

# ***Report on Modeling the Complete Process Path by an Artificial Neural Network***

## ***Detailed Study***

Tadej Kodelja  
Igor Grešovnik

*Centre of Excellence for Biosensors, Instrumentation and Process Control*

*Revision 4, April 2013.  
(revision 0: Nov. 2012)*

**Warning:** This is a long document; please don't send it to a printer!



## Contents:

<b>1</b>	<b><i>Introduction</i></b>	<b>1</b>
<b>2</b>	<b><i>Process Parameters and Final Material Properties</i></b>	<b>3</b>
<b>3</b>	<b><i>ANN Module</i></b>	<b>5</b>
<b>4</b>	<b><i>Error Estimation</i></b>	<b>7</b>
<b>4.1</b>	<b>Elongation (A)</b>	<b>7</b>
4.1.1	Errors on training points	7
4.1.2	Errors on verification points	8
<b>4.2</b>	<b>Tensile Strength (<math>R_m</math>)</b>	<b>8</b>
4.2.1	Errors on training points	8
4.2.2	Errors on verification points	9
<b>4.3</b>	<b>Yield Stress (<math>R_p</math>)</b>	<b>10</b>
4.3.1	Errors on training points	10
4.3.2	Errors on verification points	10
<b>4.4</b>	<b>Hardness After Rolling (HB)</b>	<b>11</b>
4.4.1	Errors on training points	11
4.4.2	Errors on verification points	12
<b>4.5</b>	<b>Necking (Z)</b>	<b>12</b>
4.5.1	Errors on training points	12
4.5.2	Errors on verification points	13
<b>5</b>	<b><i>Parametric studies</i></b>	<b>14</b>
<b>5.1</b>	<b>Center Point</b>	<b>14</b>
5.1.1	Elongation (A)	14
5.1.2	Tensile Strength ( $R_m$ )	32
5.1.3	Yield Stress ( $R_p$ )	49
5.1.4	Hardness After Rolling (HB)	66
5.1.5	Necking (Z)	83
<b>5.2</b>	<b>Points on Line</b>	<b>101</b>
5.2.1	Elongation (A)	101
5.2.2	Tensile Strength ( $R_m$ )	118
5.2.3	Yield Stress ( $R_p$ )	135
5.2.4	Hardness After Rolling (HB)	152
5.2.5	Necking (Z)	169
<b>6</b>	<b><i>Sensitivity Tests</i></b>	<b>187</b>
<b>6.1</b>	<b>Elongation (A)</b>	<b>187</b>
<b>6.2</b>	<b>Tensile Strength (<math>R_m</math>)</b>	<b>189</b>
<b>6.3</b>	<b>Yield Stress (<math>R_p</math>)</b>	<b>191</b>
<b>6.4</b>	<b>Hardness After Rolling (HB)</b>	<b>193</b>
<b>6.5</b>	<b>Necking (Z)</b>	<b>195</b>

## 1 INTRODUCTION

For several years artificial neural networks have been successfully used for second level process automation in basic industries. One of the fields where it is possible to exploit neural networks is to predict five important mechanical properties of steel (elongation, tensile strength, flow limit, hardness and shrinkage) on the basis of their composition and other process parameters that define the complete processing path.

The complete steel manufacturing process in the Store Steel company [1] is schematically represented in Figure 1. There are six individual processes: steel making, continuous casting of steel, hydrogen removal, reheating, multiple stage rolling, and cooling on the cooling bed. Each of these processes can be modeled either by a physics based numerical model or by an artificial neural network model. Output values of a process sometimes define the next process in the chain and thus act as input parameters (e.g. defining initial or boundary conditions) in the model of that process. Another possibility when using ANN is to build a common model of the whole production chain. In this case, we can model only outcomes after the last process and relate them to process parameters that can vary in the system.

The aim of this work is to explore the possibility of applying artificial neural networks to model the whole process chain. The resulting ANN models will be used for prediction of five mechanical properties for steel manufacturing process chain in terms of process parameters. In the scope of this work, procedures have been developed for building an ANN model of the process chain and for analyzing the model response. The concept has been demonstrated on the available data from the Štore Steel company.

The currently available data is not adequate for given complexity of the targeted models since it is not complete (not all influential parameters of the process are measured and stored), it contains errors, and the amount and spatial distribution of data are not adequate. Because of this, the models generated and analyzed here can not be considered accurate, reliable or correct. However, the applicability of the concept is demonstrated and the concept can be used in the future if adequate model data is provided. In the scope of further work, we intend to substantiate this claim on the cases where adequate data can be obtained by a numerical model suitable for generation of data that can be used to build ANN-based models. Currently, we have access to the continuous casting simulator that can be used for controlled acquisition of data for ANN-based modeling, and intend to use it to build the model of this process where errors can be estimated. Further steps are planned to link the JMatPro software for calculation of material properties with the simulator in order to build extended ANN-based casting models where chemical composition can also be varied. If this turns possible then such models will be used to study model requirements in terms of provided data, and to make estimations of how different kinds of data deficiencies influence model accuracy.

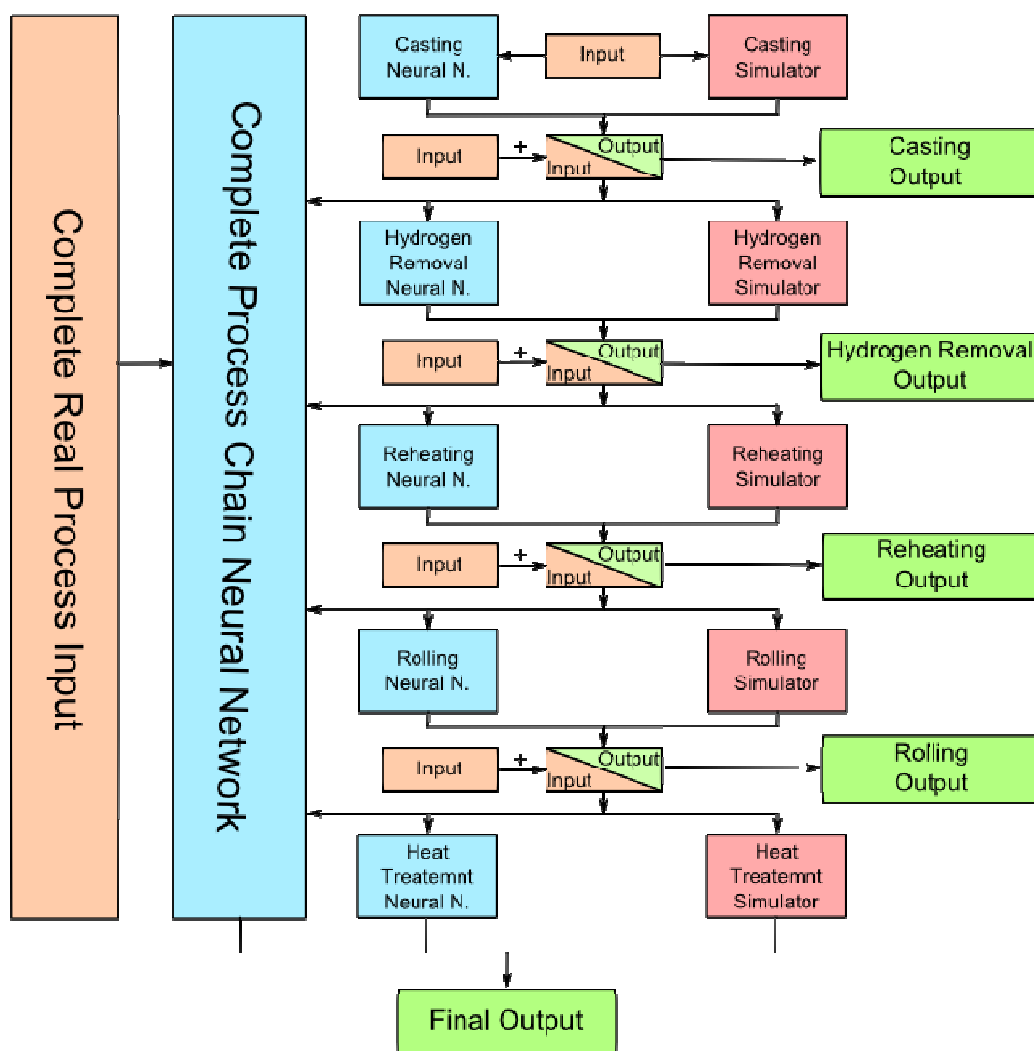


**Figure 1:** Steel manufacturing process modeling scheme.

## **2 PROCESS PARAMETERS AND FINAL MATERIAL PROPERTIES**

123 important process parameters are needed to define complete steel manufacturing process chain and are divided into seven groups (Table 1). There are 24 parameters defining the steel grade, 12 parameters for continuous casting, 2 parameters for hydrogen removal, 4 parameters for reheating furnace, 31 parameters for rolling mill, 43 parameters for continuous rolling mill and 7 parameters regarding cooling bed. On the other hand we have five basic mechanical properties of the materials that represent output values (Table 2).

**Table 1:** Process parameters (input parameters).

PROCESS	PARAMETER	NUMBER
Composition	Elements: C, Si, Mn, P, S, Cr, Mo, Ni, Al, Cu, Ti, V, W, Sn, As, Zr, Ca, Sb, B, N, O, H, Pb, Zn	24
Continuous casting of steel	Casting dimensions (140 x 140mm or 180 x 180mm)	12
	Casting temperature	
	Casting speed	
	Casting powder type	
	Mould level depth	
	Mould water flow	
	Mould inlet water temperature	
	Mould outlet water temperature	
	Wreath spray flow	
	Wreath spray temperature	
	Spray cooling system 01 spray flow	
	Cooling water 01 temperature	
Hydrogen removal	Time in the furnace	2
	Temperature in the furnace	
Biller reheating furnace	Conveyor speed	4
	Temperature in furnace Zone 1 – 3	
Rolling mill	Input dimension (140 x 140mm or 180 x 180mm)	31
	Input temperature	
	Number of rolling passes	
	Entry rolling speed pass 1 – 7	
	Radius of roll 1 – 7	
	Roll gap 1 – 7	
	Roll groove 1 – 7	
Continuous rolling mill	Input dimension	43
	Input temperature	
	Entry or outlet rolling speed	
	Roll 1 – 10 engagement yes/no	
	Radius of roll 1 – 10	
	Roll gap 1 – 10	

	Roll groove 1 – 10	
Cooling bed	Product dimension – cross-section	7
	Product dimension – length	
	Product temperature	
	Distance between two products	
	Number of bars in one spot	
	Lifting apron (radiation shield) height	
	Frequency of product moving	
	<b>TOTAL</b>	<b>123</b>

**Table 2:** Final material properties (output values).

VALUES	NUMBER
Elongation (A)	1
Tensile strength ( $R_m$ )	1
Yield stress ( $R_{p0.2}$ )	1
Hardness after rolling (HB)	1
Necking (Z)	1
<b>TOTAL</b>	<b>5</b>

### 3 ANN MODULE

We trained artificial neural network with data from the complete steel production chain in Store Steel Company. Process is completely defined with 123 process parameters (Table 1). 34 influential input parameters (Table 3) and 5 output values (Table 4) were taken into account.

**Table 3:** Process parameters used in ANN model (input parameters).

PROCESS	PARAMETER	NUMBER
Composition	Elements: C, Si, Mn, P, S, Cr, Mo, Ni, Al, Cu, Ti, V, W, Sn, As, Zr, Ca, Sb, B, N, O, H, Pb, Zn	24
Continuous casting of steel	Casting temperature	7
	Casting speed	
	Mould water flow	
	Mould inlet water temperature	
	Mould outlet water temperature	
	Wreath spray flow	
	Spray cooling system 01 spray flow	
	Cooling water 01 temperature	
Biller reheating furnace	Temperature in furnace Zone 1 – 3	3
<b>TOTAL</b>		<b>34</b>

**Table 4:** Final material properties used in ANN model (output values).

VALUES	NUMBER
Elongation (A)	1
Tensile strength ( $R_m$ )	1
Yield stress ( $R_{p0.2}$ )	1
Hardness after rolling (HB)	1
Necking (Z)	1
<b>TOTAL</b>	<b>5</b>

After separating data belonging to two billet dimensions (140mm and 180mm) and after some filtering to exclude corrupted data, 1879 data sets for dimension 140mm have been prepared. The data have been manually collected from different synchronized data bases. The main goal of the study is to train the artificial neural network in order to be capable of predicting elongation, tensile strength, flow limit, hardness after rolling and shrinkage, while changing the chemical composition and other process parameters accounted for in training procedure [3]-[5]. For practical set-up of the relevant artificial neural network we used Aforge.Net [2] library, incorporated in our software module written in C# (C sharp) [12]-[14]. The broader ANN module is based on the IGLib.NET [12], a general purpose library for developing technical applications that has its roots in long term experience gained from development of industrial optimization software [6]-[12]. Datasets were stored in predefined JSON-based format and imported from file before training. Our module allows us to check training and verification errors during the training procedure. The procedure consist of

### 3. ANN Module Report on Modeling the Complete Process Path by an Artificial Neural Network

---

five steps: reading data from a file, data preparation, training, testing and prediction of unknown output values based on different combinations of 34 input parameters listed in Table 3. During training, state of the artificial neural network is adjusted to data sets with known output values. These comprise historical cases of steel production in the past. During training, the ANN response in training and verification points is checked in order to see how well it does at predicting known and unknown output values. Verification and training points used for testing are usually a subset of historical data. Verification points are randomly chosen from datasets before training starts and are not used in training procedure, while training points are. When error on training points becomes smaller than the user specified tolerance or when the number of training cycles reaches specified number, the training stops. We tried different combinations of layouts and training parameters. We made more than 20 trainings with Aforge library. Settings for ANN are presented in Table 5.

**Table 5:** ANN settings.

Name	Value
Number of hidden layers	1
Number of neurons in hidden layer 1	15
Maximum number of epochs	100.000
Learning rate	0.3
Momentum	0.6
Input safety factor	1.4
Output safety factor	1.4

Training procedures were always performed on HP workstation HPDL380G7 with 12 Intel Xenon 2.0GHz processors, 24GB installed RAM. Trained neural network which gave us the best results was trained in approximately 18 hours.

## 4 ERROR ESTIMATION

After training of the neural network was done, errors of the approximated outputs in training and verification sets were calculated. With these tests we try to determine the accuracy of the ANN.

Relative errors in all training points represents how the ANN is approximating on these points, while relative errors in all verification points represent how the ANN is approximating in the space between training points. These errors are defined as follows:

$$\delta v_i = \left| \frac{v^{(m)}(\mathbf{p}_i) - v(\mathbf{p}_i)}{\max_{j \in I_T} (v^{(m)}(\mathbf{p}_j)) - \min_{j \in I_T} (v^{(m)}(\mathbf{p}_j))} \right|; i \in I_V, , \quad (1)$$

where  $v^{(m)}(\mathbf{p}_i)$  is the actual (measured) value of the output quantity  $v$  at the vector of input parameters  $\mathbf{p}_i$ ,  $v(\mathbf{p}_i)$  is the approximated value of this quantity at the same vector of parameters.

### 4.1 Elongation (A)

**Relative errors for elongation (A) are represented in**

Figure 2 for training points and Figure 3 for verification points.

#### 4.1.1 Errors on training points

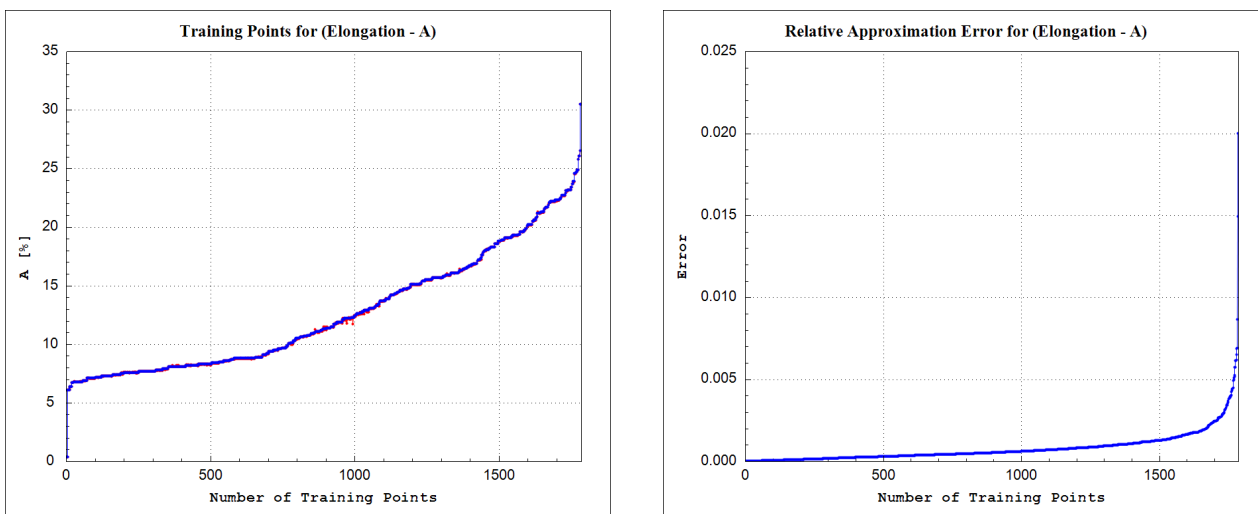


**Figure 2:** Approximation for elongation (A) in 1879 training points. Training points are represented by dots. Left: real elongation values. Right: relative error in training points.

#### 4.1.2 Errors on verification points

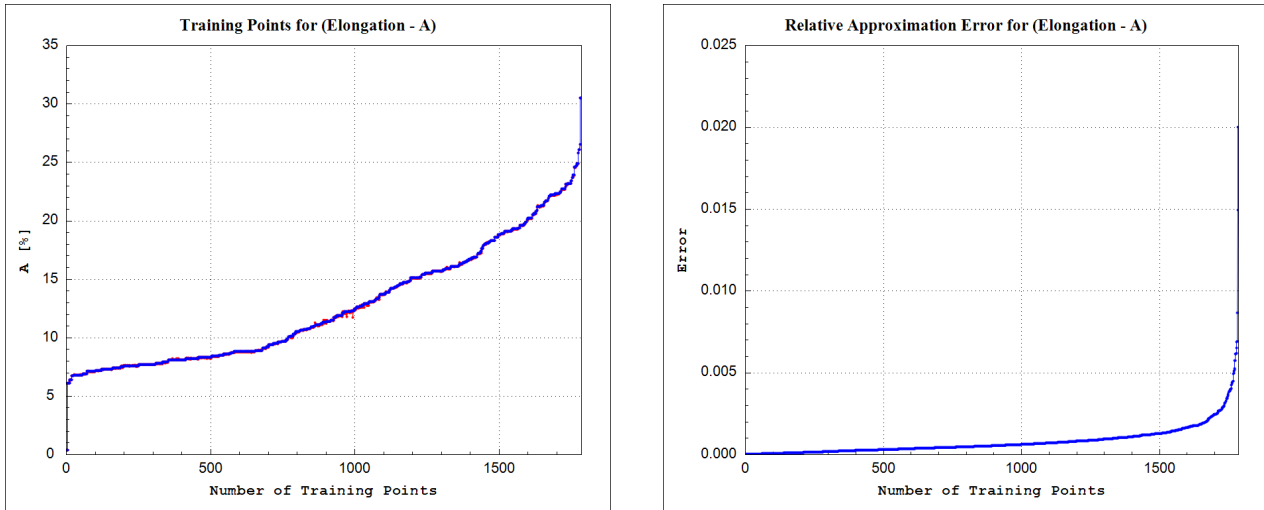


**Figure 3:** Approximation for elongation (A) in 94 verification points. Verification points are represented by dots. Left: real elongation values. Right: relative error in verification points.

### 4.2 Tensile Strength ( $R_m$ )

Relative errors for tensile strength ( $R_m$ ) are represented in Figure 4 for training points and Figure 5 for verification points.

#### 4.2.1 Errors on training points

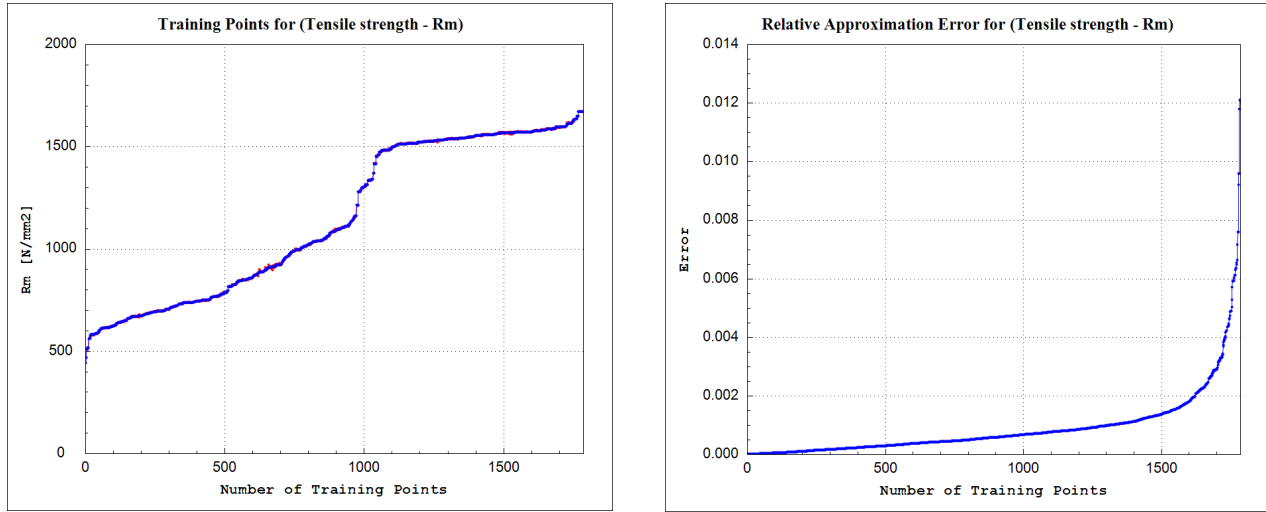


**Figure 4:** Approximation for tensile strength ( $R_m$ ) in 1879 training points. Training points are represented by dots. Left: real tensile strength values. Right: relative error in training points.

#### 4.2.2 Errors on verification points

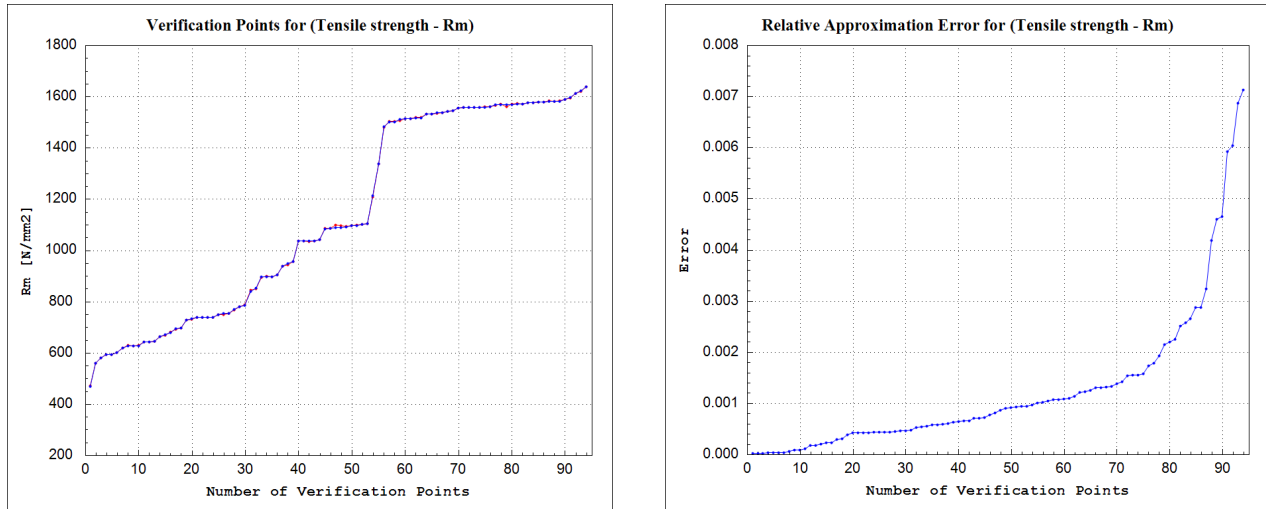


**Figure 5:** Approximation for tensile strength ( $R_m$ ) in 94 verification points. Verification points are represented by dots. Left: real tensile strength values. Right: relative error in verification points.

### 4.3 Yield Stress ( $R_p$ )

Relative errors for yield stress ( $R_p$ ) are represented in Figure 6 for training points and Figure 7 for verification points.

#### 4.3.1 Errors on training points

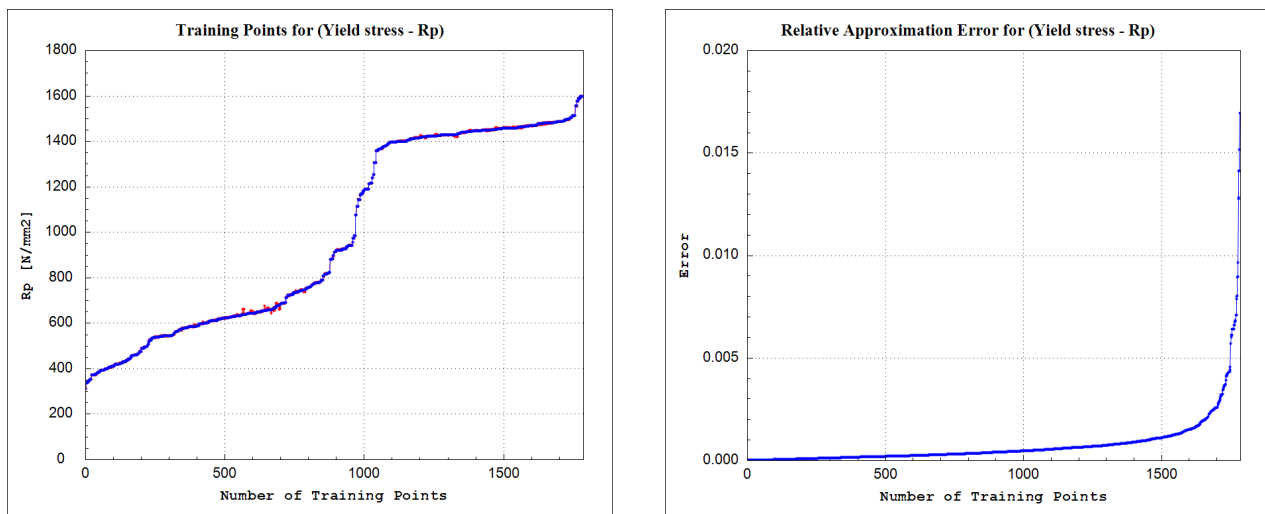


**Figure 6:** Approximation for yield stress ( $R_p$ ) in 1879 training points. Training points are represented by dots. Left: real yield stress values. Right: relative error in training points.

#### 4.3.2 Errors on verification points

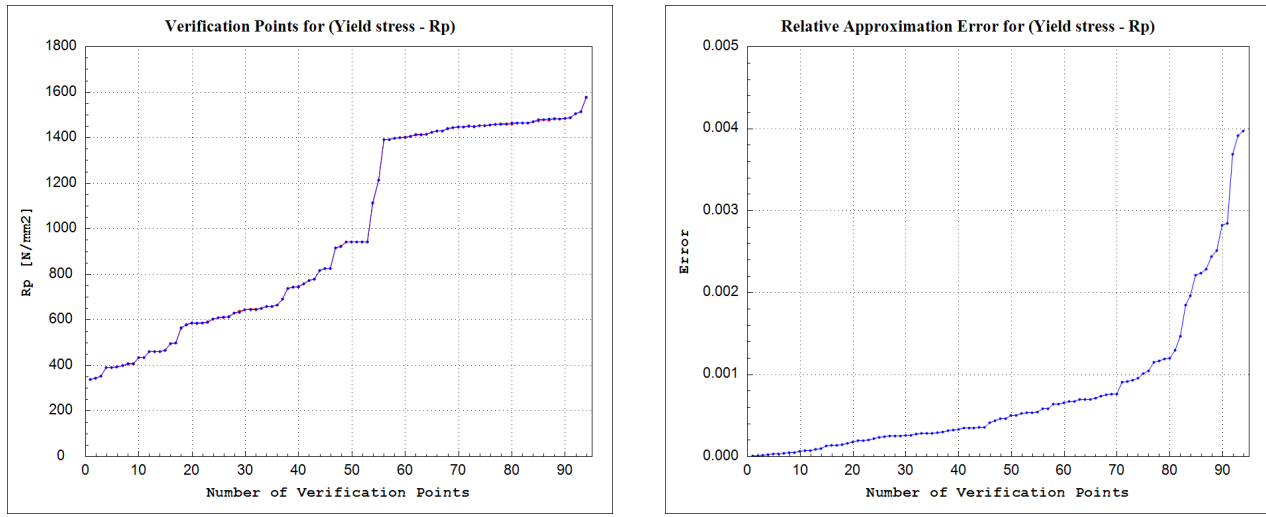


**Figure 7:** Approximation for yield stress ( $R_p$ ) in 94 verification points. Verification points are represented by dots. Left: real yield stress values. Right: relative error in verification points.

#### 4.4 Hardness After Rolling (HB)

Relative errors for hardness after rolling (HB) are represented in Figure 8 for training points and Figure 9 for verification points.

##### 4.4.1 Errors on training points

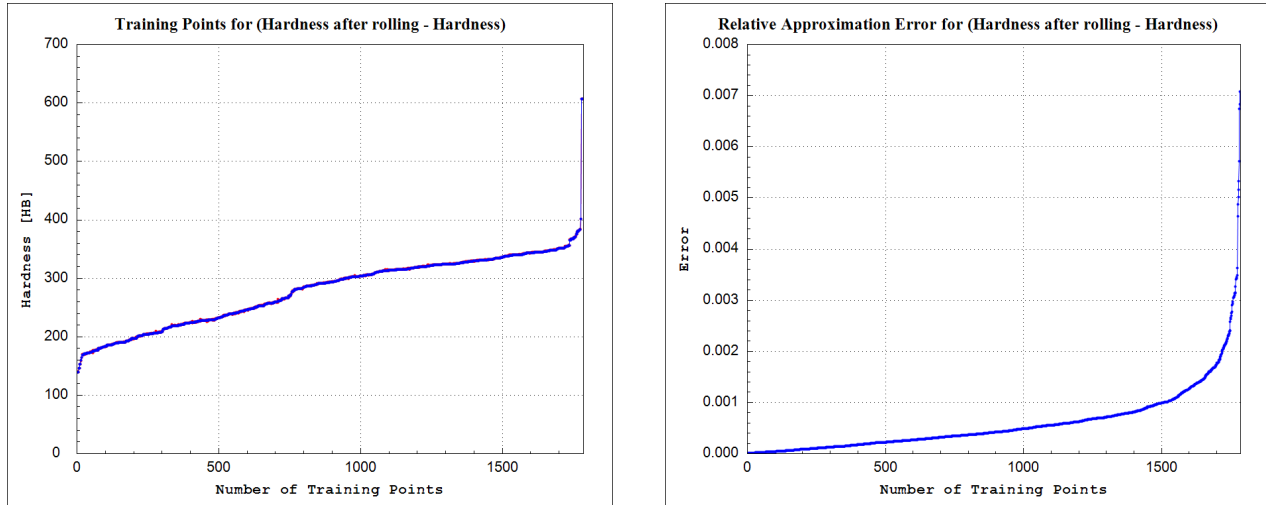


**Figure 8:** Approximation for hardness after rolling (HB) in 1879 training points. Training points are represented by dots. Left: real hardness after rolling values. Right: relative error in training points.

#### 4.4.2 Errors on verification points

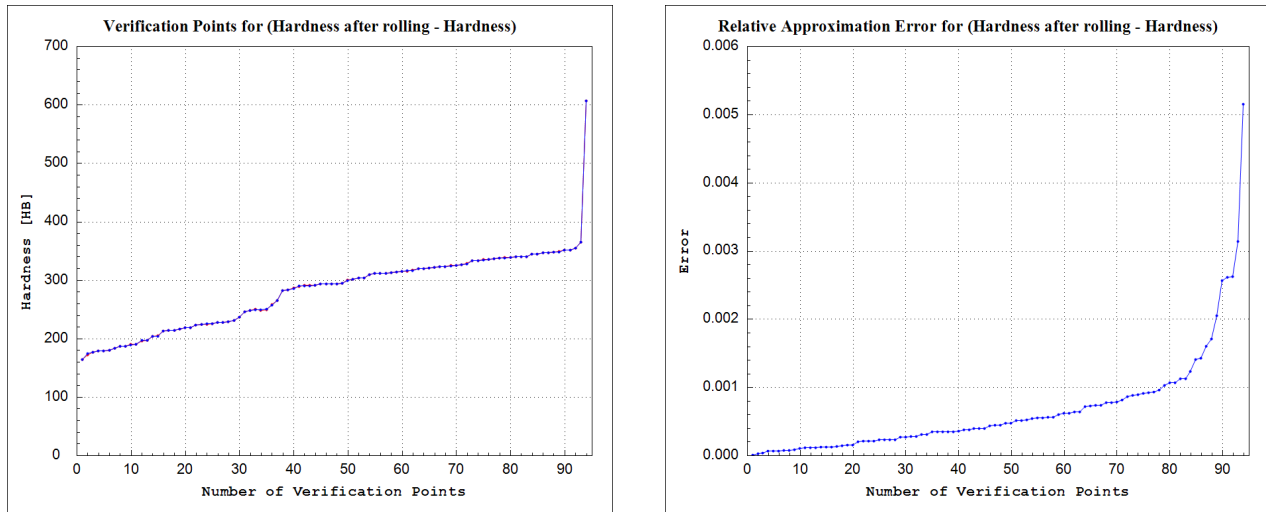


**Figure 9:** Approximation for hardness after rolling (HB) in 94 verification points. Verification points are represented by dots. Left: real hardness after rolling values. Right: relative error in verification points.

### 4.5 Necking (Z)

Relative errors for necking (Z) are represented in Figure 10 for training points and Figure 11 for verification points.

#### 4.5.1 Errors on training points

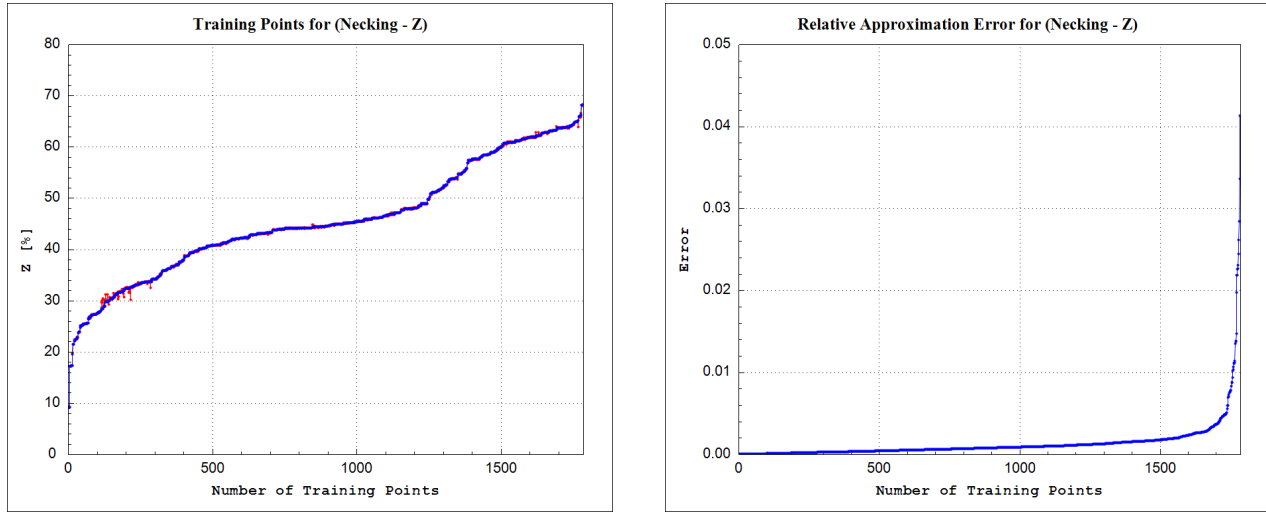


**Figure 10:** Approximation for necking ( $Z$ ) in 1879 training points. Training points are represented by dots. Left: real necking values. Right: relative error in training points.

#### 4.5.2 Errors on verification points

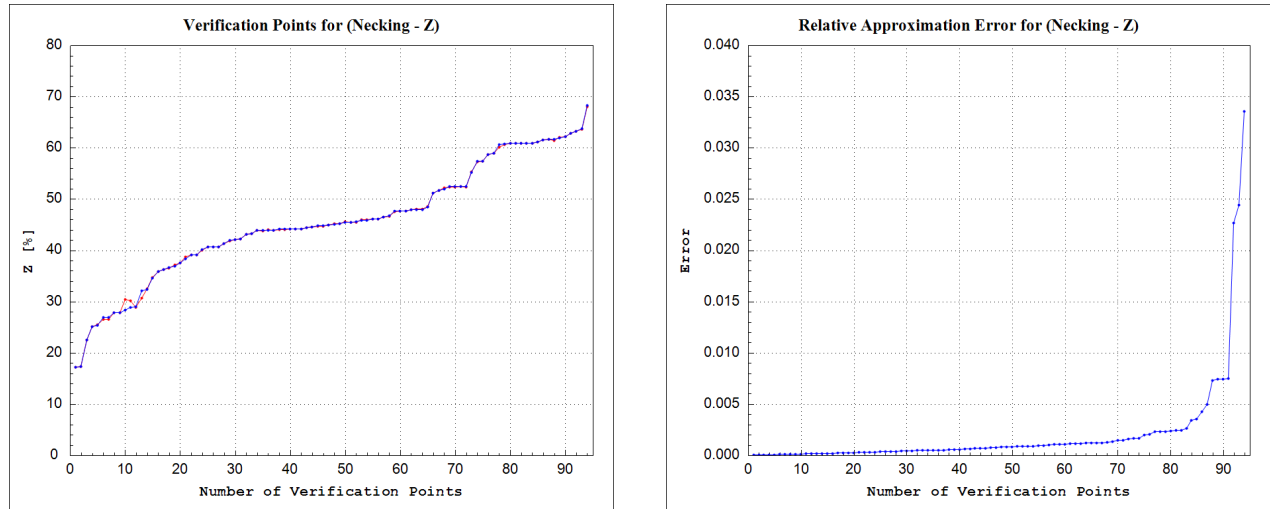


**Figure 11:** Approximation for necking ( $Z$ ) in 94 verification points. Verification points are represented by dots. Left: real necking values. Right: relative error in verification points.

## 5 PARAMETRIC STUDIES

After performing error estimation tests, some parametric studies were performed. With these parametric tests we try to determine the accuracy of the ANN and also verify dependences between parameters.

### 5.1 *Center Point*

In this study we calculated one center point from training data set and one point from verification data set. Center point for training point was defined as:

$$\mathbf{r}_T = \frac{\sum_{i=0}^{I_T} (\mathbf{p}_i)}{I_T}; i \in I_T, \quad (2)$$

while center point for verification set was defined as,

$$\mathbf{r}_V = \frac{\sum_{i=0}^{I_V} (\mathbf{p}_i)}{I_T}; i \in I_V. \quad (3)$$

In each chosen point we varied one parameter, while other parameters were fixed. Parameter was varied within the range defined by the minimum and maximum value of that parameter over all dataset used in training. These kind of tests help us find out how the change of one parameter, influences on final material properties. We performed these tests for all 34 input parameters. The influences are shown from Figure 12 to Figure 181.

#### 5.1.1 Elongation (A)

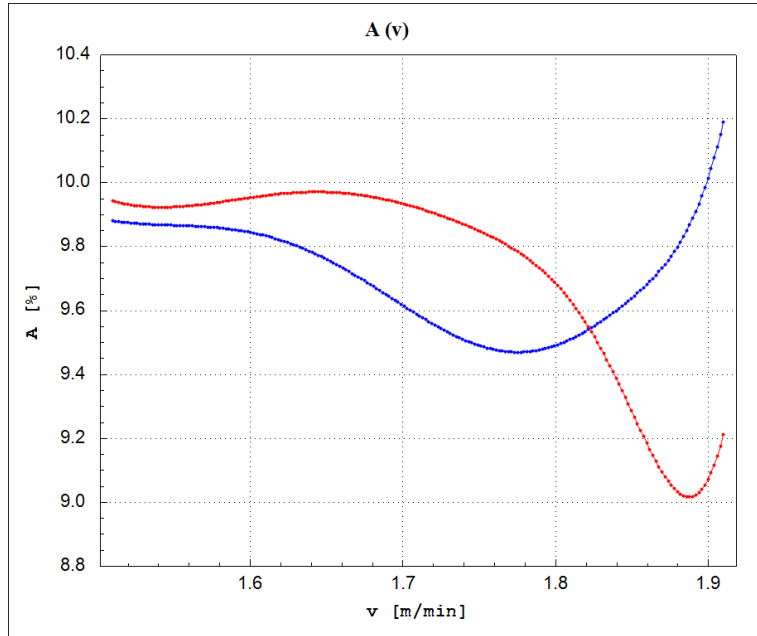


**Figure 12:** Elongation as a function of the continuous casting speed, calculated by the ANN model on centered verification point (red line) and centered training point (blue line).

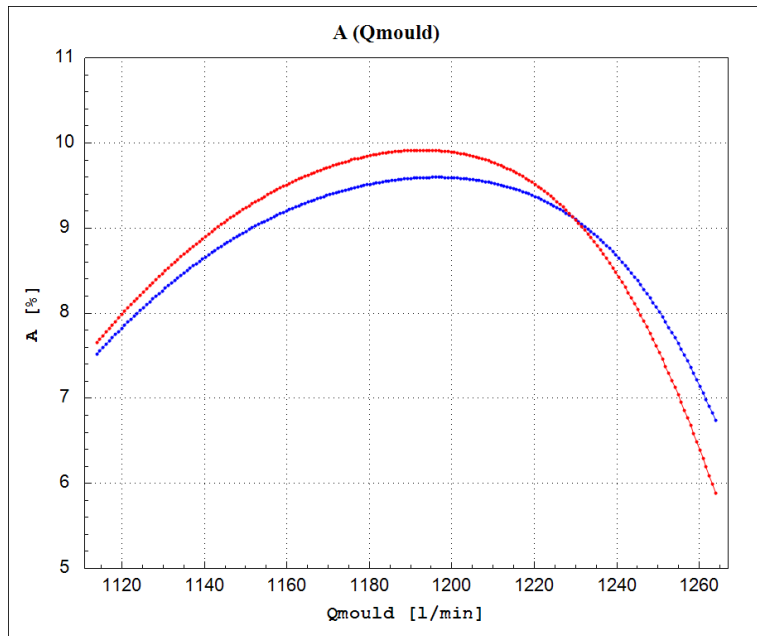


**Figure 13:** Elongation as a function of the cooling flow rate in the mould, calculated by the ANN model on centered verification point (red line) and centered training point (blue line).

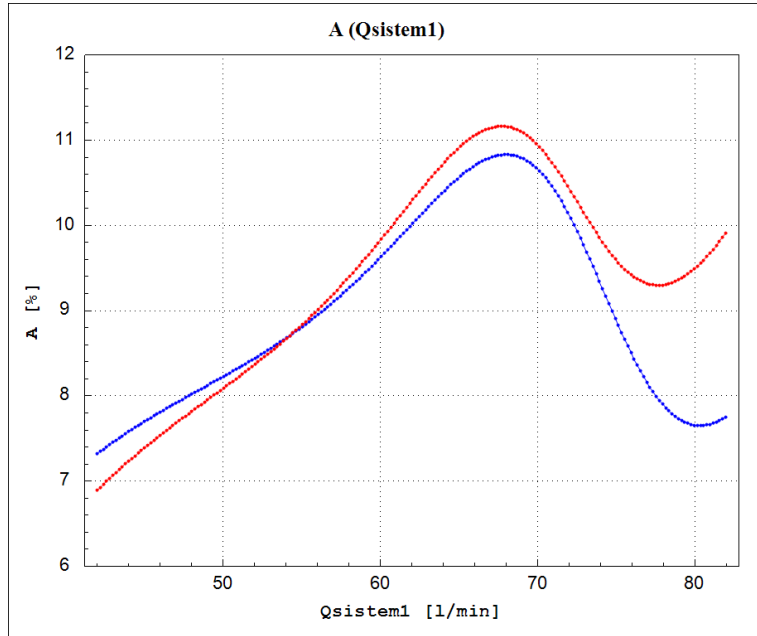


**Figure 14:** Elongation as a function of the cooling flow rate in 1<sup>st</sup> spray system, calculated by the ANN model on centered verification point (red line) and centered training point (blue line).

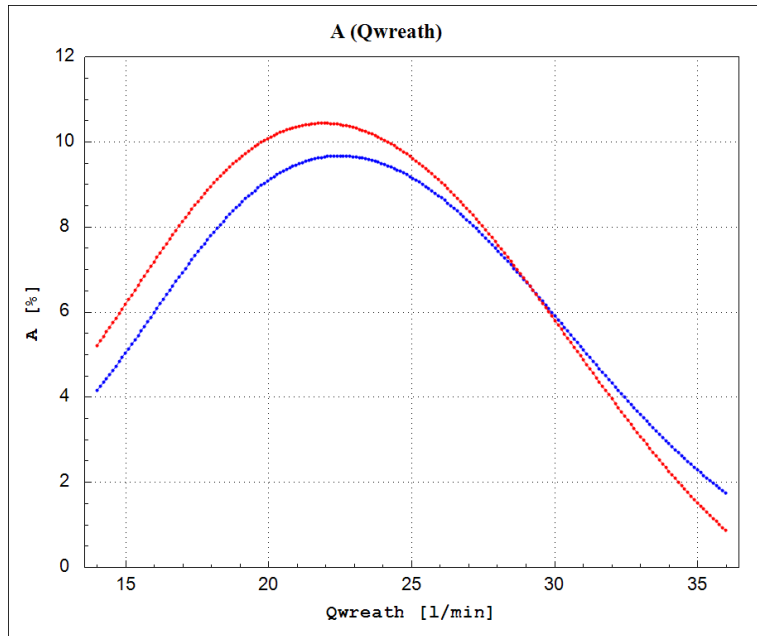


**Figure 15:** Elongation as a function of the cooling flow rate in wreath spray system, calculated by the ANN model on centered verification point (red line) and centered training point (blue line).

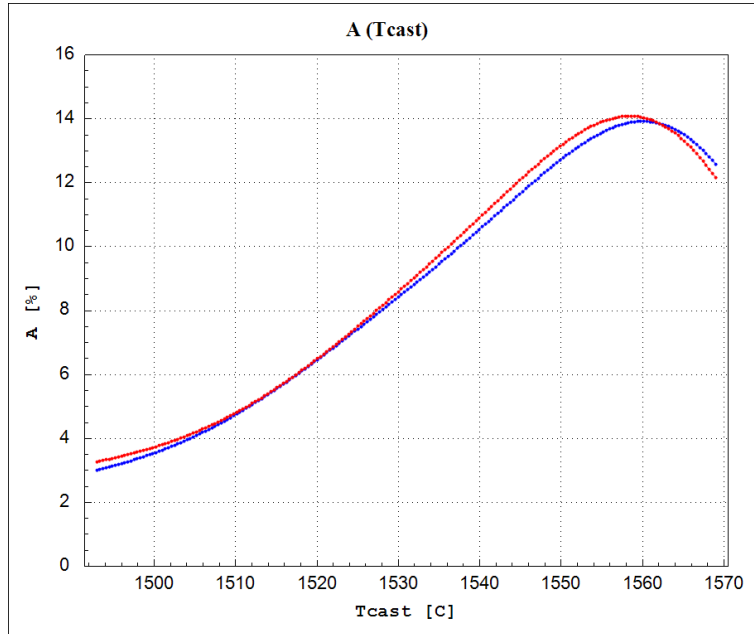


**Figure 16:** Elongation as a function of the casting temperature, calculated by the ANN model on centered verification point (red line) and centered training point (blue line).

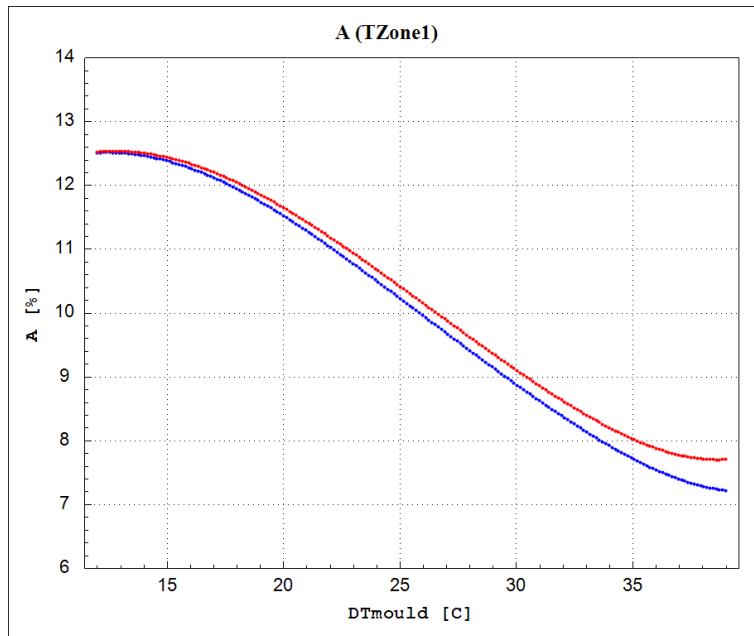


**Figure 17:** Elongation as a function of the water temperature in Zone 1, calculated by the ANN model on centered verification point (red line) and centered training point (blue line).

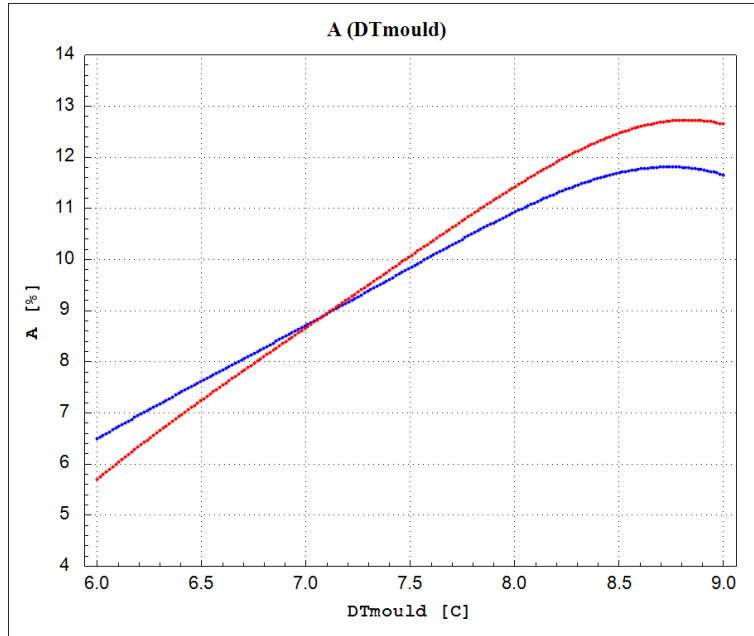


**Figure 18:** Elongation as a function of the delta T, calculated by the ANN model on centered verification point (red line) and centered training point (blue line).

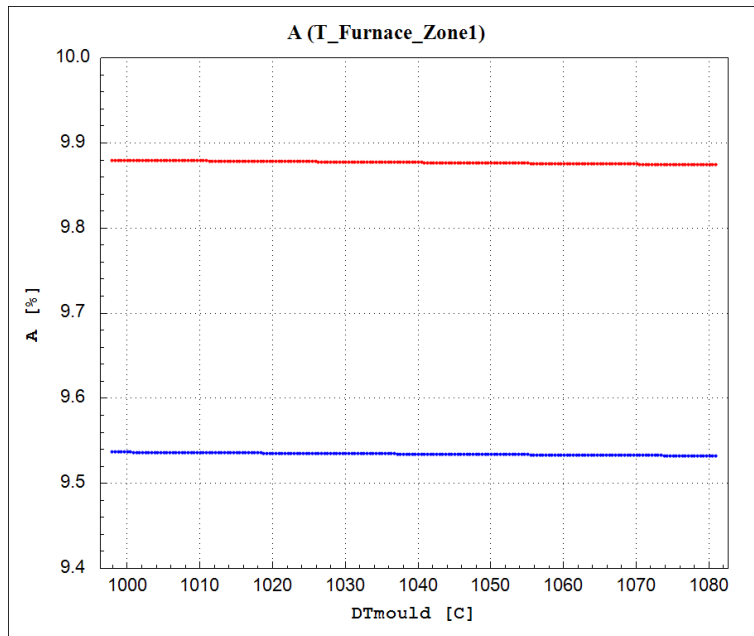


**Figure 19:** Elongation as a function of the average on temperature in zone 1, calculated by the ANN model on centered verification point (red line) and centered training point (blue line).

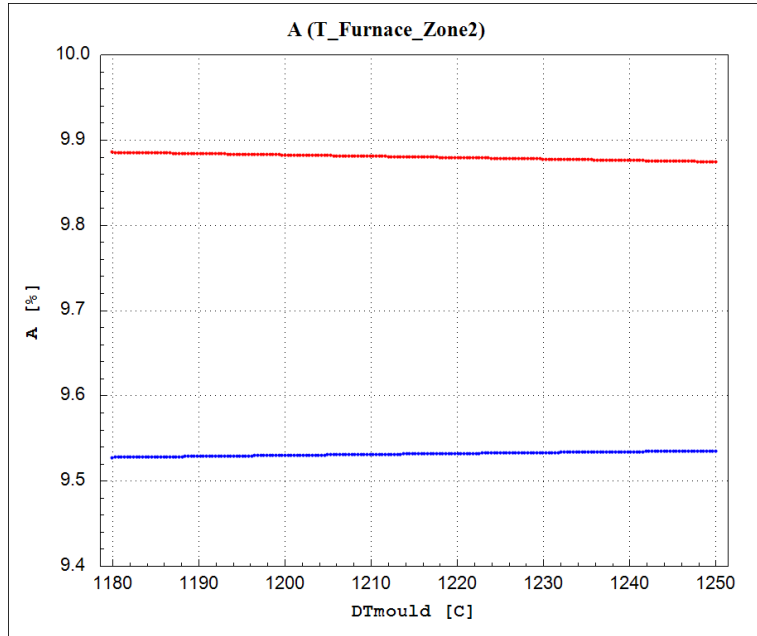


**Figure 20:** Elongation as a function of the average on temperature in zone 2, calculated by the ANN model on centered verification point (red line) and centered training point (blue line).

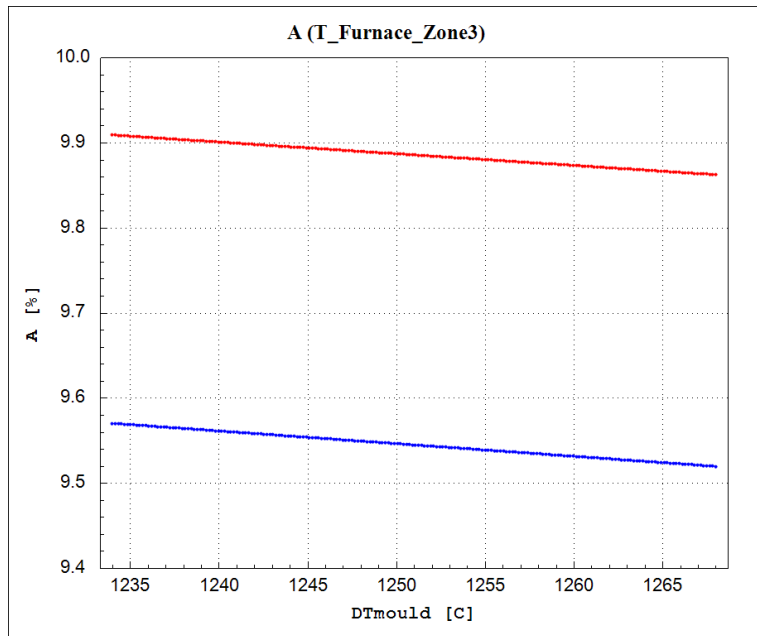


**Figure 21:** Elongation as a function of the average on temperature in zone 3, calculated by the ANN model on centered verification point (red line) and centered training point (blue line).

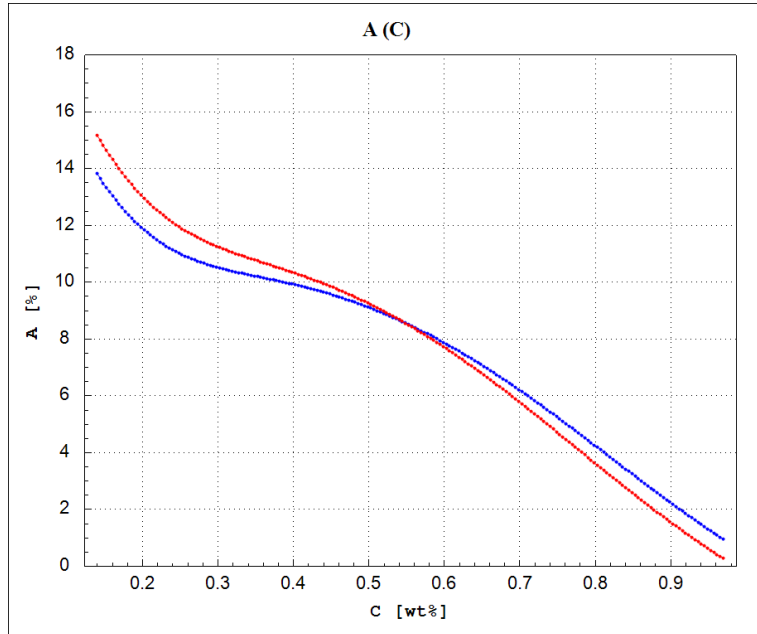


**Figure 22:** Elongation as a function of the Carbon concentration (C), calculated by the ANN model on centered verification point (red line) and centered training point (blue line).

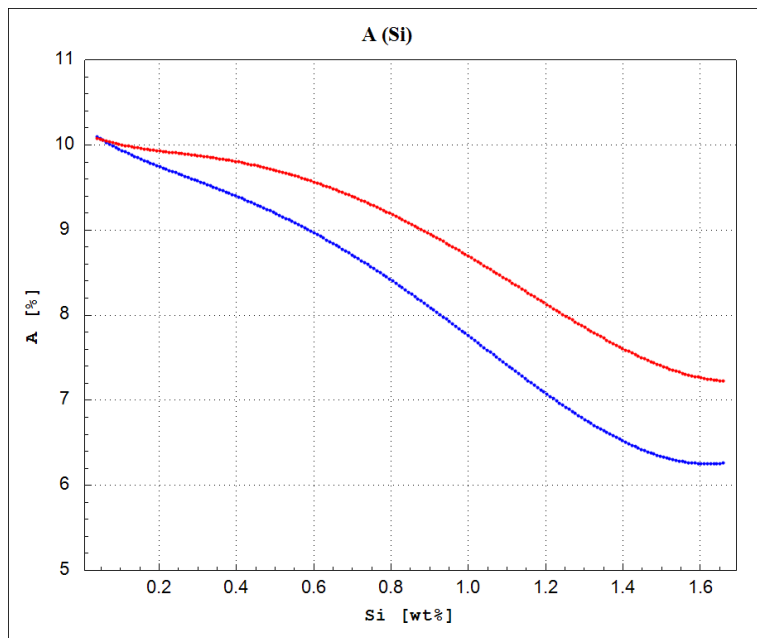


**Figure 23:** Elongation as a function of the Silicon concentration (Si), calculated by the ANN model on centered verification point (red line) and centered training point (blue line).

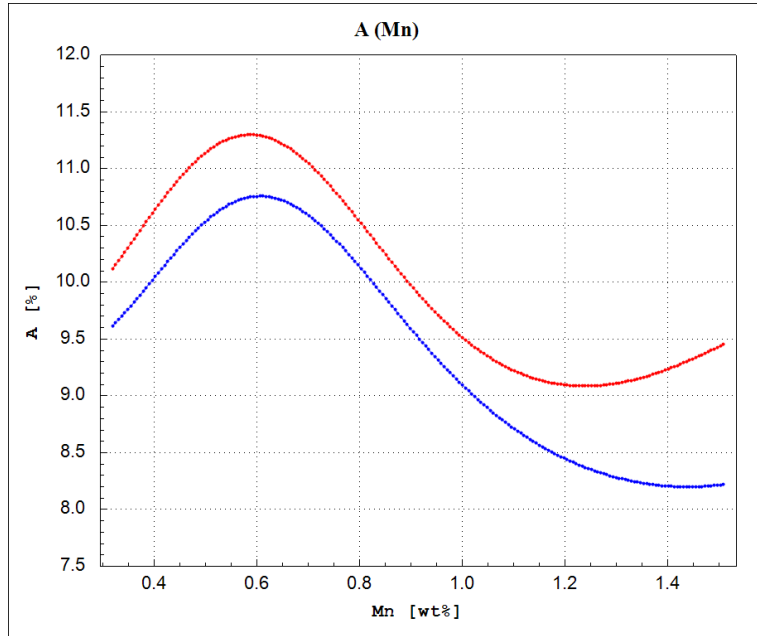


**Figure 24:** Elongation as a function of the Manganese concentration (Mn), calculated by the ANN model on centered verification point (red line) and centered training point (blue line).

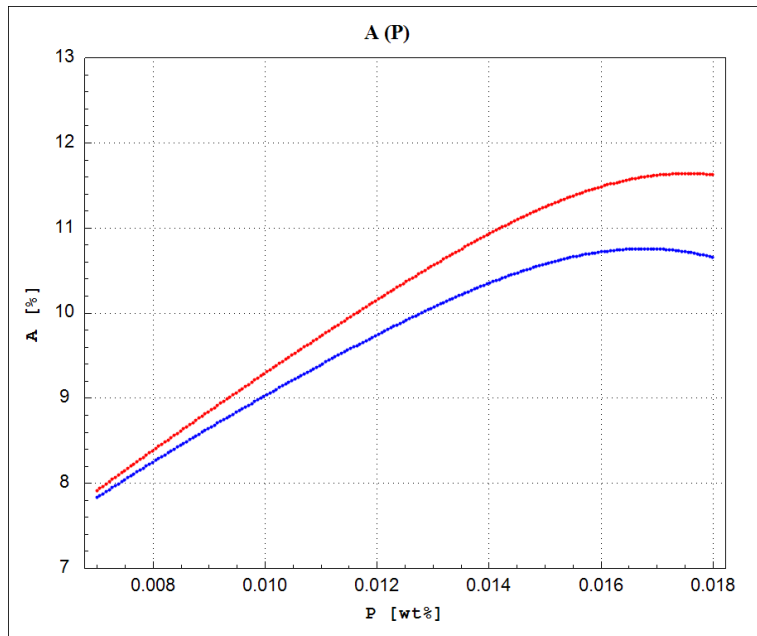


**Figure 25:** Elongation as a function of the Phosphorus concentration (P), calculated by the ANN model on centered verification point (red line) and centered training point (blue line).

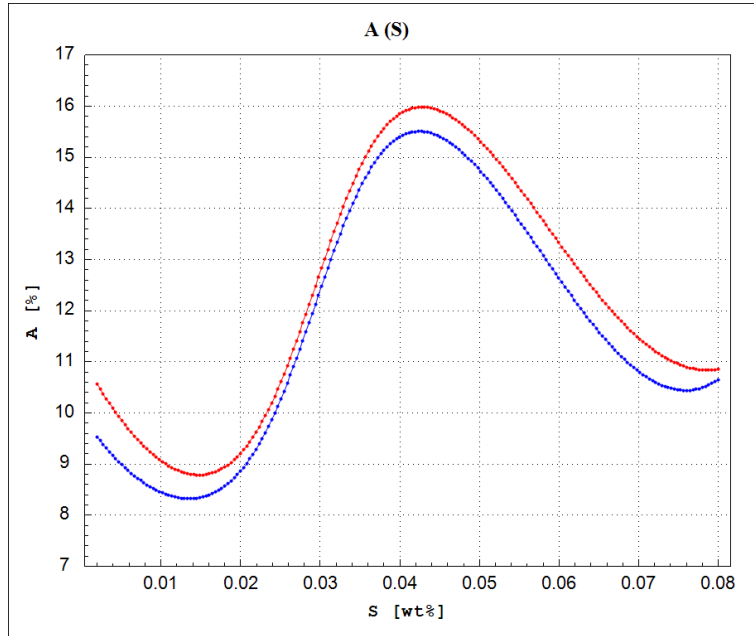


**Figure 26:** Elongation as a function of the Sulphur concentration (S), calculated by the ANN model on centered verification point (red line) and centered training point (blue line).

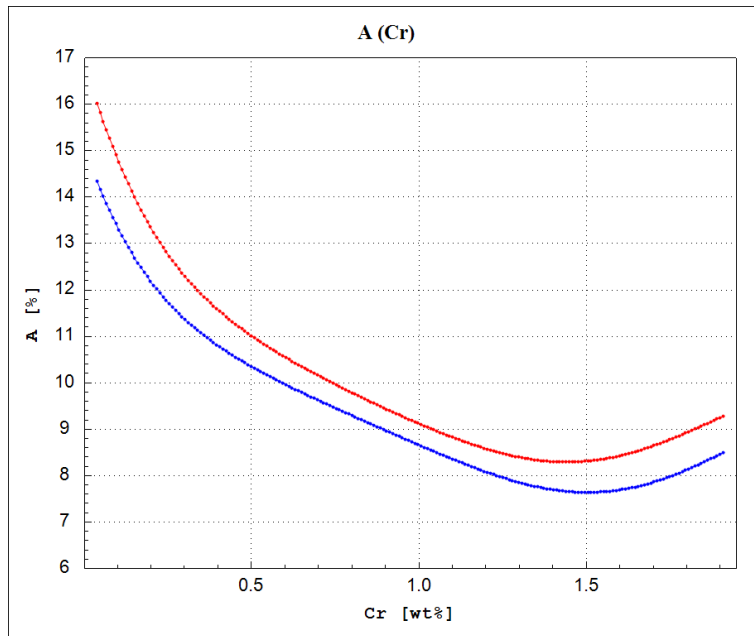


**Figure 27:** Elongation as a function of the Chromium concentration (Cr), calculated by the ANN model on centered verification point (red line) and centered training point (blue line).

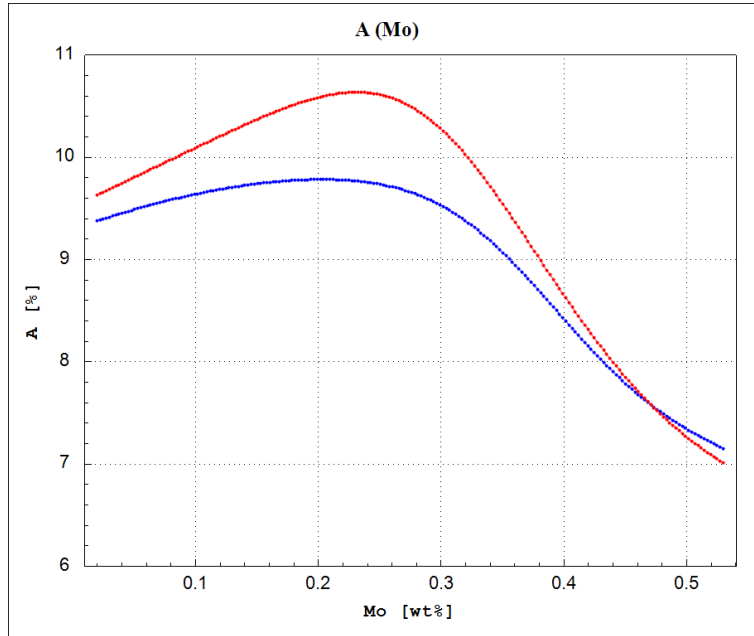


**Figure 28:** Elongation as a function of the Molybdenum concentration (Mo), calculated by the ANN model on centered verification point (red line) and centered training point (blue line).

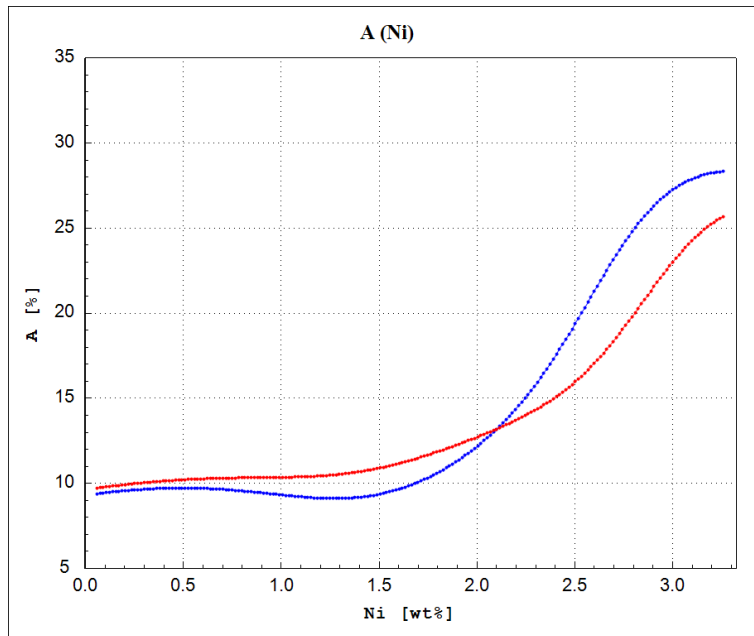


**Figure 29:** Elongation as a function of the Nickel concentration (Ni), calculated by the ANN model on centered verification point (red line) and centered training point (blue line).

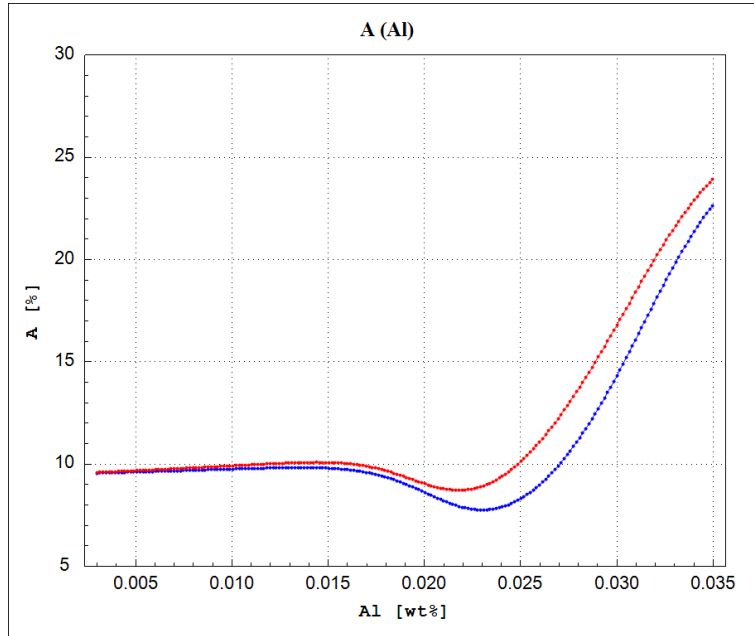


**Figure 30:** Elongation as a function of the Aluminium concentration (Al), calculated by the ANN model on centered verification point (red line) and centered training point (blue line).

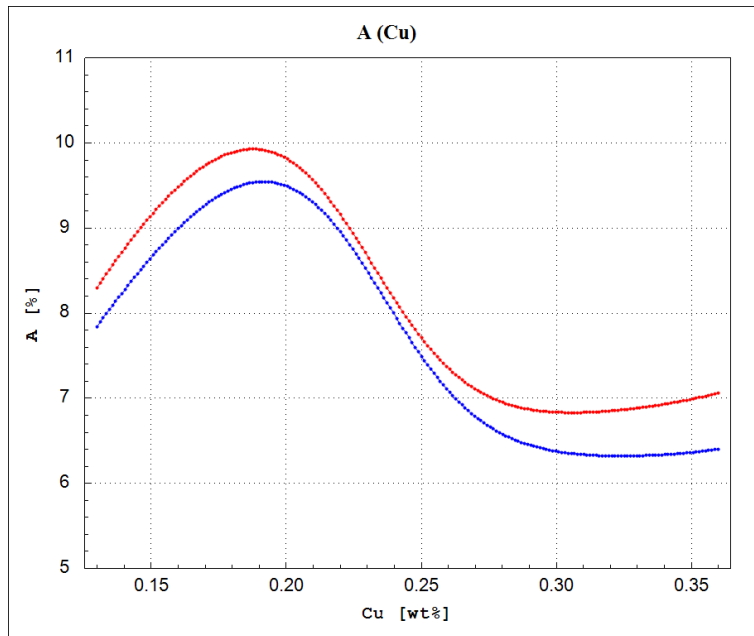


**Figure 31:** Elongation as a function of the Copper concentration (Cu), calculated by the ANN model on centered verification point (red line) and centered training point (blue line).

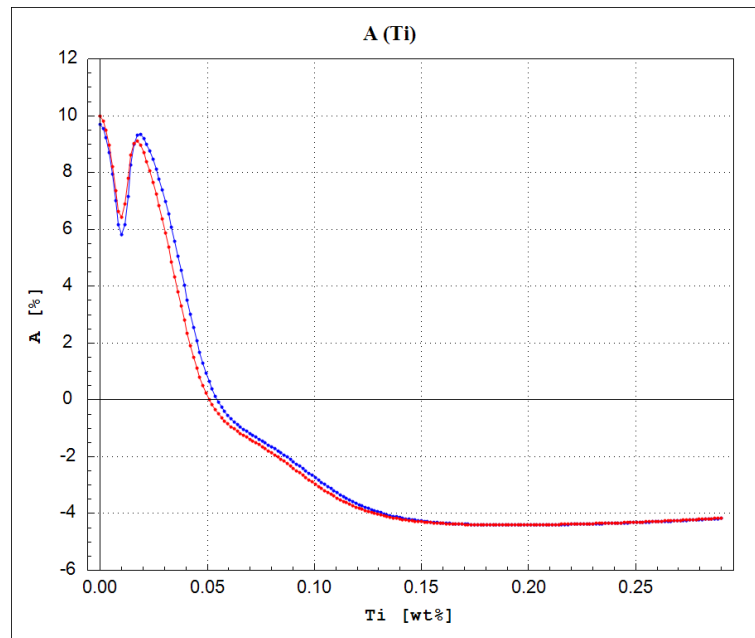


**Figure 32:** Elongation as a function of the Titanium concentration (Ti), calculated by the ANN model on centered verification point (red line) and centered training point (blue line).

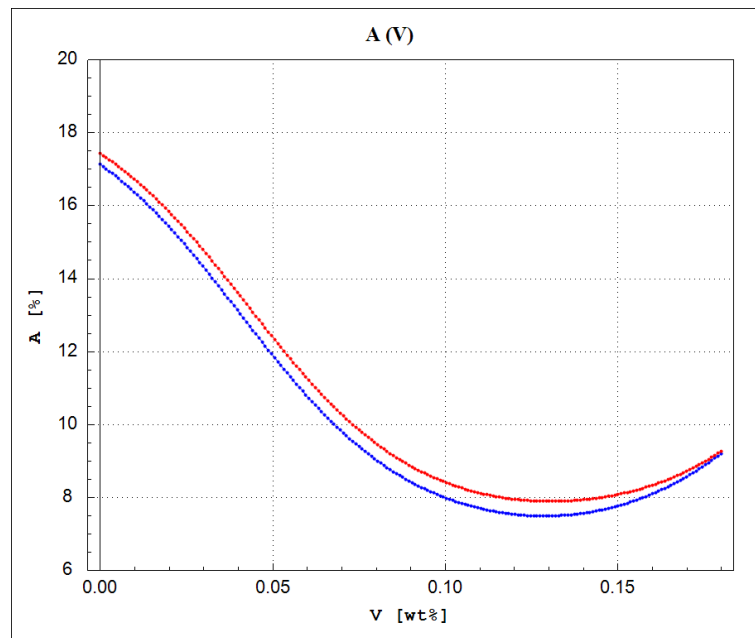


**Figure 33:** Elongation as a function of the Vanadium concentration (V), calculated by the ANN model on centered verification point (red line) and centered training point (blue line).

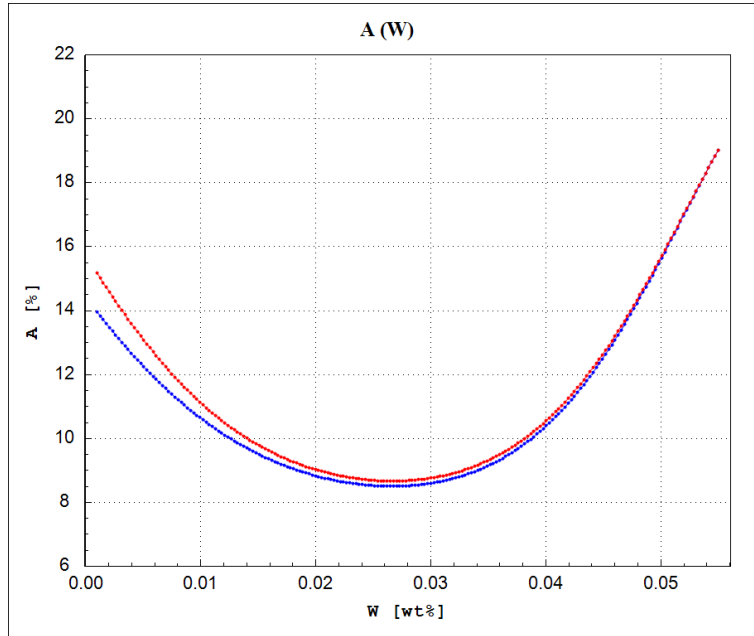


**Figure 34:** Elongation as a function of the Tungsten concentration (W), calculated by the ANN model on centered verification point (red line) and centered training point (blue line).

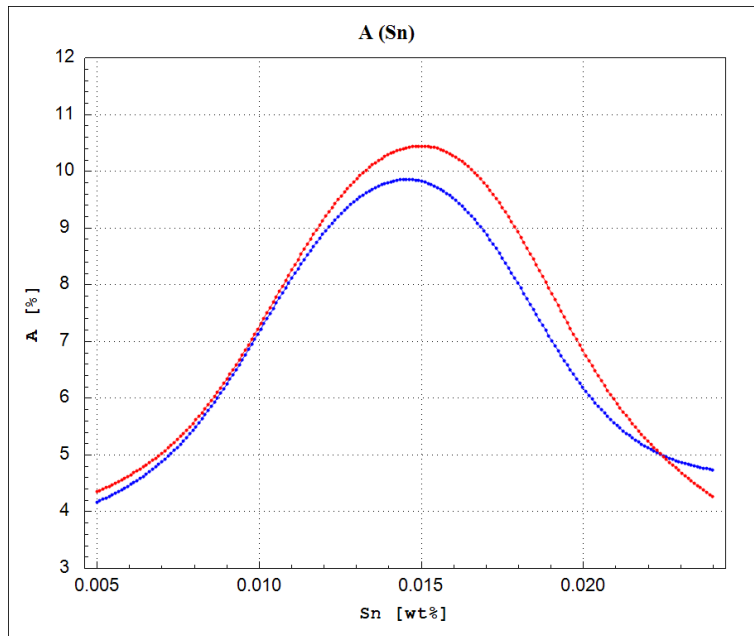


**Figure 35:** Elongation as a function of the Tin concentration (Sn), calculated by the ANN model on centered verification point (red line) and centered training point (blue line).

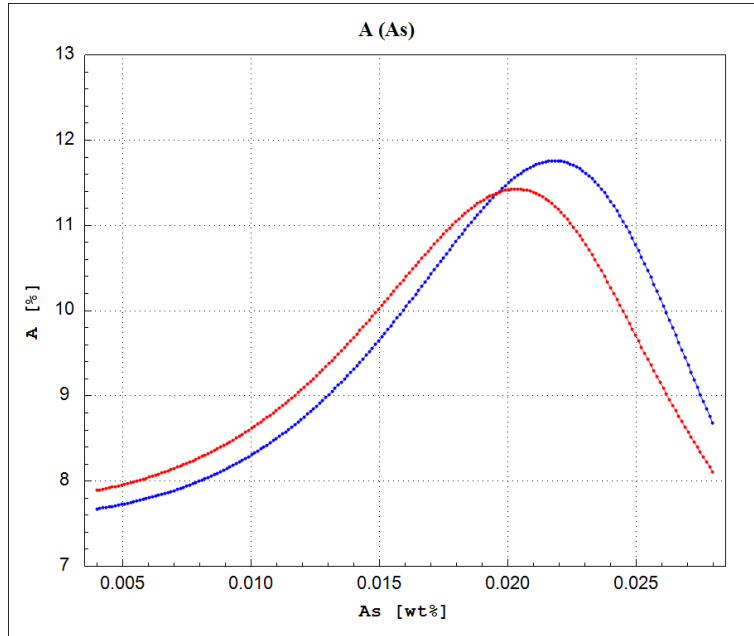


**Figure 36:** Elongation as a function of the Arsenic concentration (As), calculated by the ANN model on centered verification point (red line) and centered training point (blue line).

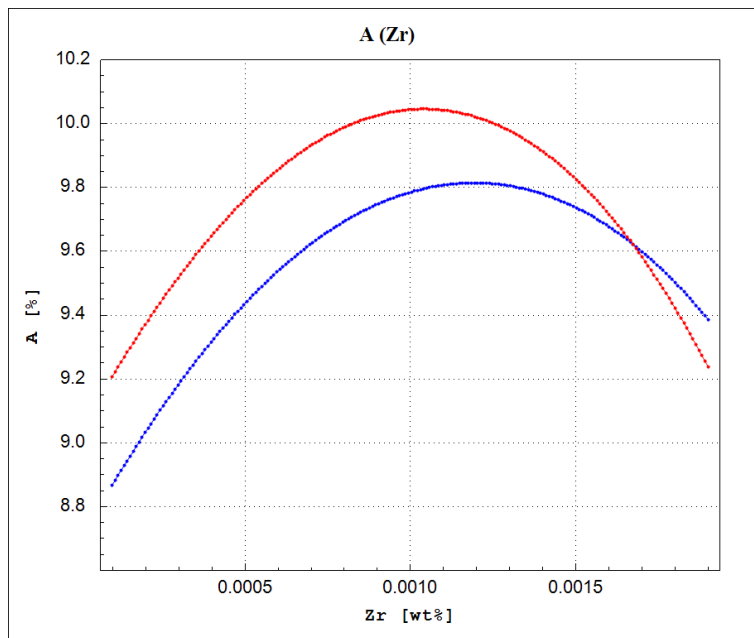


**Figure 37:** Elongation as a function of the Zirconium concentration (Zr), calculated by the ANN model on centered verification point (red line) and centered training point (blue line).

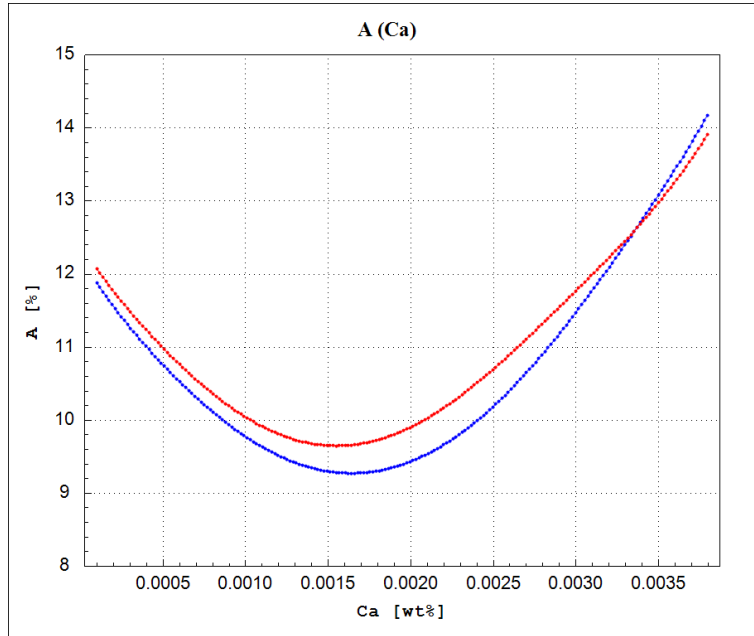


**Figure 38:** Elongation as a function of the Calcium concentration (Ca), calculated by the ANN model on centered verification point (red line) and centered training point (blue line).

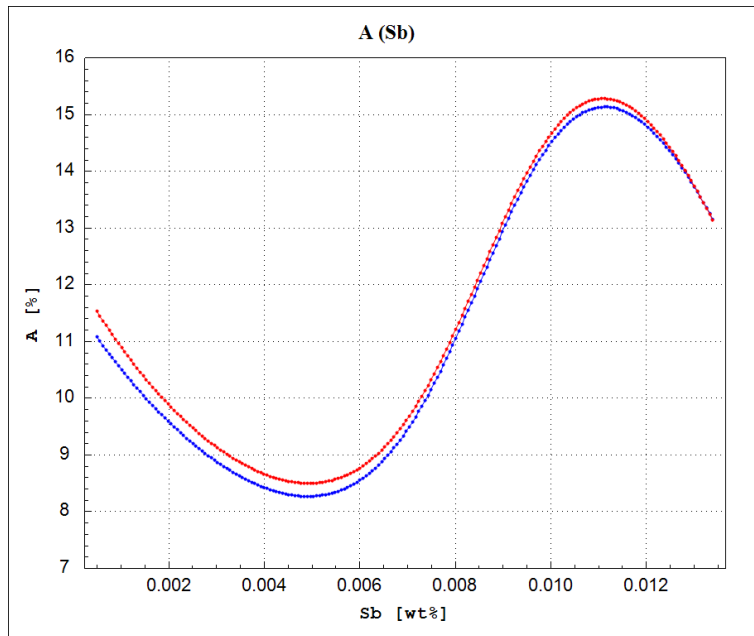


**Figure 39:** Elongation as a function of the Antimony concentration (Sb), calculated by the ANN model on centered verification point (red line) and centered training point (blue line).

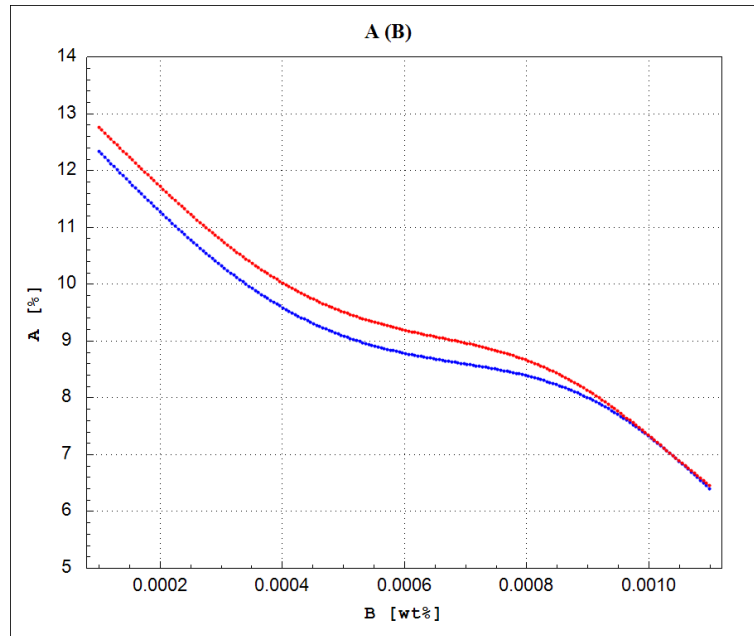


**Figure 40:** Elongation as a function of the Boron concentration (B), calculated by the ANN model on centered verification point (red line) and centered training point (blue line).

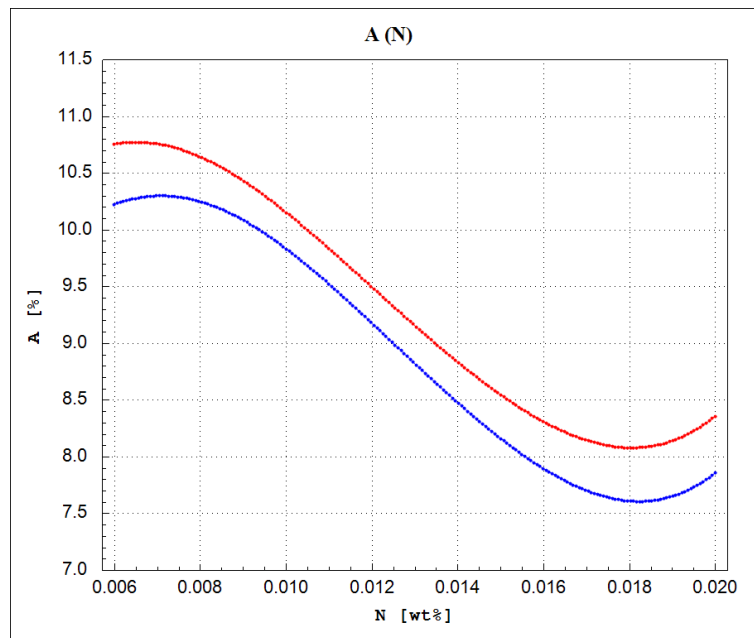


**Figure 41:** Elongation as a function of the Nitrogen concentration (N), calculated by the ANN model on centered verification point (red line) and centered training point (blue line).

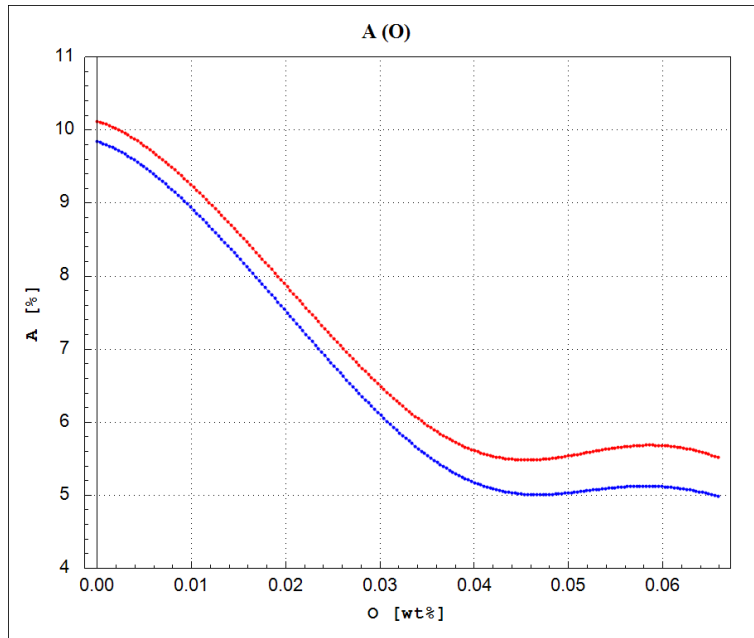


**Figure 42:** Elongation as a function of the Oxygen concentration (O), calculated by the ANN model on centered verification point (red line) and centered training point (blue line).

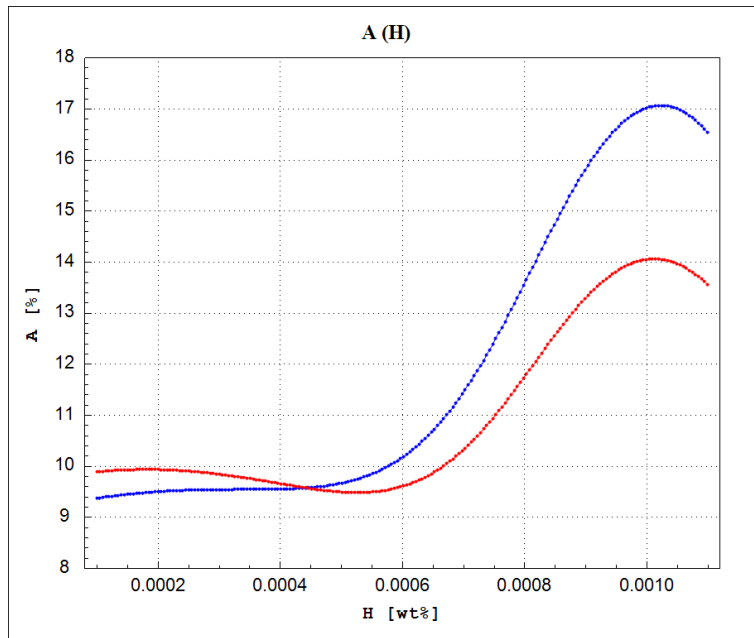


**Figure 43:** Elongation as a function of the Hydrogen concentration (H), calculated by the ANN model on centered verification point (red line) and centered training point (blue line).

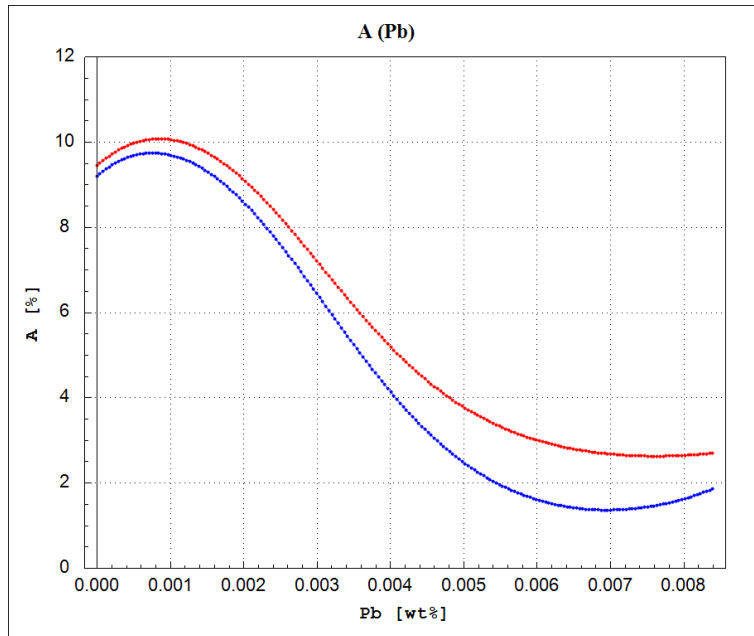


**Figure 44:** Elongation as a function of the Lead concentration (Pb), calculated by the ANN model on centered verification point (red line) and centered training point (blue line).

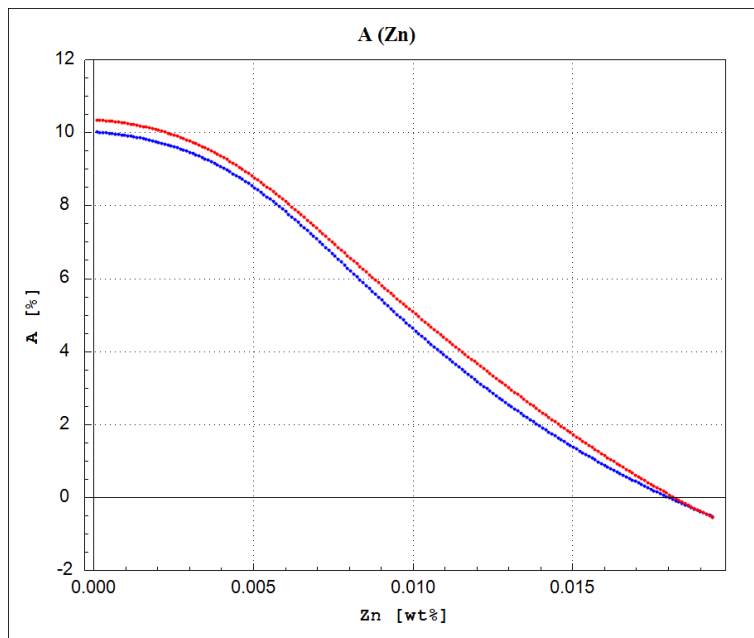


**Figure 45:** Elongation as a function of the Zinc concentration (Zn), calculated by the ANN model on centered verification point (red line) and centered training point (blue line).

### 5.1.2 Tensile Strength ( $R_m$ )

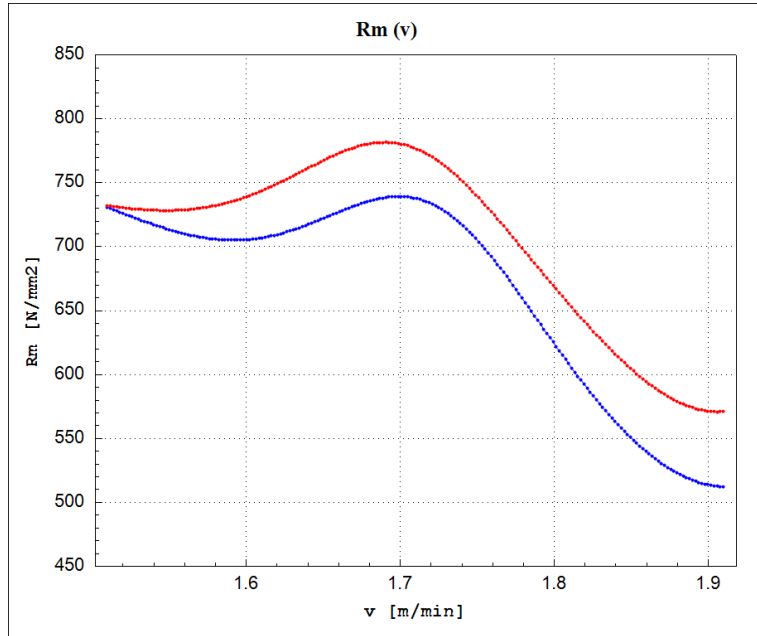


**Figure 46:** Tensile strength as a function of the continuous casting speed, calculated by the ANN model on centered verification point (red line) and centered training point (blue line).

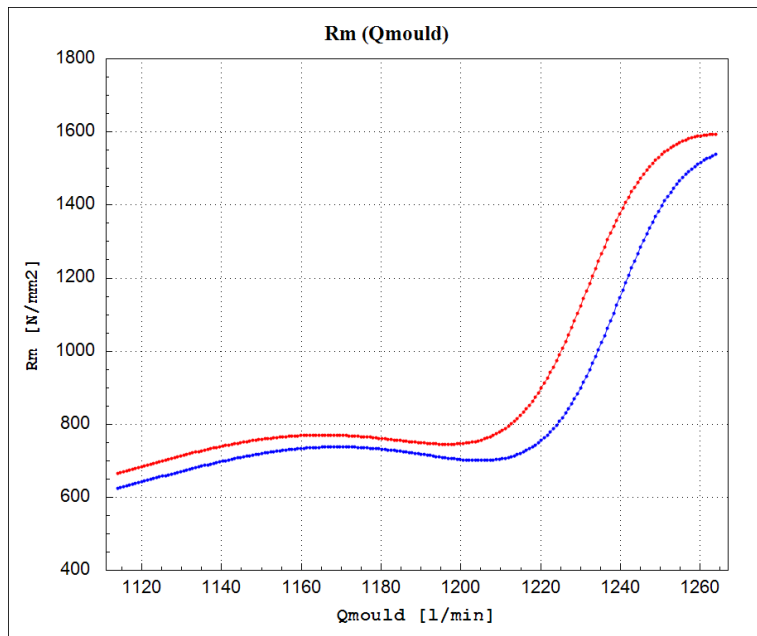


**Figure 47:** Tensile strength as a function of the cooling flow rate in the mould, calculated by the ANN model on centered verification point (red line) and centered training point (blue line).

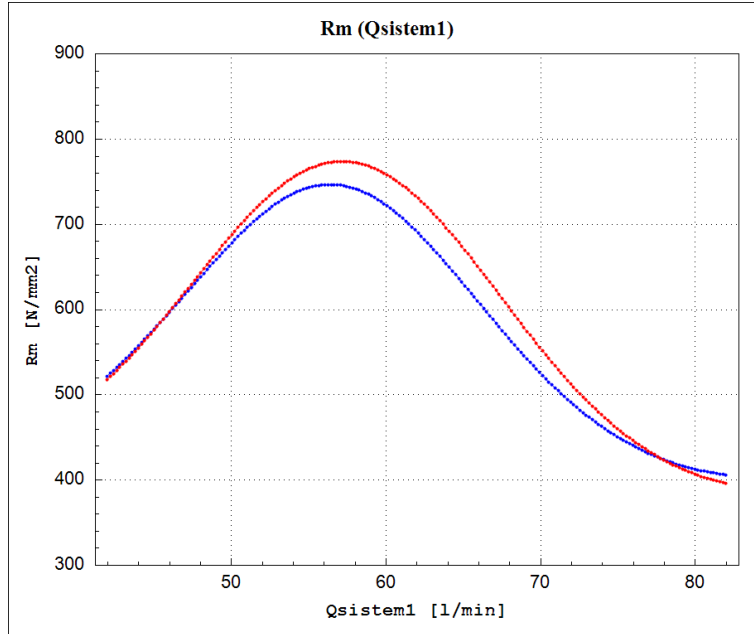


**Figure 48:** Tensile strength as a function of the cooling flow rate in 1<sup>st</sup> spray system, calculated by the ANN model on centered verification point (red line) and centered training point (blue line).

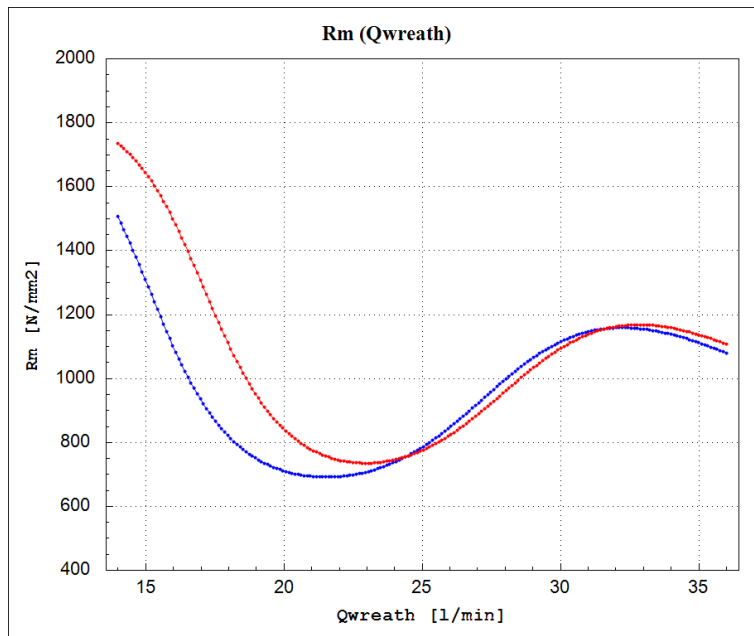


**Figure 49:** Tensile strength as a function of the cooling flow rate in wreath spray system, calculated by the ANN model on centered verification point (red line) and centered training point (blue line).

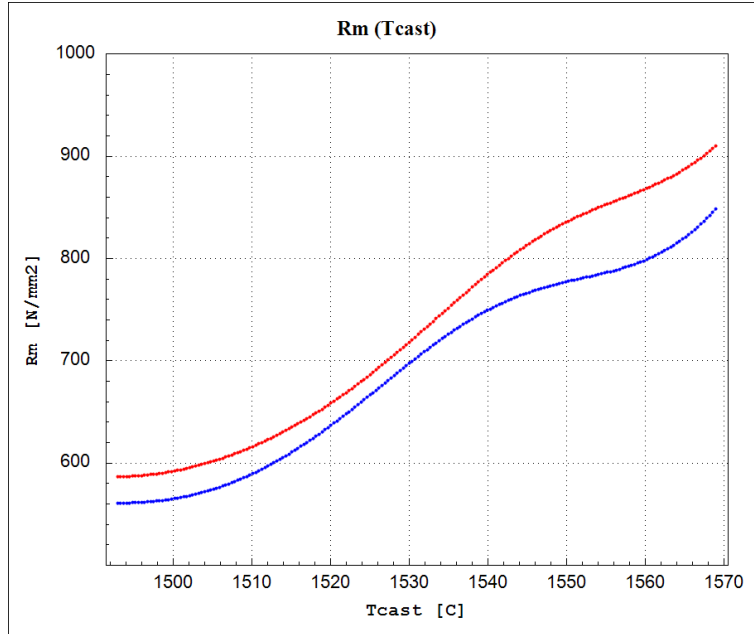


**Figure 50:** Tensile strength as a function of the casting temperature, calculated by the ANN model on centered verification point (red line) and centered training point (blue line).

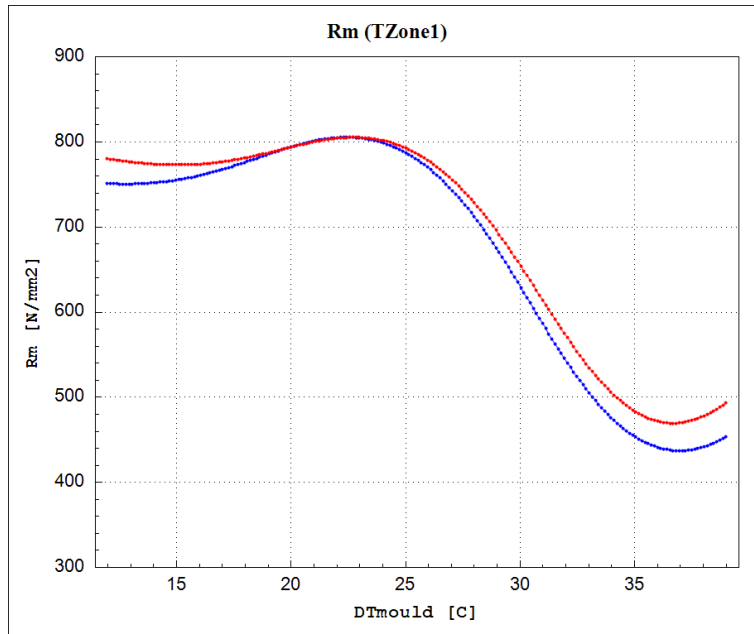


**Figure 51:** Tensile strength as a function of the water temperature in Zone 1, calculated by the ANN model on centered verification point (red line) and centered training point (blue line).

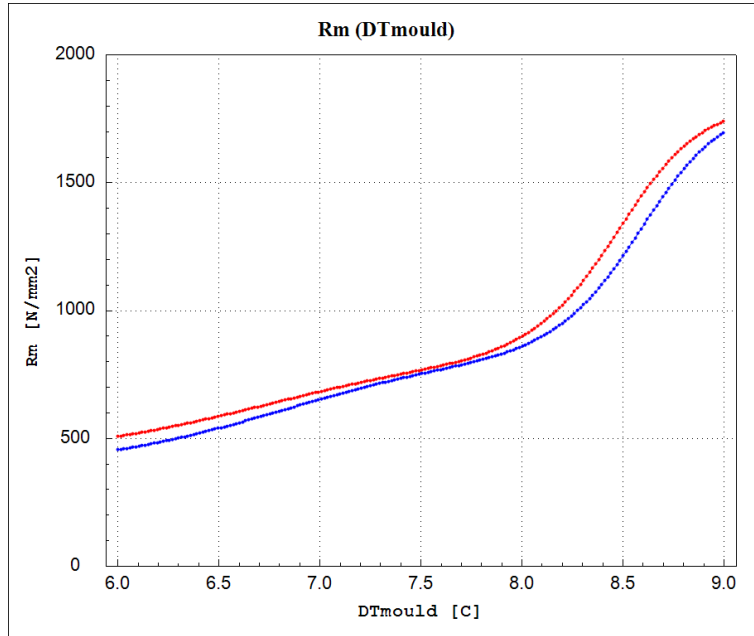


**Figure 52:** Tensile strength as a function of the delta T, calculated by the ANN model on centered verification point (red line) and centered training point (blue line).

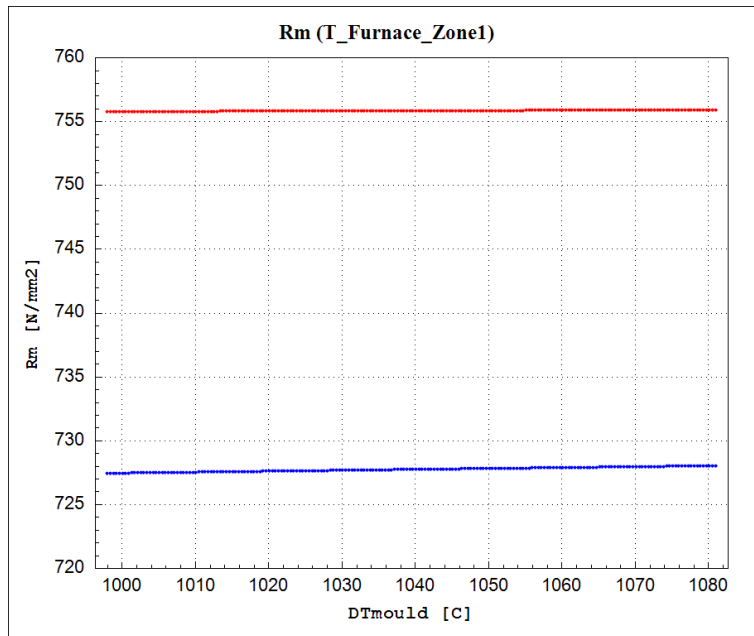


**Figure 53:** Tensile strength as a function of the average on temperature in zone 1, calculated by the ANN model on centered verification point (red line) and centered training point (blue line).

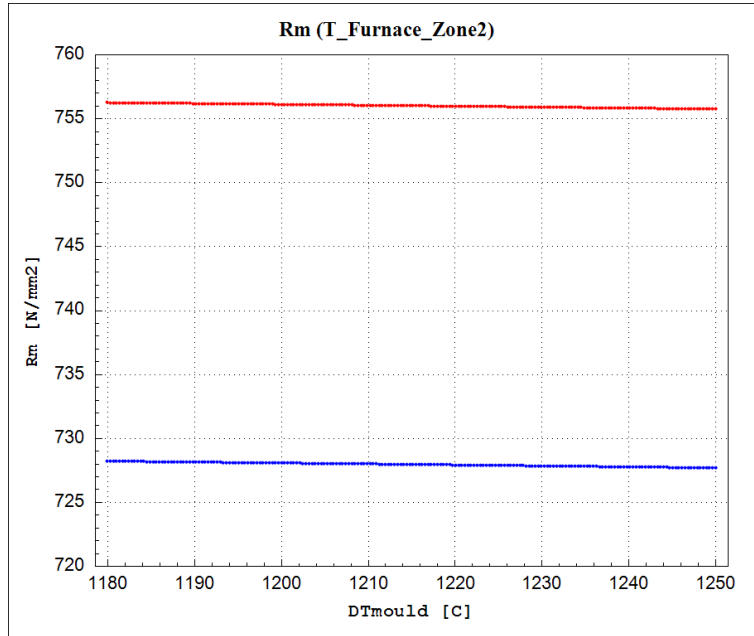


**Figure 54:** Tensile strength as a function of the average on temperature in zone 2, calculated by the ANN model on centered verification point (red line) and centered training point (blue line).

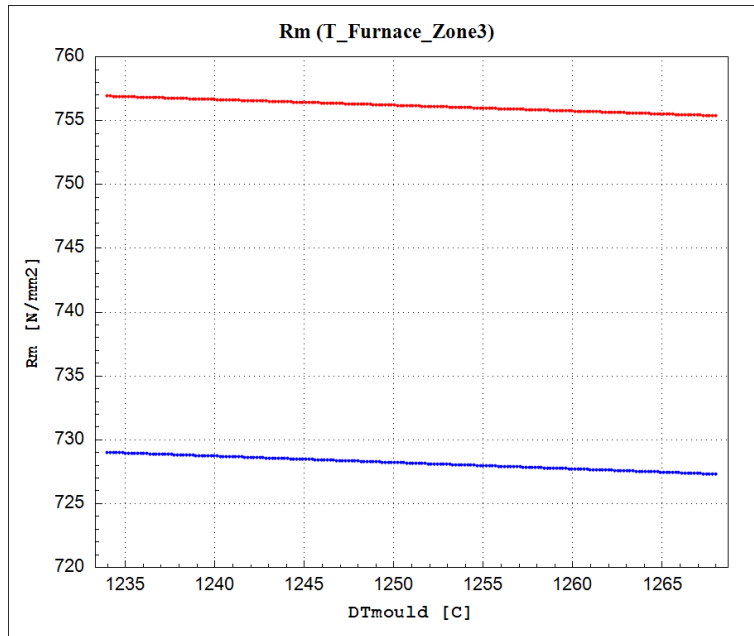


**Figure 55:** Tensile strength as a function of the average on temperature in zone 3, calculated by the ANN model on centered verification point (red line) and centered training point (blue line).

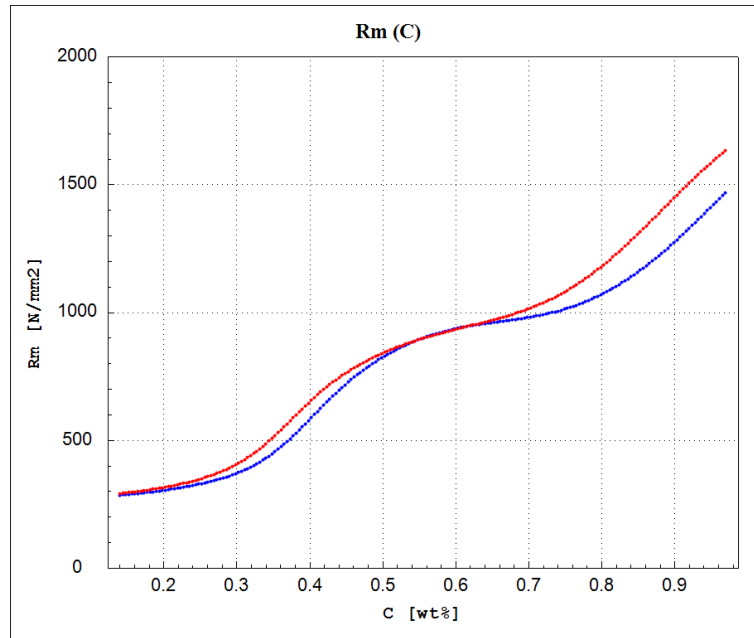


**Figure 56:** Tensile strength as a function of the Carbon concentration (C), calculated by the ANN model on centered verification point (red line) and centered training point (blue line).

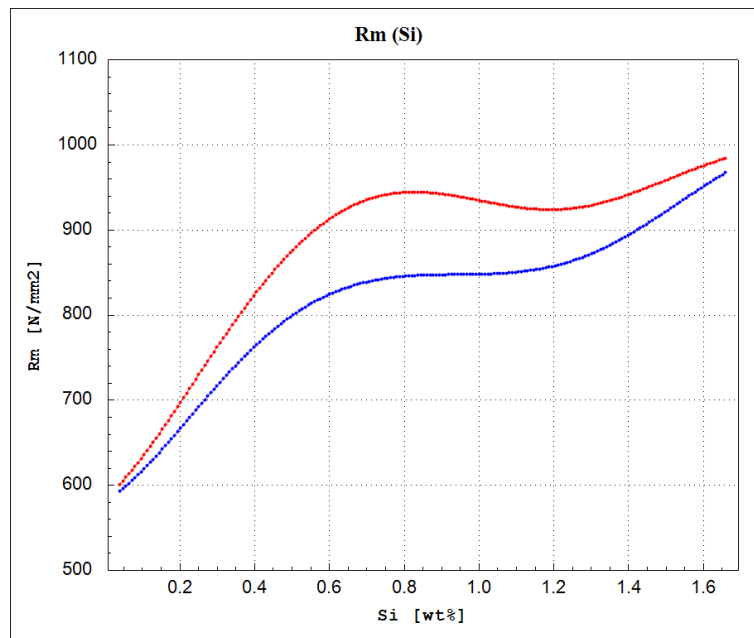


**Figure 57:** Tensile strength as a function of the Silicon concentration (Si), calculated by the ANN model on centered verification point (red line) and centered training point (blue line).

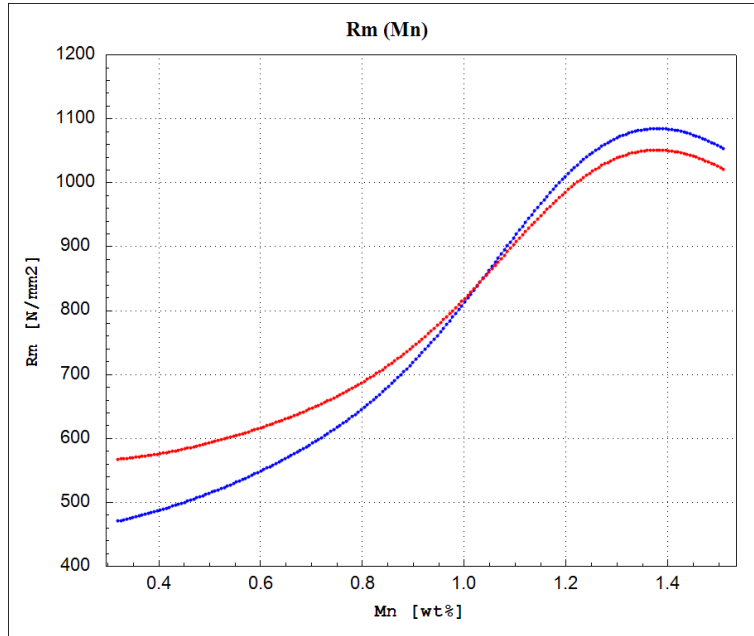


**Figure 58:** Tensile strength as a function of the Manganese concentration (Mn), calculated by the ANN model on centered verification point (red line) and centered training point (blue line).

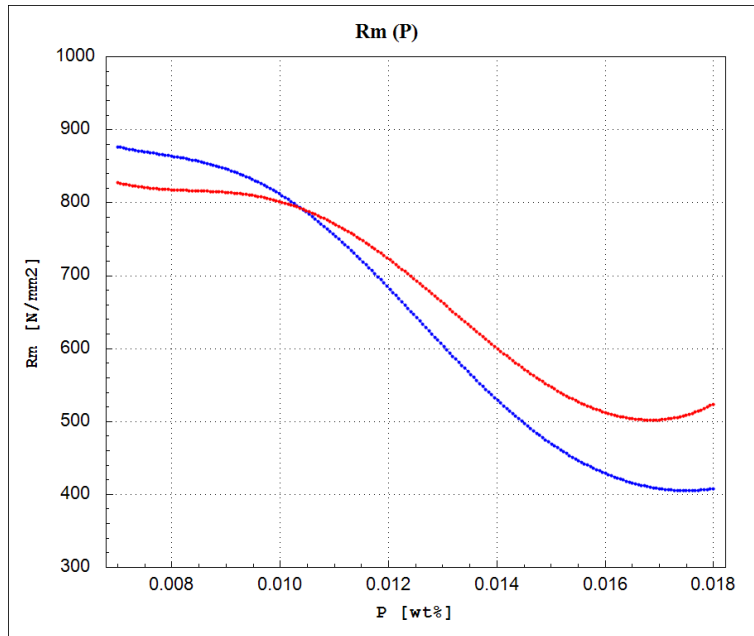


**Figure 59:** Tensile strength as a function of the Phosphorus concentration (P), calculated by the ANN model on centered verification point (red line) and centered training point (blue line).

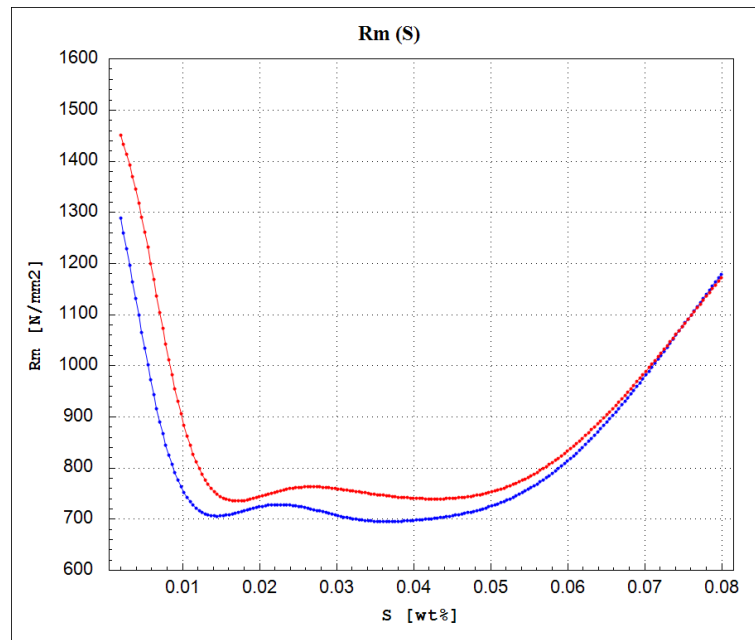


**Figure 60:** Tensile strength as a function of the Sulphur concentration (S), calculated by the ANN model on centered verification point (red line) and centered training point (blue line).

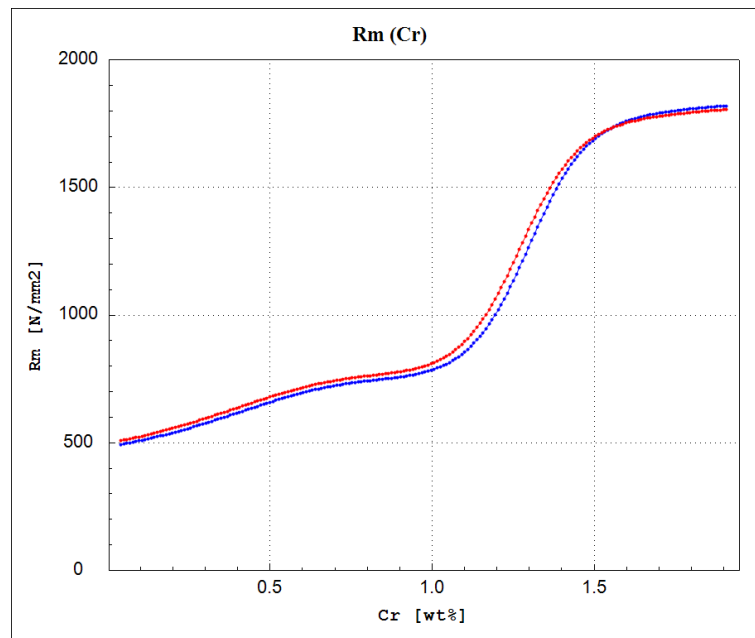


**Figure 61:** Tensile strength as a function of the Chromium concentration (Cr), calculated by the ANN model on centered verification point (red line) and centered training point (blue line).

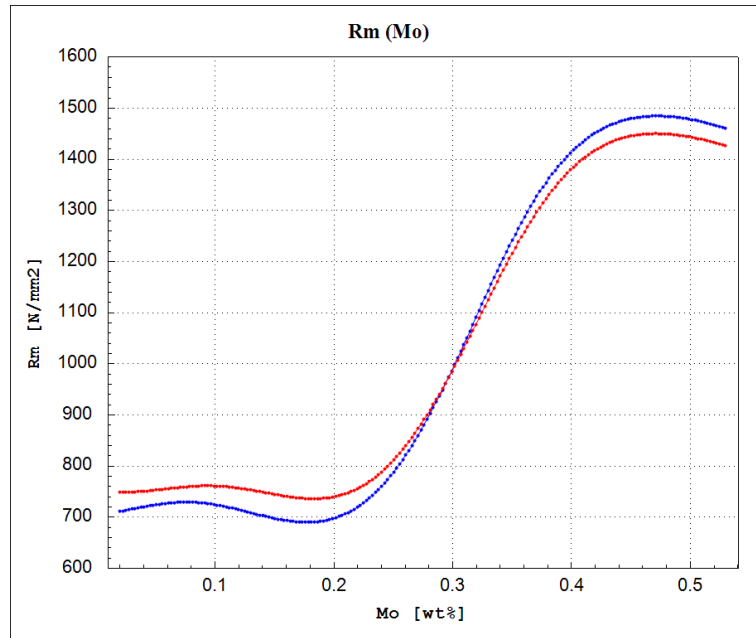


**Figure 62:** Tensile strength as a function of the Molybdenum concentration (Mo), calculated by the ANN model on centered verification point (red line) and centered training point (blue line).

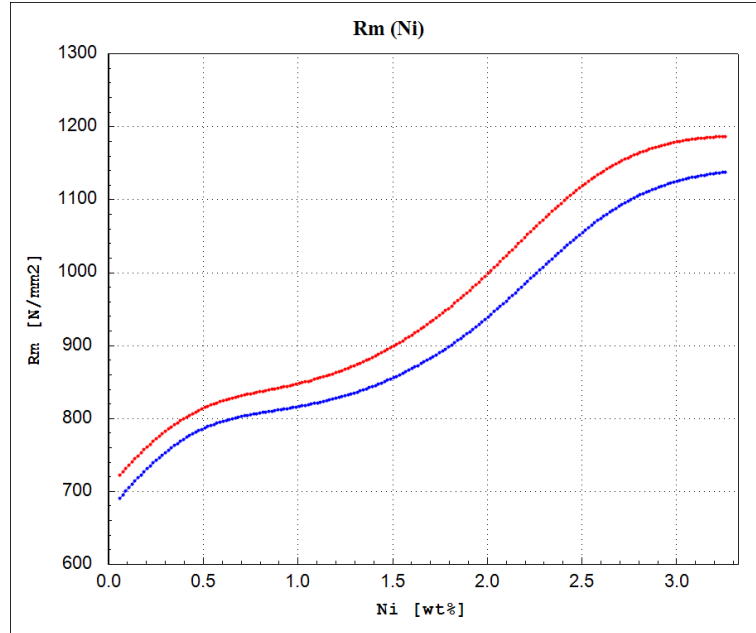


**Figure 63:** Tensile strength as a function of the Nickel concentration (Ni), calculated by the ANN model on centered verification point (red line) and centered training point (blue line).

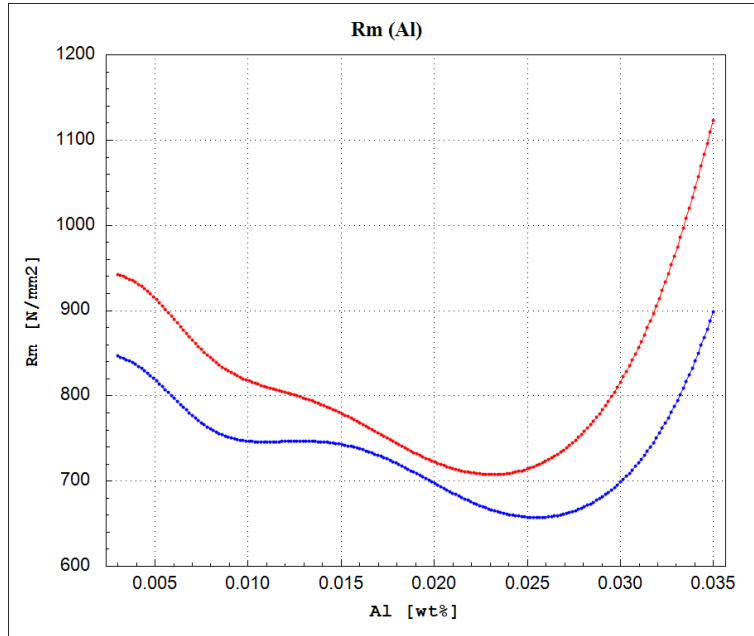


**Figure 64:** Tensile strength as a function of the Aluminium concentration (Al), calculated by the ANN model on centered verification point (red line) and centered training point (blue line).

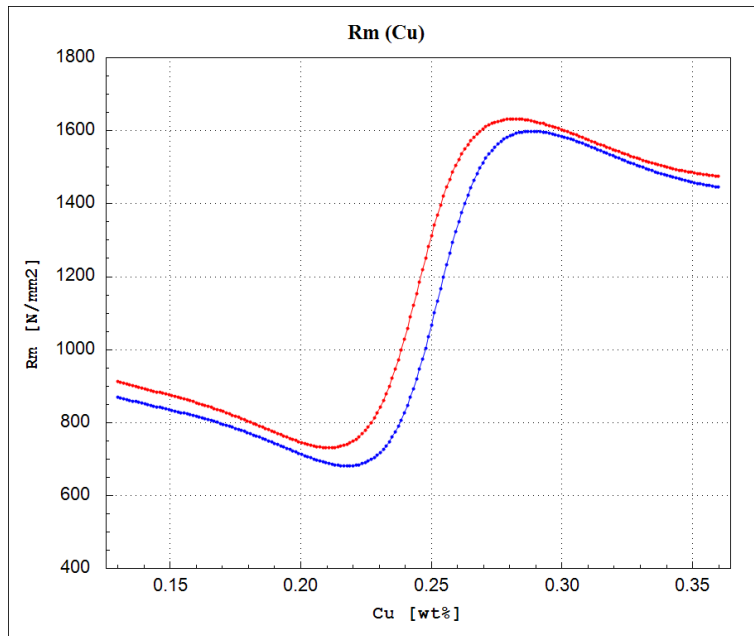


**Figure 65:** Tensile strength as a function of the Copper concentration (Cu), calculated by the ANN model on centered verification point (red line) and centered training point (blue line).

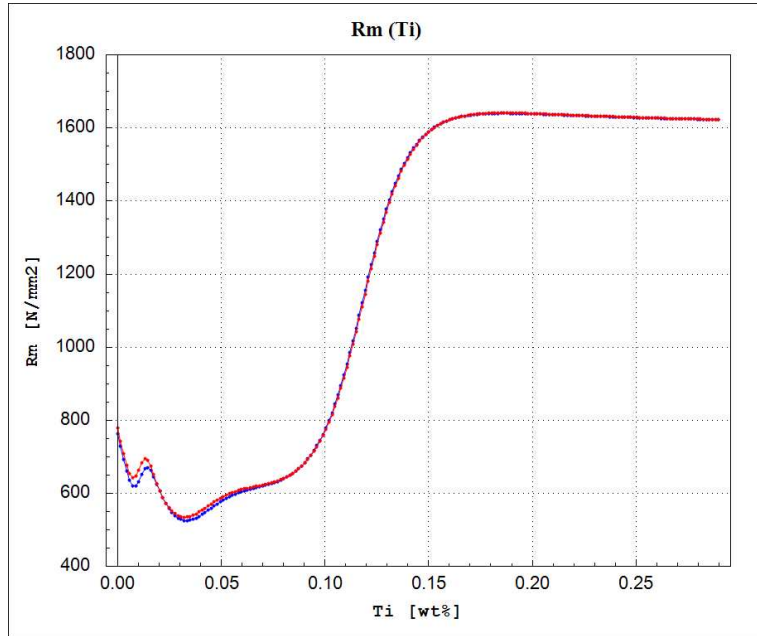


**Figure 66:** Tensile strength as a function of the Titanium concentration (Ti), calculated by the ANN model on centered verification point (red line) and centered training point (blue line).

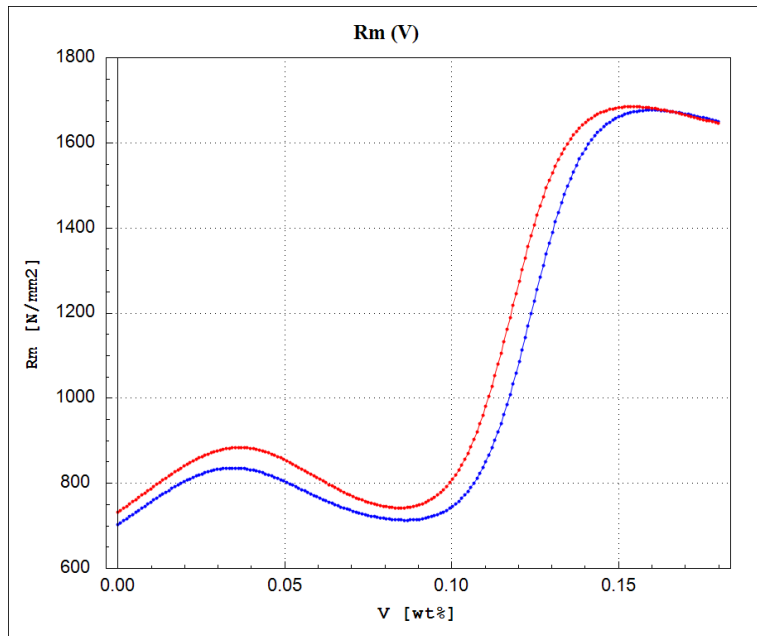


**Figure 67:** Tensile strength as a function of the Vanadium concentration (V), calculated by the ANN model on centered verification point (red line) and centered training point (blue line).

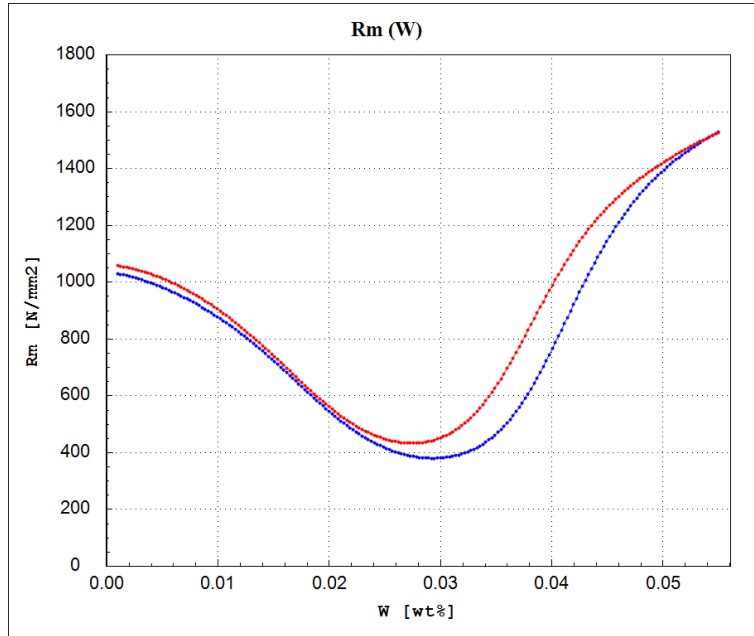


**Figure 68:** Tensile strength as a function of the Tungsten concentration (W), calculated by the ANN model on centered verification point (red line) and centered training point (blue line).

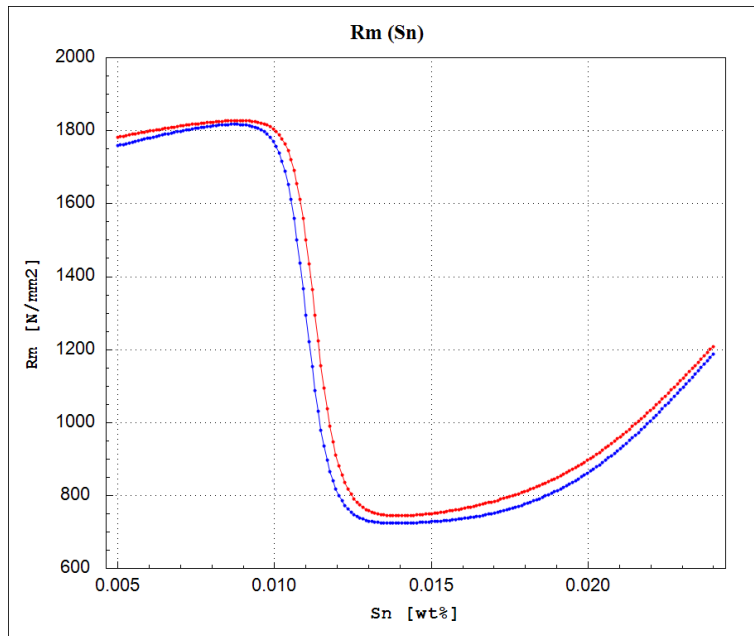


**Figure 69:** Tensile strength as a function of the Tin concentration (Sn), calculated by the ANN model on centered verification point (red line) and centered training point (blue line).

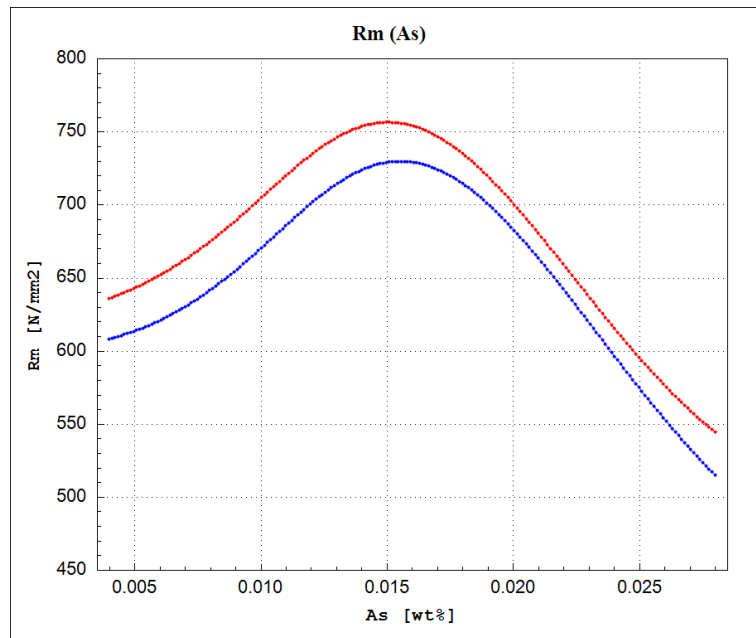


**Figure 70:** Tensile strength as a function of the Arsenic concentration (As), calculated by the ANN model on centered verification point (red line) and centered training point (blue line).

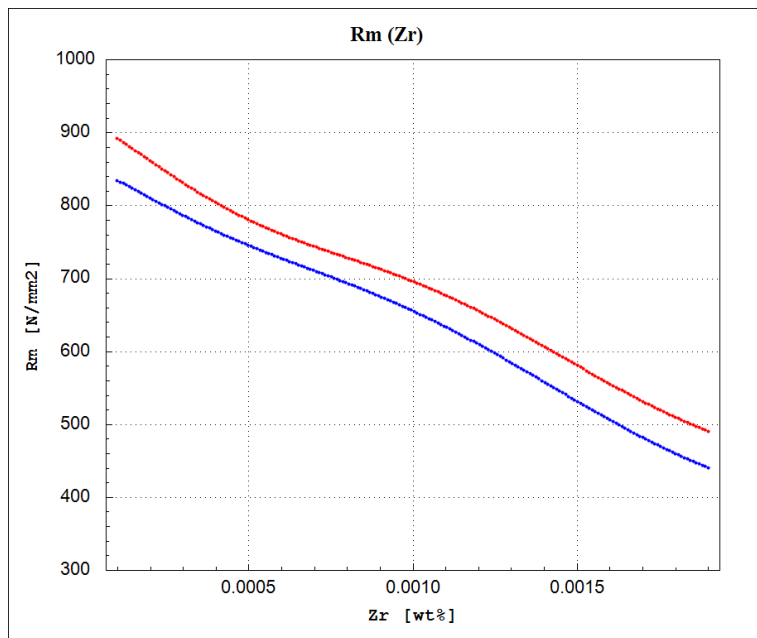


**Figure 71:** Tensile strength as a function of the Zirconium concentration (Zr), calculated by the ANN model on centered verification point (red line) and centered training point (blue line).

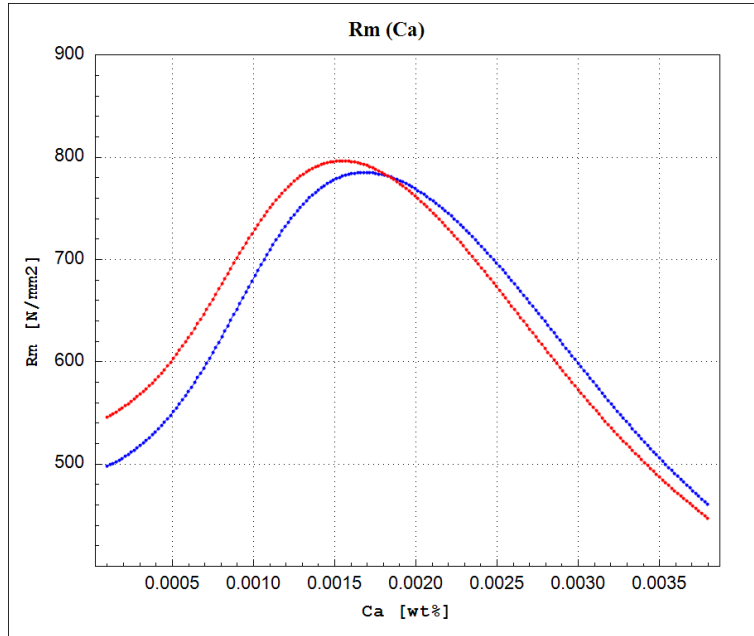


**Figure 72:** Tensile strength as a function of the Calcium concentration (Ca), calculated by the ANN model on centered verification point (red line) and centered training point (blue line).

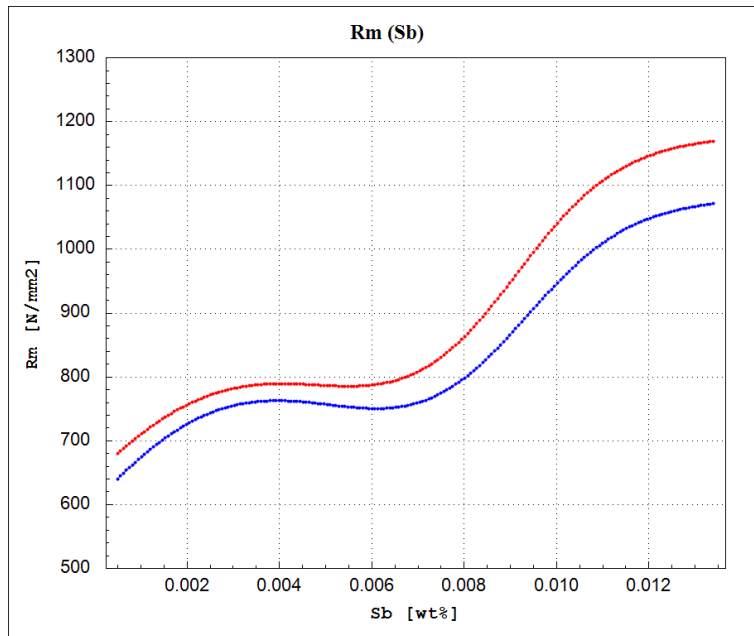


**Figure 73:** Tensile strength as a function of the Antimony concentration (Sb), calculated by the ANN model on centered verification point (red line) and centered training point (blue line).

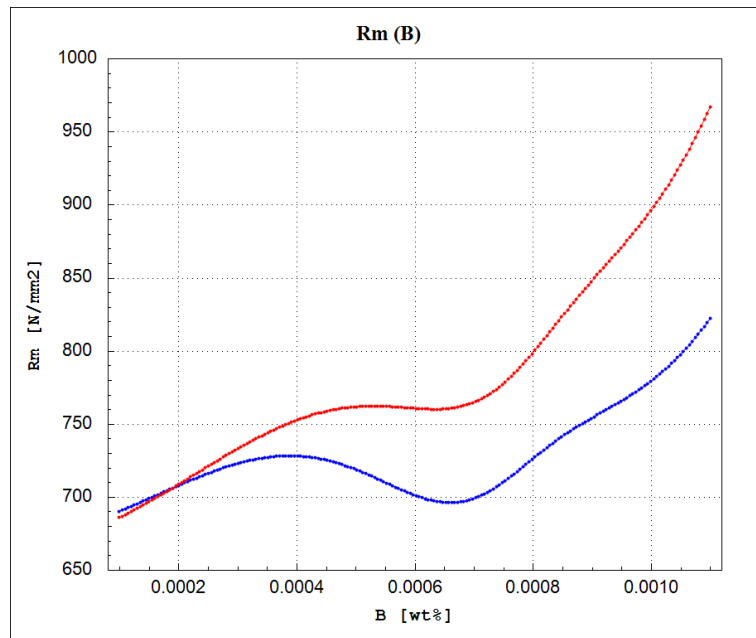


**Figure 74:** Tensile strength as a function of the Boron concentration (B), calculated by the ANN model on centered verification point (red line) and centered training point (blue line).

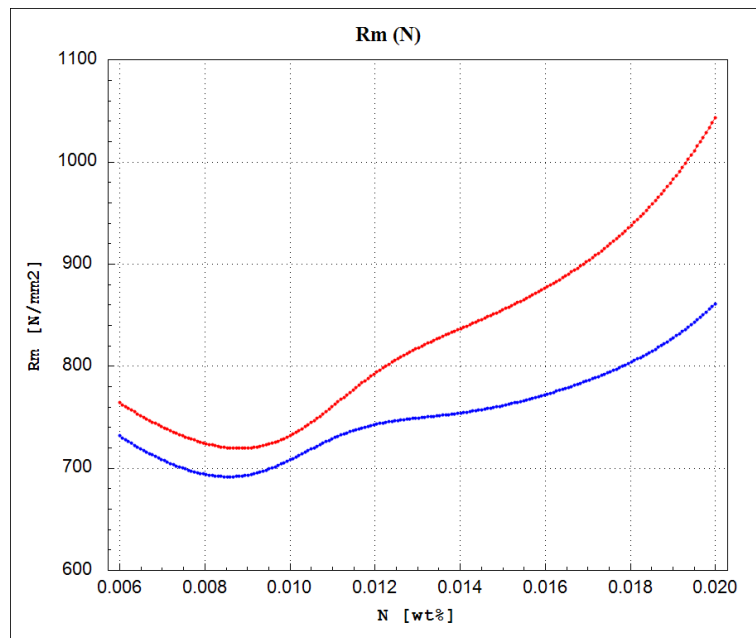


**Figure 75:** Tensile strength as a function of the Nitrogen concentration (N), calculated by the ANN model on centered verification point (red line) and centered training point (blue line).

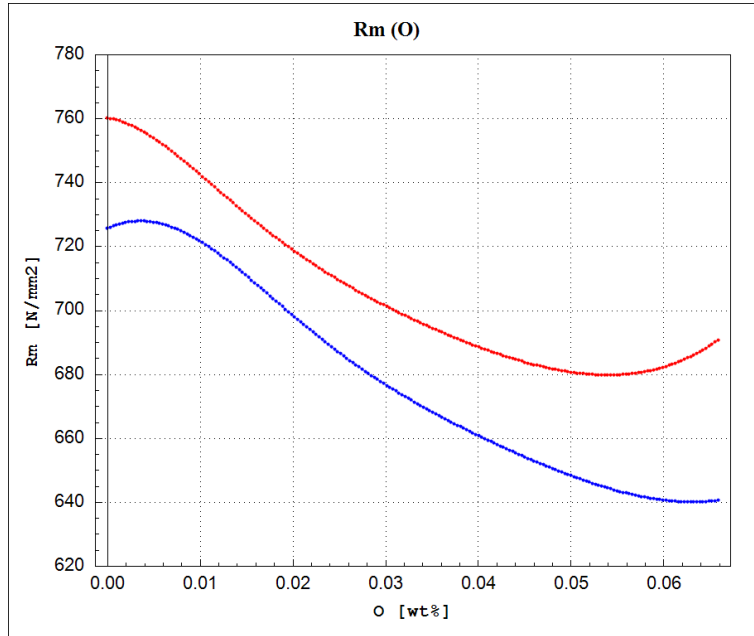


**Figure 76:** Tensile strength as a function of the Oxygen concentration (O), calculated by the ANN model on centered verification point (red line) and centered training point (blue line).

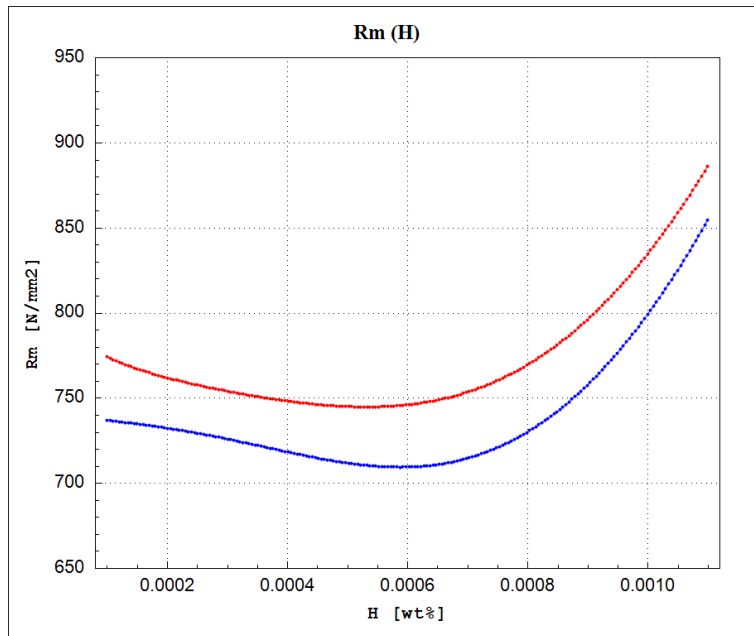


**Figure 77:** Tensile strength as a function of the Hydrogen concentration (H), calculated by the ANN model on centered verification point (red line) and centered training point (blue line).

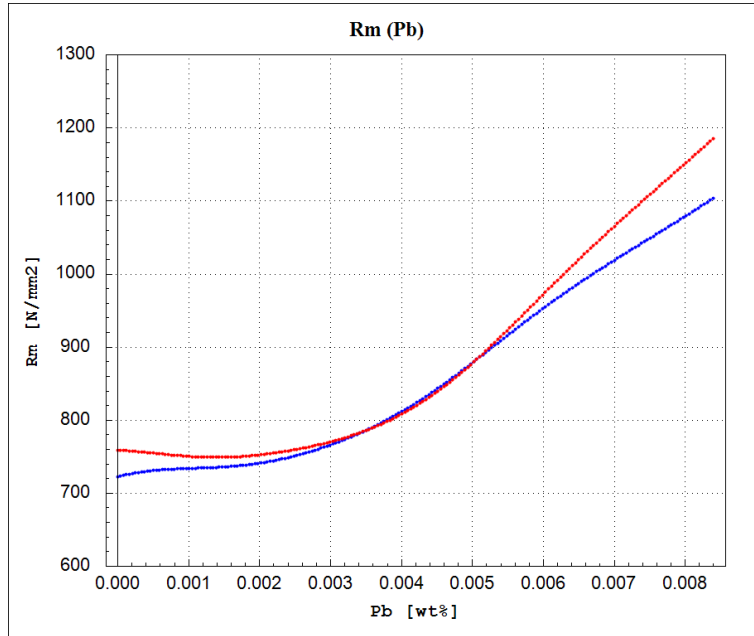


**Figure 78:** Tensile strength as a function of the Lead concentration (Pb), calculated by the ANN model on centered verification point (red line) and centered training point (blue line).

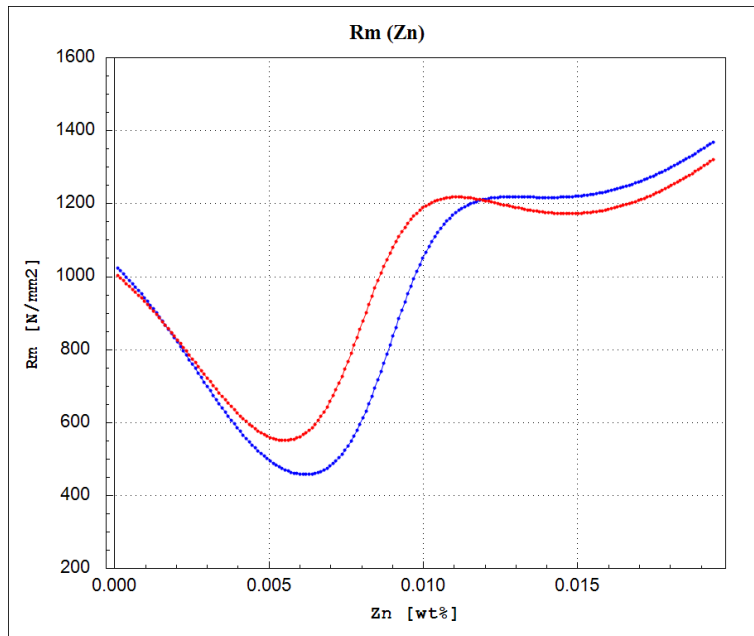


**Figure 79:** Tensile strength as a function of the Zinc concentration (Zn), calculated by the ANN model on centered verification point (red line) and centered training point (blue line).

### 5.1.3 Yield Stress ( $R_p$ )

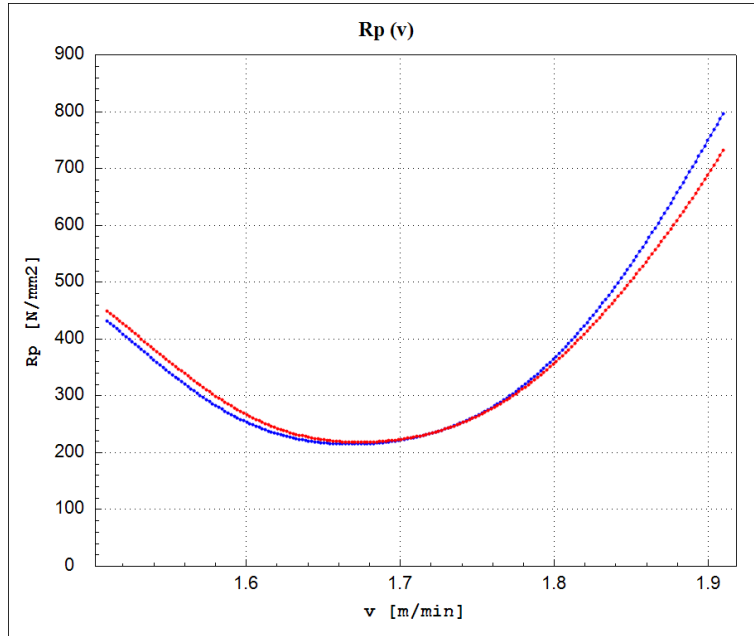


**Figure 80:** Yield stress as a function of the continuous casting speed, calculated by the ANN model on centered verification point (red line) and centered training point (blue line).

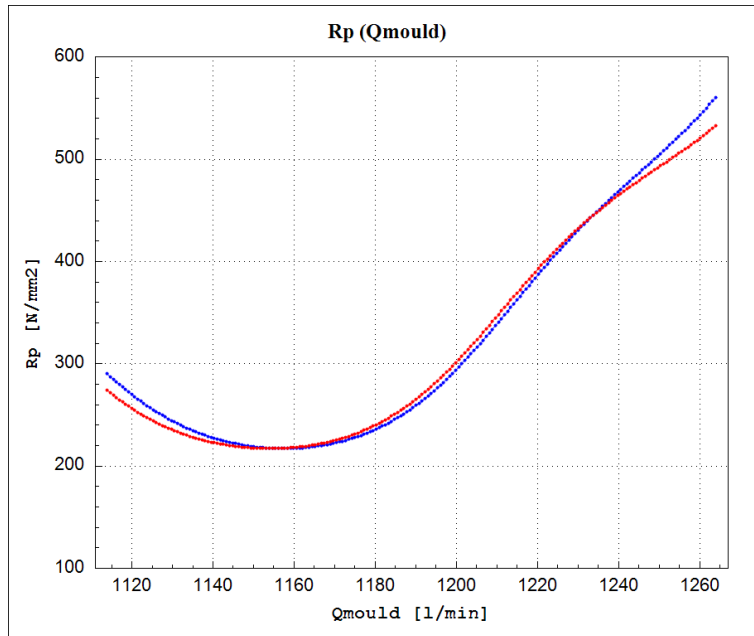


**Figure 81:** Yield stress as a function of the cooling flow rate in the mould, calculated by the ANN model on centered verification point (red line) and centered training point (blue line).

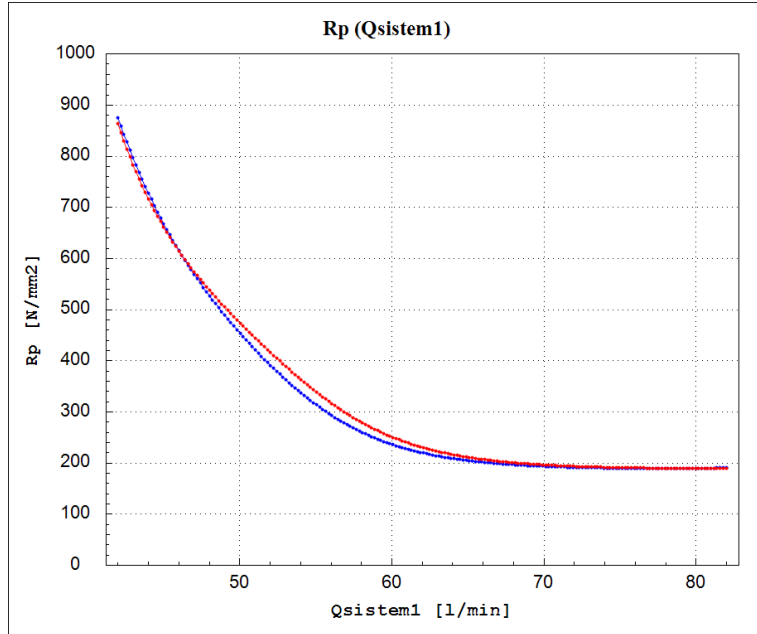


**Figure 82:** Yield stress as a function of the cooling flow rate in 1<sup>st</sup> spray system, calculated by the ANN model on centered verification point (red line) and centered training point (blue line).

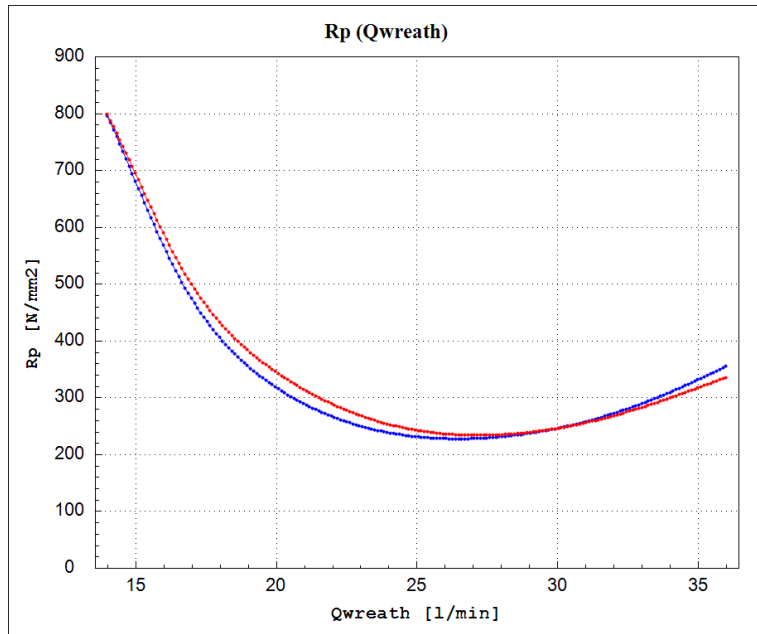


**Figure 83:** Yield stress as a function of the cooling flow rate in wreath spray system, calculated by the ANN model on centered verification point (red line) and centered training point (blue line).

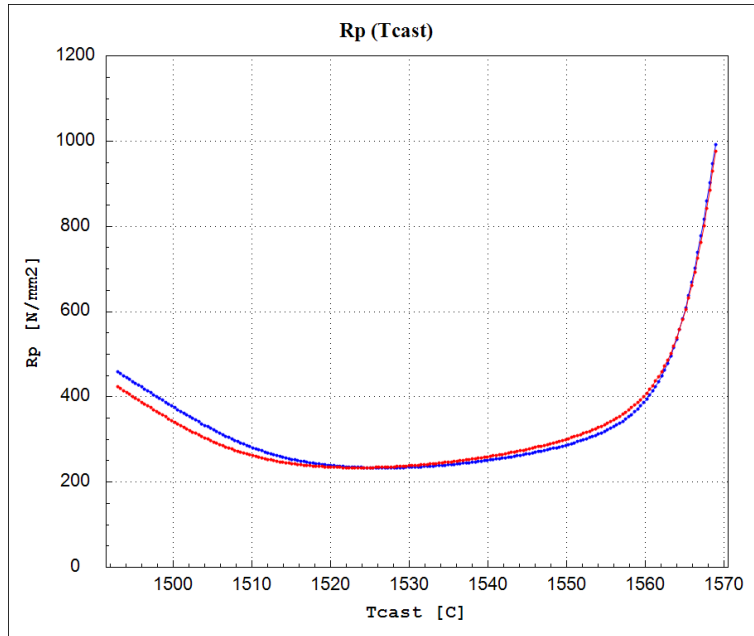


**Figure 84:** Yield stress as a function of the casting temperature, calculated by the ANN model on centered verification point (red line) and centered training point (blue line).

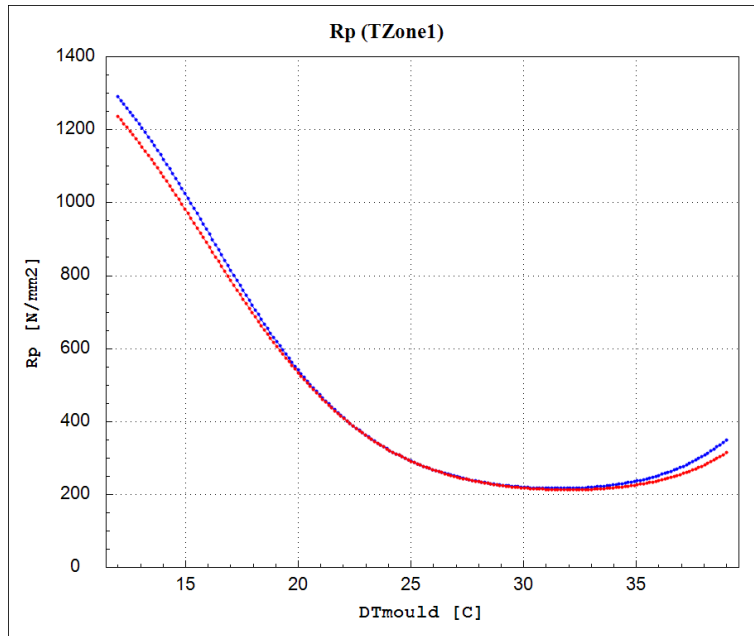


**Figure 85:** Yield stress as a function of the water temperature in Zone 1, calculated by the ANN model on centered verification point (red line) and centered training point (blue line).

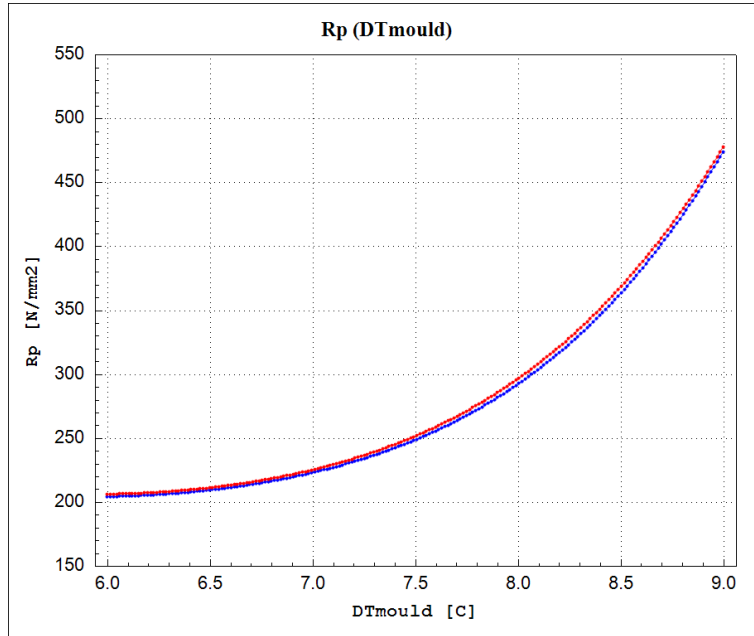


**Figure 86:** Yield stress as a function of the delta  $T$ , calculated by the ANN model on centered verification point (red line) and centered training point (blue line).

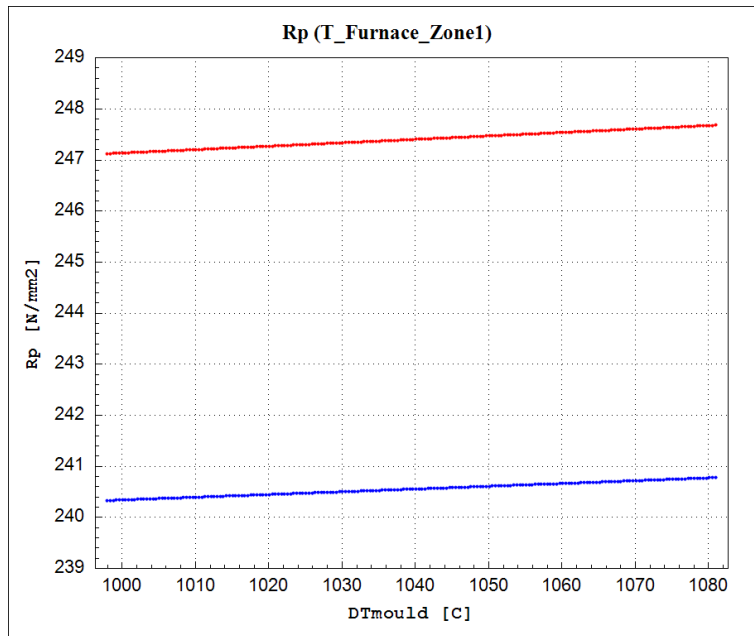


**Figure 87:** Yield stress as a function of the average on temperature in zone 1, calculated by the ANN model on centered verification point (red line) and centered training point (blue line).

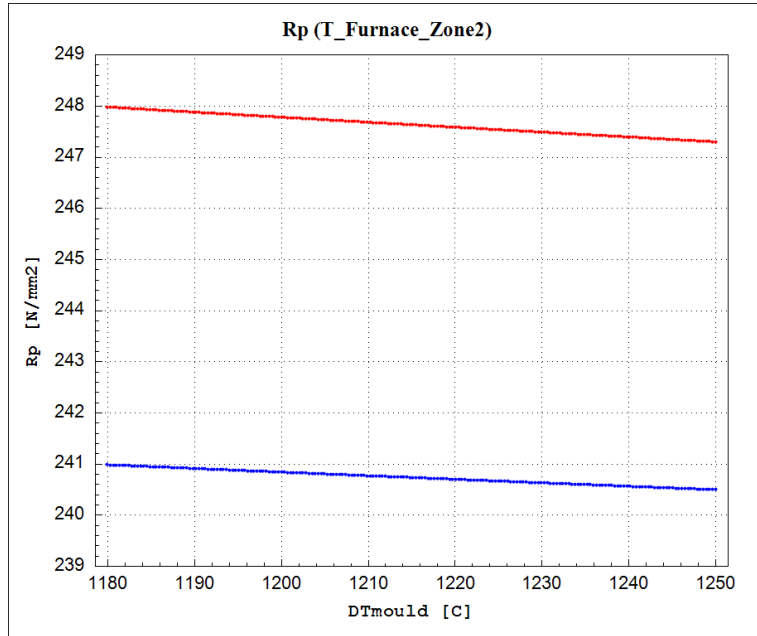


**Figure 88:** Yield stress as a function of the average on temperature in zone 2, calculated by the ANN model on centered verification point (red line) and centered training point (blue line).

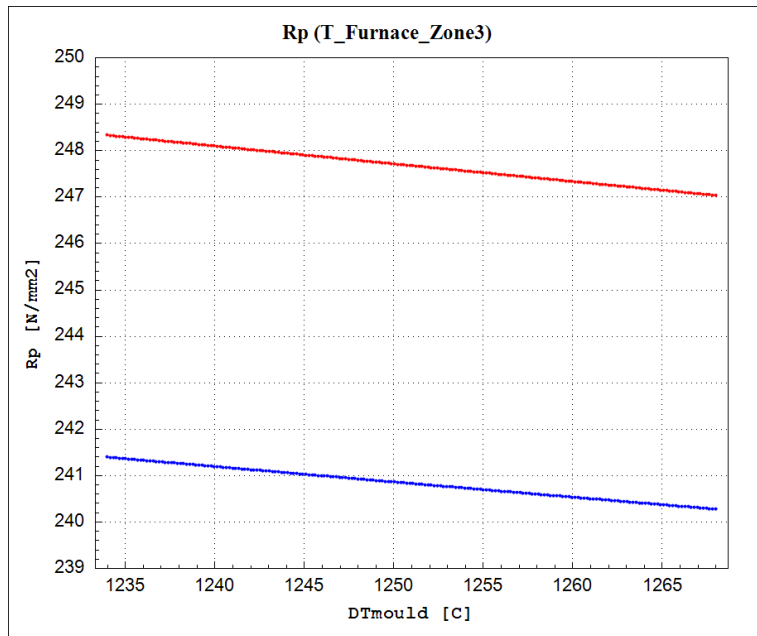


**Figure 89:** Yield stress as a function of the average on temperature in zone 3, calculated by the ANN model on centered verification point (red line) and centered training point (blue line).

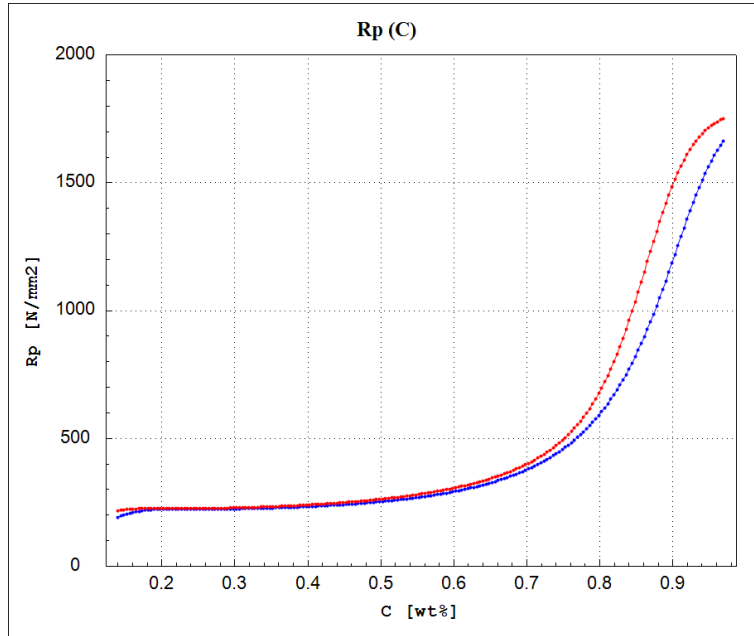


**Figure 90:** Yield stress as a function of the Carbon concentration (C), calculated by the ANN model on centered verification point (red line) and centered training point (blue line).

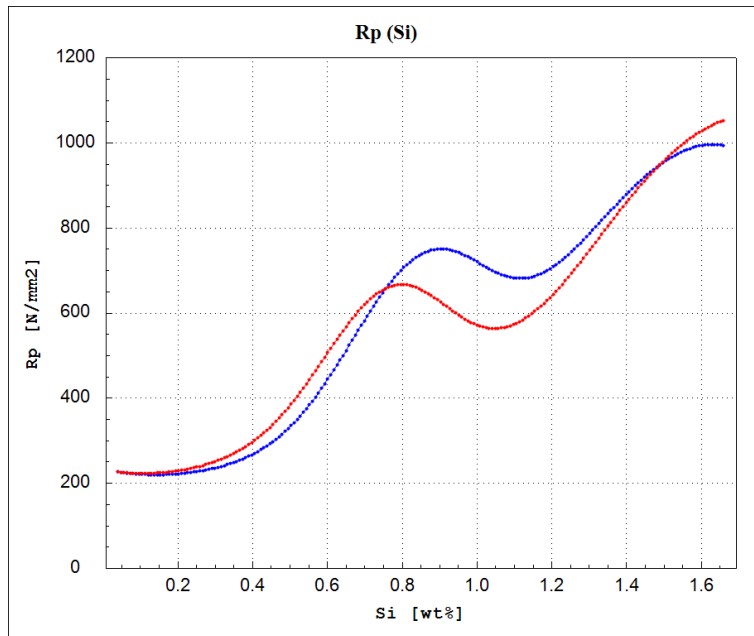


**Figure 91:** Yield stress as a function of the Silicon concentration (Si), calculated by the ANN model on centered verification point (red line) and centered training point (blue line).

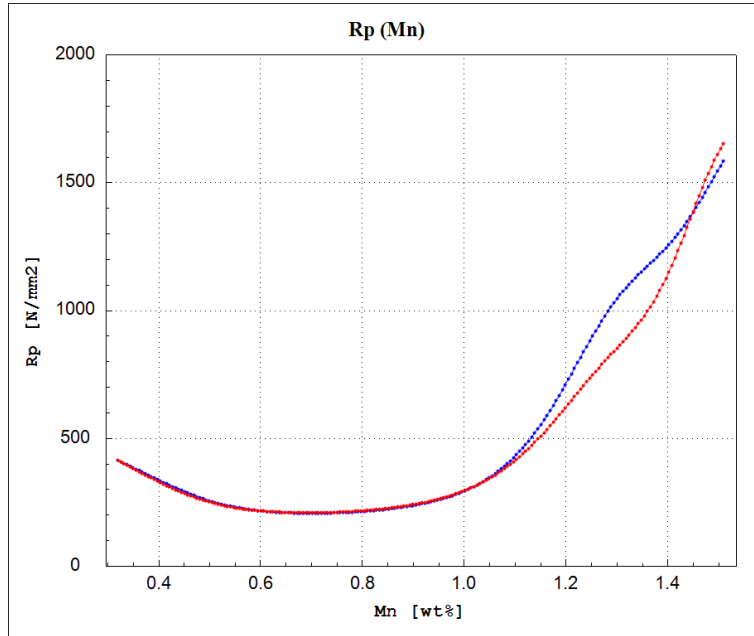


**Figure 92:** Yield stress as a function of the Manganese concentration (Mn), calculated by the ANN model on centered verification point (red line) and centered training point (blue line).

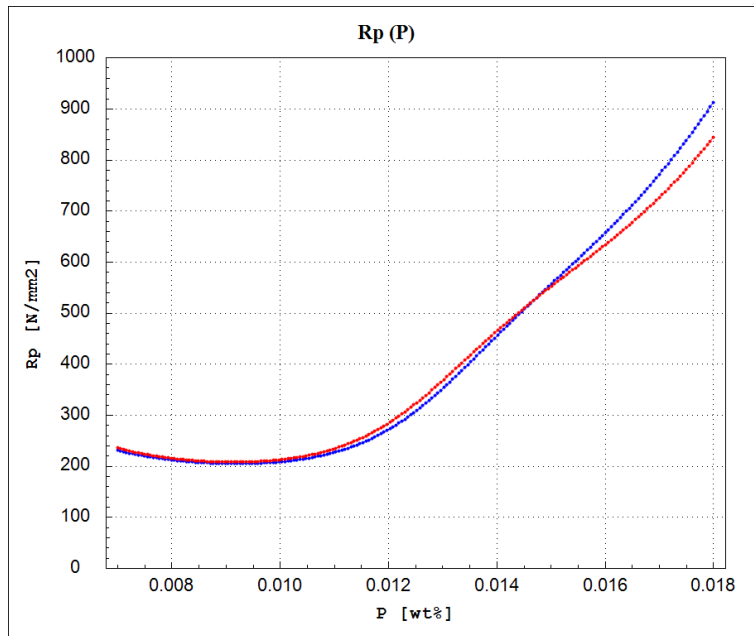


**Figure 93:** Yield stress as a function of the Phosphorus concentration (P), calculated by the ANN model on centered verification point (red line) and centered training point (blue line).

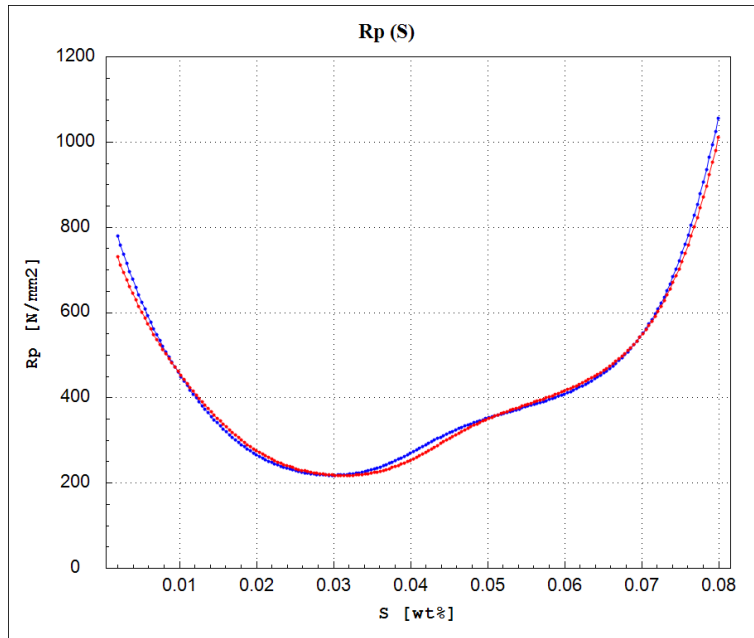


**Figure 94:** Yield stress as a function of the Sulphur concentration (S), calculated by the ANN model on centered verification point (red line) and centered training point (blue line).

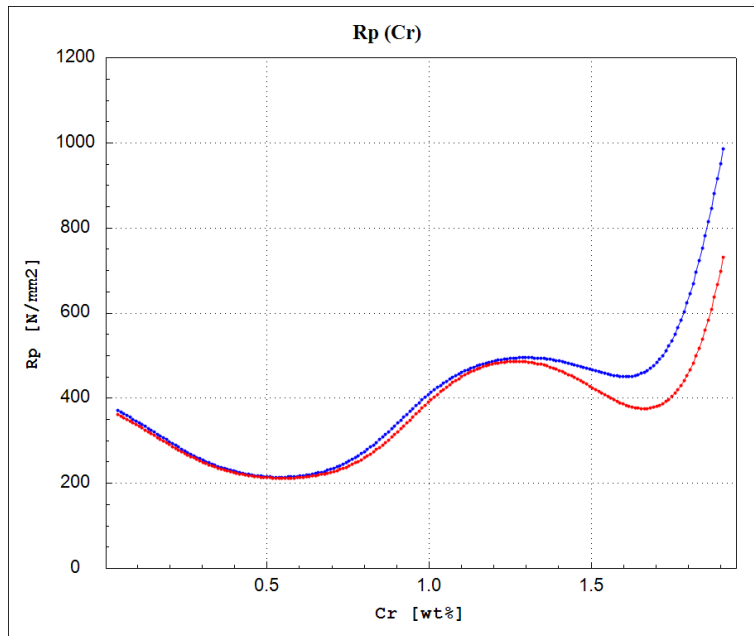


**Figure 95:** Yield stress as a function of the Chromium concentration (Cr), calculated by the ANN model on centered verification point (red line) and centered training point (blue line).

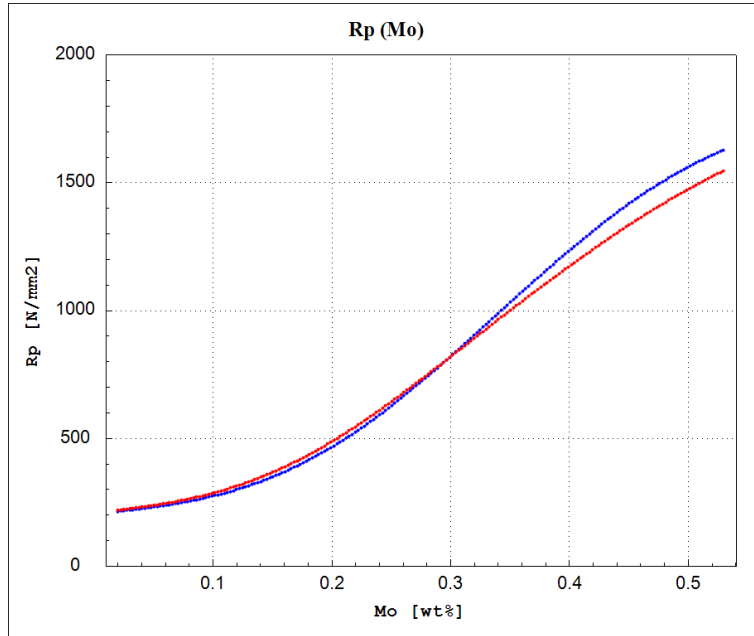


**Figure 96:** Yield stress as a function of the Molybdenum concentration (Mo), calculated by the ANN model on centered verification point (red line) and centered training point (blue line).

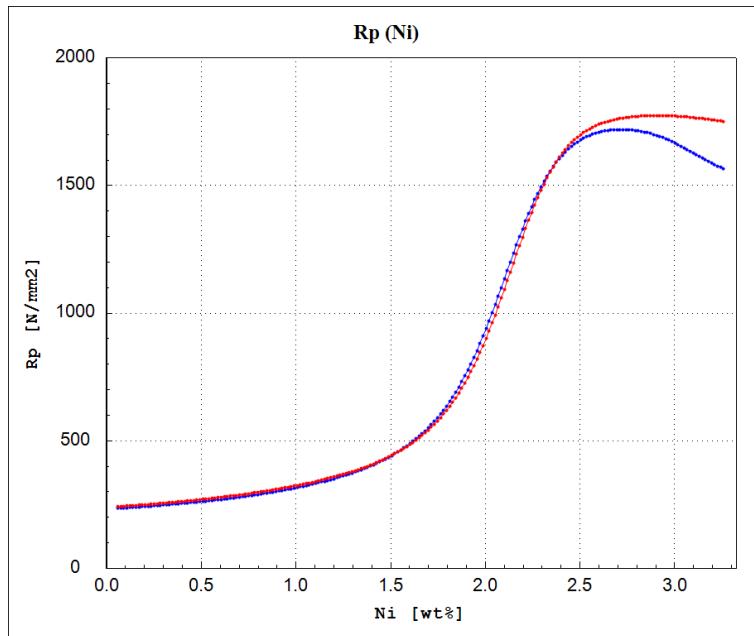


**Figure 97:** Yield stress as a function of the Nickel concentration (Ni), calculated by the ANN model on centered verification point (red line) and centered training point (blue line).

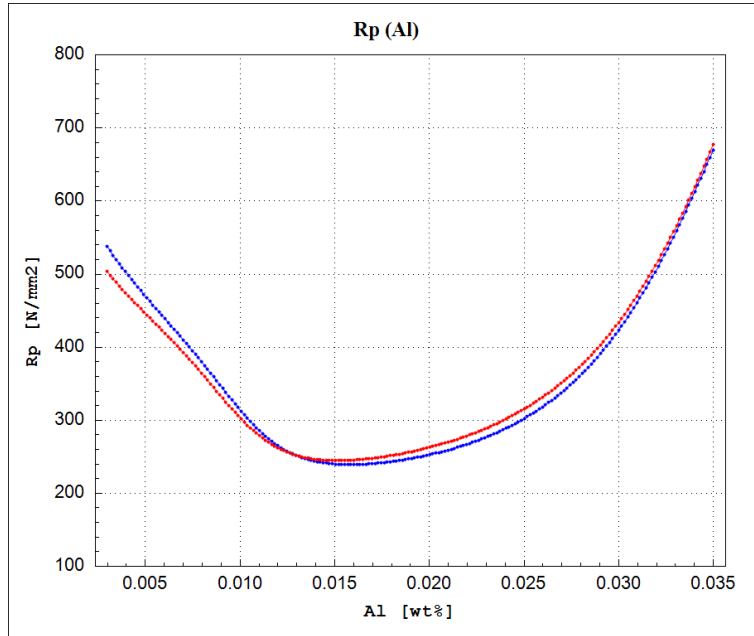


**Figure 98:** Yield stress as a function of the Aluminium concentration (Al), calculated by the ANN model on centered verification point (red line) and centered training point (blue line).

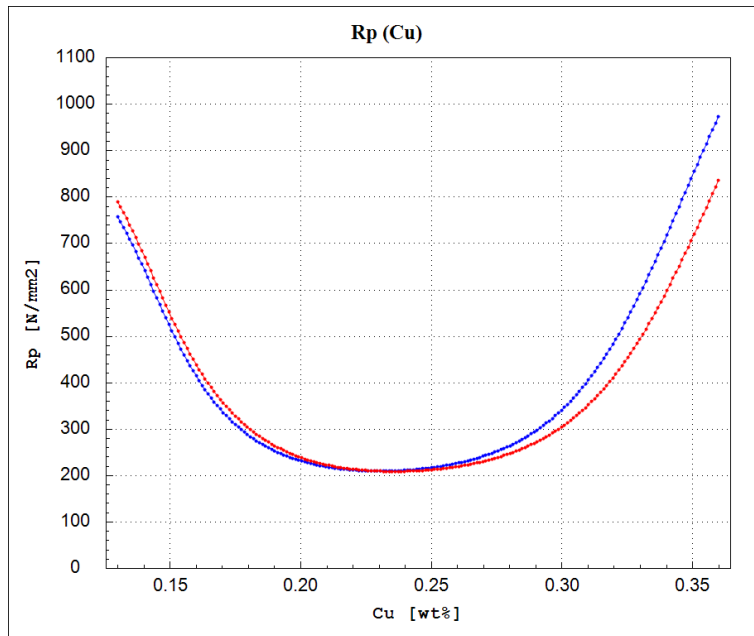


**Figure 99:** Yield stress as a function of the Copper concentration (Cu), calculated by the ANN model on centered verification point (red line) and centered training point (blue line).

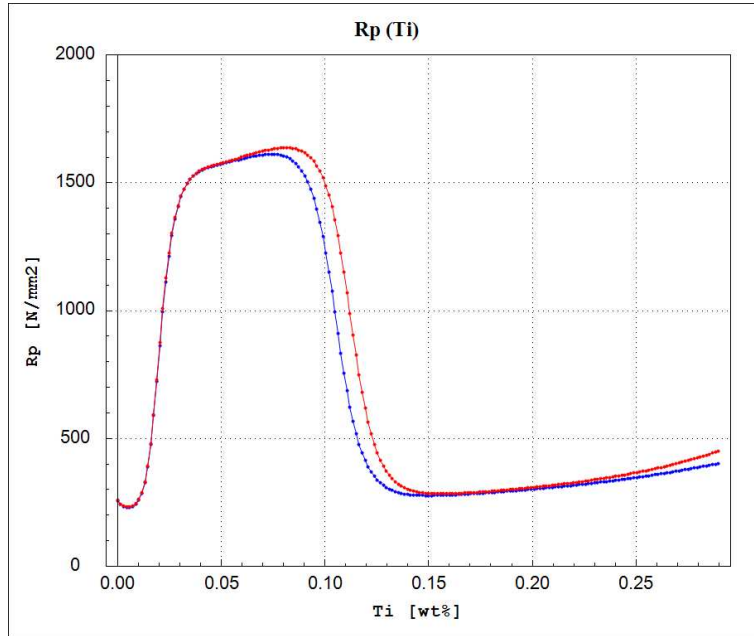


**Figure 100:** Yield stress as a function of the Titanium concentration (Ti), calculated by the ANN model on centered verification point (red line) and centered training point (blue line).

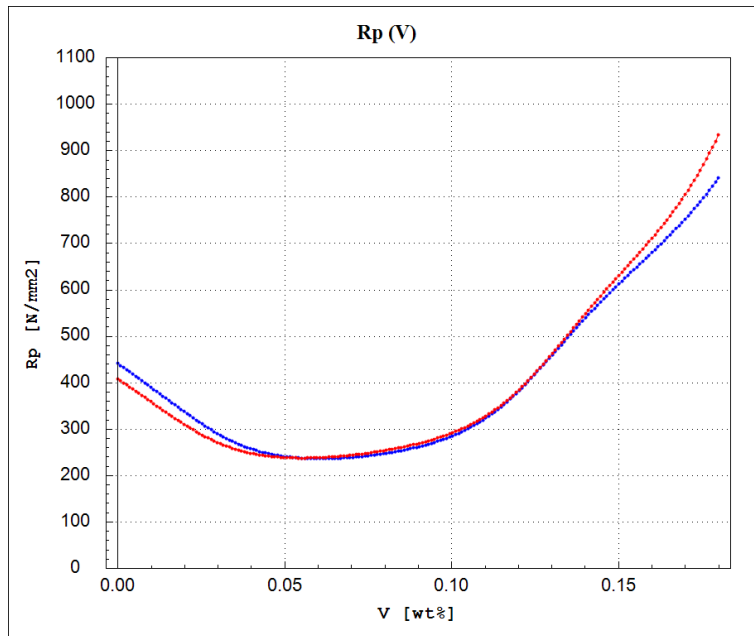


**Figure 101:** Yield stress as a function of the Vanadium concentration (V), calculated by the ANN model on centered verification point (red line) and centered training point (blue line).

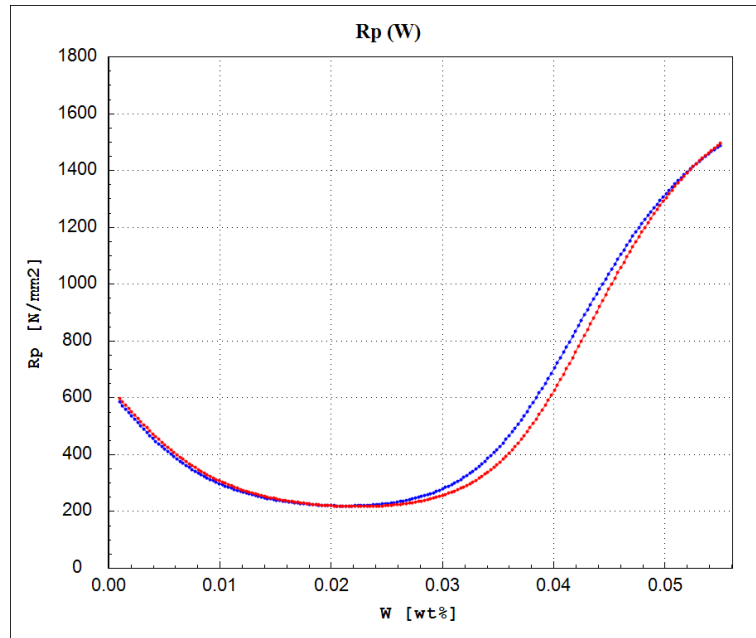


**Figure 102:** Yield stress as a function of the Tungsten concentration (W), calculated by the ANN model on centered verification point (red line) and centered training point (blue line).

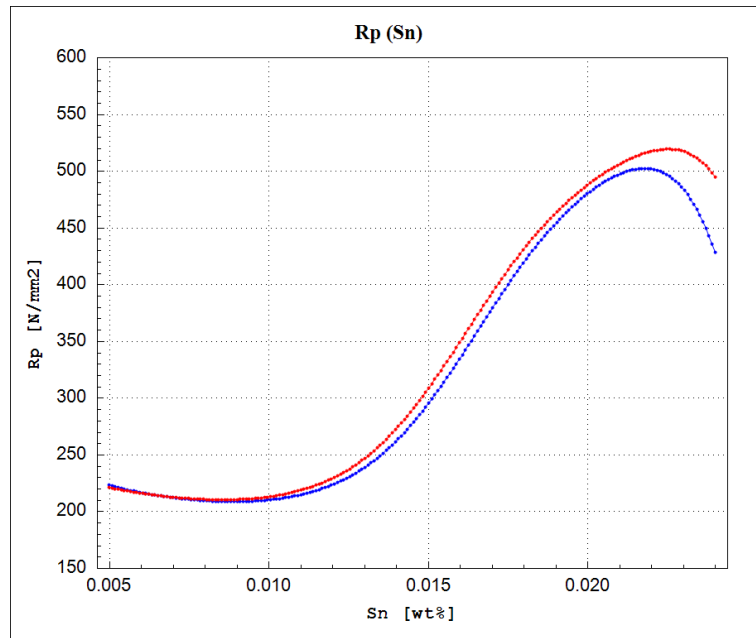


**Figure 103:** Yield stress as a function of the Tin concentration (Sn), calculated by the ANN model on centered verification point (red line) and centered training point (blue line).

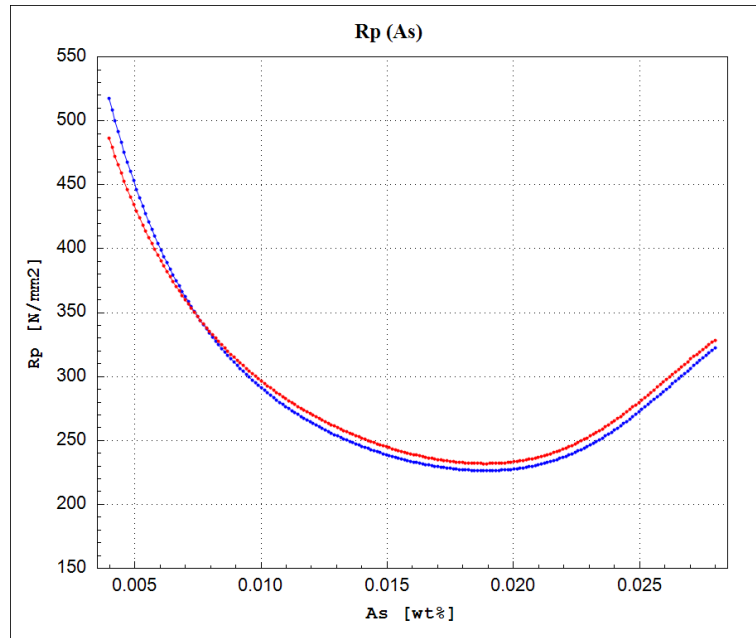


**Figure 104:** Yield stress as a function of the Arsenic concentration (As), calculated by the ANN model on centered verification point (red line) and centered training point (blue line).

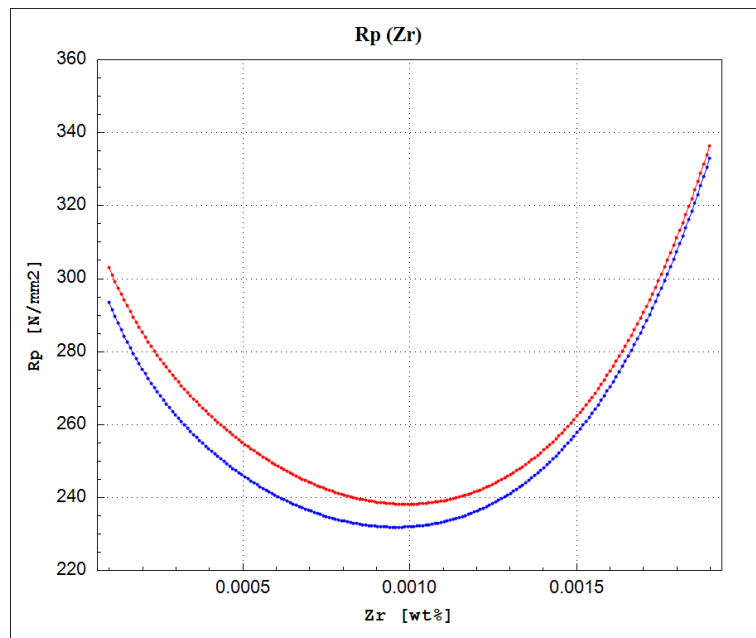


**Figure 105:** Yield stress as a function of the Zirconium concentration (Zr), calculated by the ANN model on centered verification point (red line) and centered training point (blue line).

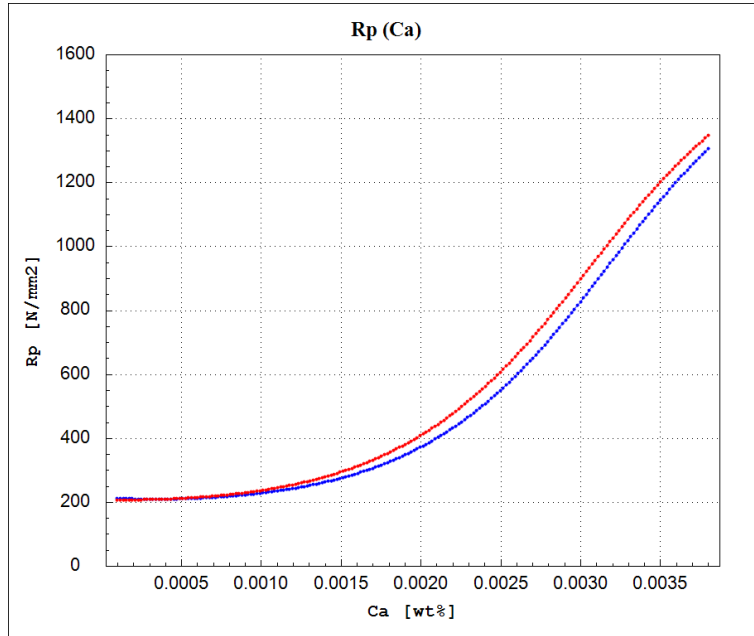


**Figure 106:** Yield stress as a function of the Calcium concentration (Ca), calculated by the ANN model on centered verification point (red line) and centered training point (blue line).

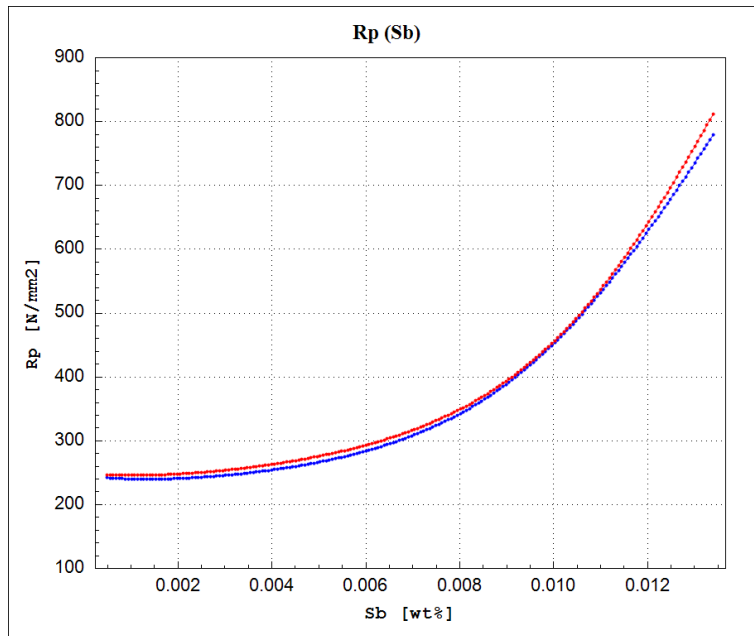


**Figure 107:** Yield stress as a function of the Antimony concentration (Sb), calculated by the ANN model on centered verification point (red line) and centered training point (blue line).

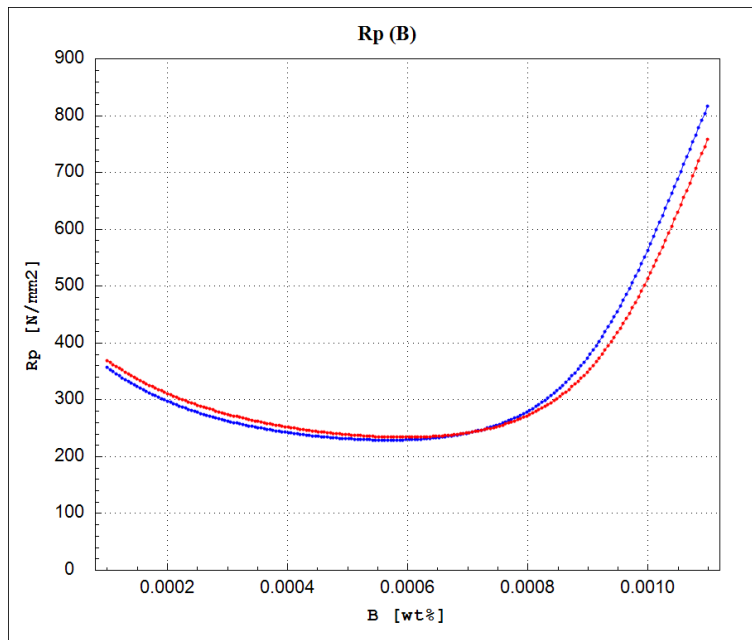


**Figure 108:** Yield stress as a function of the Boron concentration (B), calculated by the ANN model on centered verification point (red line) and centered training point (blue line).

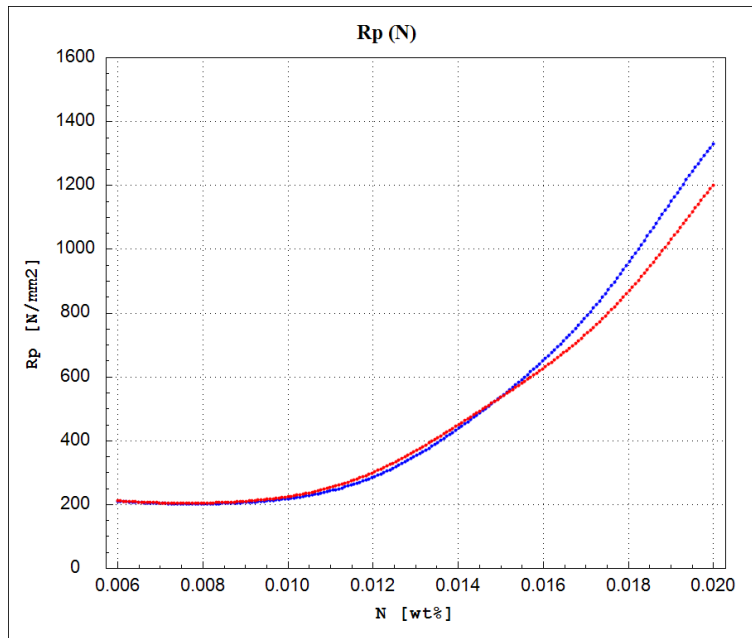


**Figure 109:** Yield stress as a function of the Nitrogen concentration (N), calculated by the ANN model on centered verification point (red line) and centered training point (blue line).

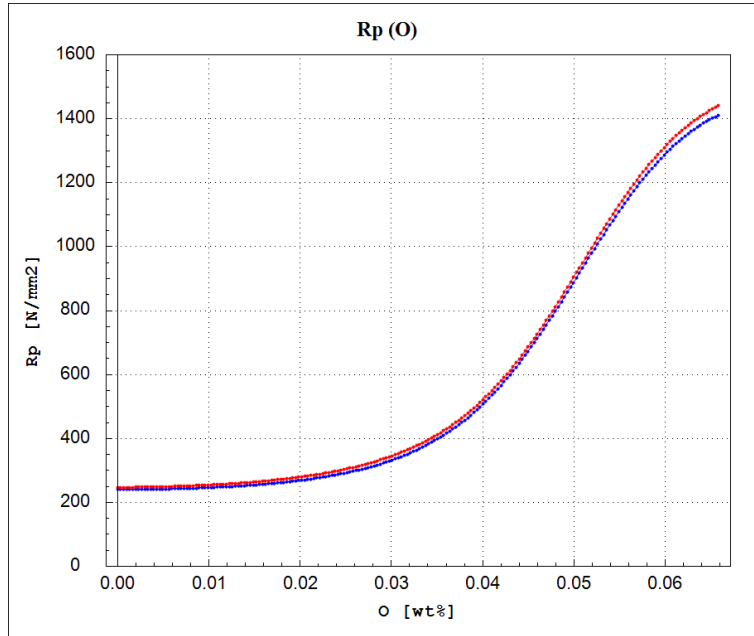


**Figure 110:** Yield stress as a function of the Oxigen concentration (O), calculated by the ANN model on centered verification point (red line) and centered training point (blue line).

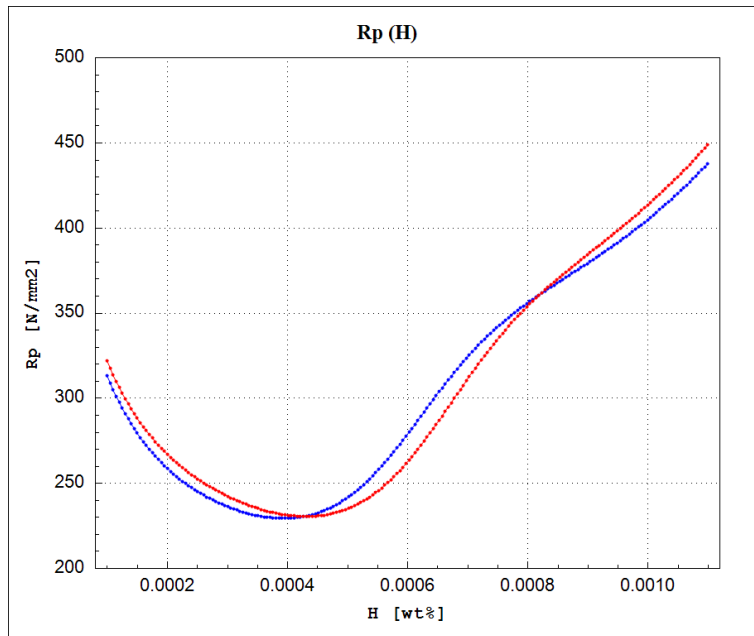


**Figure 111:** Yield stress as a function of the Hydrogen concentration (H), calculated by the ANN model on centered verification point (red line) and centered training point (blue line).

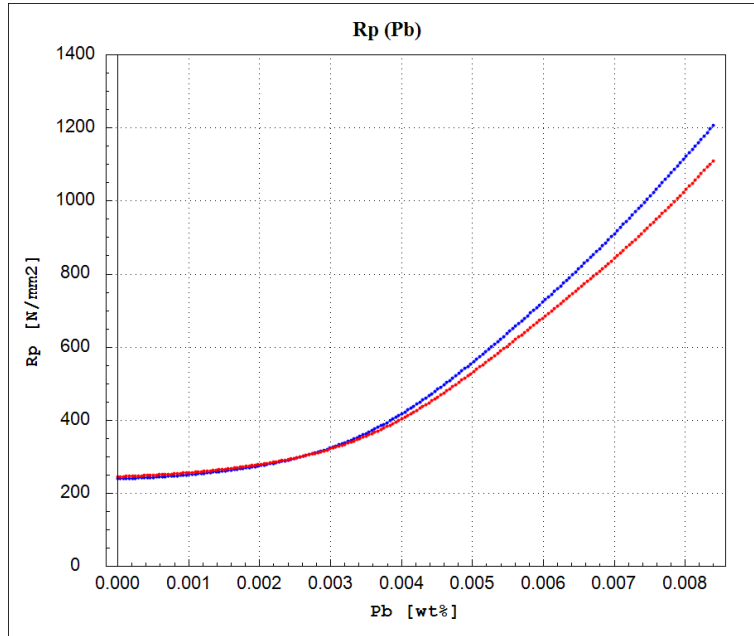


**Figure 112:** Yield stress as a function of the Lead concentration (Pb), calculated by the ANN model on centered verification point (red line) and centered training point (blue line).

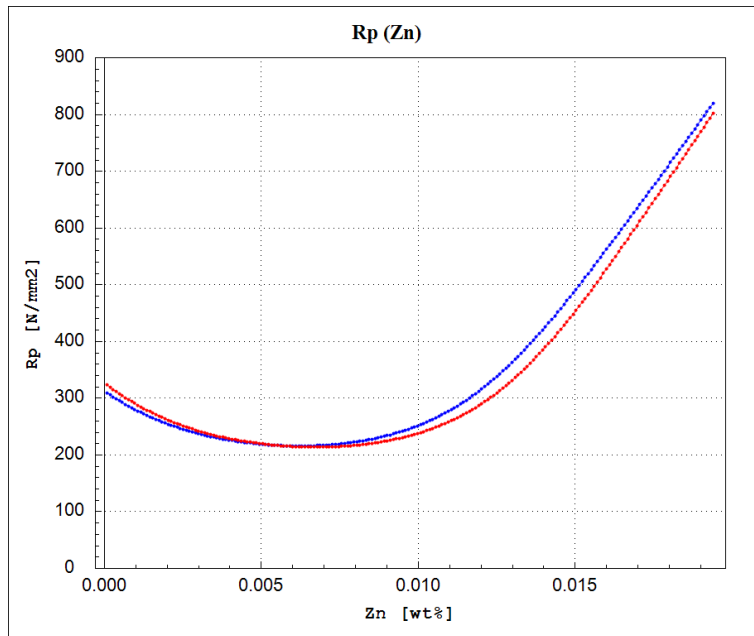


**Figure 113:** Yield stress as a function of the Zinc concentration (Zn), calculated by the ANN model on centered verification point (red line) and centered training point (blue line).

### 5.1.4 Hardness After Rolling (HB)

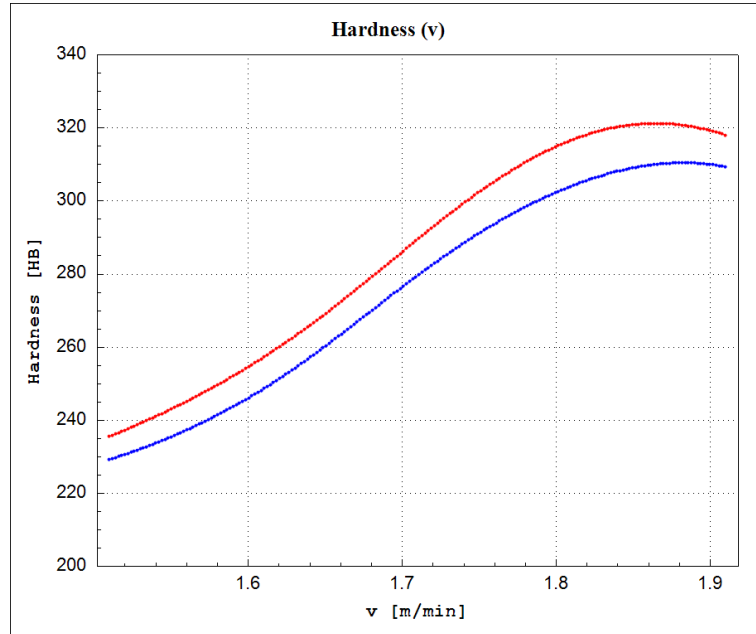


**Figure 114:** Hardness after rolling as a function of the continuous casting speed, calculated by the ANN model on centered verification point (red line) and centered training point (blue line).

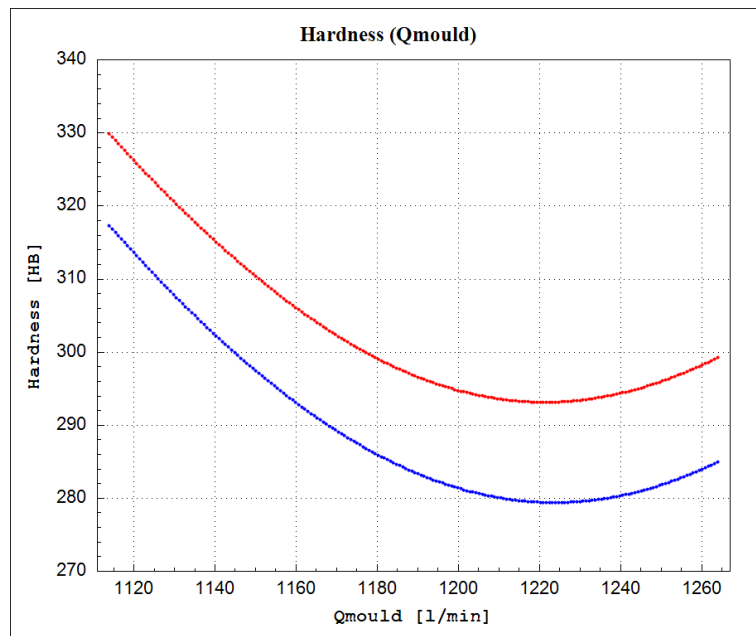


**Figure 115:** Hardness after rolling as a function of the cooling flow rate in the mould, calculated by the ANN model on centered verification point (red line) and centered training point (blue line).

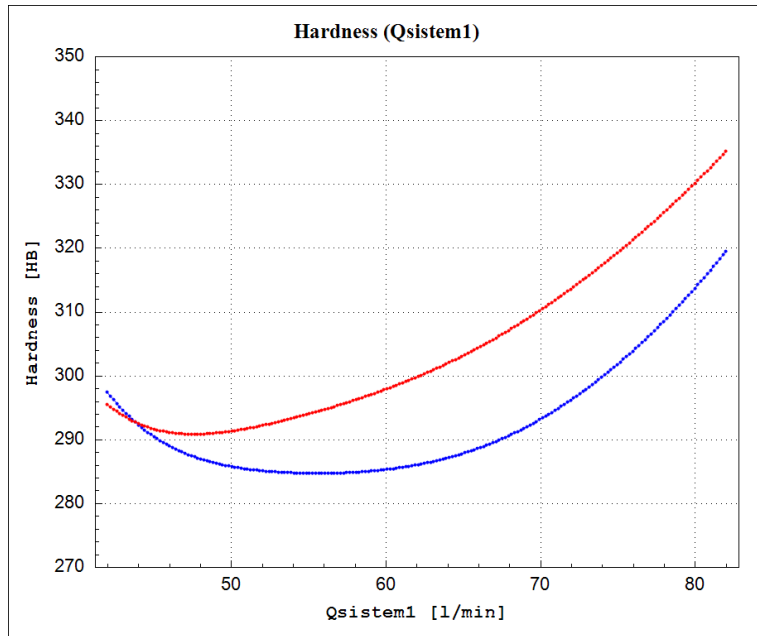


**Figure 116:** Hardness after rolling as a function of the cooling flow rate in 1<sup>st</sup> spray system, calculated by the ANN model on centered verification point (red line) and centered training point (blue line).

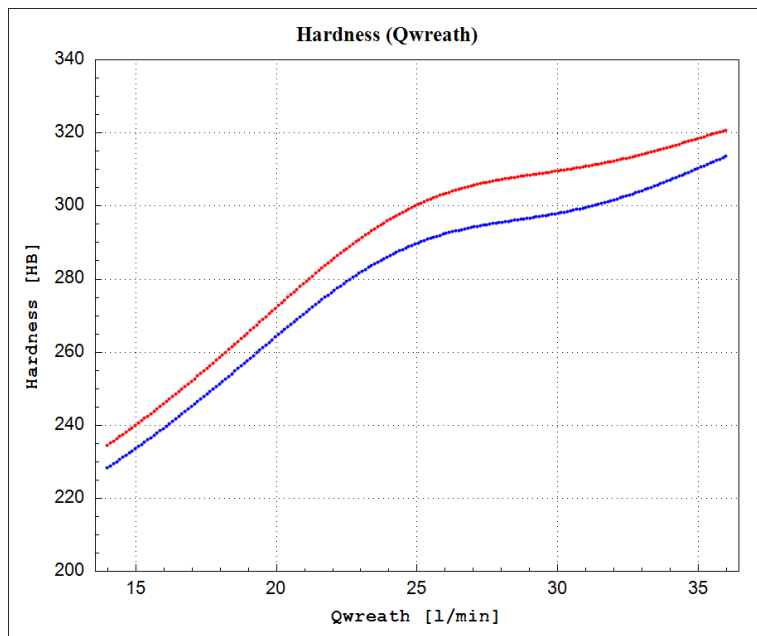


**Figure 117:** Hardness after rolling as a function of the cooling flow rate in wreath spray system, calculated by the ANN model on centered verification point (red line) and centered training point (blue line).

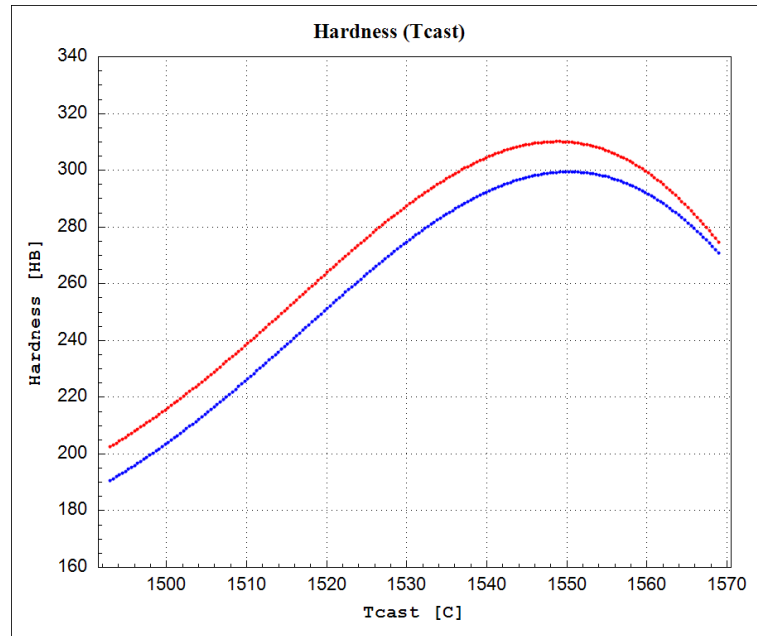


**Figure 118:** Hardness after rolling as a function of the casting temperature, calculated by the ANN model on centered verification point (red line) and centered training point (blue line).

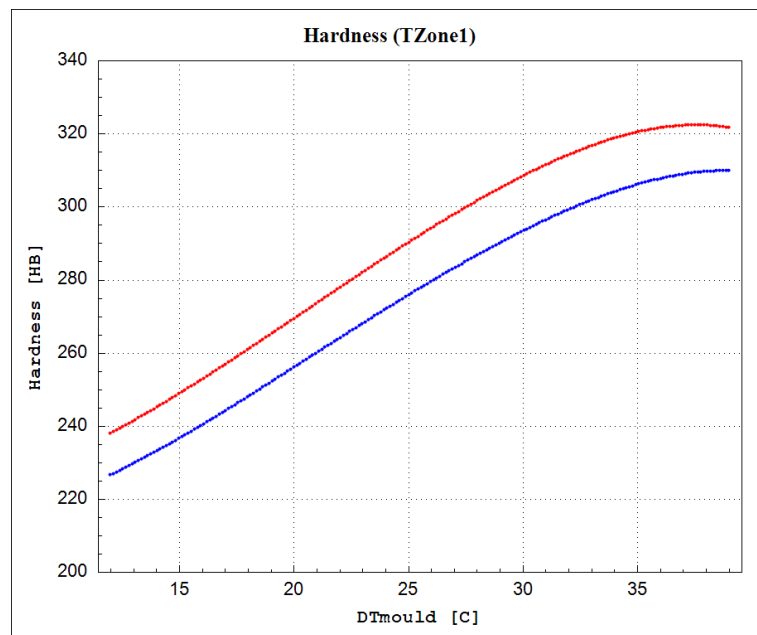


**Figure 119:** Hardness after rolling as a function of the water temperature in Zone 1, calculated by the ANN model on centered verification point (red line) and centered training point (blue line).

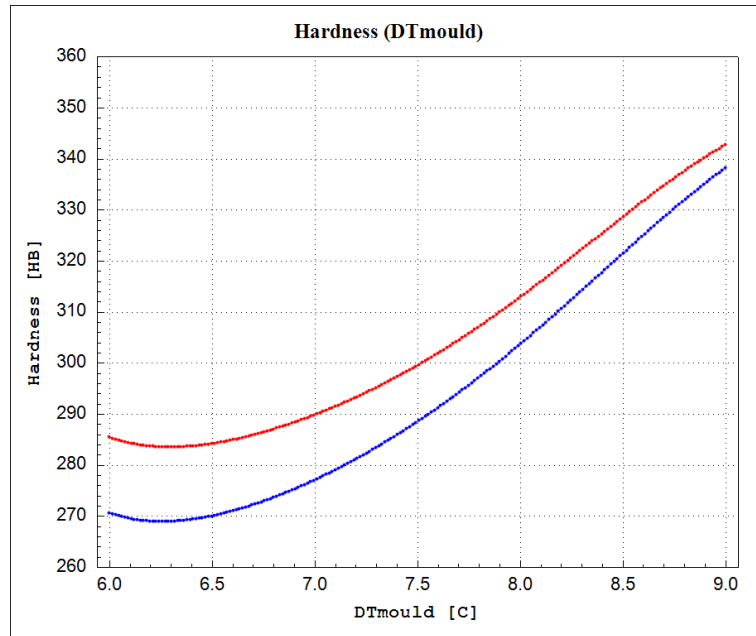


**Figure 120:** Hardness after rolling as a function of the delta T, calculated by the ANN model on centered verification point (red line) and centered training point (blue line).

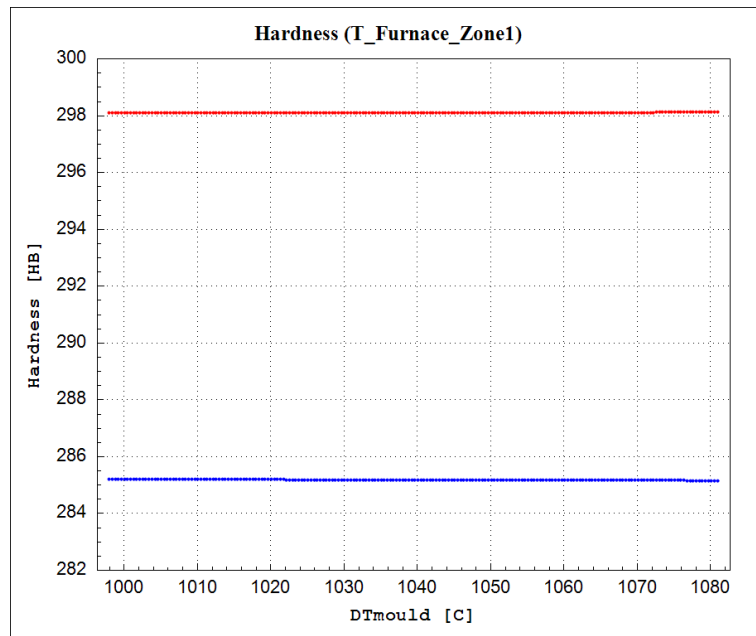


**Figure 121:** Hardness after rolling as a function of the average on temperature in zone 1, calculated by the ANN model on centered verification point (red line) and centered training point (blue line).

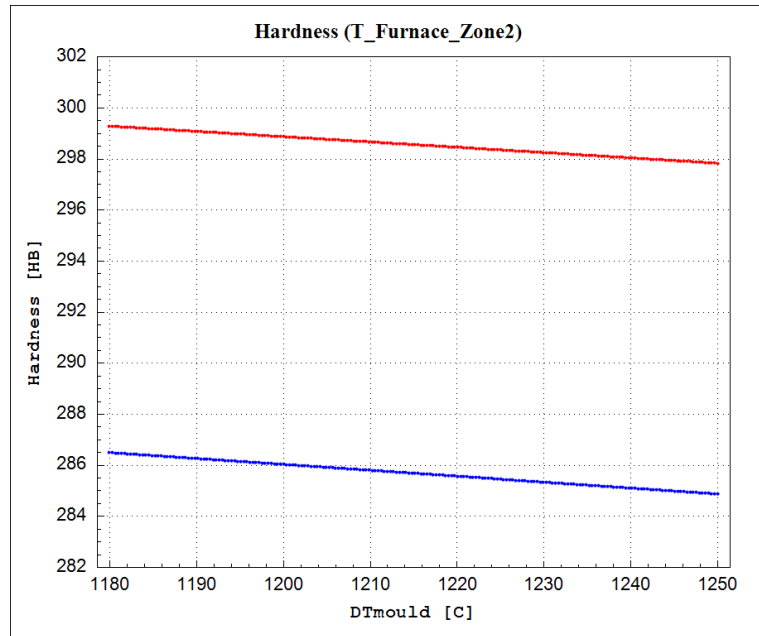


**Figure 122:** Hardness after rolling as a function of the average on temperature in zone 2, calculated by the ANN model on centered verification point (red line) and centered training point (blue line).

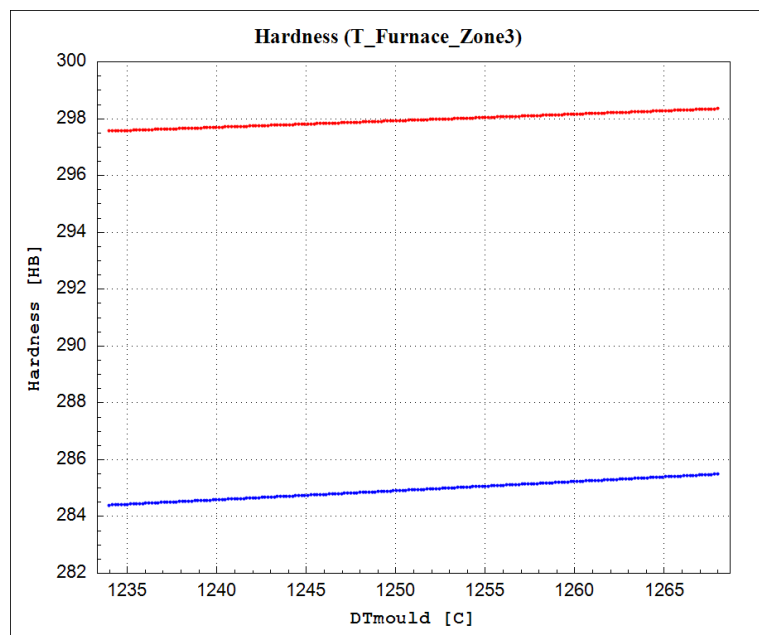


**Figure 123:** Hardness after rolling as a function of the average on temperature in zone 3, calculated by the ANN model on centered verification point (red line) and centered training point (blue line).

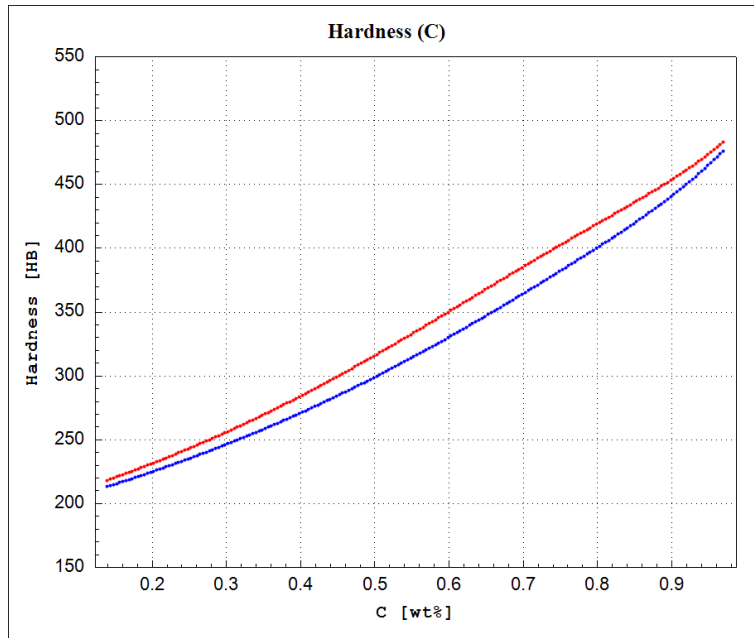


**Figure 124:** Hardness after rolling as a function of the Carbon concentration (C), calculated by the ANN model on centered verification point (red line) and centered training point (blue line).

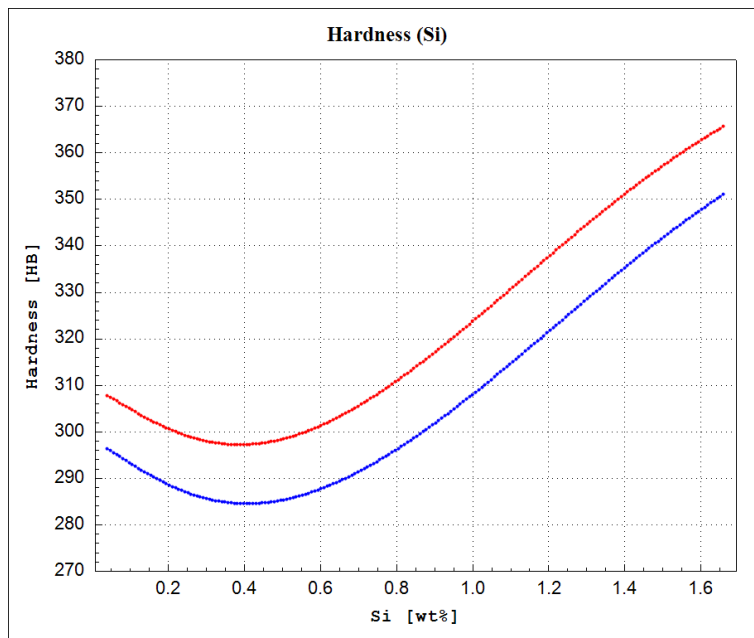


**Figure 125:** Hardness after rolling as a function of the Silicon concentration (Si), calculated by the ANN model on centered verification point (red line) and centered training point (blue line).

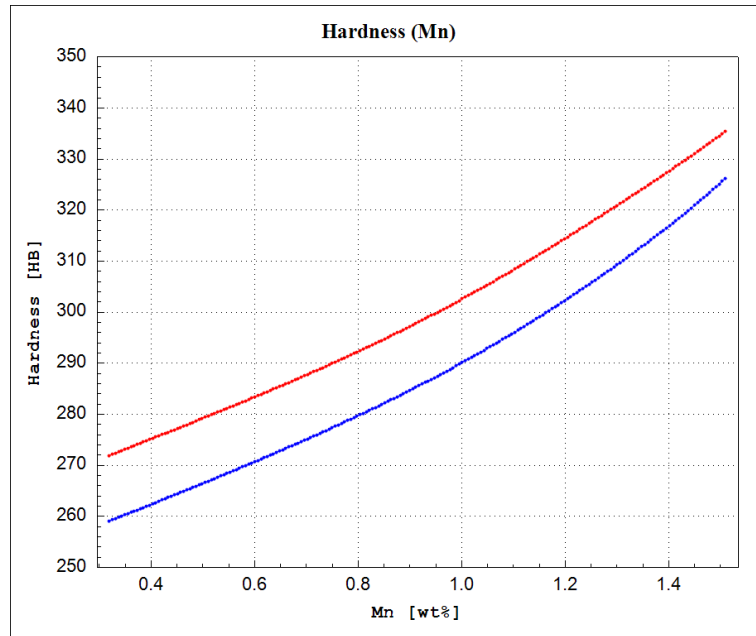


**Figure 126:** Hardness after rolling as a function of the Manganese concentration (Mn), calculated by the ANN model on centered verification point (red line) and centered training point (blue line).

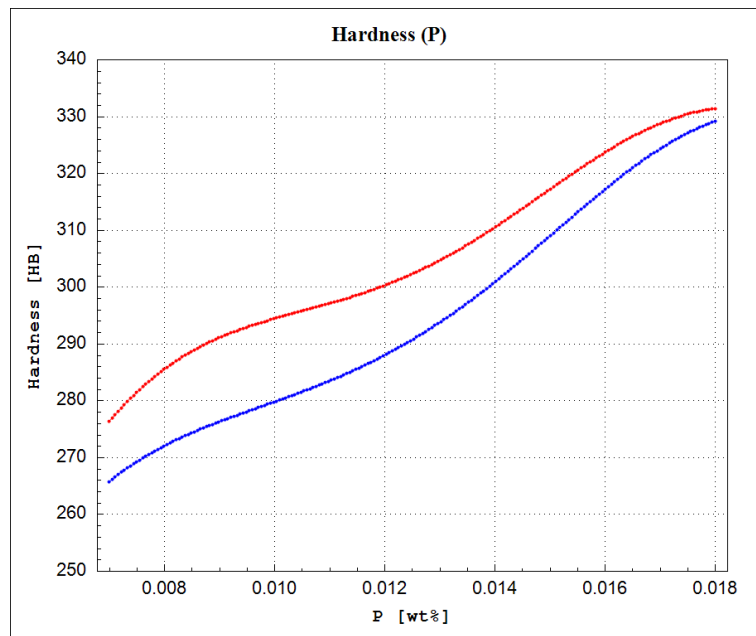


**Figure 127:** Hardness after rolling as a function of the Phosphorus concentration (P), calculated by the ANN model on centered verification point (red line) and centered training point (blue line).

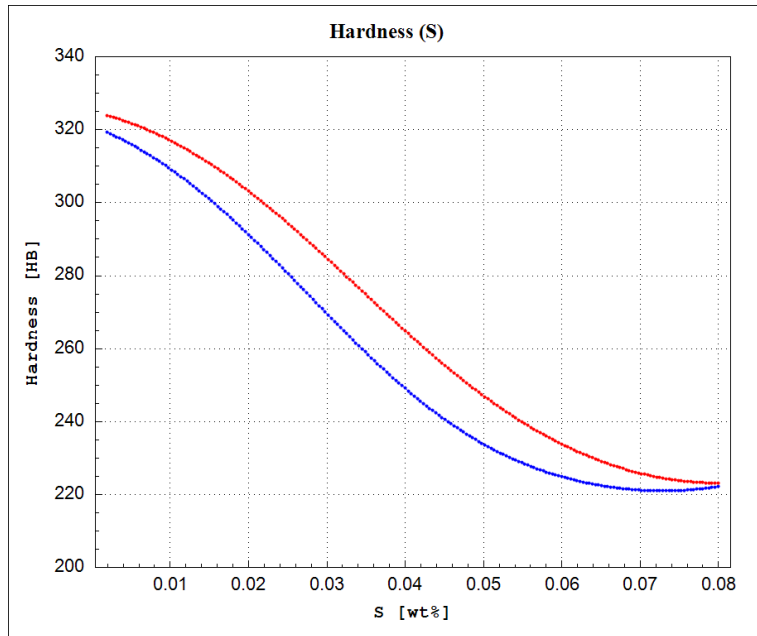


**Figure 128:** Hardness after rolling as a function of the Sulphur concentration (S), calculated by the ANN model on centered verification point (red line) and centered training point (blue line).

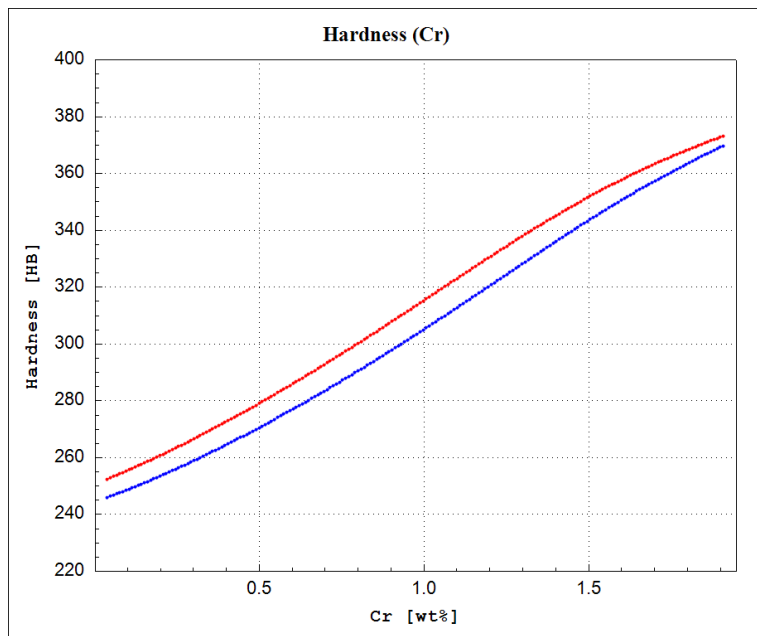


**Figure 129:** Hardness after rolling as a function of the Chromium concentration (Cr), calculated by the ANN model on centered verification point (red line) and centered training point (blue line).

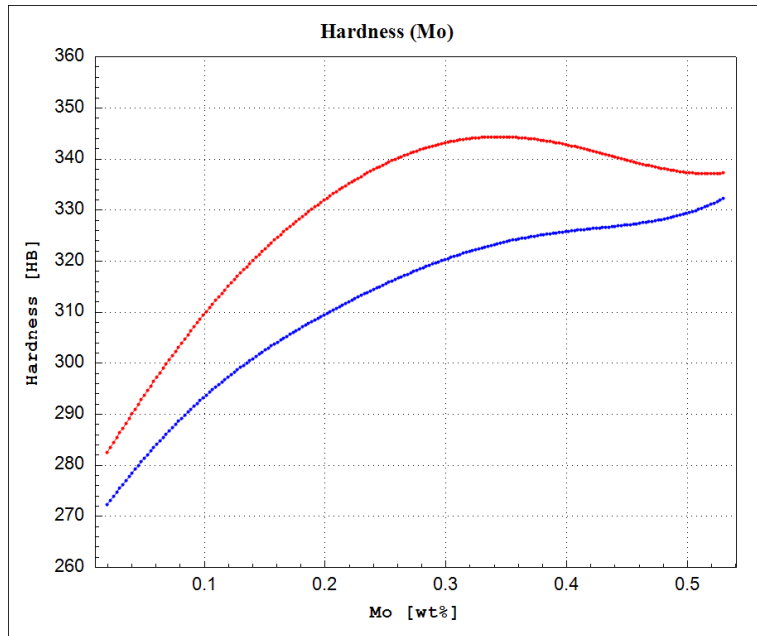


**Figure 130:** Hardness after rolling as a function of the Molybdenum concentration (Mo), calculated by the ANN model on centered verification point (red line) and centered training point (blue line).

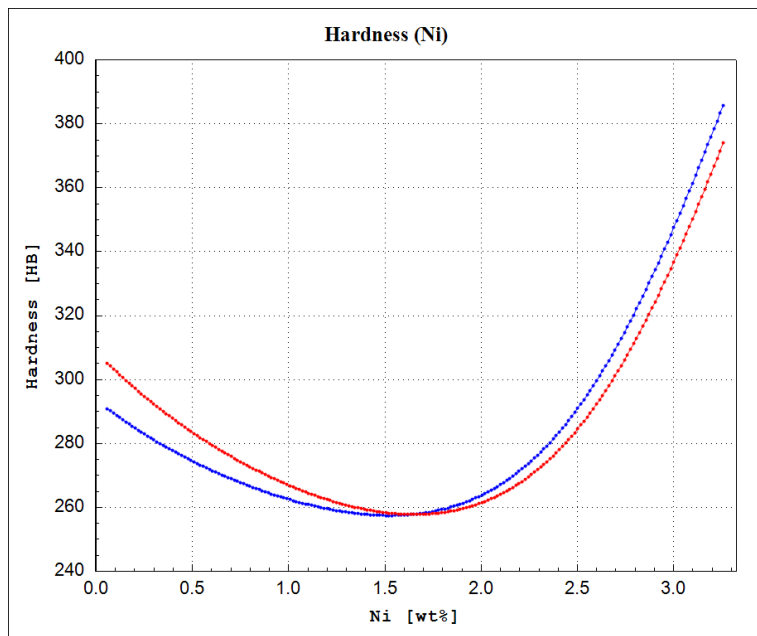


**Figure 131:** Hardness after rolling as a function of the Nickel concentration (Ni), calculated by the ANN model on centered verification point (red line) and centered training point (blue line).

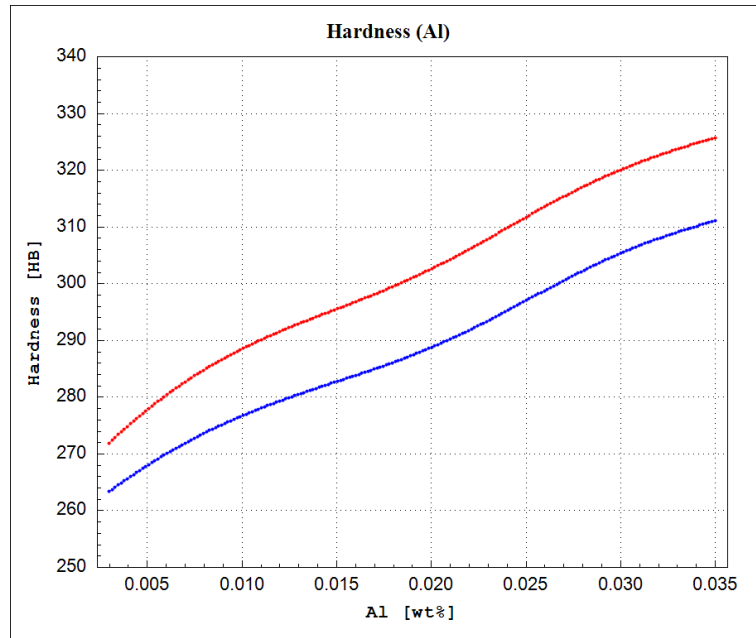


**Figure 132:** Hardness after rolling as a function of the Aluminium concentration (Al), calculated by the ANN model on centered verification point (red line) and centered training point (blue line).

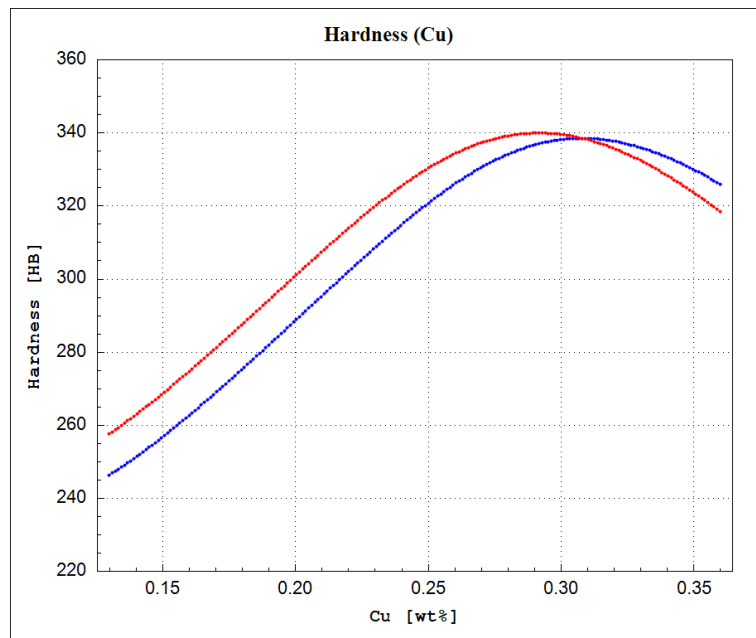


**Figure 133:** Hardness after rolling as a function of the Copper concentration (Cu), calculated by the ANN model on centered verification point (red line) and centered training point (blue line).

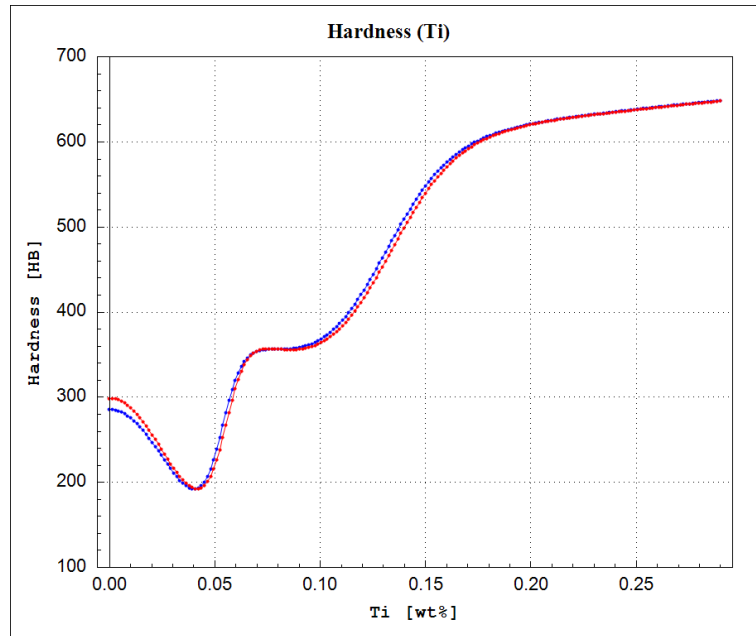


**Figure 134:** Hardness after rolling as a function of the Titanium concentration (Ti), calculated by the ANN model on centered verification point (red line) and centered training point (blue line).

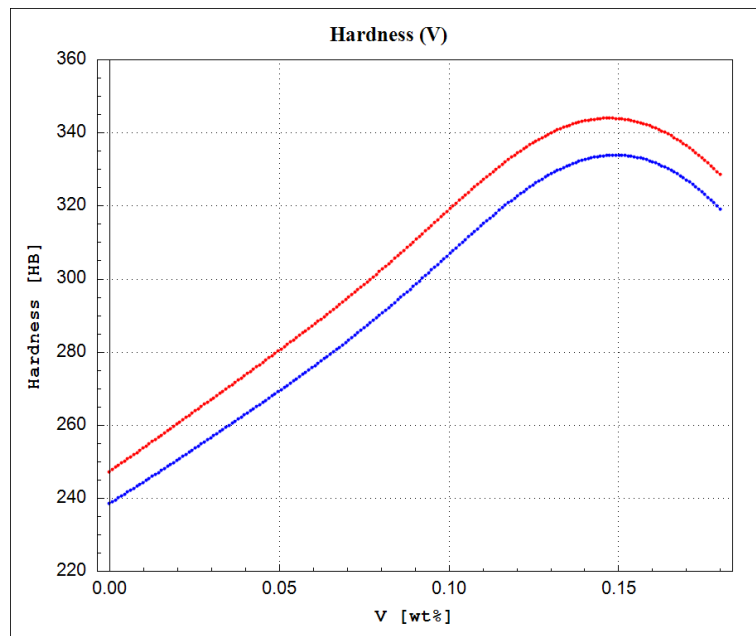


**Figure 135:** Hardness after rolling as a function of the Vanadium concentration (V), calculated by the ANN model on centered verification point (red line) and centered training point (blue line).

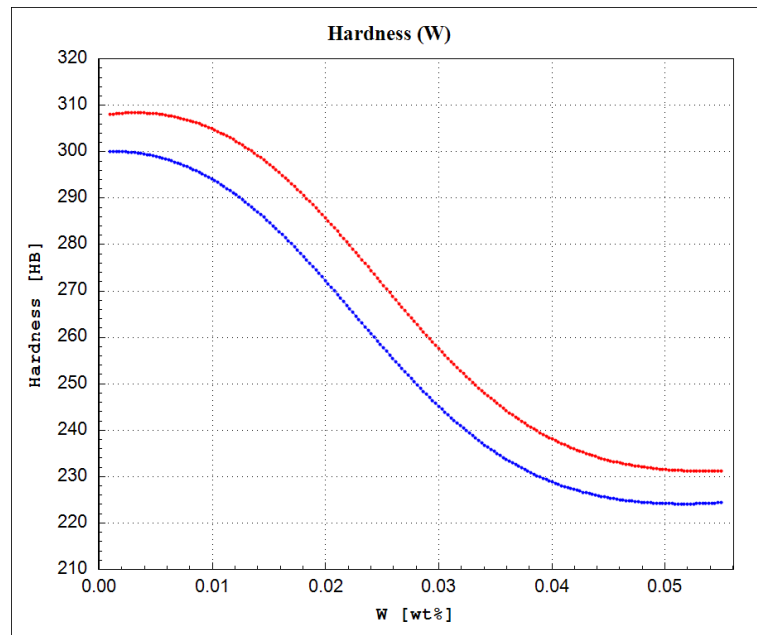


**Figure 136:** Hardness after rolling as a function of the Tungsten concentration (W), calculated by the ANN model on centered verification point (red line) and centered training point (blue line).

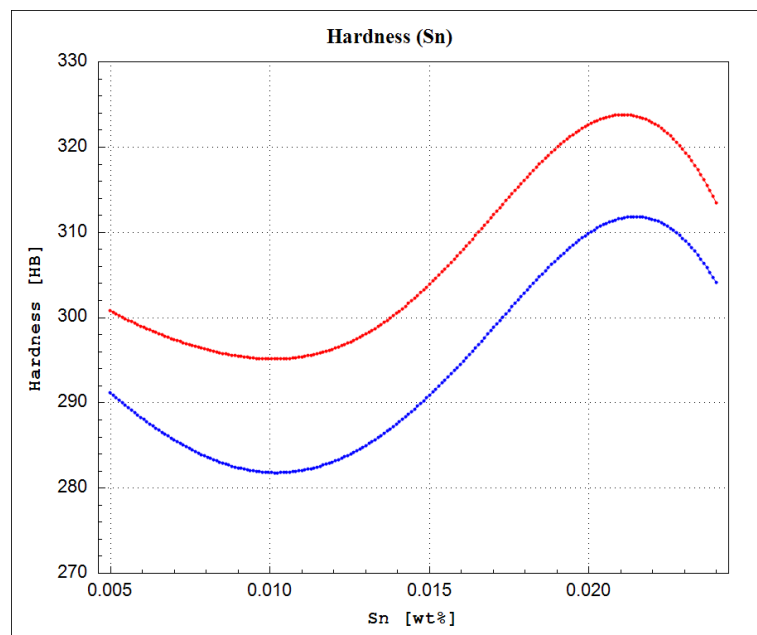


**Figure 137:** Hardness after rolling as a function of the Tin concentration (Sn), calculated by the ANN model on centered verification point (red line) and centered training point (blue line).

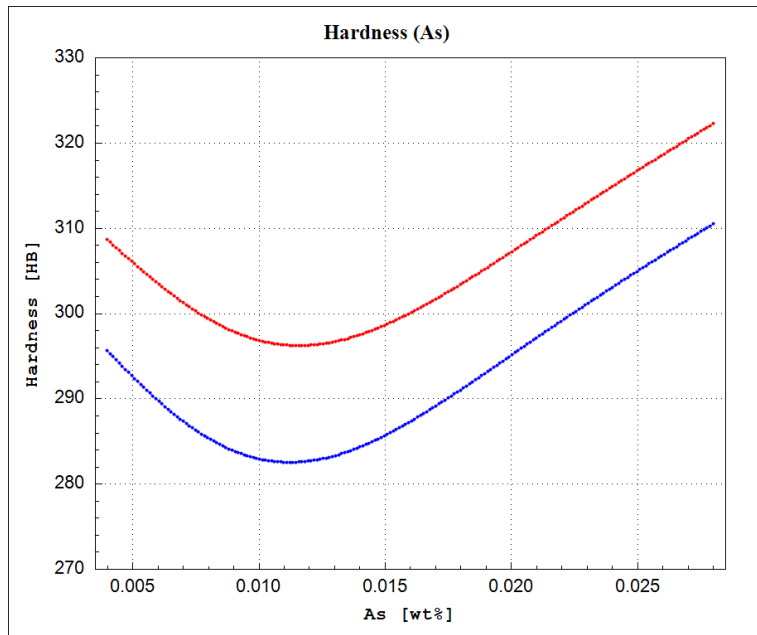


**Figure 138:** Hardness after rolling as a function of the Arsenic concentration (As), calculated by the ANN model on centered verification point (red line) and centered training point (blue line).

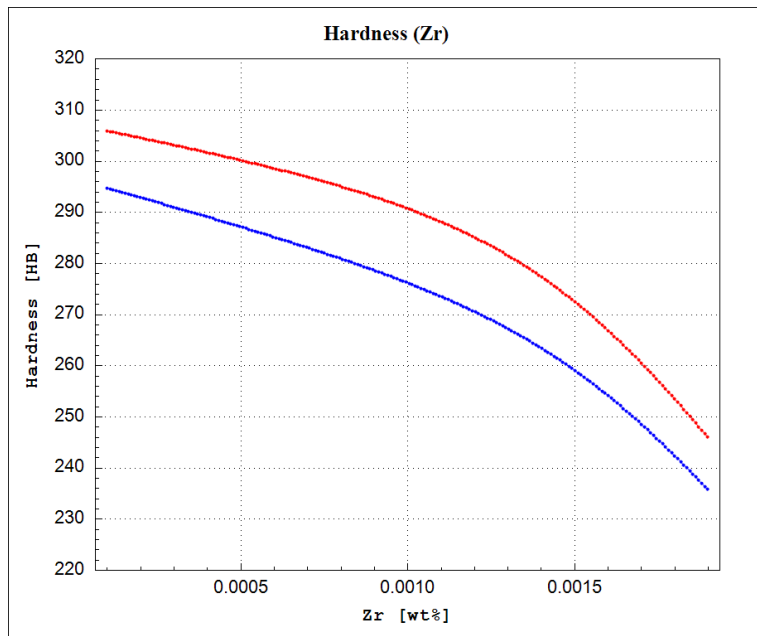


**Figure 139:** Hardness after rolling as a function of the Zirconium concentration (Zr), calculated by the ANN model on centered verification point (red line) and centered training point (blue line).

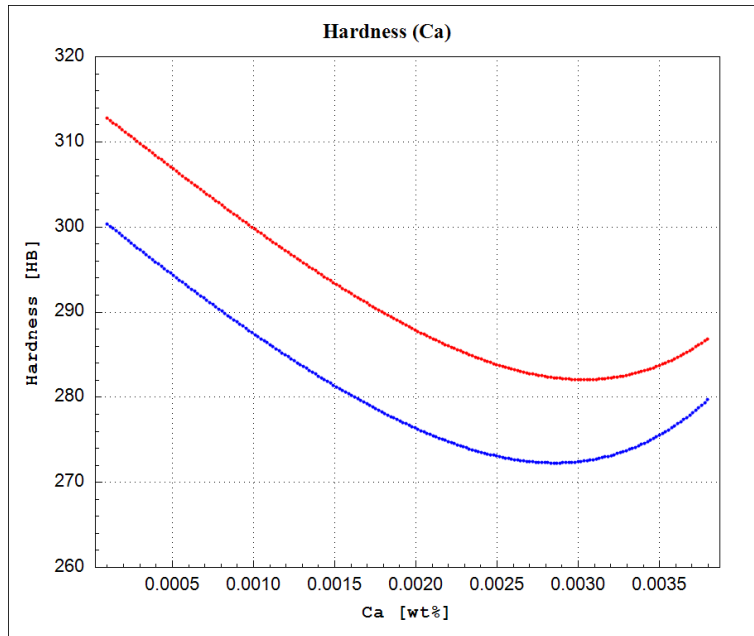


**Figure 140:** Hardness after rolling as a function of the Calcium concentration (Ca), calculated by the ANN model on centered verification point (red line) and centered training point (blue line).

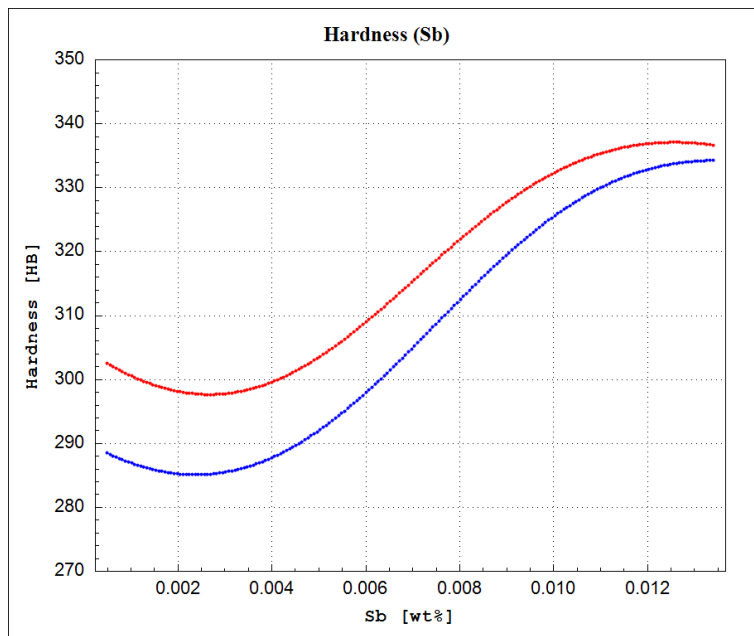


**Figure 141:** Hardness after rolling as a function of the Antimony concentration (Sb), calculated by the ANN model on centered verification point (red line) and centered training point (blue line).

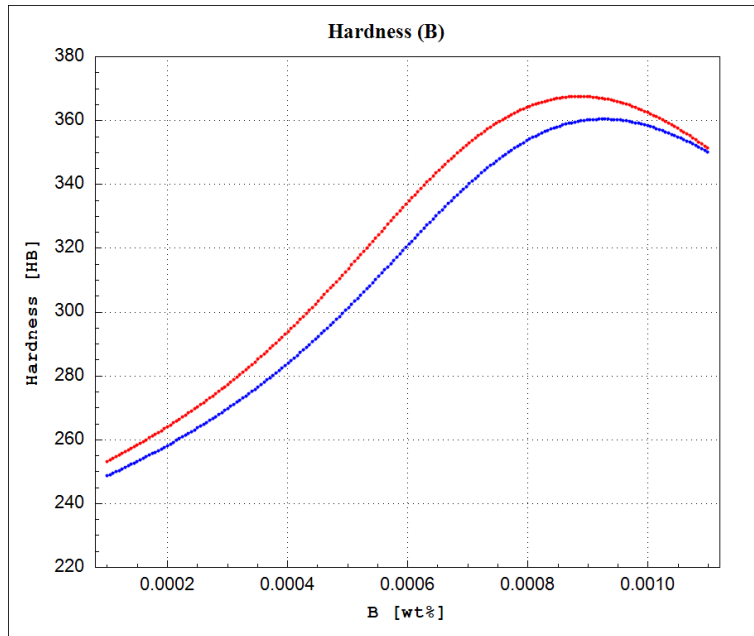


**Figure 142:** Hardness after rolling as a function of the Boron concentration (B), calculated by the ANN model on centered verification point (red line) and centered training point (blue line).

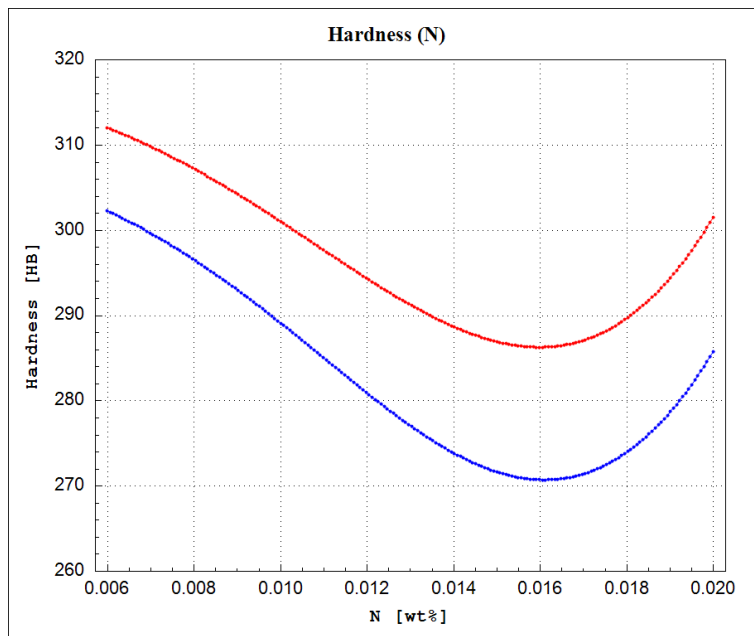


**Figure 143:** Hardness after rolling as a function of the Nitrogen concentration (N), calculated by the ANN model on centered verification point (red line) and centered training point (blue line).

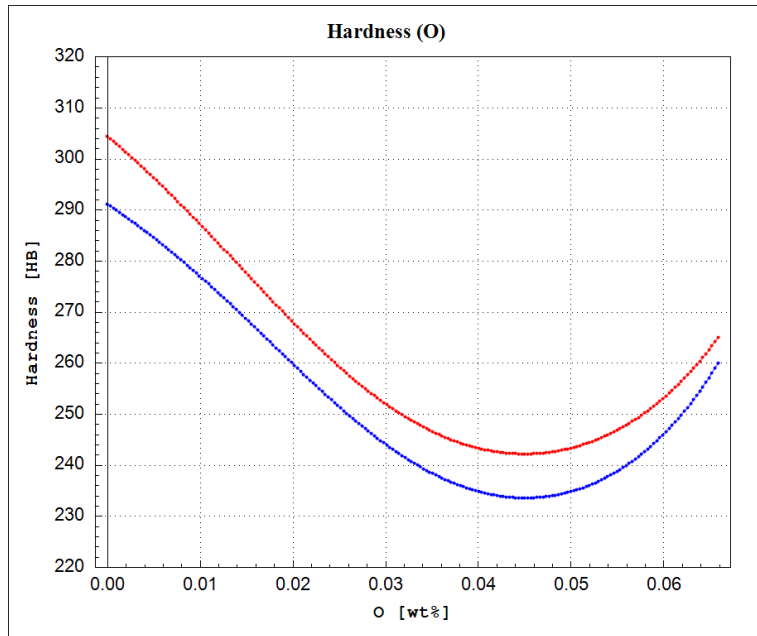


**Figure 144:** Hardness after rolling as a function of the Oxigen concentration (O), calculated by the ANN model on centered verification point (red line) and centered training point (blue line).

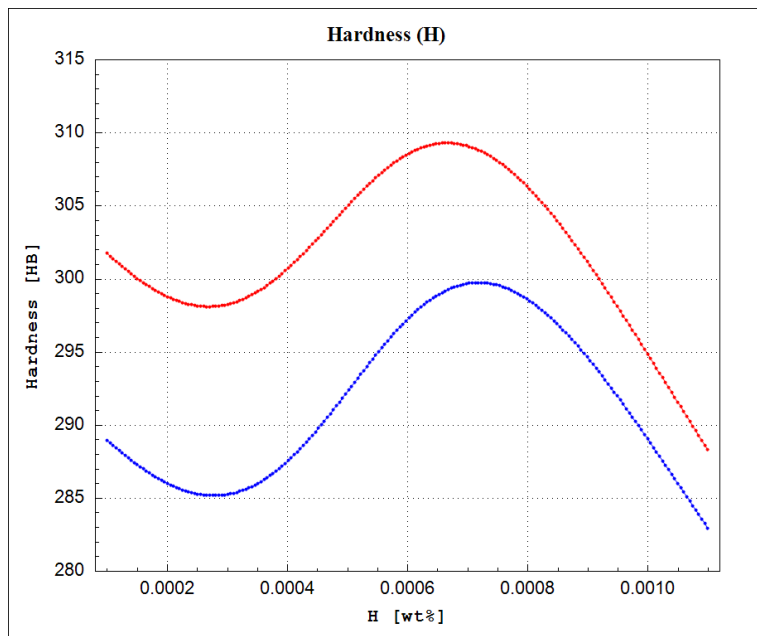


**Figure 145:** Hardness after rolling as a function of the Hydrogen concentration (H), calculated by the ANN model on centered verification point (red line) and centered training point (blue line).

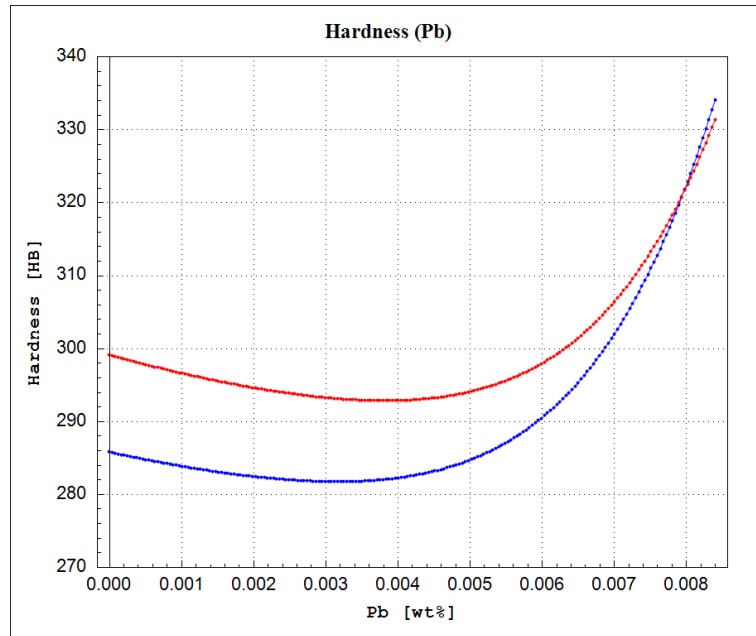


**Figure 146:** Hardness after rolling as a function of the Lead concentration (Pb), calculated by the ANN model on centered verification point (red line) and centered training point (blue line).

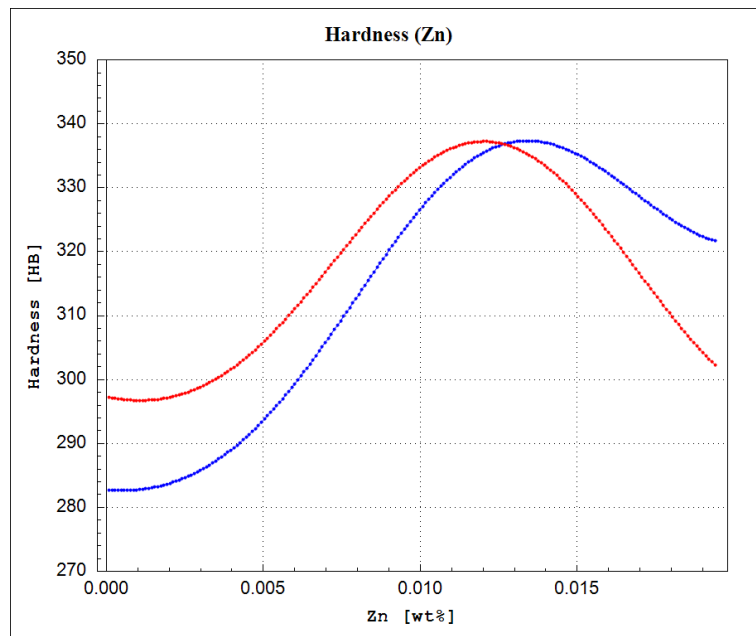


**Figure 147:** Hardness after rolling as a function of the Zinc concentration (Zn), calculated by the ANN model on centered verification point (red line) and centered training point (blue line).

### 5.1.5 Necking (Z)

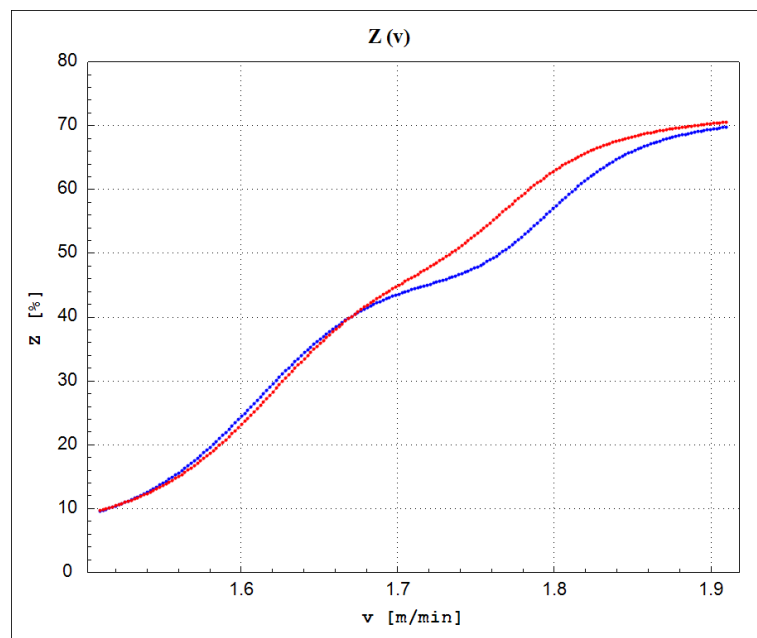


**Figure 148:** Necking as a function of the continuous casting speed, calculated by the ANN model on centered verification point (red line) and centered training point (blue line).

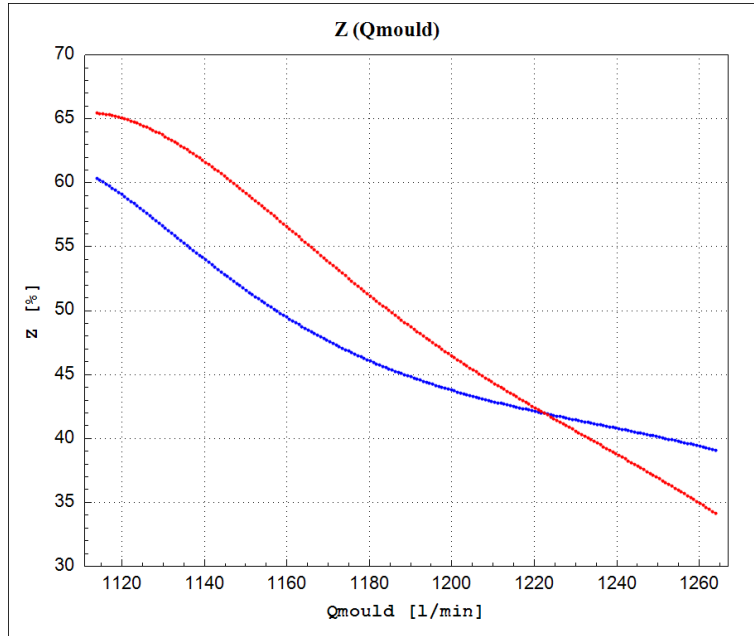


**Figure 149:** Necking as a function of the cooling flow rate in the mould, calculated by the ANN model on centered verification point (red line) and centered training point (blue line).

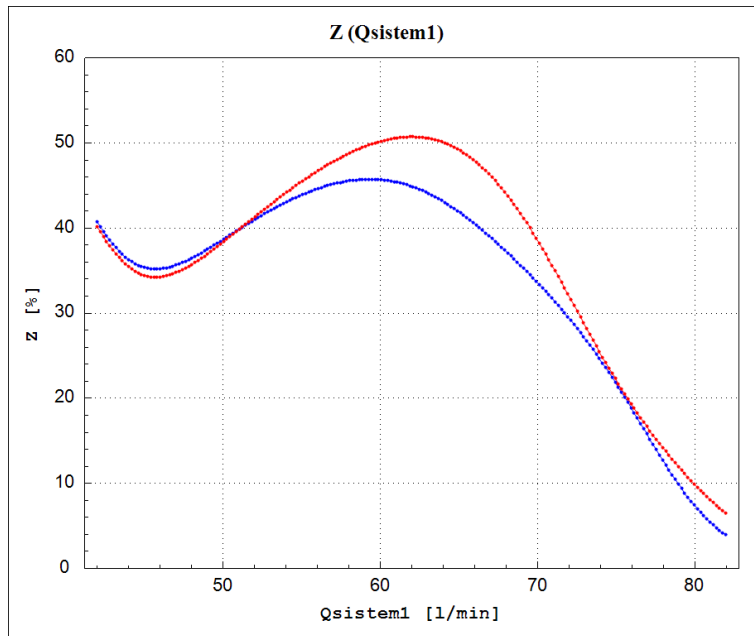


**Figure 150:** Necking as a function of the cooling flow rate in 1<sup>st</sup> spray system, calculated by the ANN model on centered verification point (red line) and centered training point (blue line).

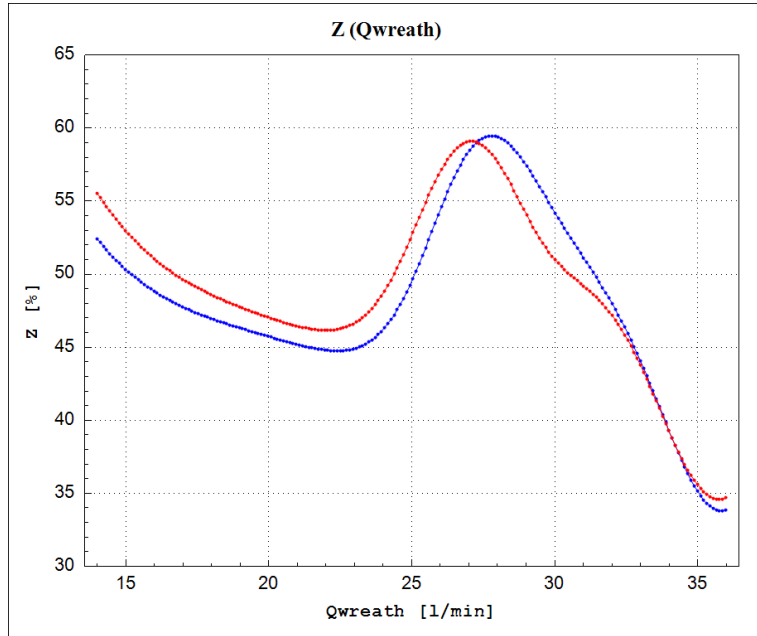


**Figure 151:** Necking as a function of the cooling flow rate in wreath spray system, calculated by the ANN model on centered verification point (red line) and centered training point (blue line).

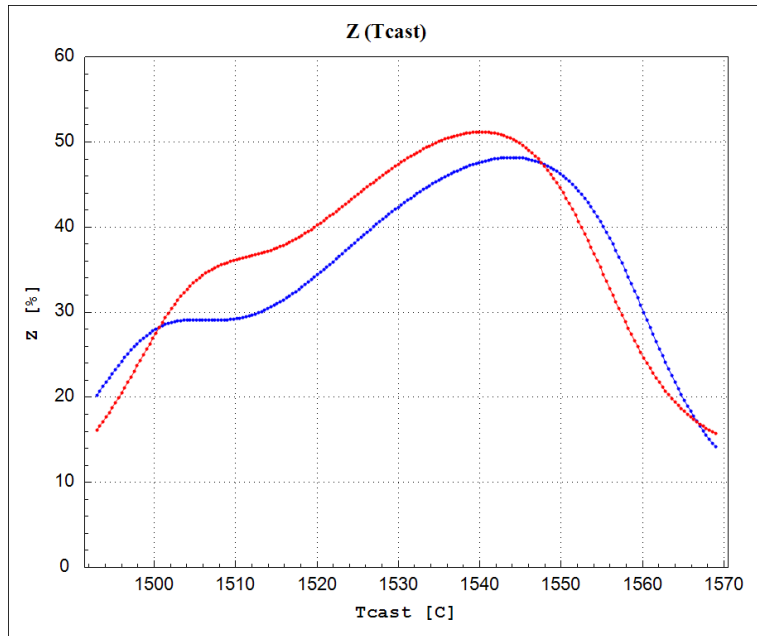


**Figure 152:** Necking as a function of the casting temperature, calculated by the ANN model on centered verification point (red line) and centered training point (blue line).

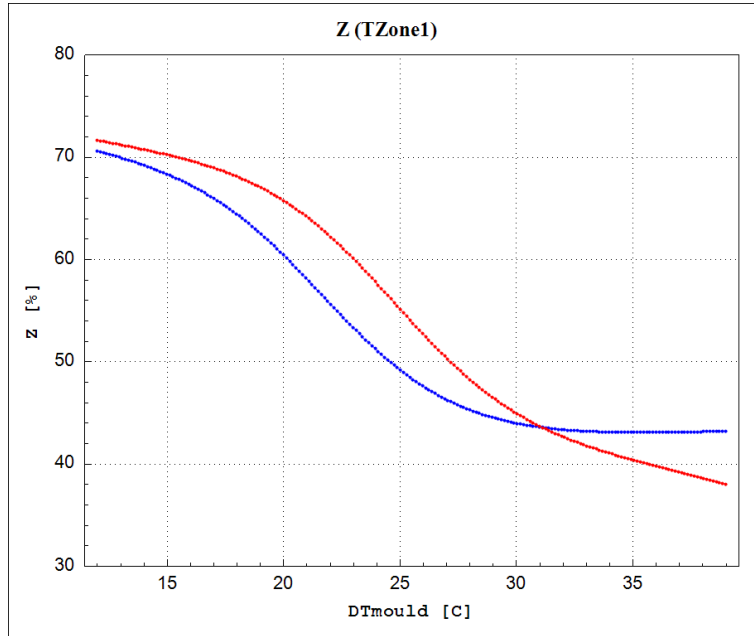


**Figure 153:** Necking as a function of the water temperature in Zone 1, calculated by the ANN model on centered verification point (red line) and centered training point (blue line).

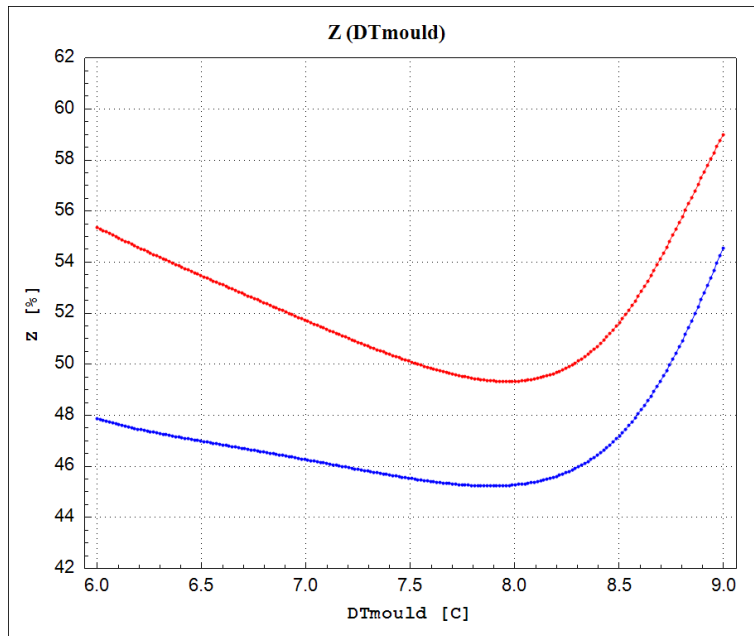


**Figure 154:** Necking as a function of the delta T, calculated by the ANN model on centered verification point (red line) and centered training point (blue line).

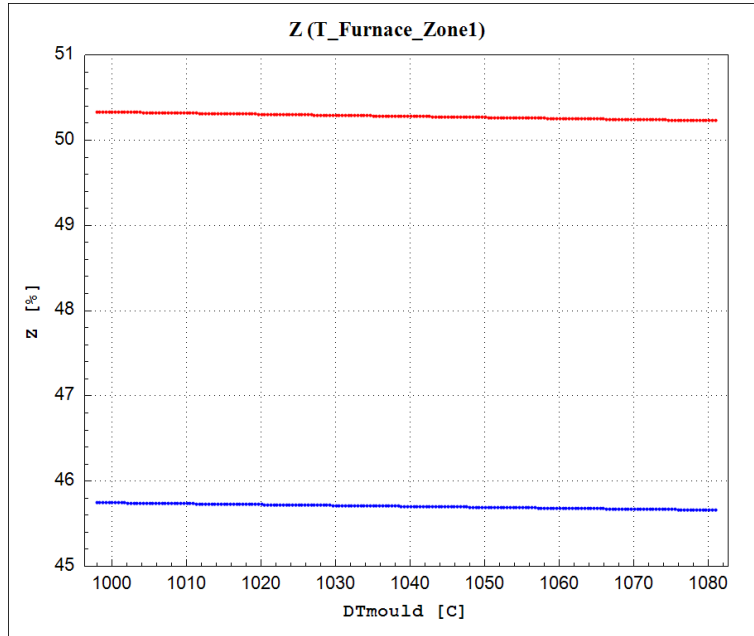


**Figure 155:** Necking as a function of the average on temperature in zone 1, calculated by the ANN model on centered verification point (red line) and centered training point (blue line).

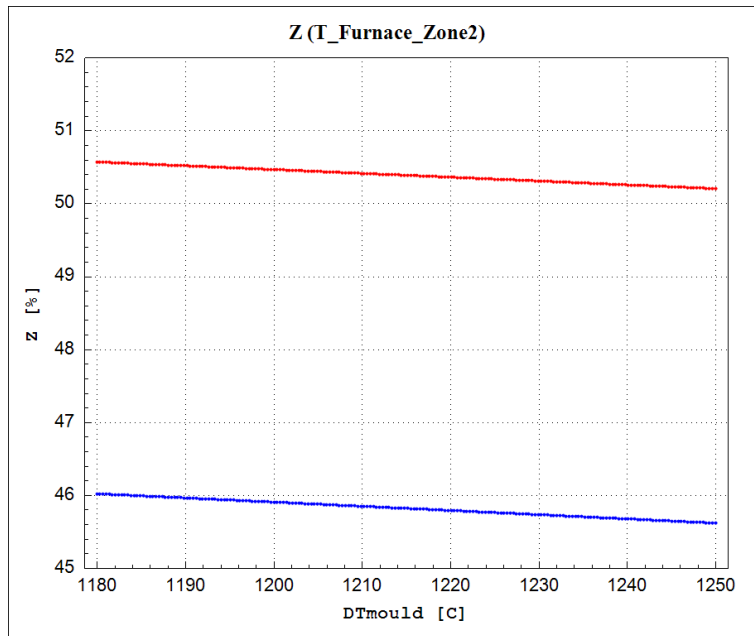


**Figure 156:** Necking as a function of the average on temperature in zone 2, calculated by the ANN model on centered verification point (red line) and centered training point (blue line).

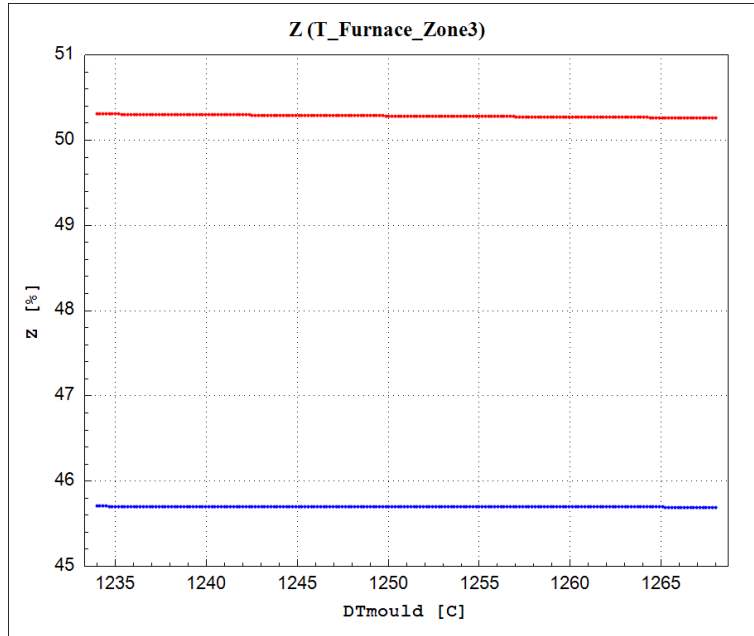


**Figure 157:** Necking as a function of the average on temperature in zone 3, calculated by the ANN model on centered verification point (red line) and centered training point (blue line).

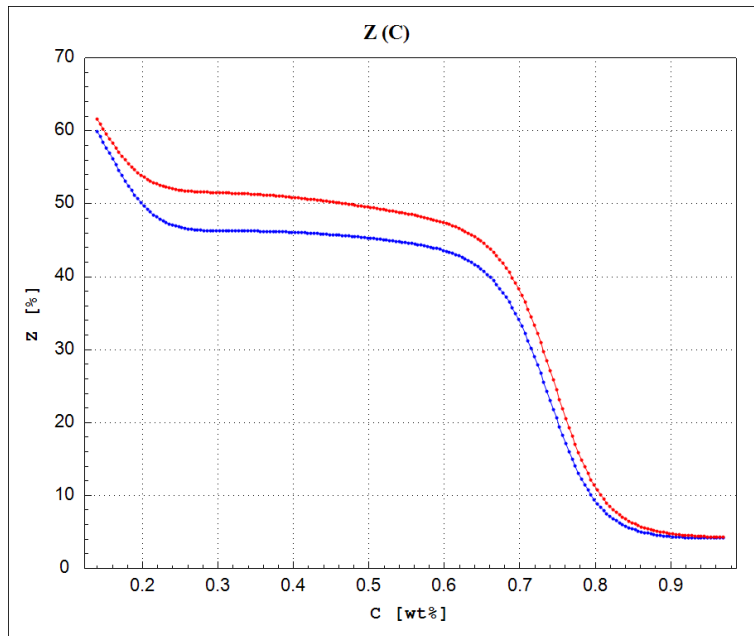


**Figure 158:** Necking as a function of the Carbon concentration (C), calculated by the ANN model on centered verification point (red line) and centered training point (blue line).

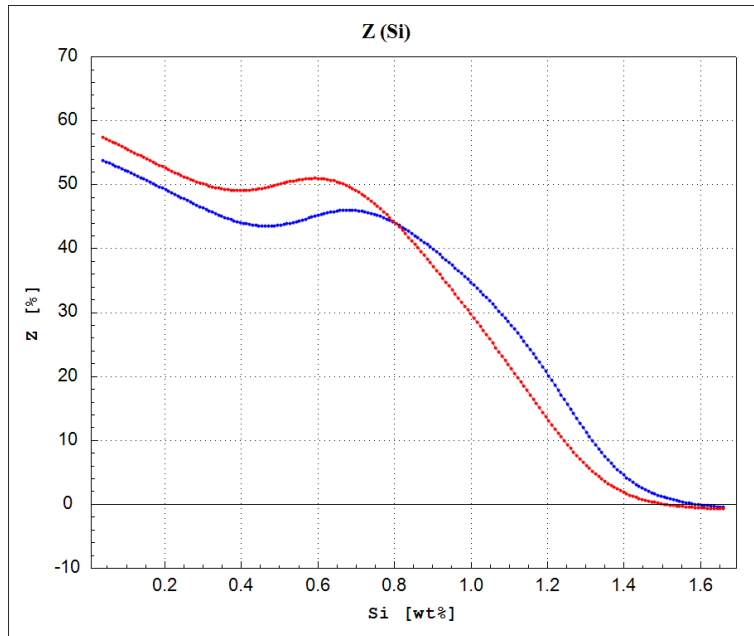


**Figure 159:** Necking as a function of the Silicon concentration (Si), calculated by the ANN model on centered verification point (red line) and centered training point (blue line).

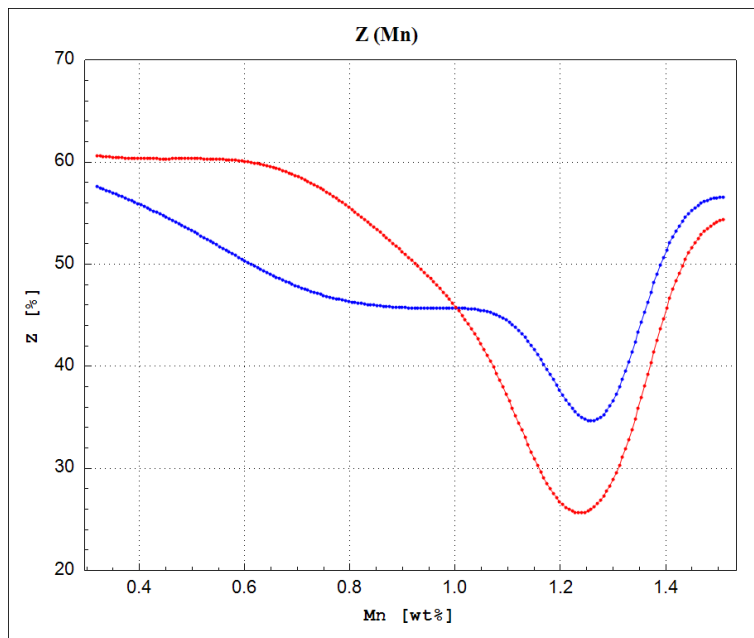


**Figure 160:** Necking as a function of the Manganese concentration (Mn), calculated by the ANN model on centered verification point (red line) and centered training point (blue line).

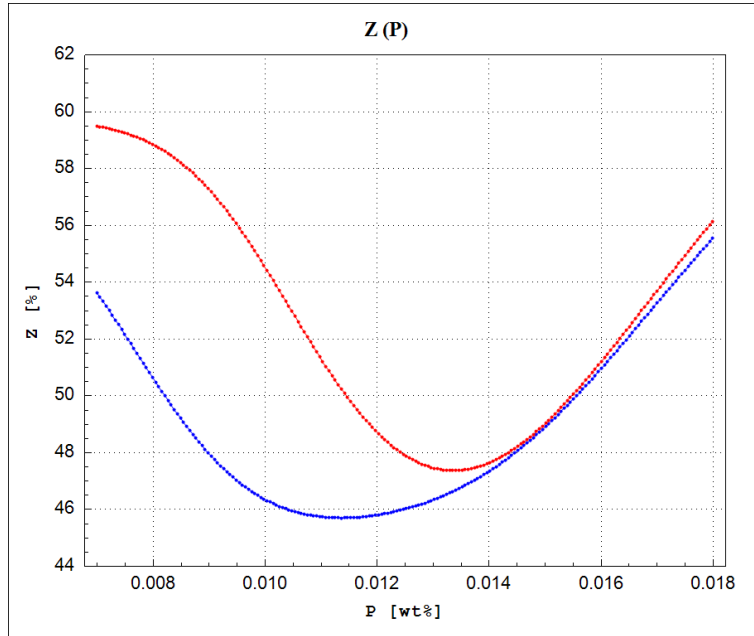


**Figure 161:** Necking as a function of the Phosphorus concentration (P), calculated by the ANN model on centered verification point (red line) and centered training point (blue line).

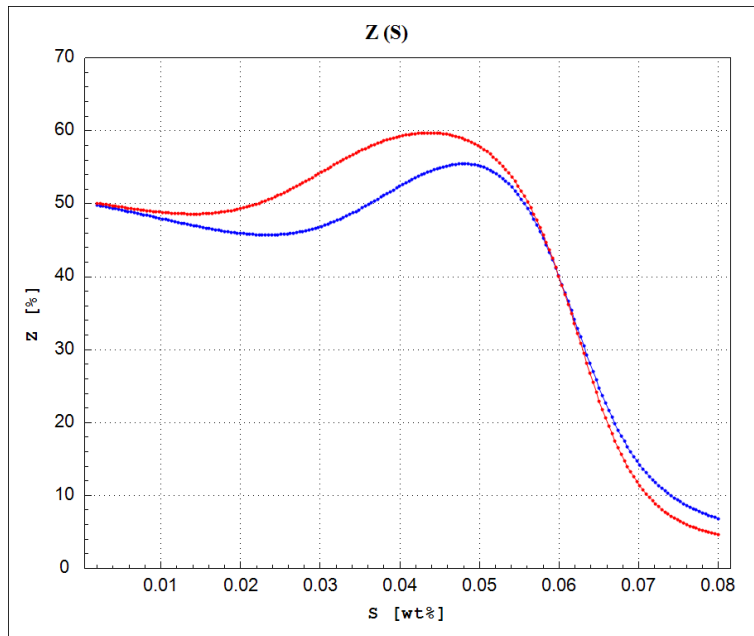


**Figure 162:** Necking as a function of the Sulphur concentration (S), calculated by the ANN model on centered verification point (red line) and centered training point (blue line).

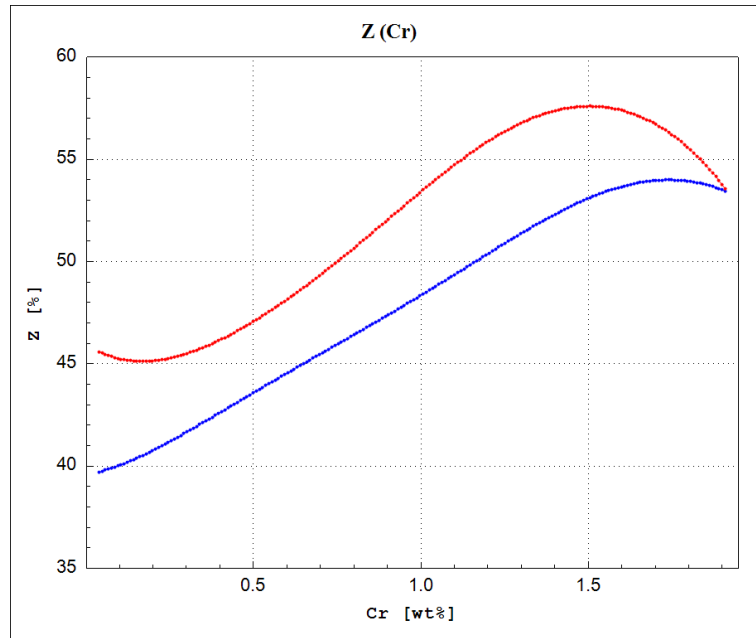


**Figure 163:** Necking as a function of the Chromium concentration (Cr), calculated by the ANN model on centered verification point (red line) and centered training point (blue line).

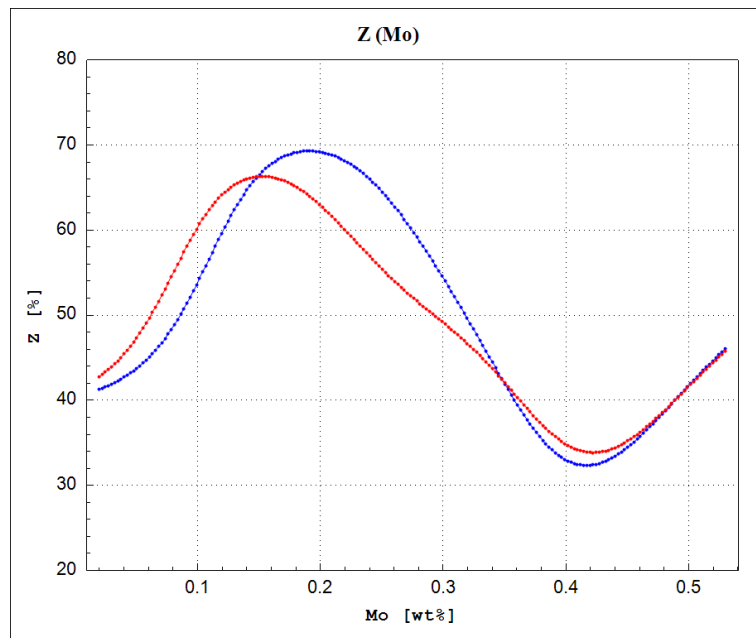


**Figure 164:** Necking as a function of the Molybdenum concentration (Mo), calculated by the ANN model on centered verification point (red line) and centered training point (blue line).

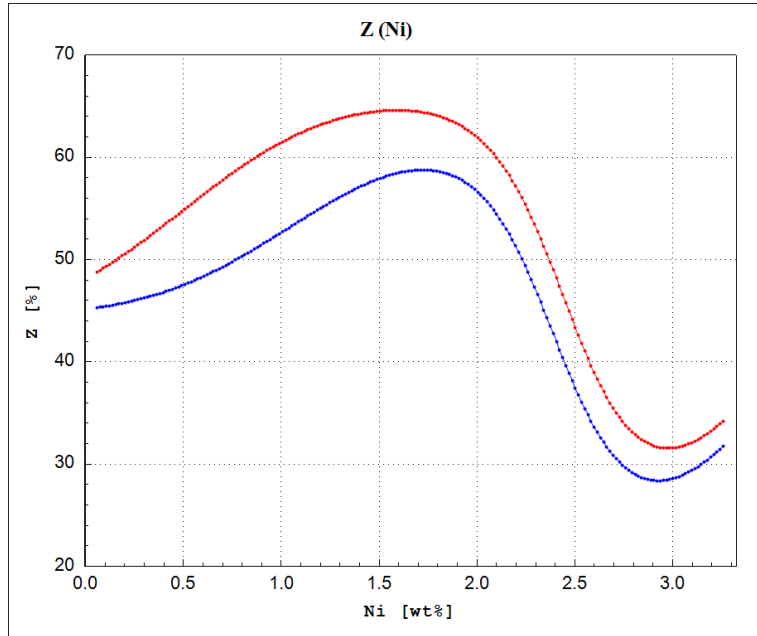


**Figure 165:** Necking as a function of the Nickel concentration (Ni), calculated by the ANN model on centered verification point (red line) and centered training point (blue line).

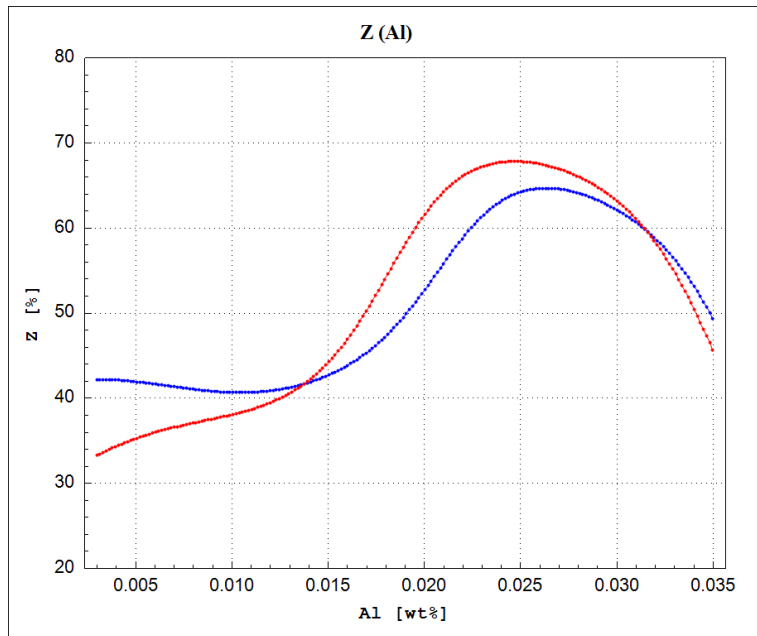


**Figure 166:** Necking as a function of the Aluminium concentration (Al), calculated by the ANN model on centered verification point (red line) and centered training point (blue line).

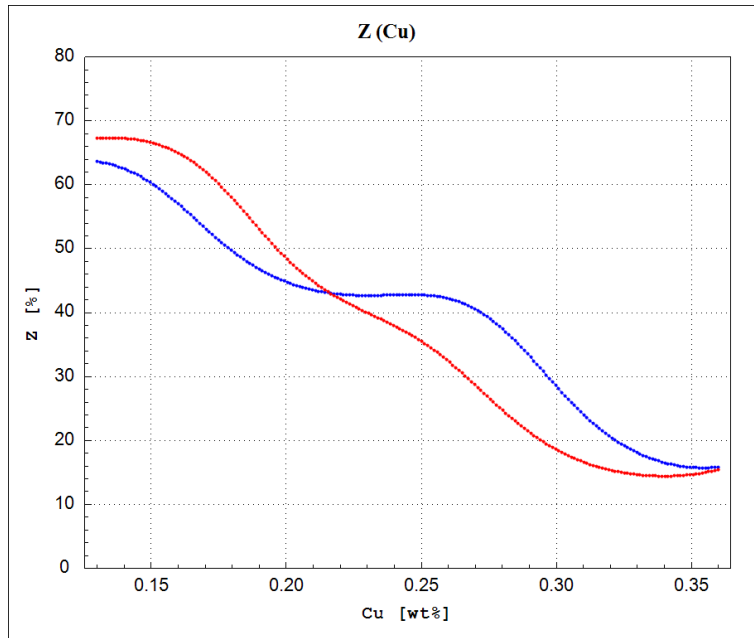


**Figure 167:** Necking as a function of the Copper concentration (Cu), calculated by the ANN model on centered verification point (red line) and centered training point (blue line).

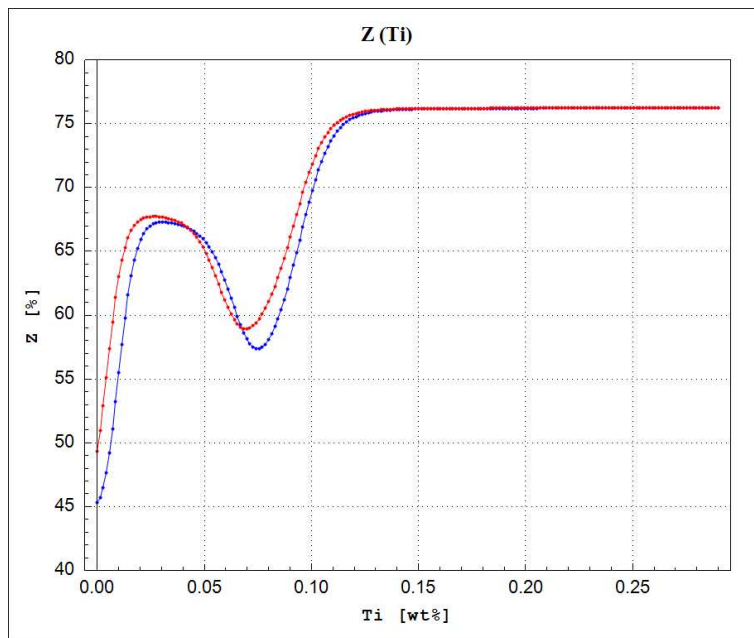


**Figure 168:** Necking as a function of the Titanium concentration (Ti), calculated by the ANN model on centered verification point (red line) and centered training point (blue line).

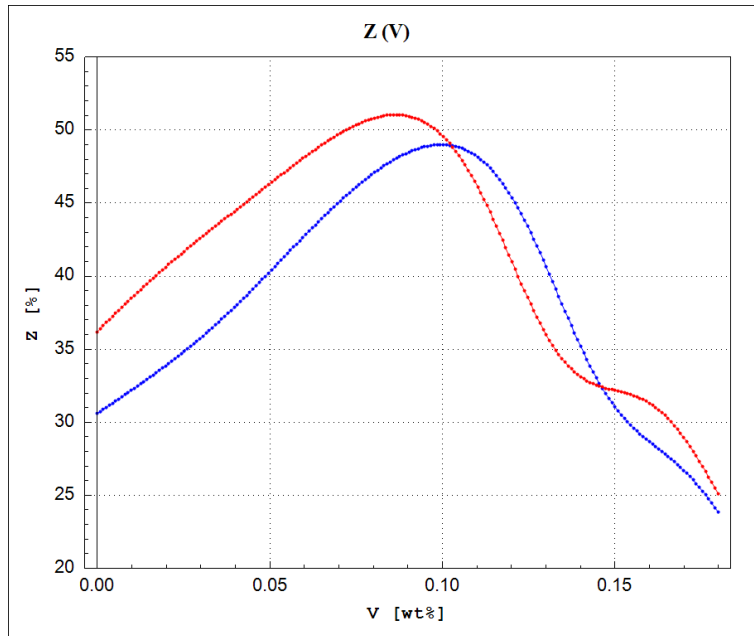


**Figure 169:** Necking as a function of the Vanadium concentration (V), calculated by the ANN model on centered verification point (red line) and centered training point (blue line).

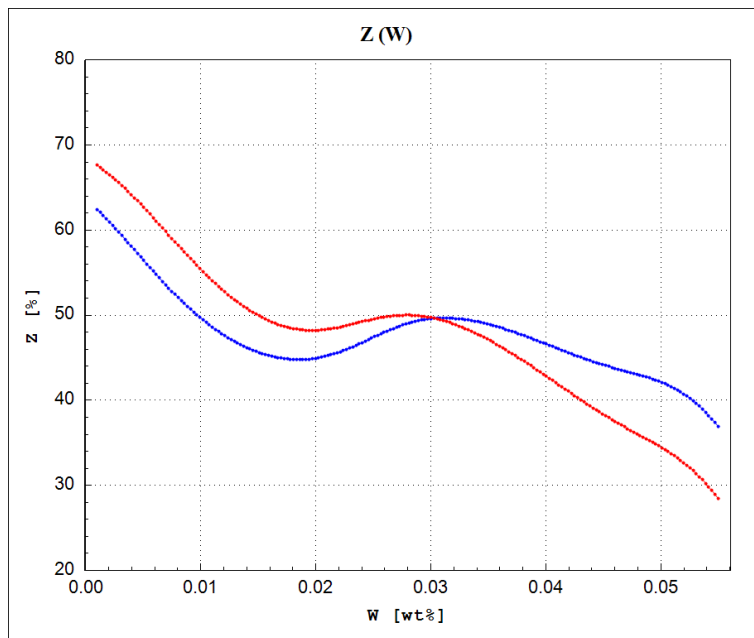


**Figure 170:** Necking as a function of the Tungsten concentration (W), calculated by the ANN model on centered verification point (red line) and centered training point (blue line).

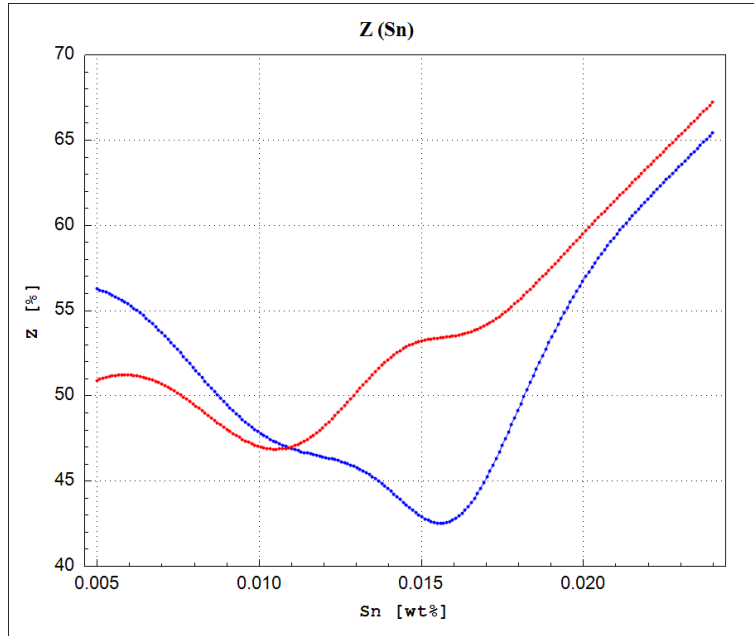


**Figure 171:** Necking as a function of the Tin concentration (Sn), calculated by the ANN model on centered verification point (red line) and centered training point (blue line).

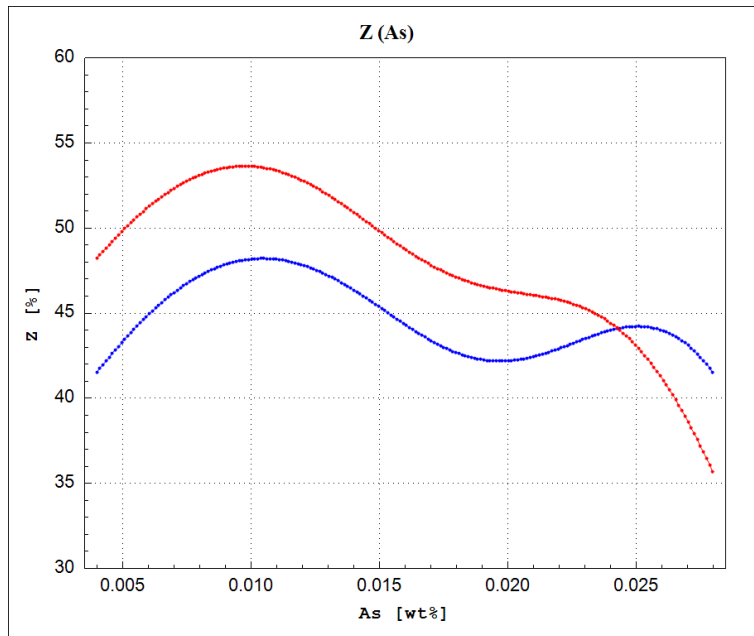


**Figure 172:** Necking as a function of the Arsenic concentration (As), calculated by the ANN model on centered verification point (red line) and centered training point (blue line).

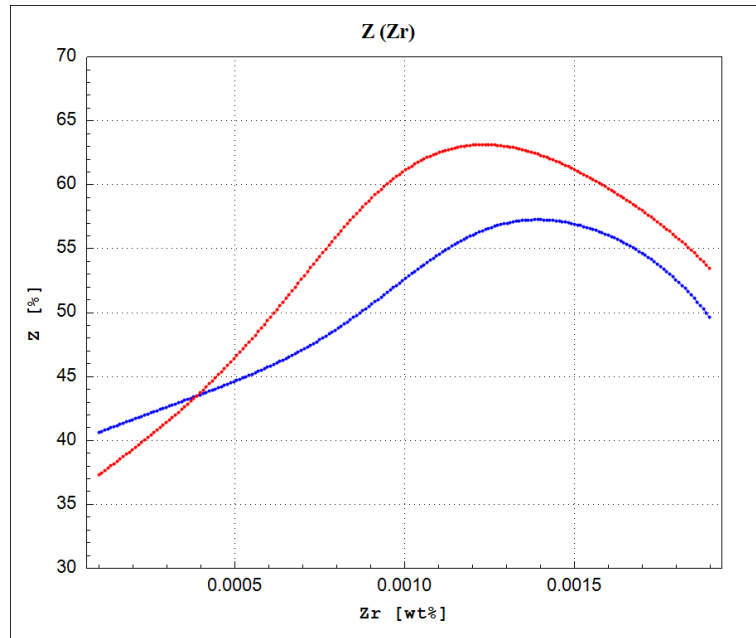


**Figure 173:** Necking as a function of the Zirconium concentration (Zr), calculated by the ANN model on centered verification point (red line) and centered training point (blue line).

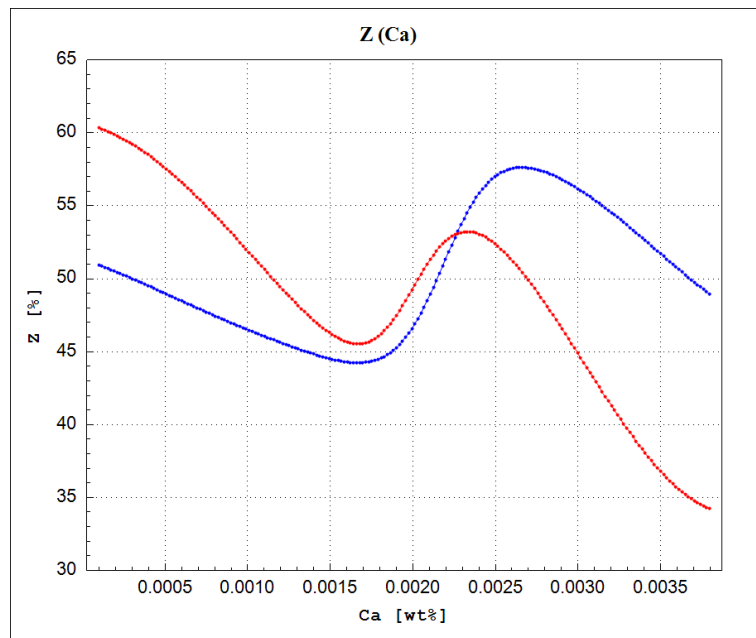


**Figure 174:** Necking as a function of the Calcium concentration (Ca), calculated by the ANN model on centered verification point (red line) and centered training point (blue line).

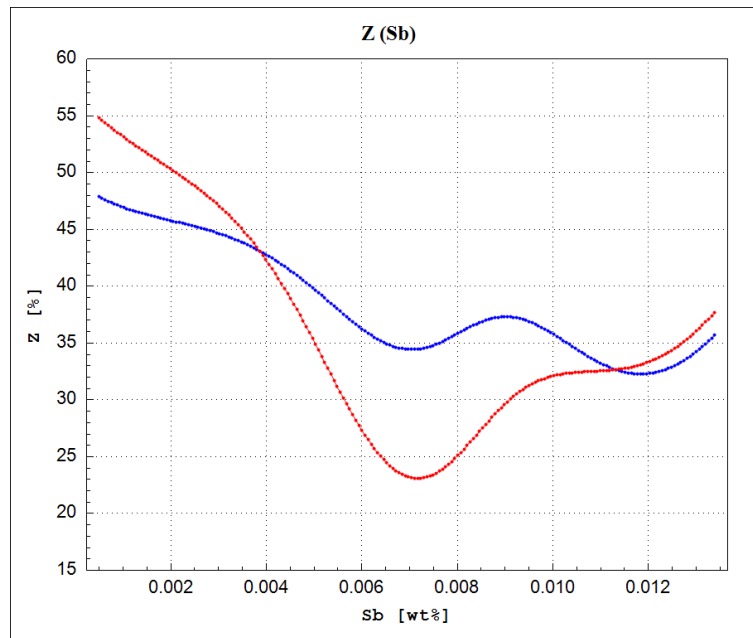


**Figure 175:** Necking as a function of the Antimony concentration (Sb), calculated by the ANN model on centered verification point (red line) and centered training point (blue line).

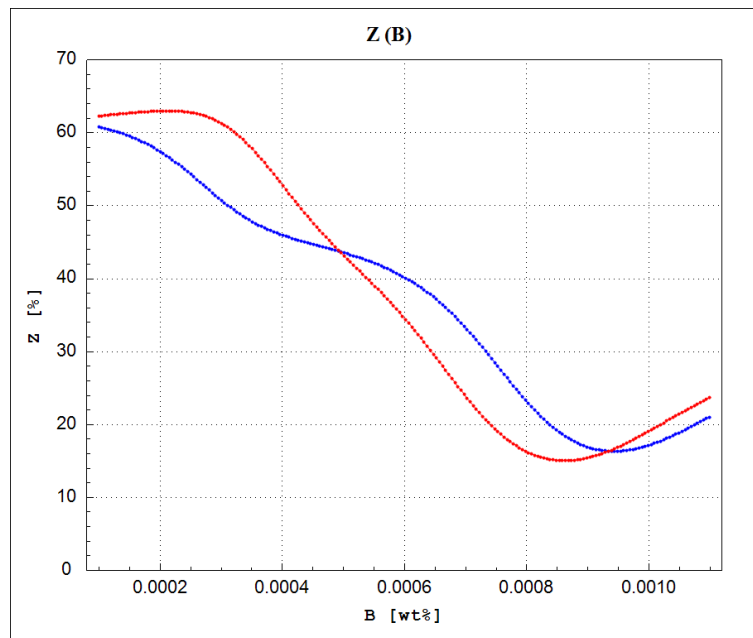


**Figure 176:** Necking as a function of the Boron concentration (B), calculated by the ANN model on centered verification point (red line) and centered training point (blue line).

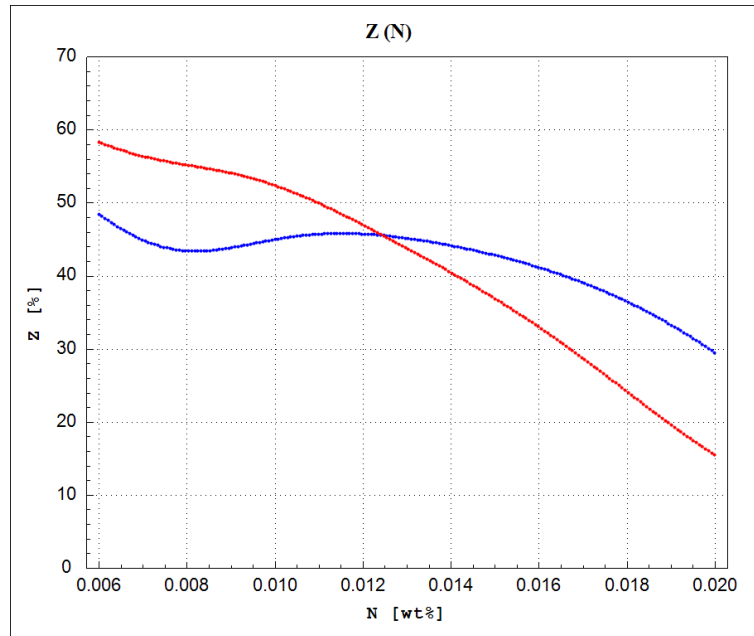


**Figure 177:** Necking as a function of the Nitrogen concentration (N), calculated by the ANN model on centered verification point (red line) and centered training point (blue line).

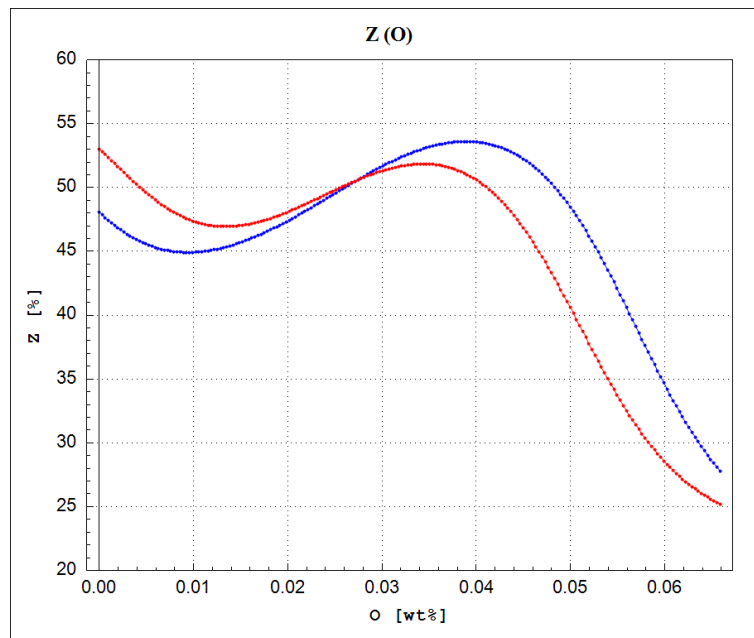


**Figure 178:** Necking as a function of the Oxygen concentration (O), calculated by the ANN model on centered verification point (red line) and centered training point (blue line).

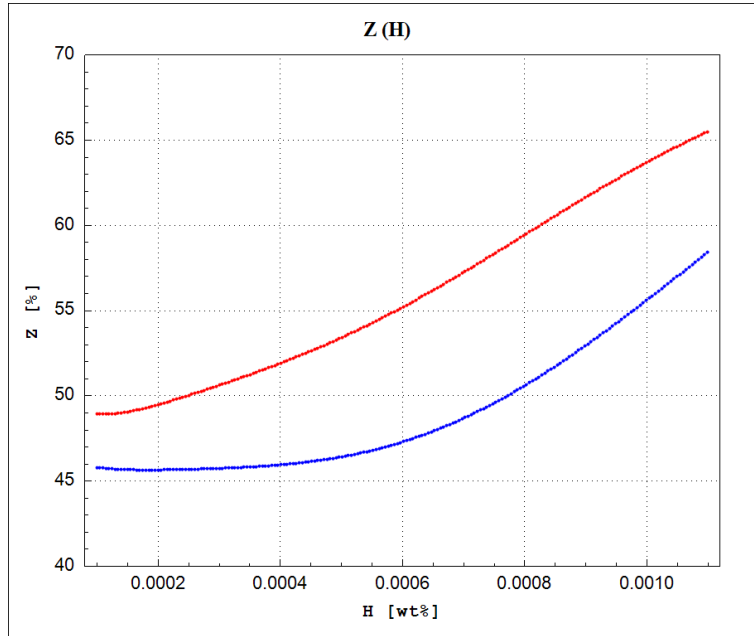


**Figure 179:** Necking as a function of the Hydrogen concentration (H), calculated by the ANN model on centered verification point (red line) and centered training point (blue line).

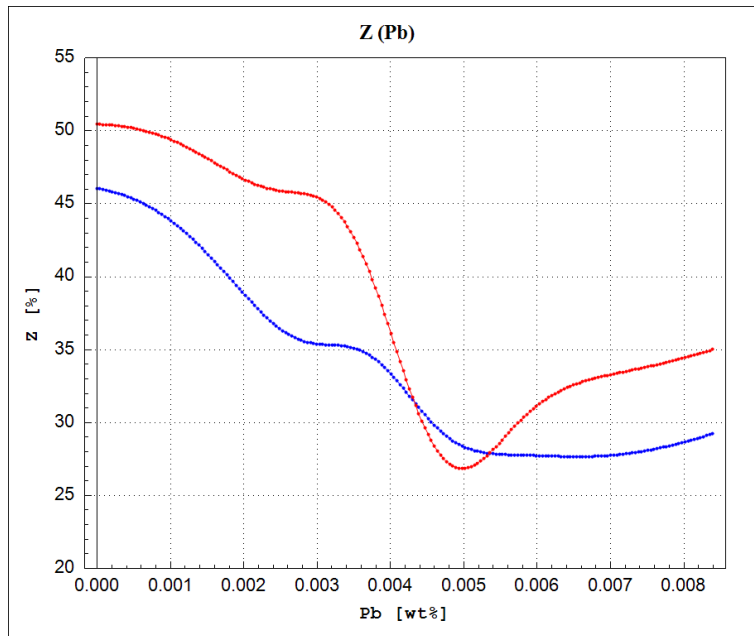


**Figure 180:** Necking as a function of the Lead concentration (Pb), calculated by the ANN model on centered verification point (red line) and centered training point (blue line).

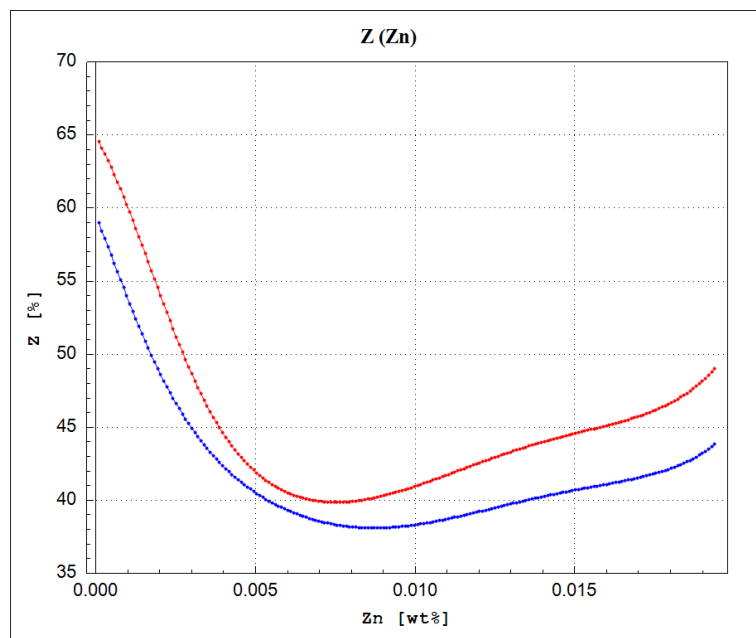


**Figure 181:** Necking as a function of the Zinc concentration (Zn), calculated by the ANN model on centered verification point (red line) and centered training point (blue line).

## 5.2 Points on Line

We chose two points ( $\mathbf{p}_I, \mathbf{p}_F$ ) from the training data-set and from verification data-set.  $\mathbf{p}_I$  represents initial point with minimum parameters from elected data-set, and  $\mathbf{p}_F$  represents final point, with maximum parameters from that data-set. Then we took a certain number of equally spaced points on the line segment between these two points (including the chosen points). The effects of variation of certain parameters were done for all points and are represented from Figure 182 to Figure 351. The intermediate points  $\mathbf{p}_j$  were calculated according to

$$\mathbf{p}_j = \mathbf{p}_I + (\mathbf{p}_F - \mathbf{p}_I) \frac{j}{n+1}; \quad j = 0, 1, 2, \dots, n+1, \quad (4)$$

where  $j$  is the number of the intermediate points.

### 5.2.1 Elongation (A)

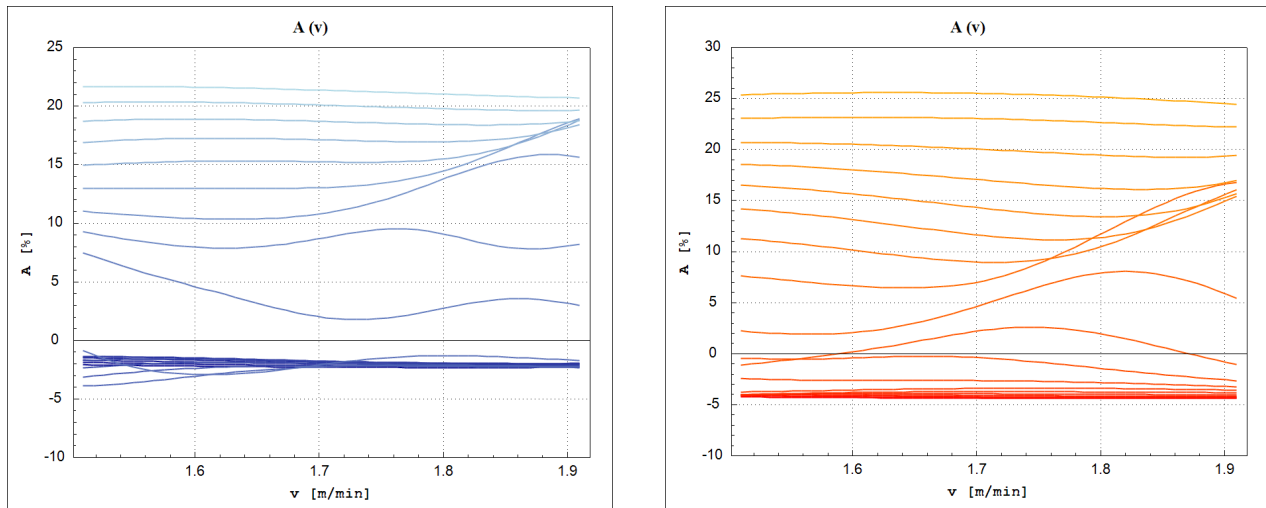


**Figure 182:** Elongation as a function of the continuous casting speed, calculated by the ANN model in two points from the data set, and for 18 other points on the line between them. Left: training data set. Right: verification data set.

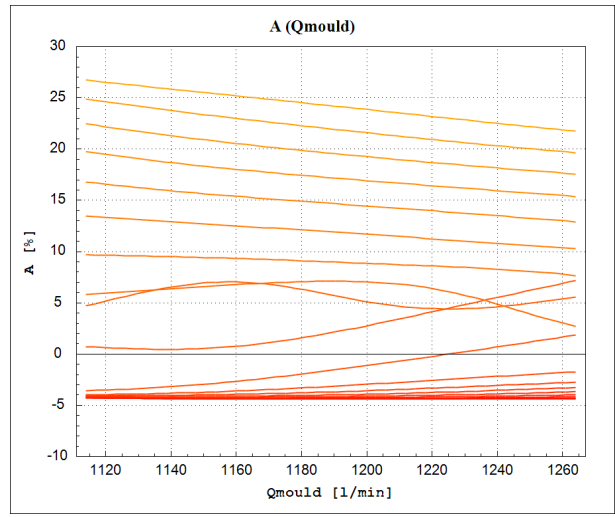
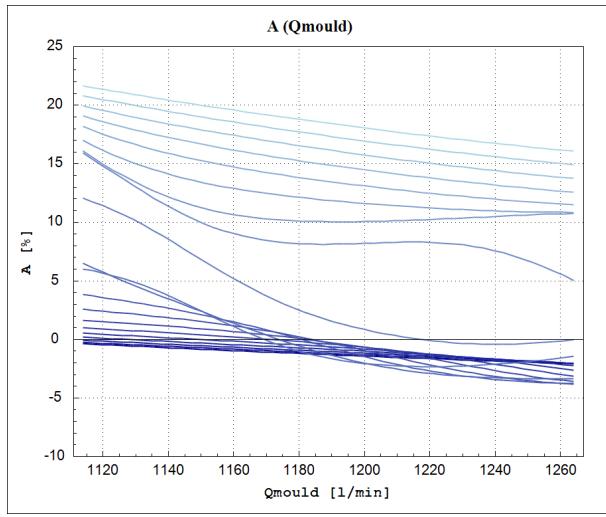


**Figure 183:** Elongation as a function of the cooling flow rate in the mould, calculated by the ANN model on centered verification point (red line) and centered training point (blue line).

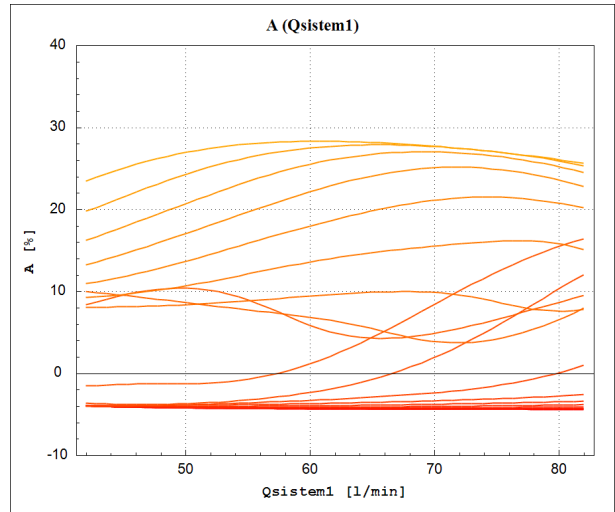
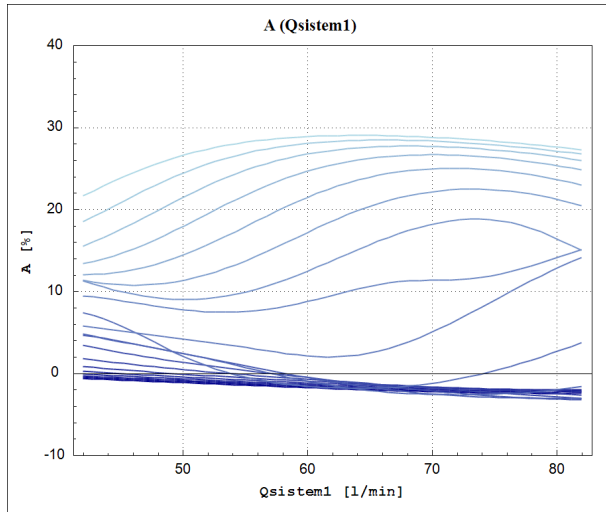


**Figure 184:** Elongation as a function of the cooling flow rate in 1<sup>st</sup> spray system, calculated by the ANN model on centered verification point (red line) and centered training point (blue line).

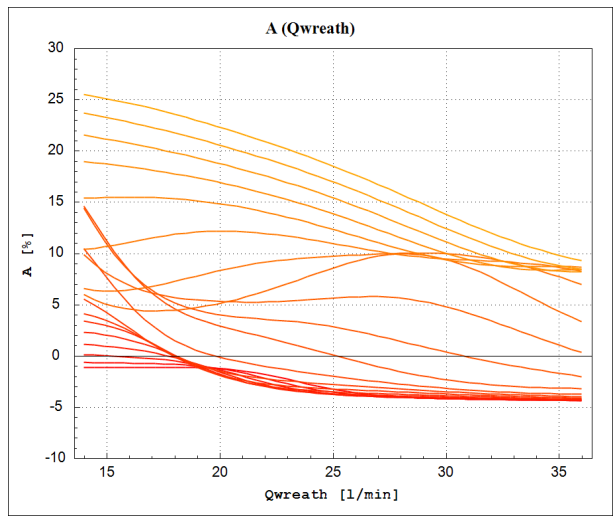
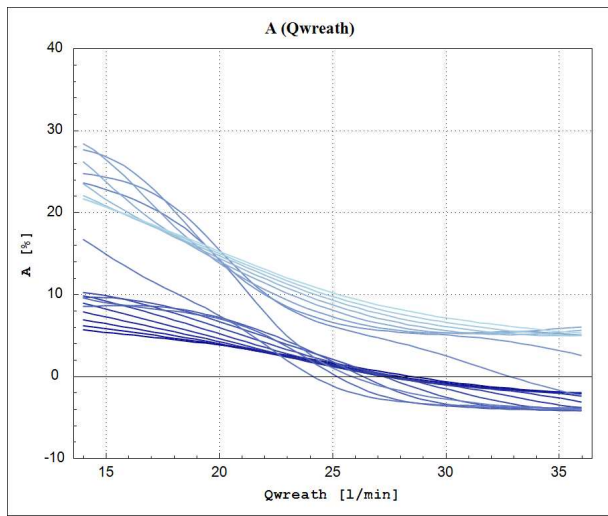


**Figure 185:** Elongation as a function of the cooling flow rate in wreath spray system, calculated by the ANN model on centered verification point (red line) and centered training point (blue line).

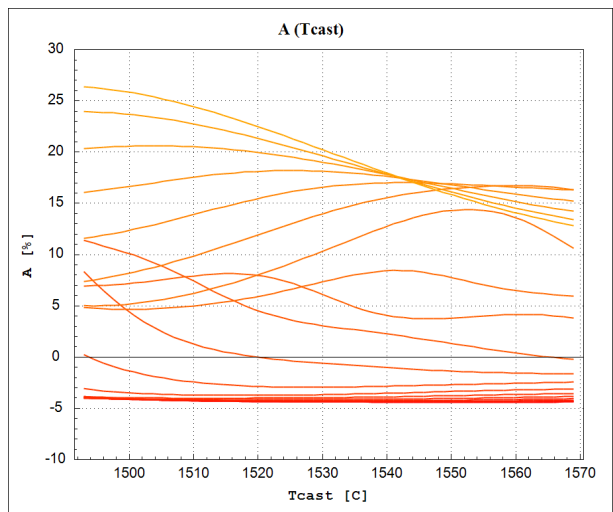
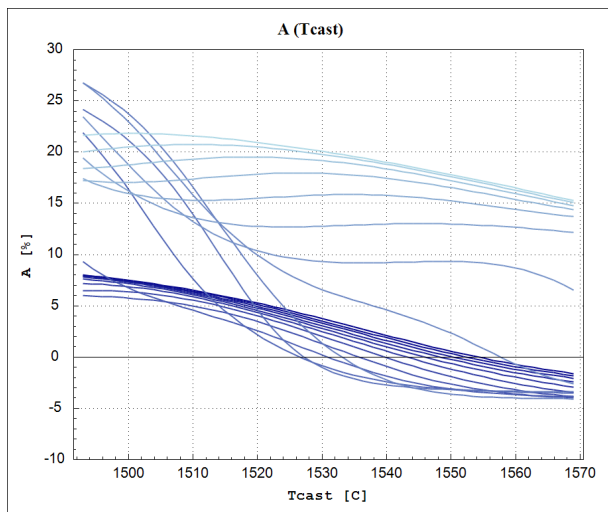


**Figure 186:** Elongation as a function of the casting temperature, calculated by the ANN model on centered verification point (red line) and centered training point (blue line).

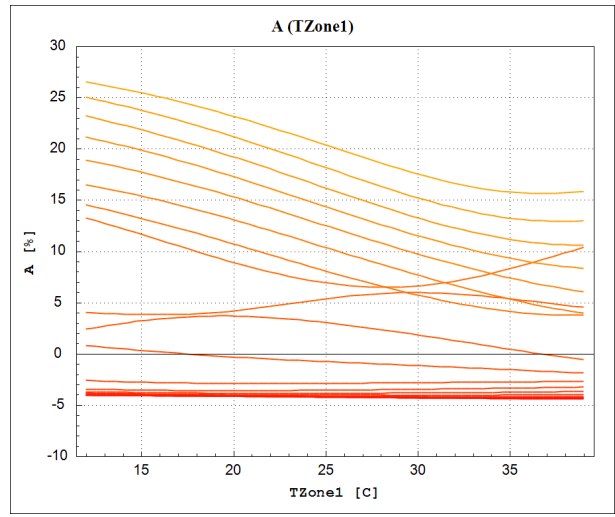
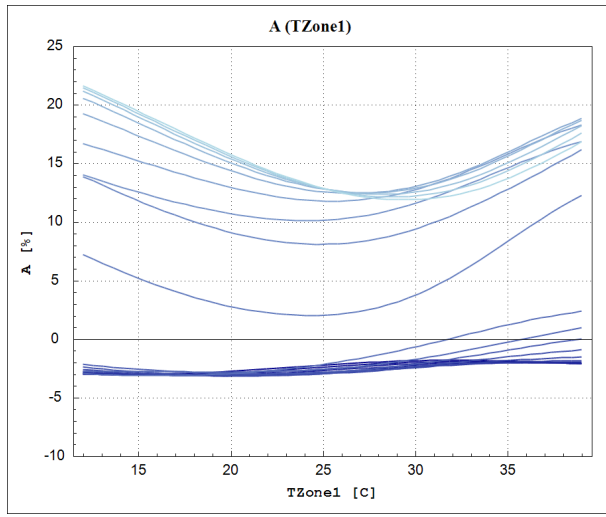


**Figure 187:** Elongation as a function of the water temperature in Zone 1, calculated by the ANN model on centered verification point (red line) and centered training point (blue line).

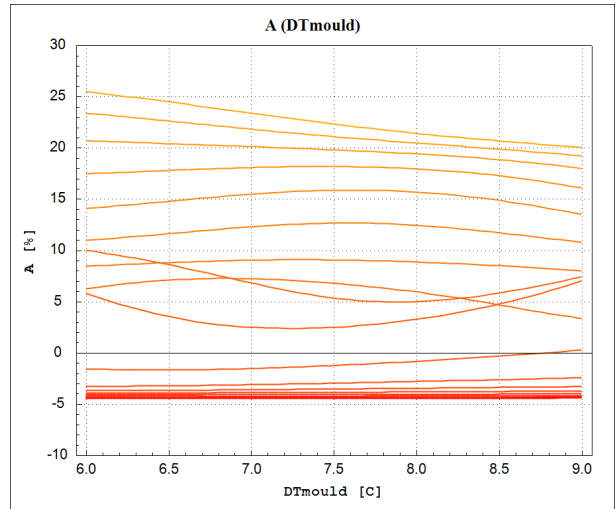
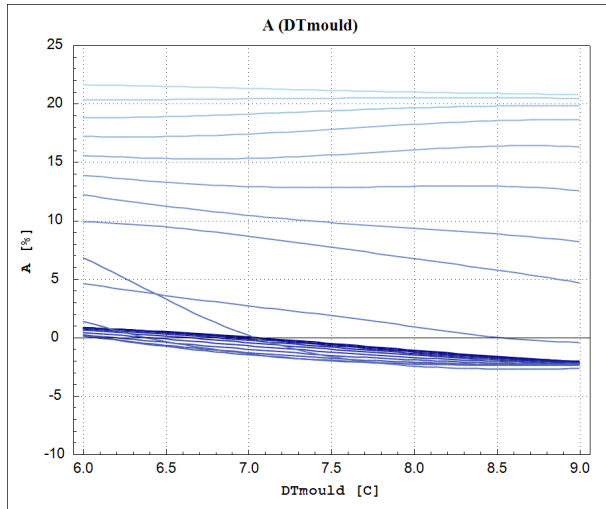


**Figure 188:** Elongation as a function of the delta T, calculated by the ANN model on centered verification point (red line) and centered training point (blue line).

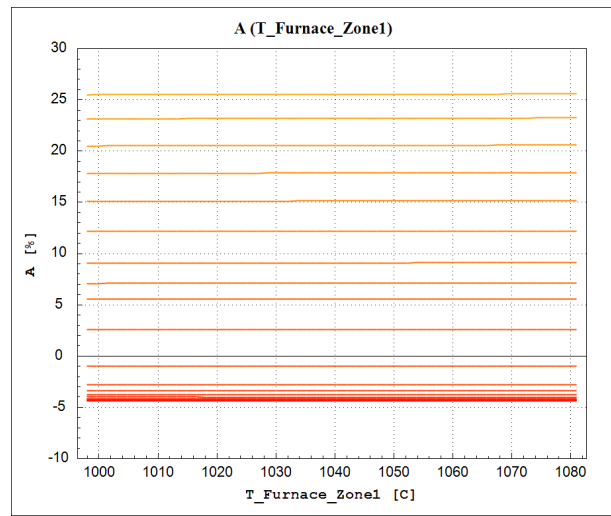
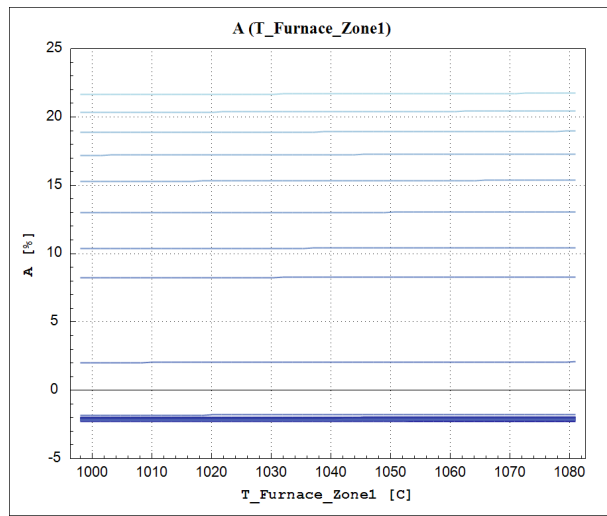


**Figure 189:** Elongation as a function of the average on temperature in zone 1, calculated by the ANN model on centered verification point (red line) and centered training point (blue line).

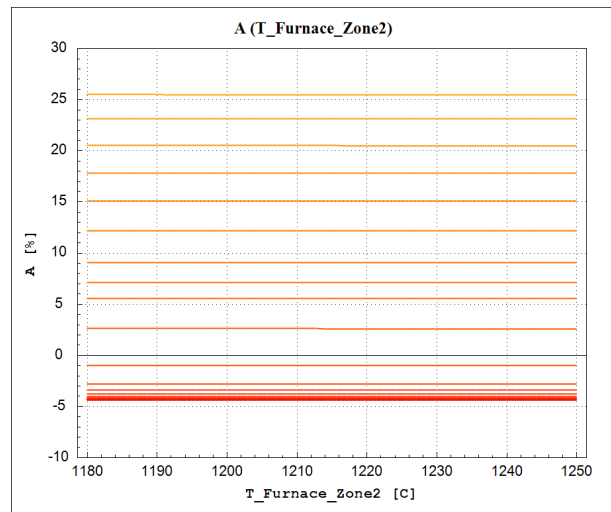
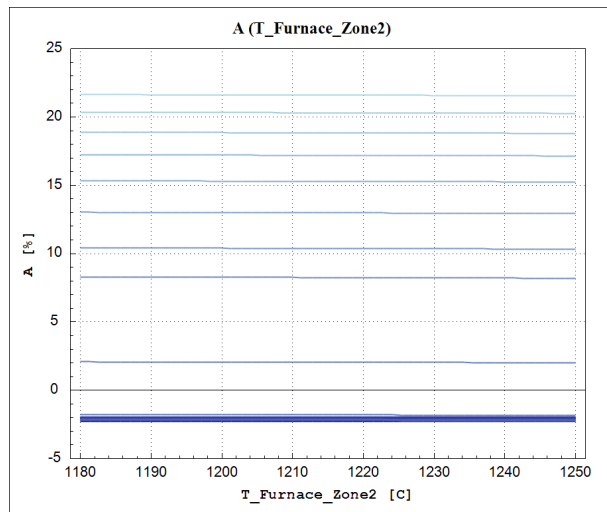


**Figure 190:** Elongation as a function of the average on temperature in zone 2, calculated by the ANN model on centered verification point (red line) and centered training point (blue line).

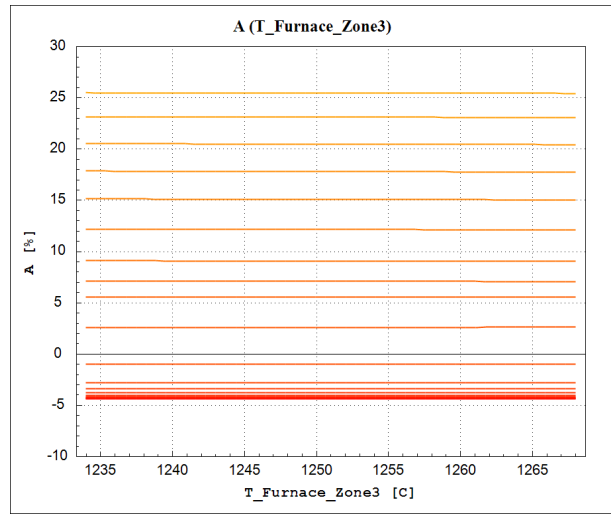
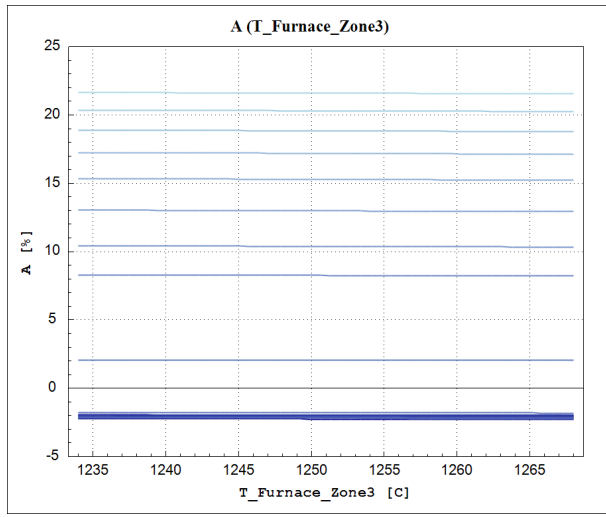


**Figure 191:** Elongation as a function of the average on temperature in zone 3, calculated by the ANN model on centered verification point (red line) and centered training point (blue line).

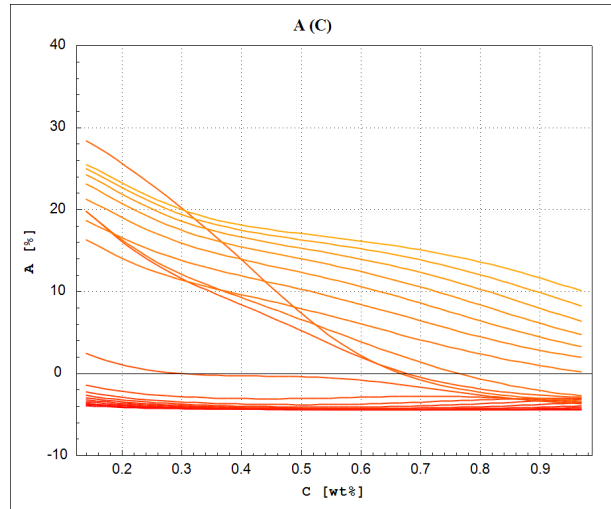
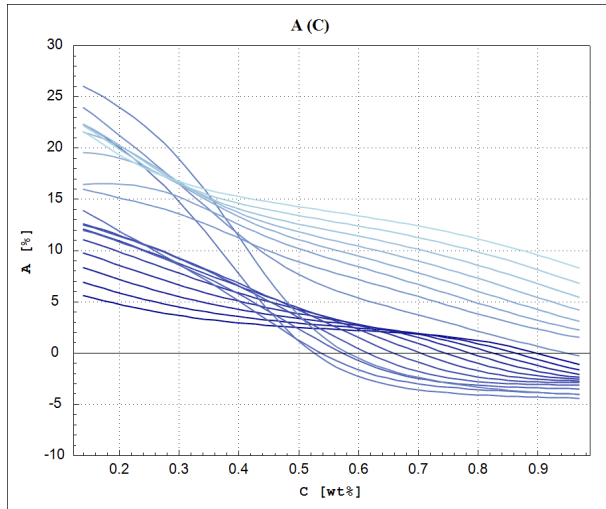


**Figure 192:** Elongation as a function of the Carbon concentration (C), calculated by the ANN model on centered verification point (red line) and centered training point (blue line).

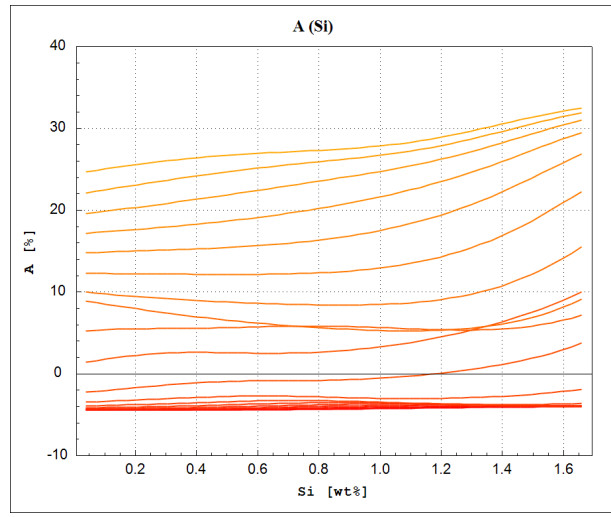
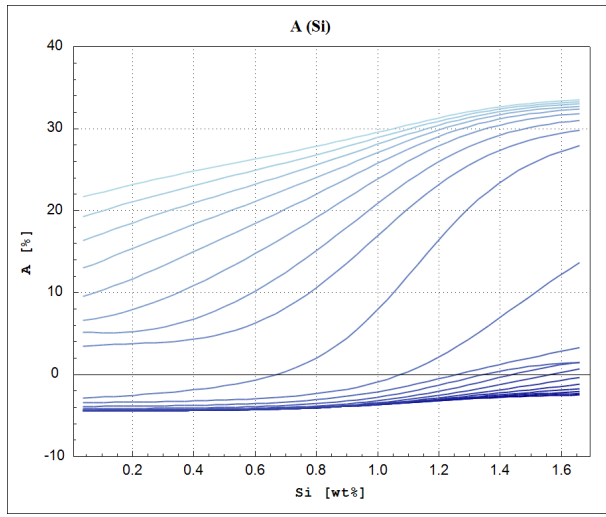


**Figure 193:** Elongation as a function of the Silicon concentration (Si), calculated by the ANN model on centered verification point (red line) and centered training point (blue line).

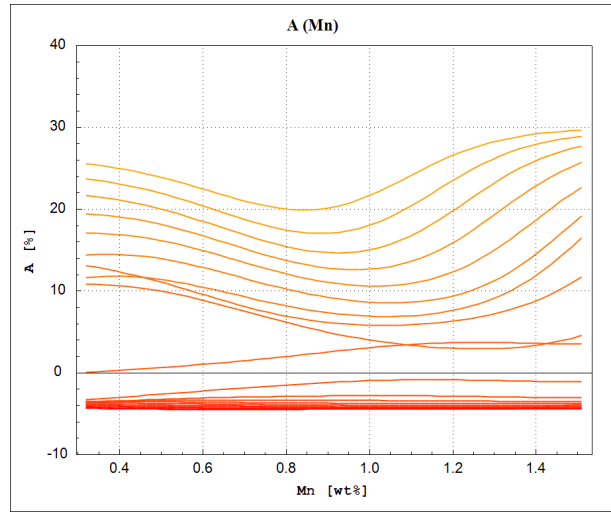
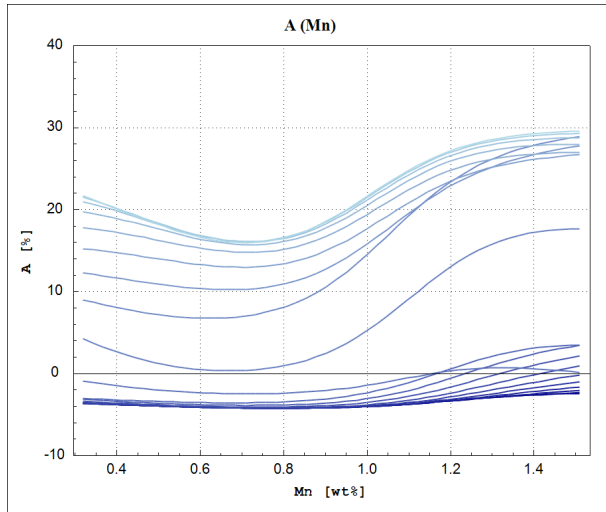


**Figure 194:** Elongation as a function of the Manganese concentration (Mn), calculated by the ANN model on centered verification point (red line) and centered training point (blue line).

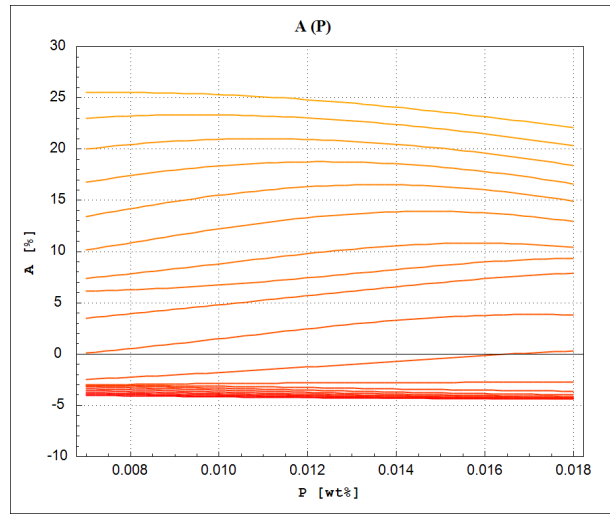
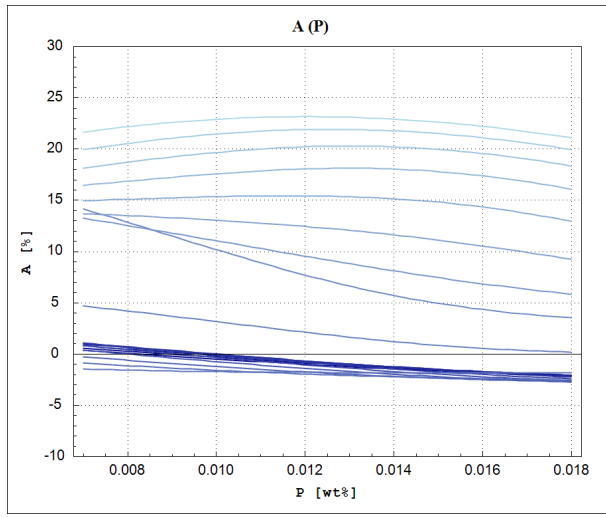


**Figure 195:** Elongation as a function of the Phosphorus concentration (P), calculated by the ANN model on centered verification point (red line) and centered training point (blue line).

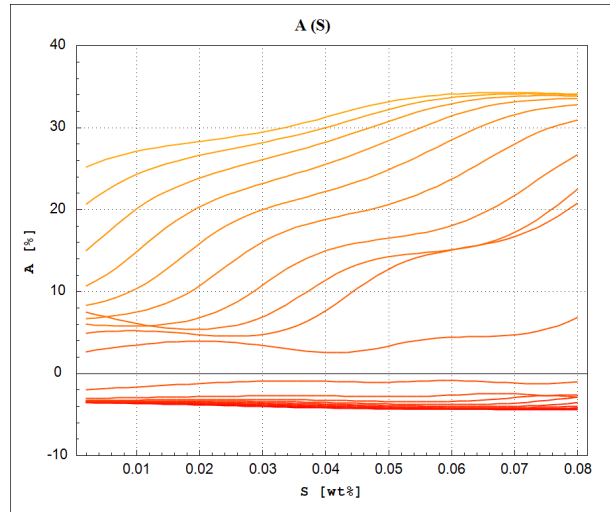
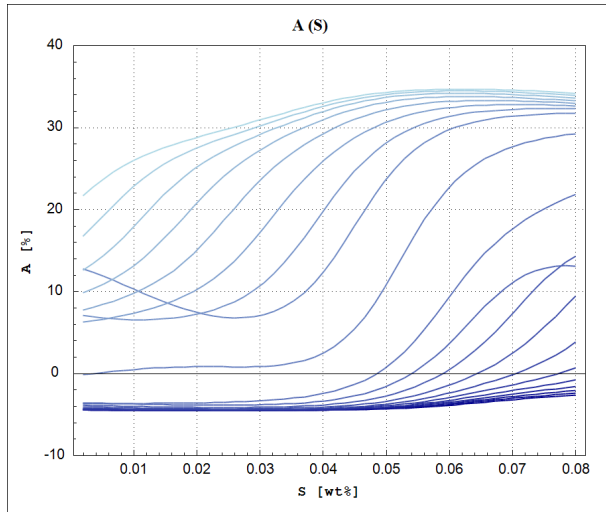


**Figure 196:** Elongation as a function of the Sulphur concentration (S), calculated by the ANN model on centered verification point (red line) and centered training point (blue line).

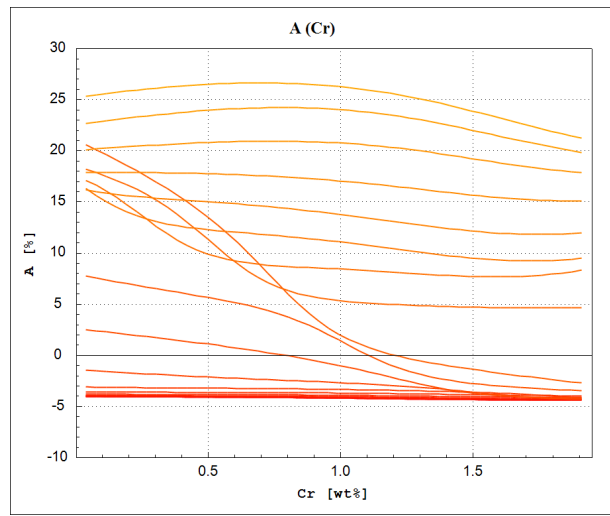
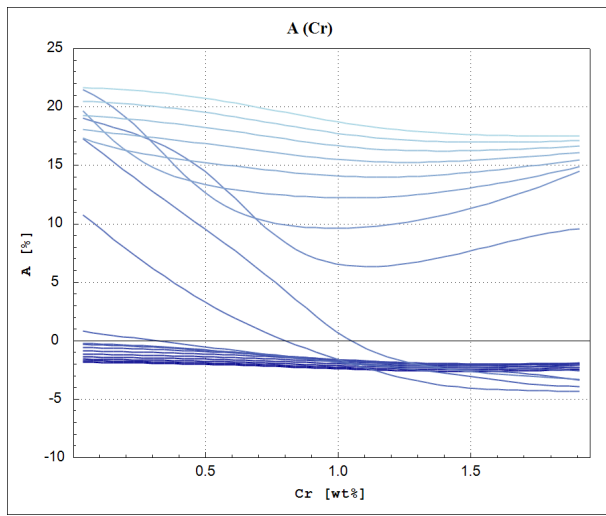


**Figure 197:** Elongation as a function of the Chromium concentration (Cr), calculated by the ANN model on centered verification point (red line) and centered training point (blue line).

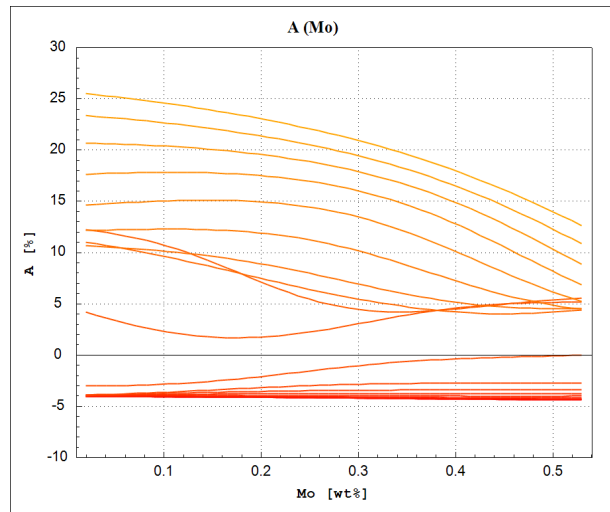
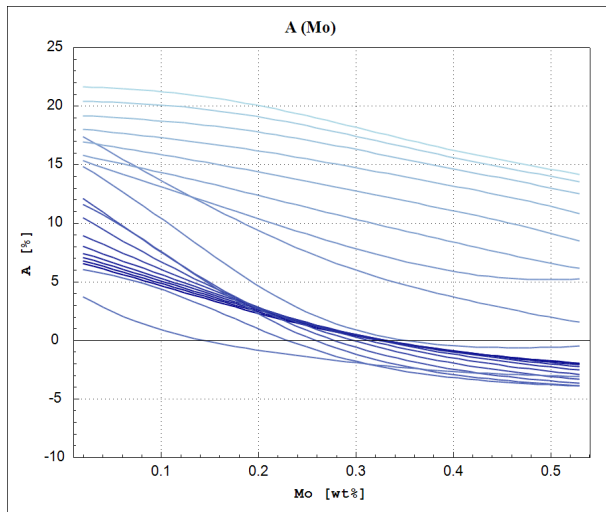


**Figure 198:** Elongation as a function of the Molybdenum concentration (Mo), calculated by the ANN model on centered verification point (red line) and centered training point (blue line).

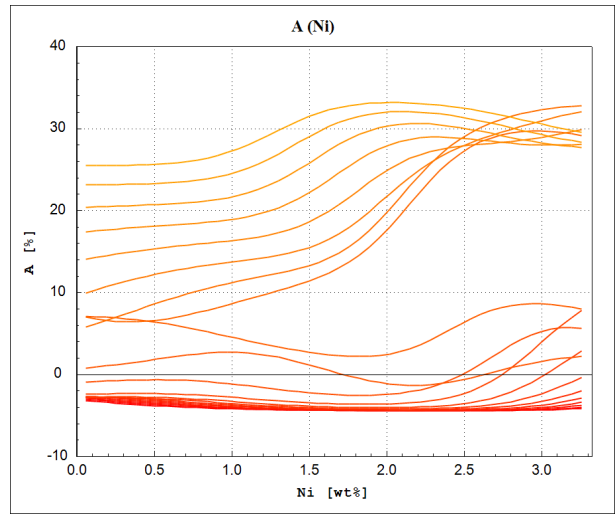
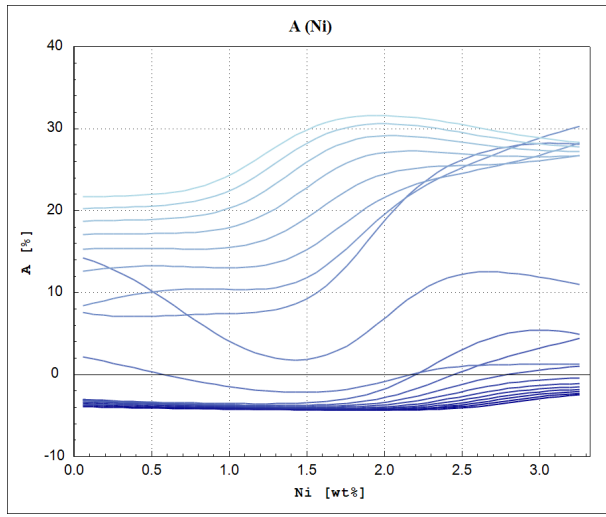


**Figure 199:** Elongation as a function of the Nickel concentration (Ni), calculated by the ANN model on centered verification point (red line) and centered training point (blue line).

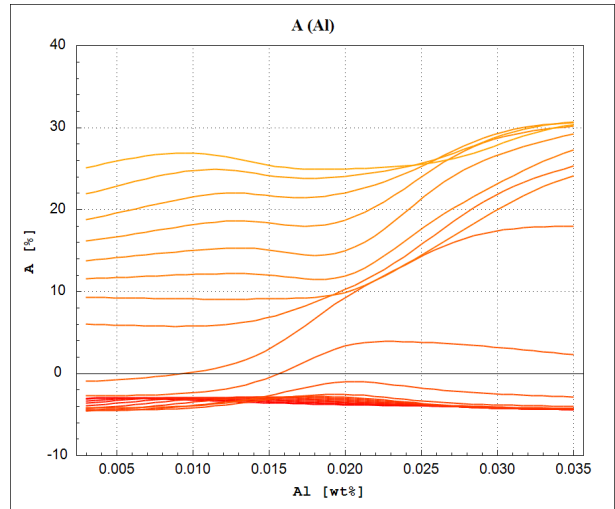
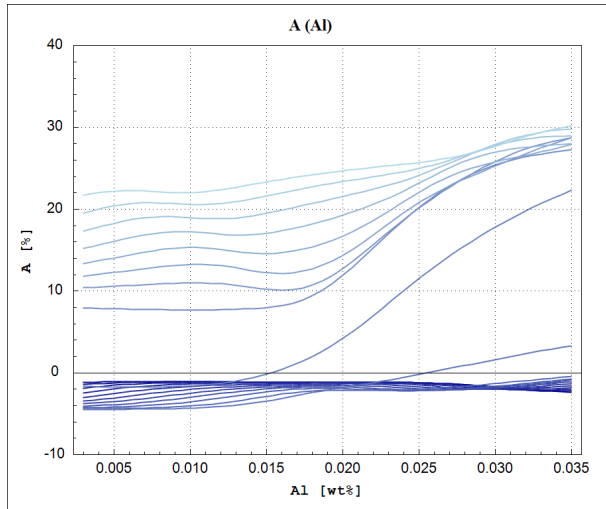


**Figure 200:** Elongation as a function of the Aluminium concentration (Al), calculated by the ANN model on centered verification point (red line) and centered training point (blue line).

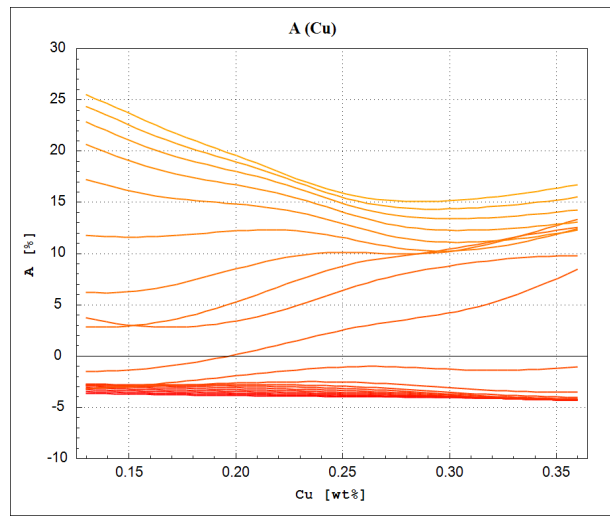
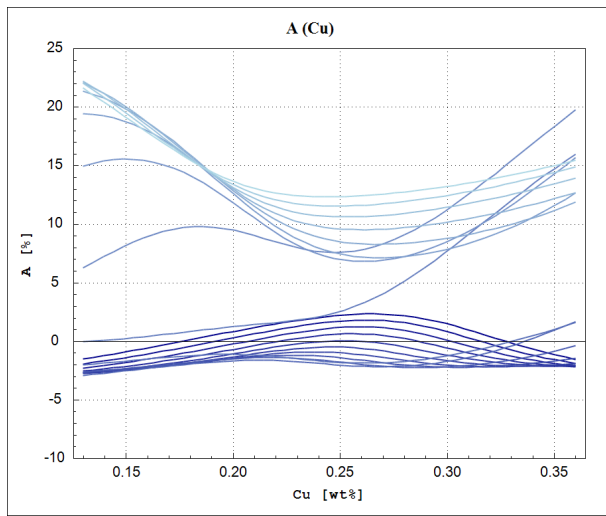


**Figure 201:** Elongation as a function of the Copper concentration (Cu), calculated by the ANN model on centered verification point (red line) and centered training point (blue line).

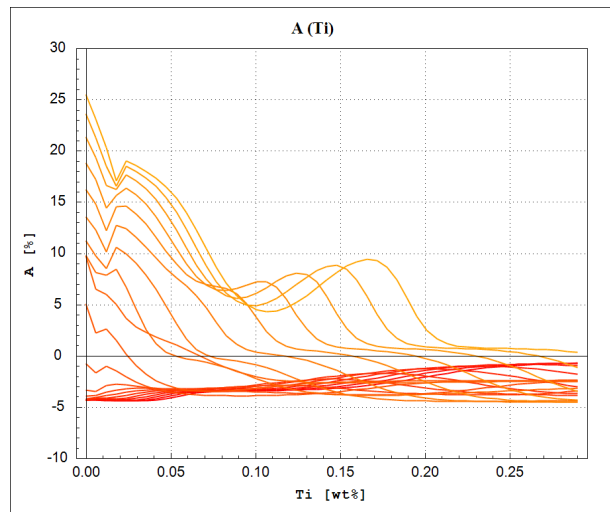
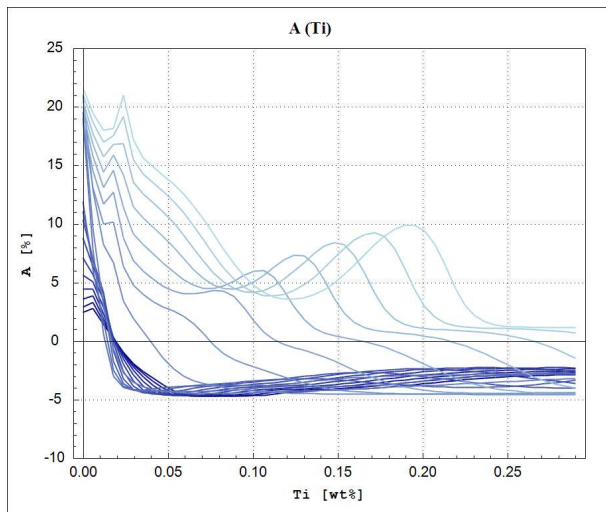


**Figure 202:** Elongation as a function of the Titanium concentration (Ti), calculated by the ANN model on centered verification point (red line) and centered training point (blue line).

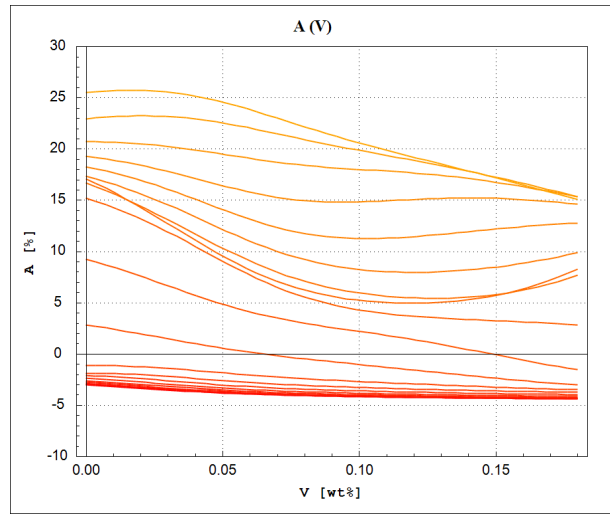
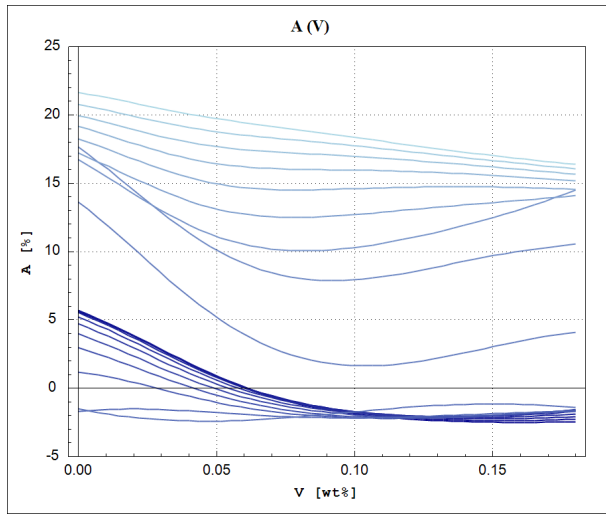


**Figure 203:** Elongation as a function of the Vanadium concentration (V), calculated by the ANN model on centered verification point (red line) and centered training point (blue line).

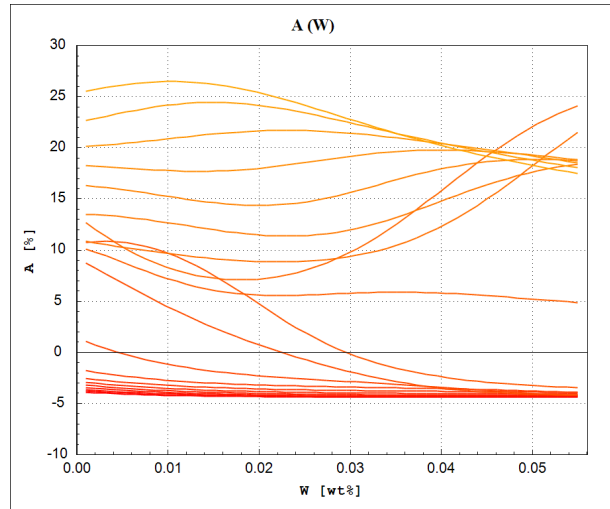
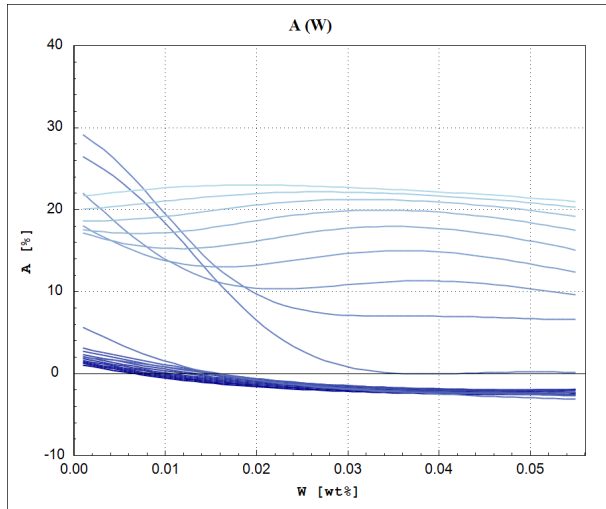


**Figure 204:** Elongation as a function of the Tungsten concentration (W), calculated by the ANN model on centered verification point (red line) and centered training point (blue line).

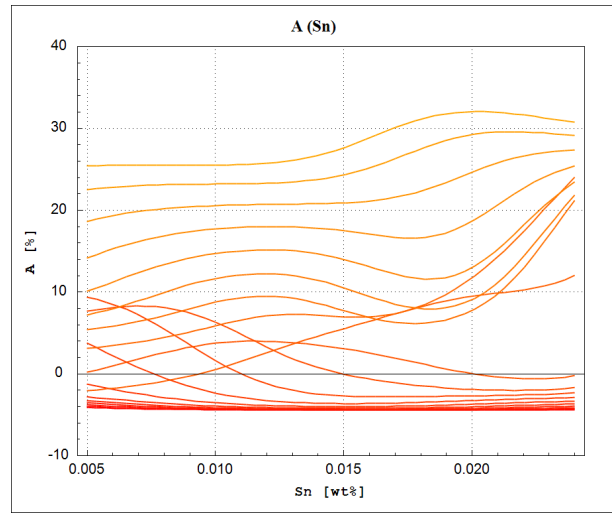
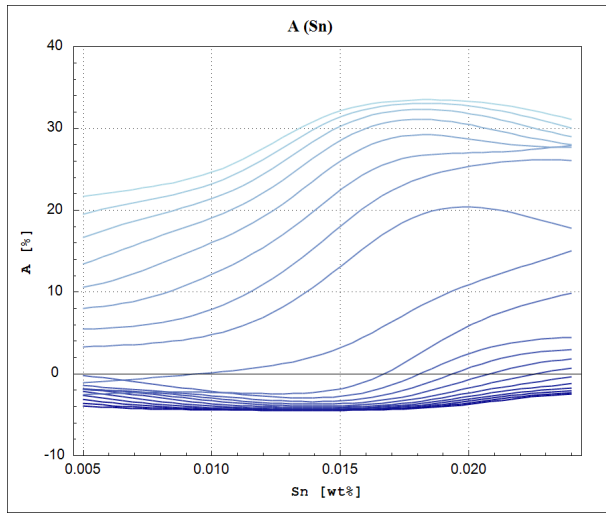


**Figure 205:** Elongation as a function of the Tin concentration (Sn), calculated by the ANN model on centered verification point (red line) and centered training point (blue line).

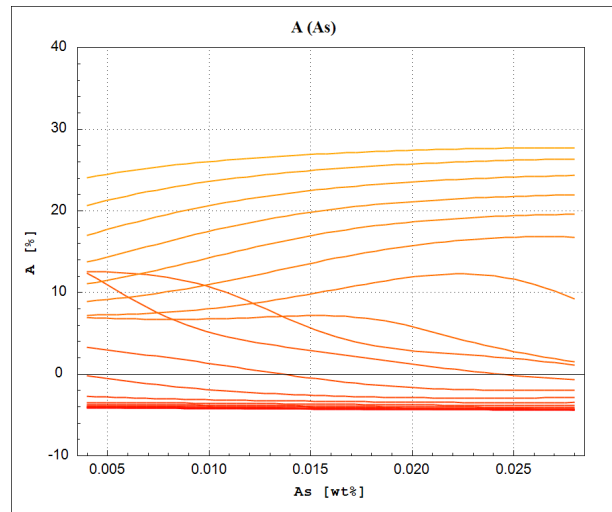
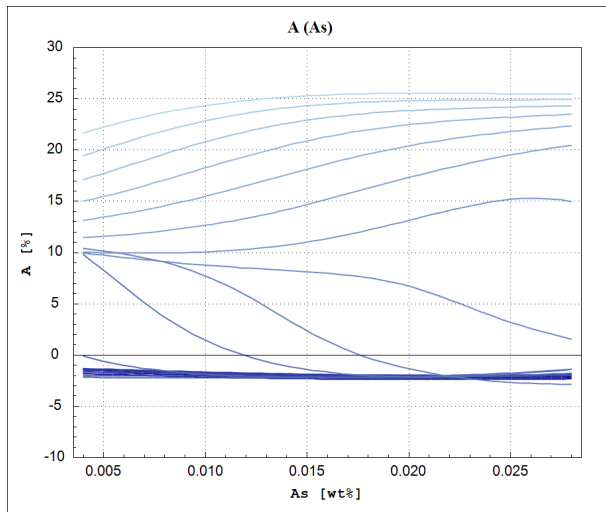


**Figure 206:** Elongation as a function of the Arsenic concentration (As), calculated by the ANN model on centered verification point (red line) and centered training point (blue line).

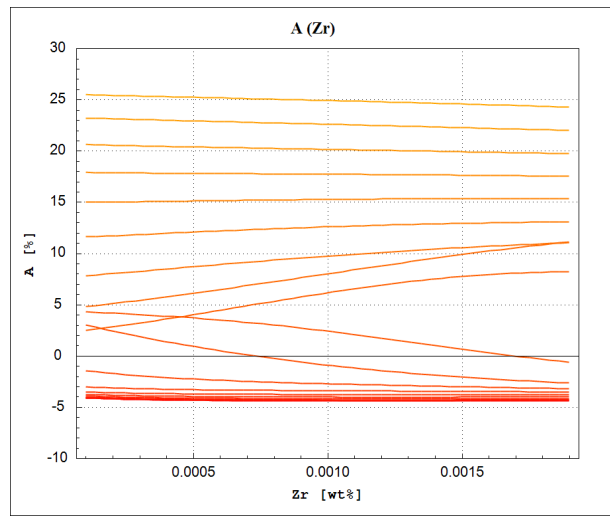
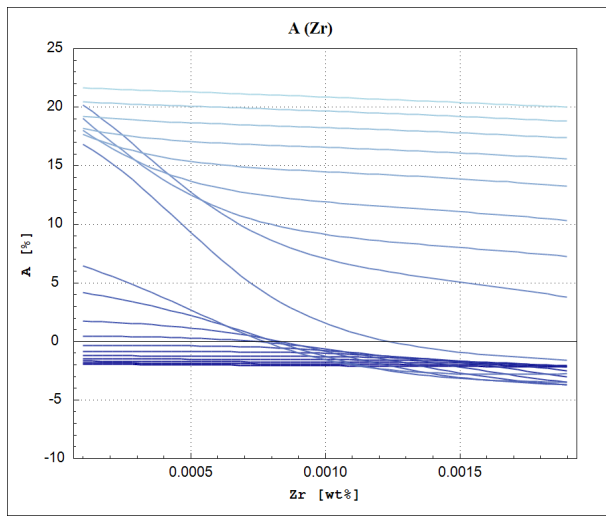


**Figure 207:** Elongation as a function of the Zirconium concentration (Zr), calculated by the ANN model on centered verification point (red line) and centered training point (blue line).

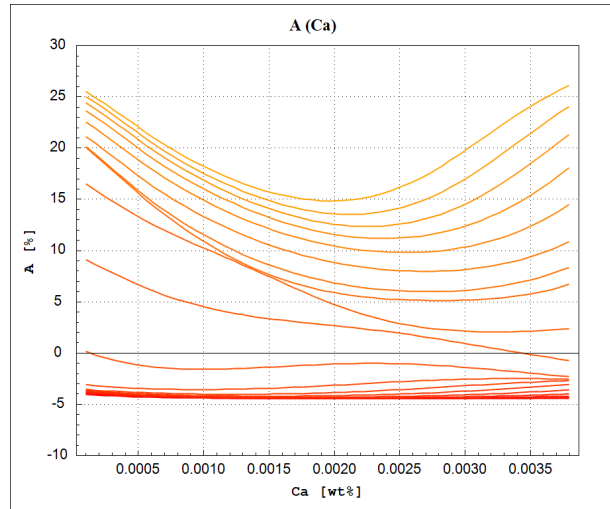
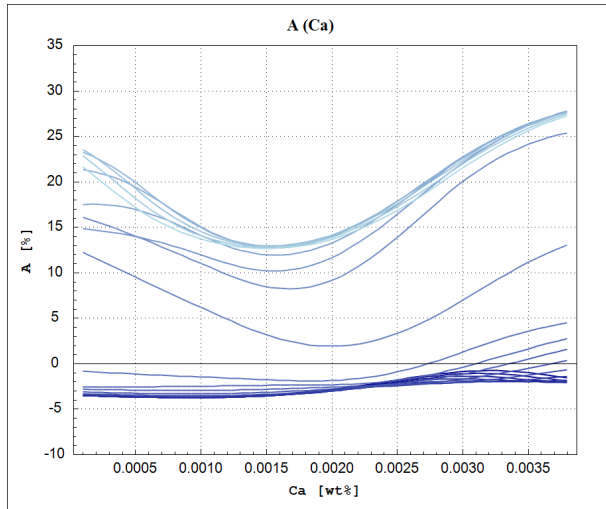


**Figure 208:** Elongation as a function of the Calcium concentration (Ca), calculated by the ANN model on centered verification point (red line) and centered training point (blue line).

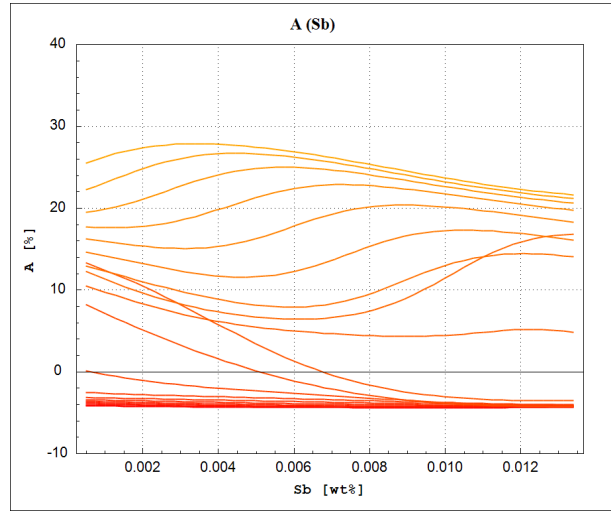
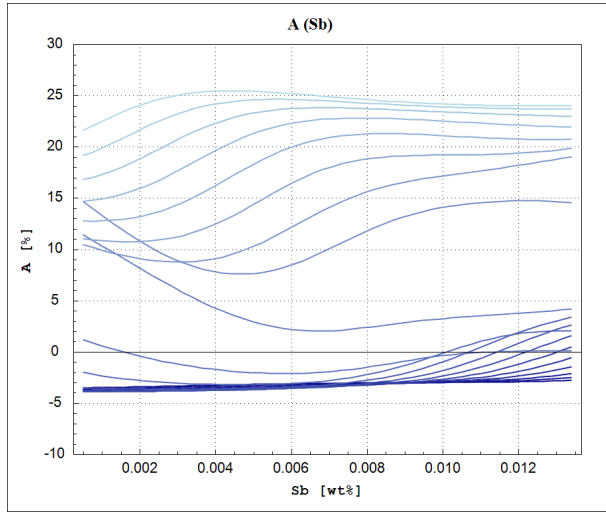


**Figure 209:** Elongation as a function of the Antimony concentration (Sb), calculated by the ANN model on centered verification point (red line) and centered training point (blue line).

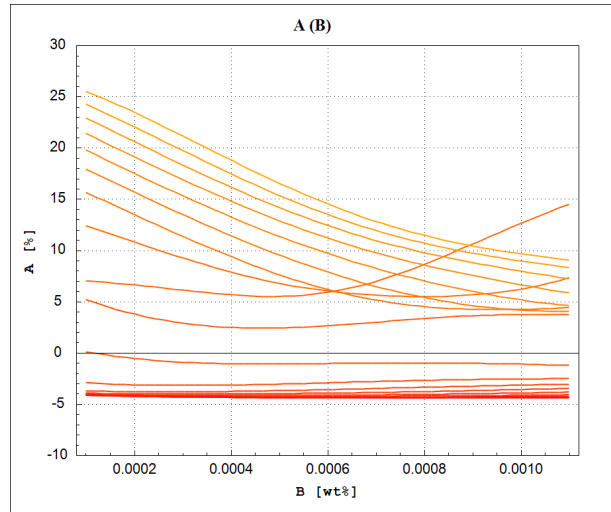
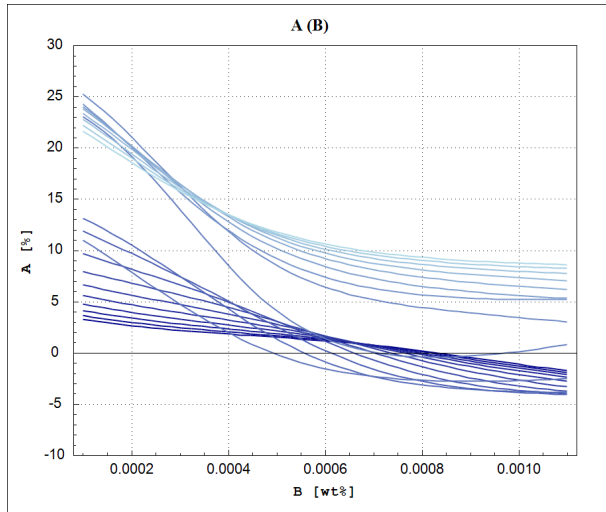


**Figure 210:** Elongation as a function of the Boron concentration (B), calculated by the ANN model on centered verification point (red line) and centered training point (blue line).

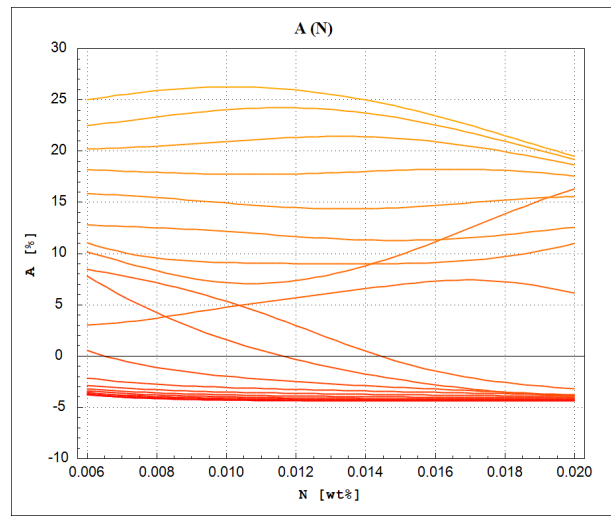
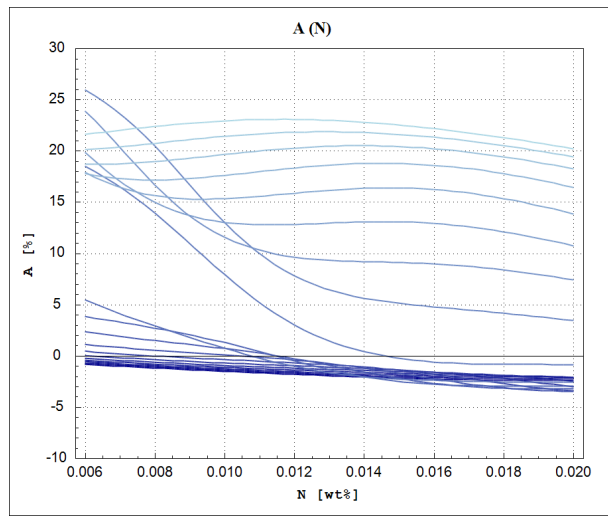


**Figure 211:** Elongation as a function of the Nitrogen concentration (N), calculated by the ANN model on centered verification point (red line) and centered training point (blue line).

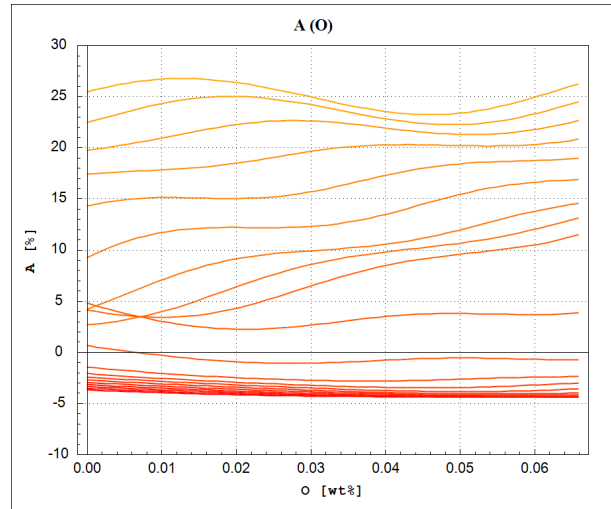
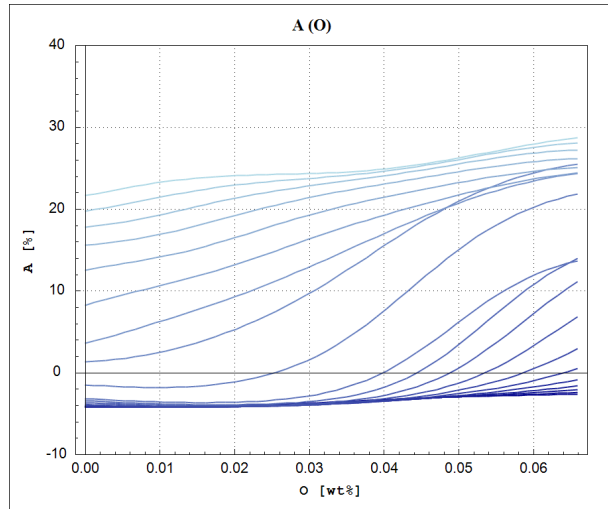


**Figure 212:** Elongation as a function of the Oxigen concentration (O), calculated by the ANN model on centered verification point (red line) and centered training point (blue line).

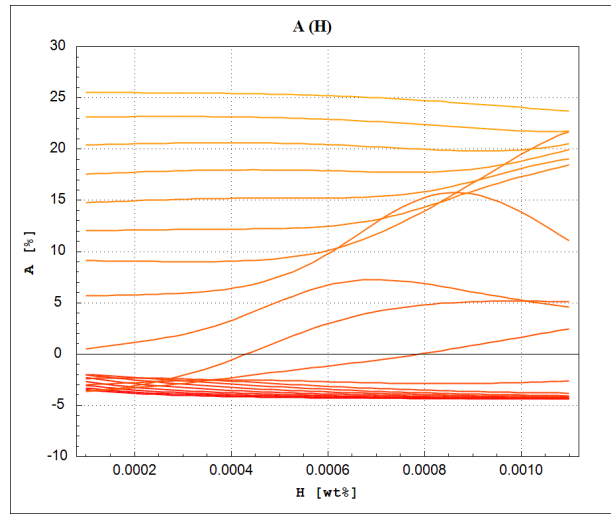
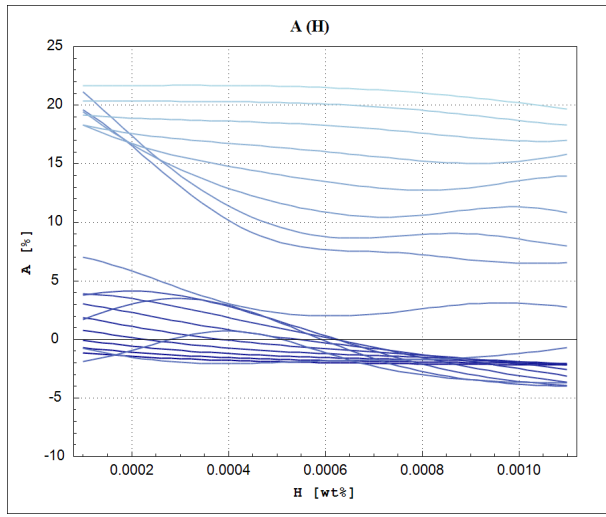


**Figure 213:** Elongation as a function of the Hydrogen concentration (H), calculated by the ANN model on centered verification point (red line) and centered training point (blue line).

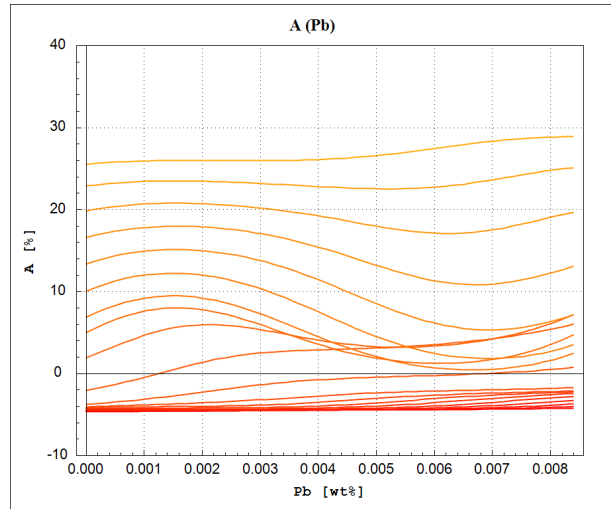
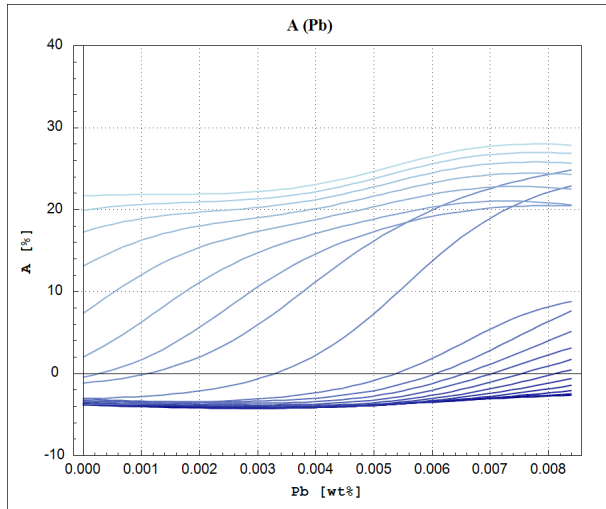


**Figure 214:** Elongation as a function of the Lead concentration (Pb), calculated by the ANN model on centered verification point (red line) and centered training point (blue line).

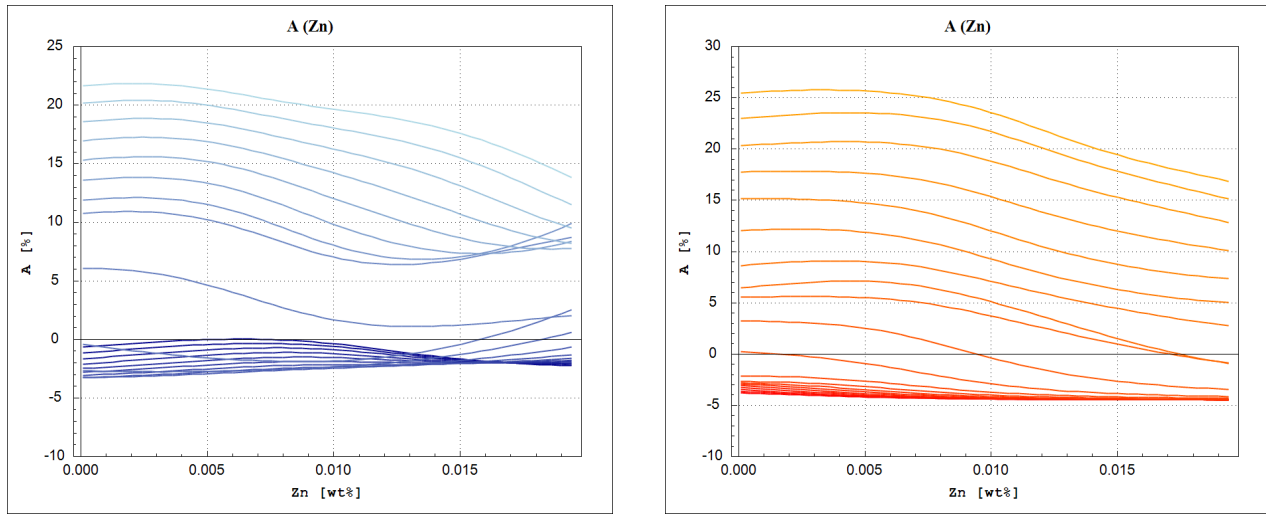


**Figure 215:** Elongation as a function of the Zinc concentration (Zn), calculated by the ANN model on centered verification point (red line) and centered training point (blue line).

### 5.2.2 Tensile Strength ( $R_m$ )

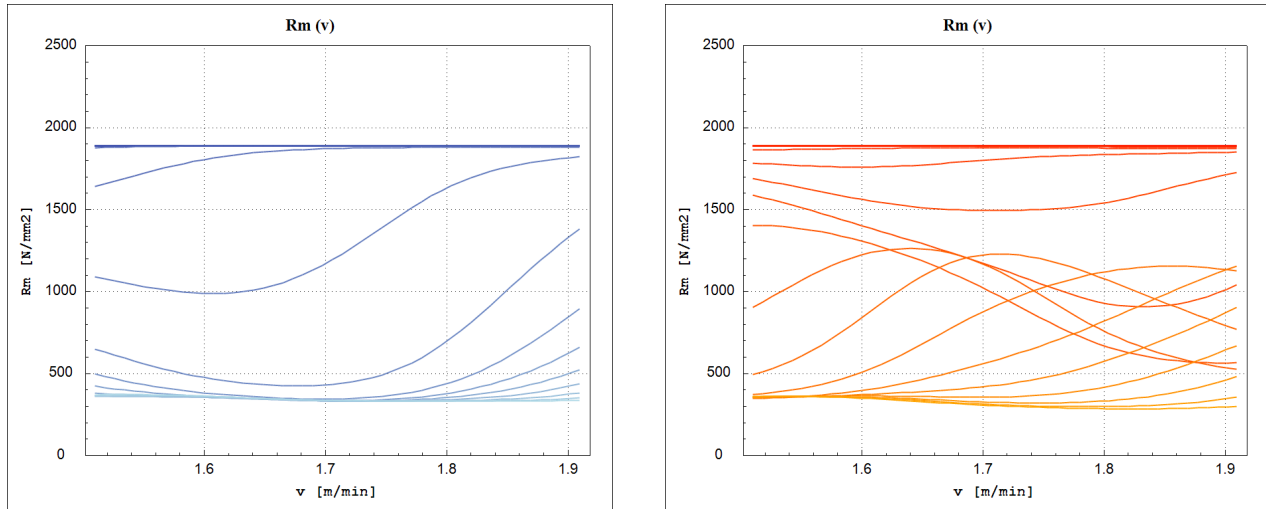


**Figure 216:** Tensile strength as a function of the continuous casting speed, calculated by the ANN model on centered verification point (red line) and centered training point (blue line).

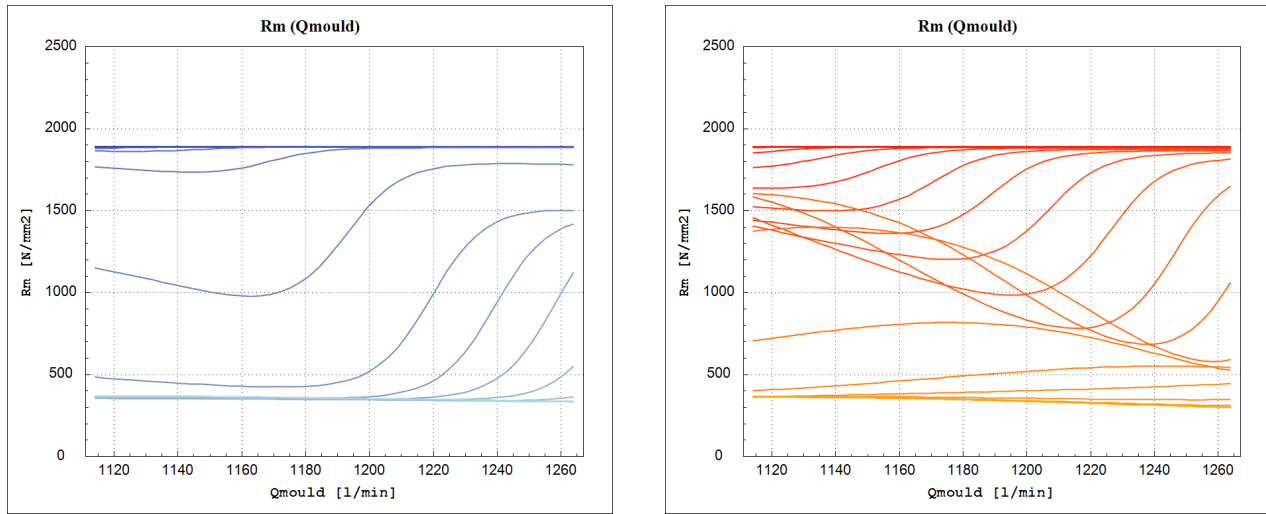


**Figure 217:** Tensile strength as a function of the cooling flow rate in the mould, calculated by the ANN model on centered verification point (red line) and centered training point (blue line).

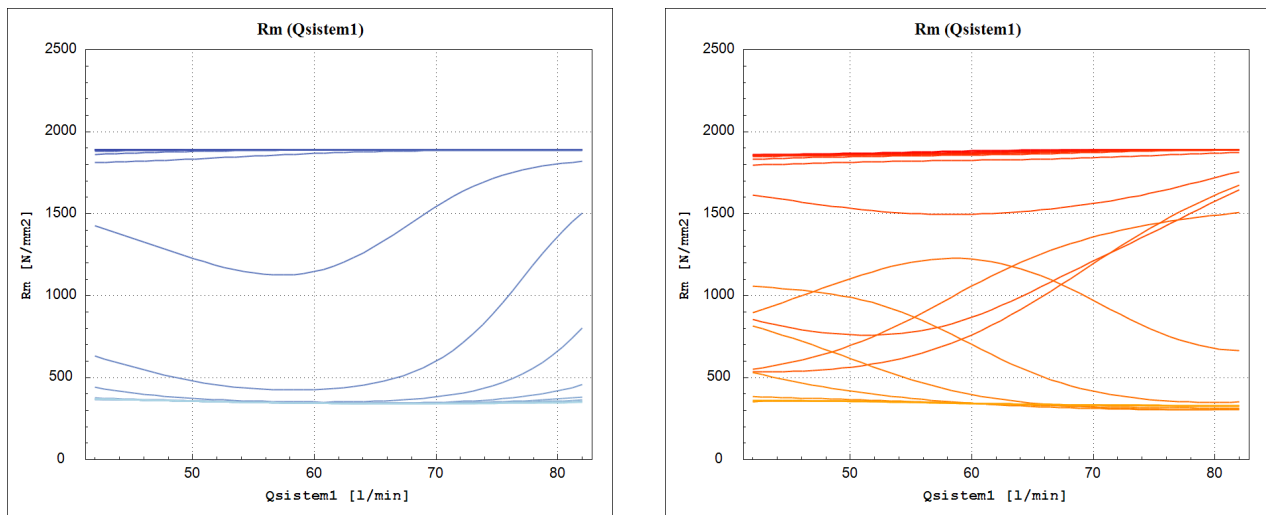


**Figure 218:** Tensile strength as a function of the cooling flow rate in 1<sup>st</sup> spray system, calculated by the ANN model on centered verification point (red line) and centered training point (blue line).

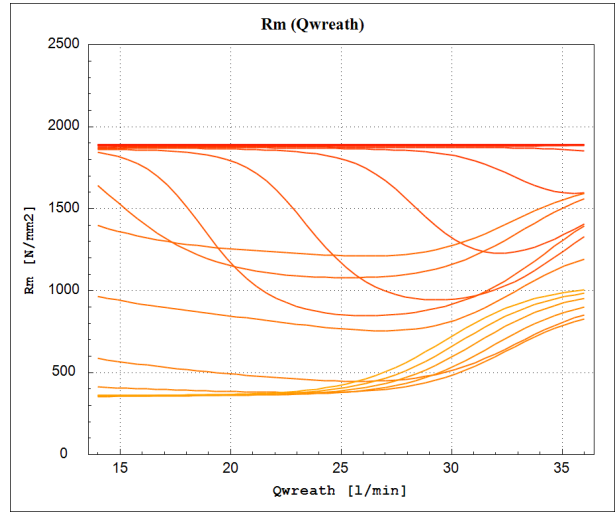
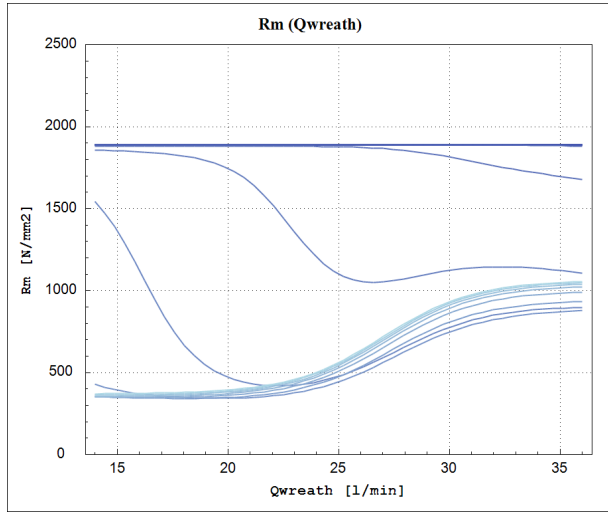


**Figure 219:** Tensile strength as a function of the cooling flow rate in wreath spray system, calculated by the ANN model on centered verification point (red line) and centered training point (blue line).

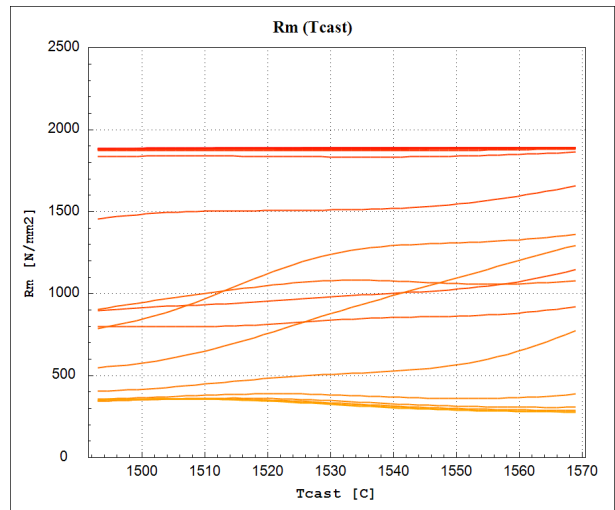
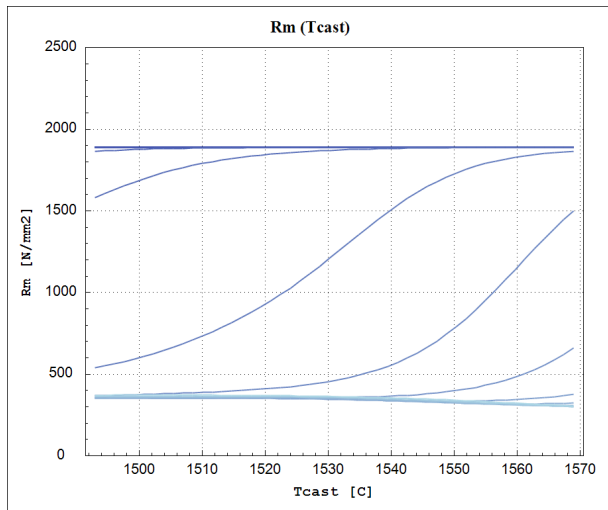


**Figure 220:** Tensile strength as a function of the casting temperature, calculated by the ANN model on centered verification point (red line) and centered training point (blue line).

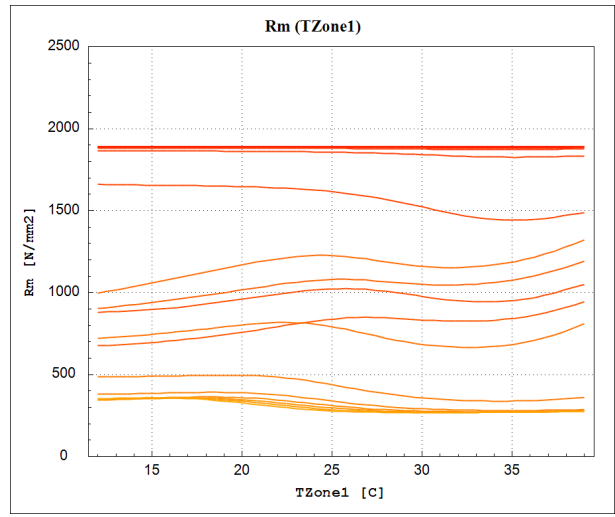
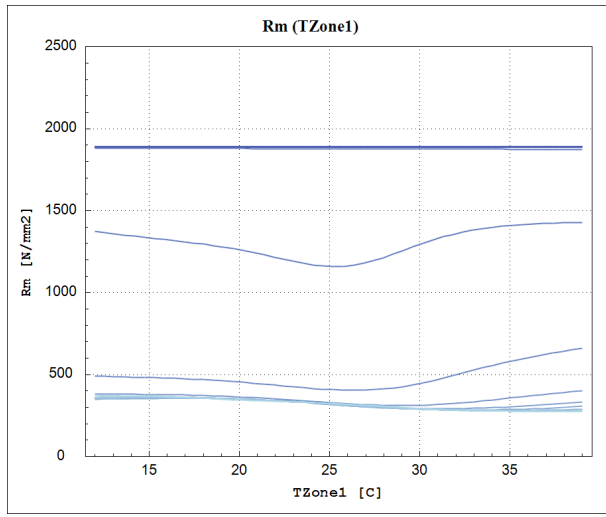


**Figure 221:** Tensile strength as a function of the water temperature in Zone 1, calculated by the ANN model on centered verification point (red line) and centered training point (blue line).

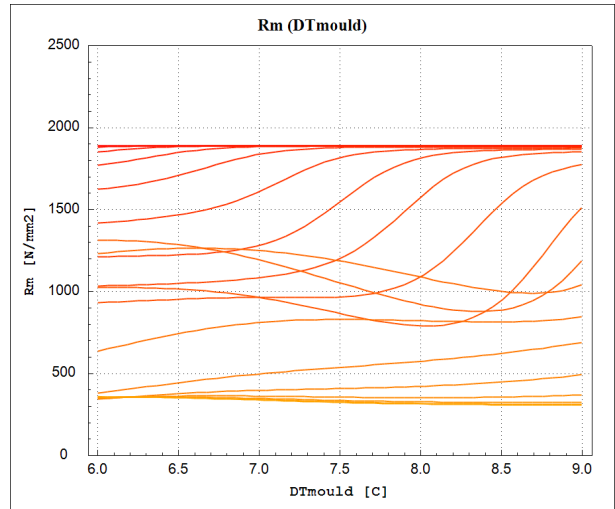
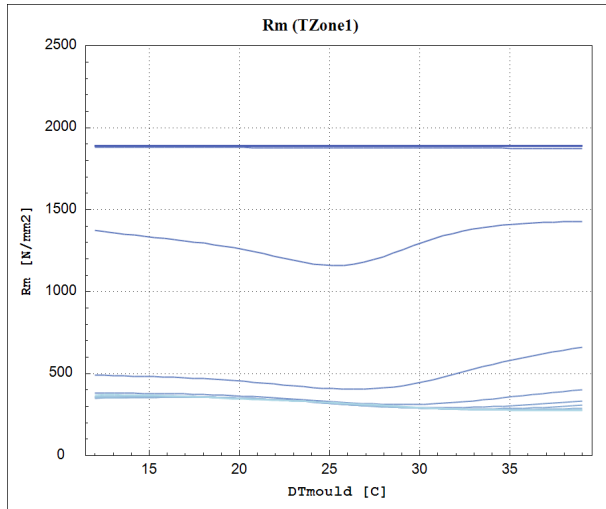


**Figure 222:** Tensile strength as a function of the delta  $T$ , calculated by the ANN model on centered verification point (red line) and centered training point (blue line).

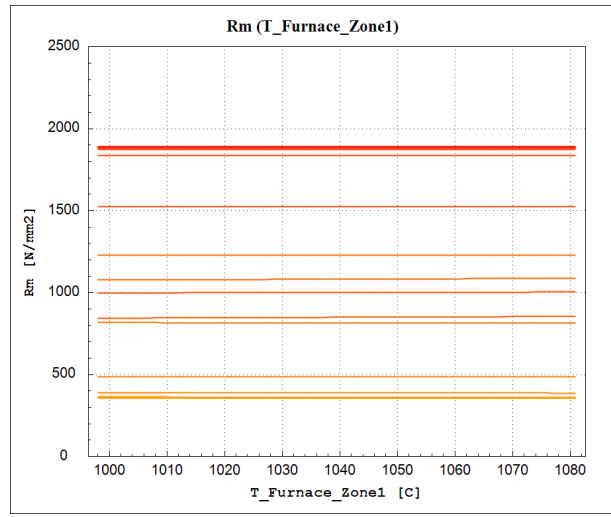
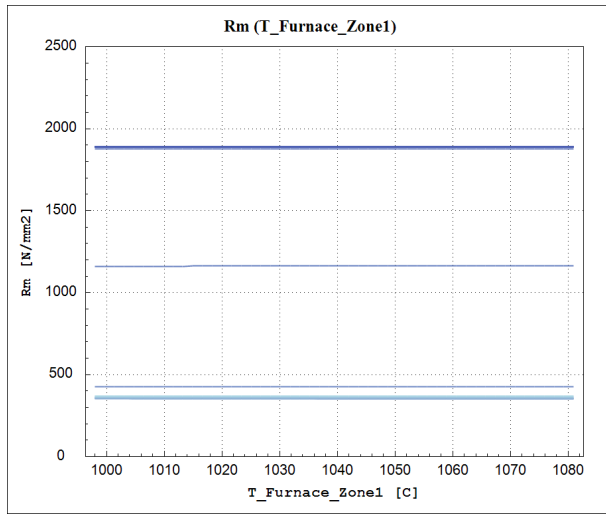


**Figure 223:** Tensile strength as a function of the average on temperature in zone 1, calculated by the ANN model on centered verification point (red line) and centered training point (blue line).

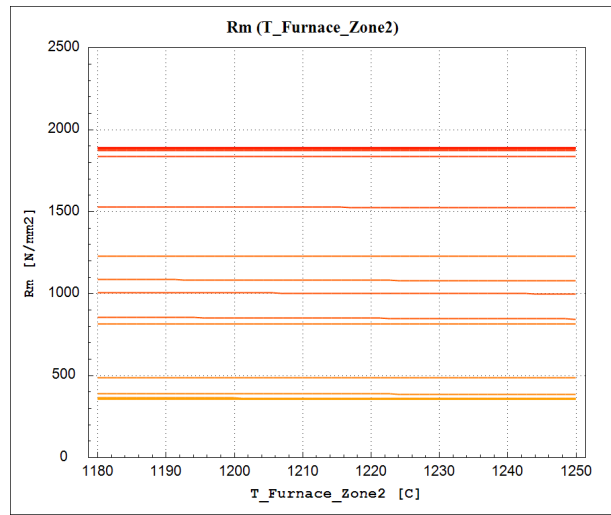
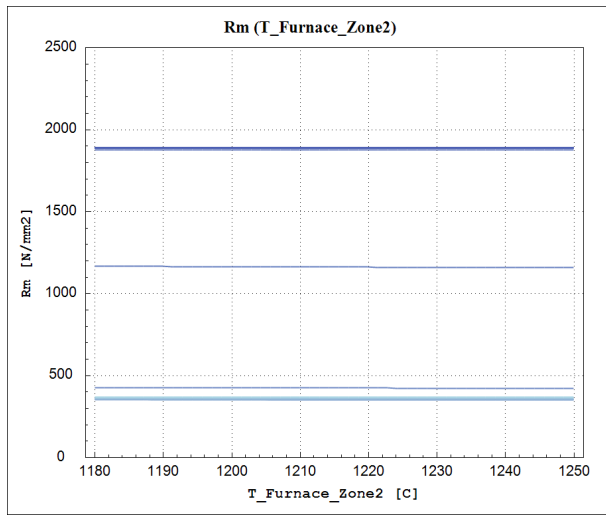


**Figure 224:** Tensile strength as a function of the average on temperature in zone 2, calculated by the ANN model on centered verification point (red line) and centered training point (blue line).

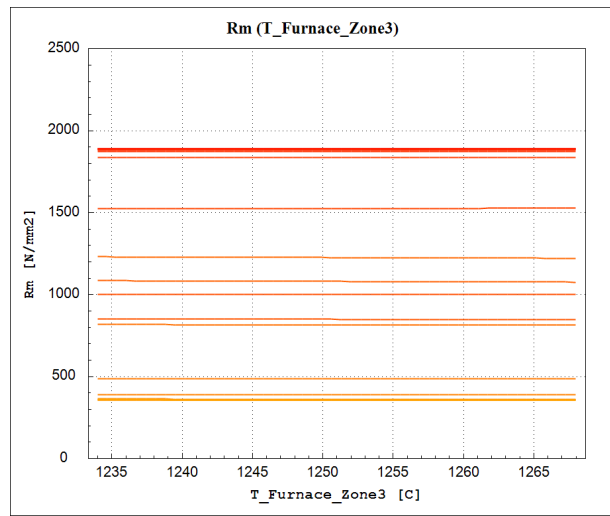
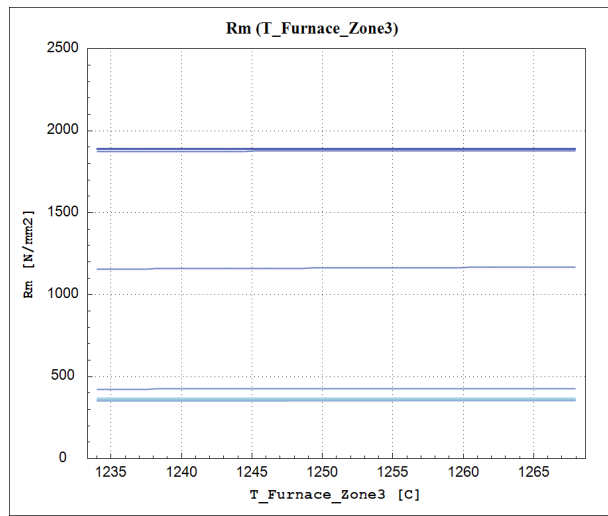


**Figure 225:** Tensile strength as a function of the average on temperature in zone 3, calculated by the ANN model on centered verification point (red line) and centered training point (blue line).

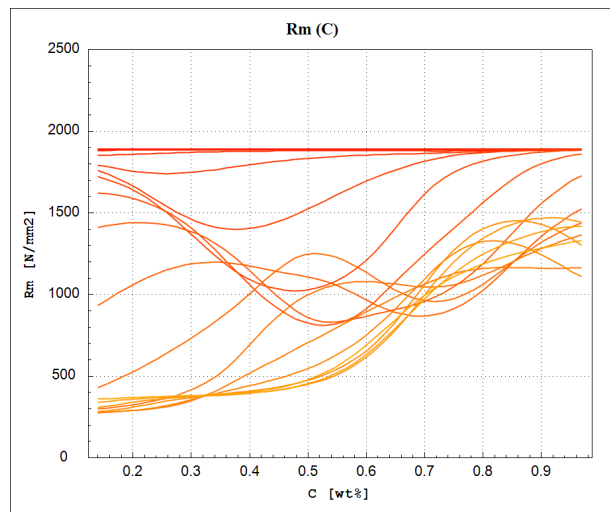
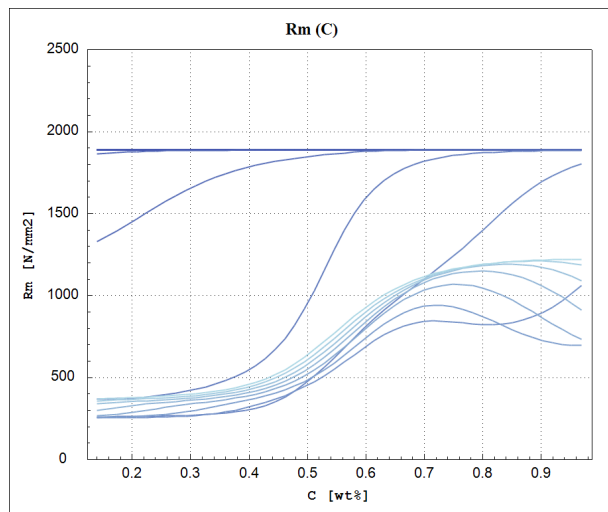


**Figure 226:** Tensile strength as a function of the Carbon concentration ( $C$ ), calculated by the ANN model on centered verification point (red line) and centered training point (blue line).

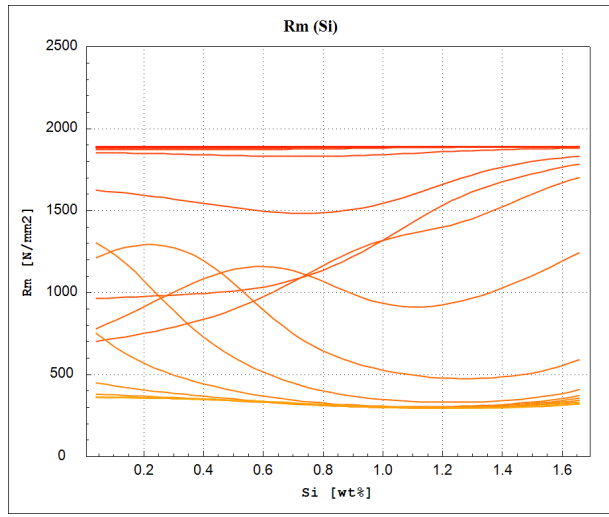
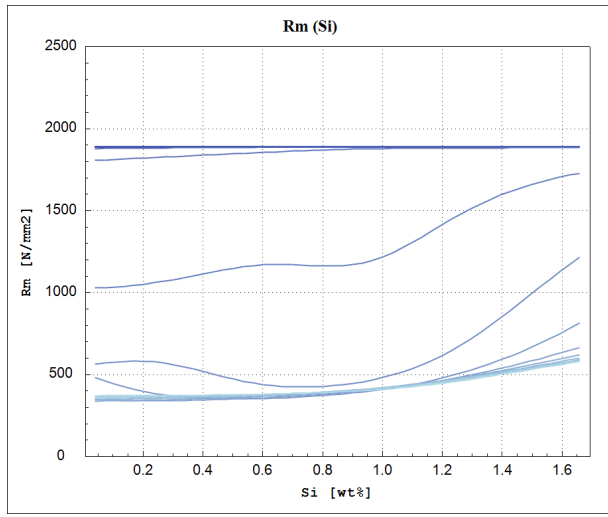


**Figure 227:** Tensile strength as a function of the Silicon concentration (Si), calculated by the ANN model on centered verification point (red line) and centered training point (blue line).

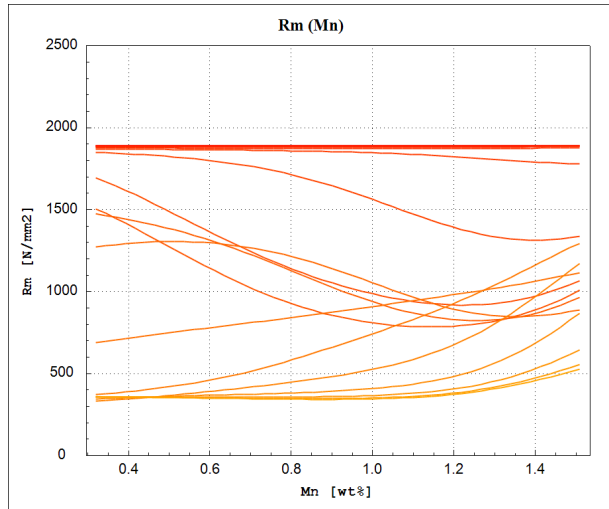
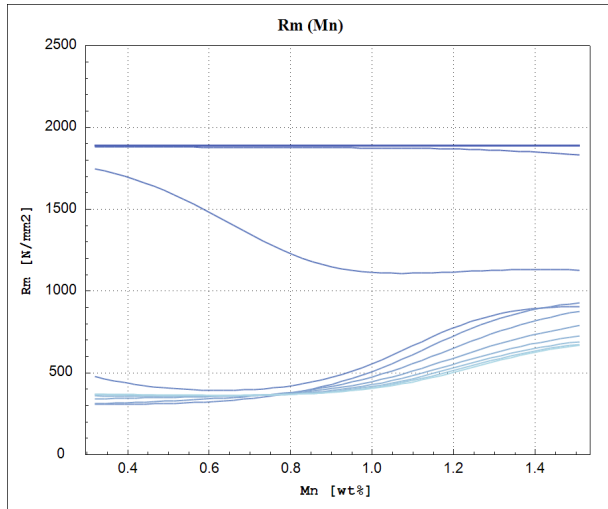


**Figure 228:** Tensile strength as a function of the Manganese concentration (Mn), calculated by the ANN model on centered verification point (red line) and centered training point (blue line).

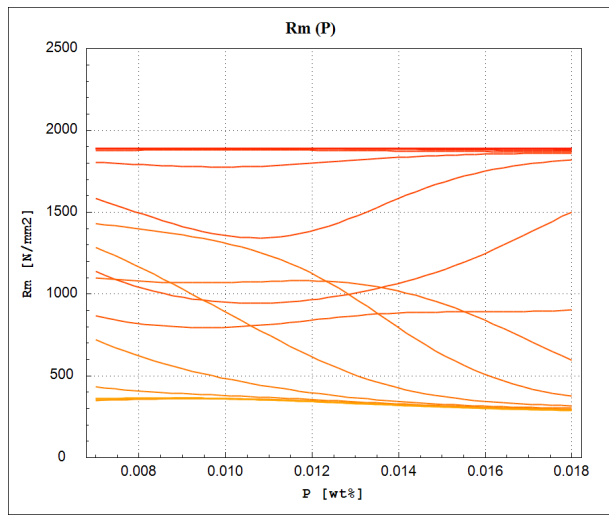
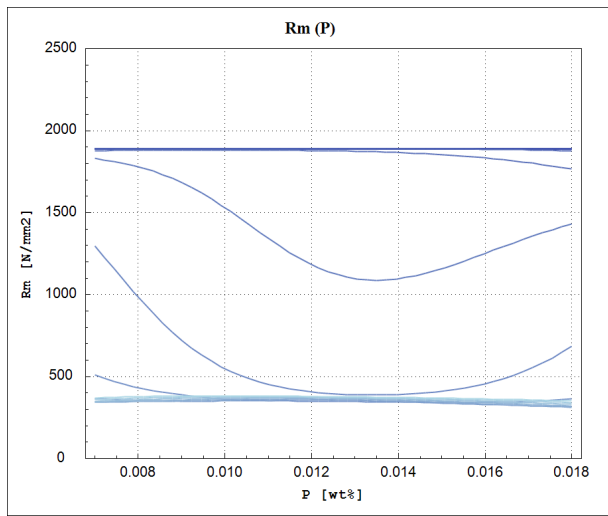


**Figure 229:** Tensile strength as a function of the Phosphorus concentration (P), calculated by the ANN model on centered verification point (red line) and centered training point (blue line).

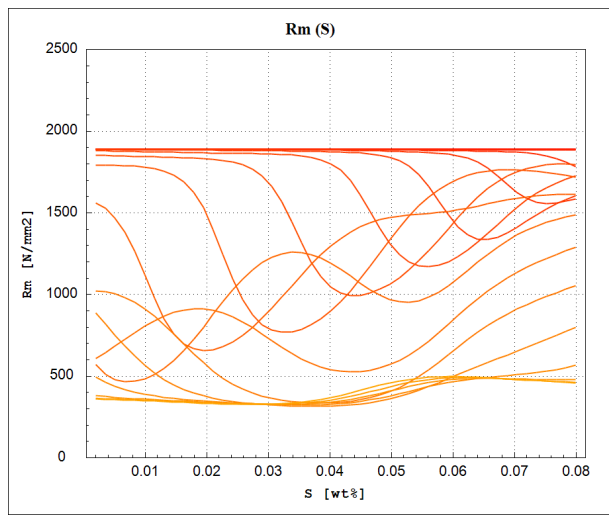
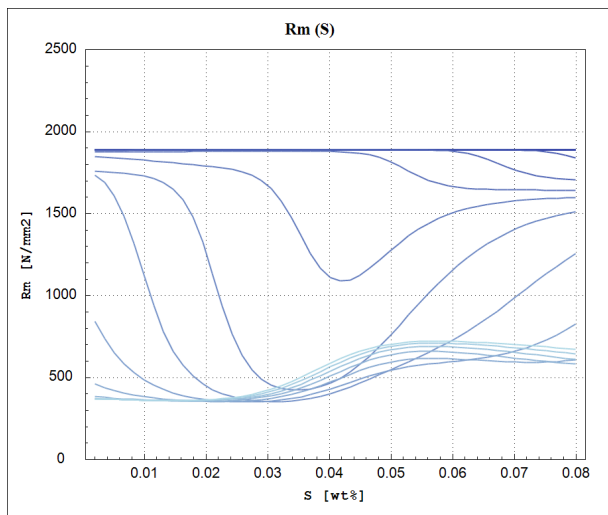


**Figure 230:** Tensile strength as a function of the Sulphur concentration (S), calculated by the ANN model on centered verification point (red line) and centered training point (blue line).

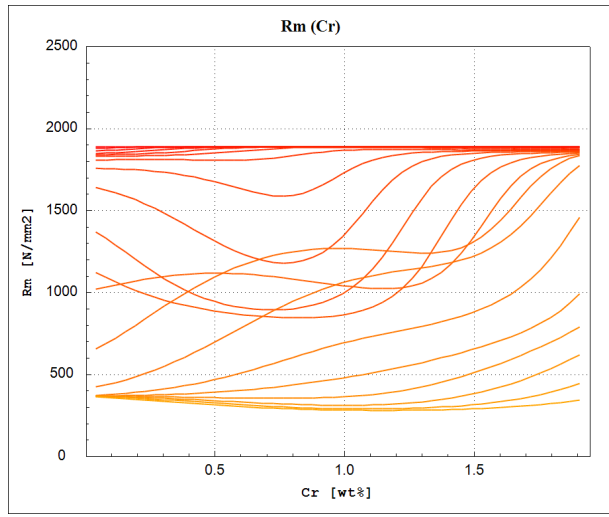
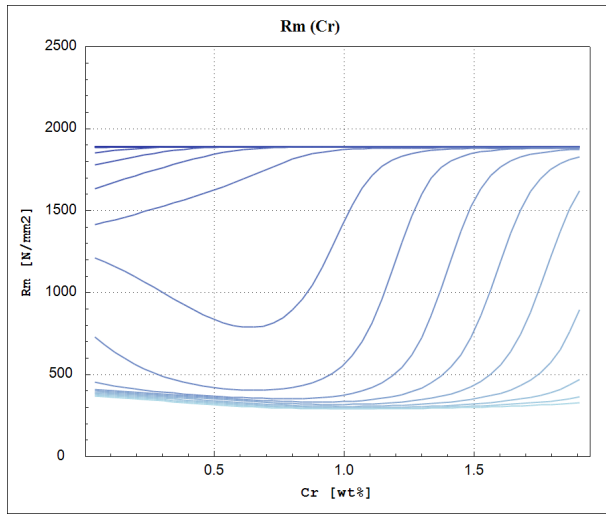


**Figure 231:** Tensile strength as a function of the Chromium concentration (Cr), calculated by the ANN model on centered verification point (red line) and centered training point (blue line).

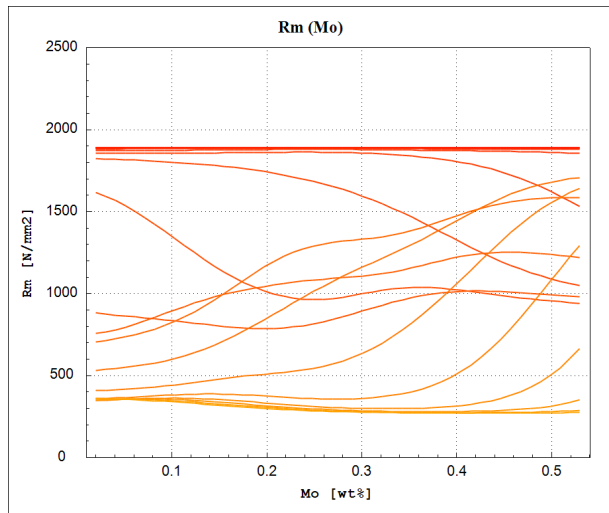
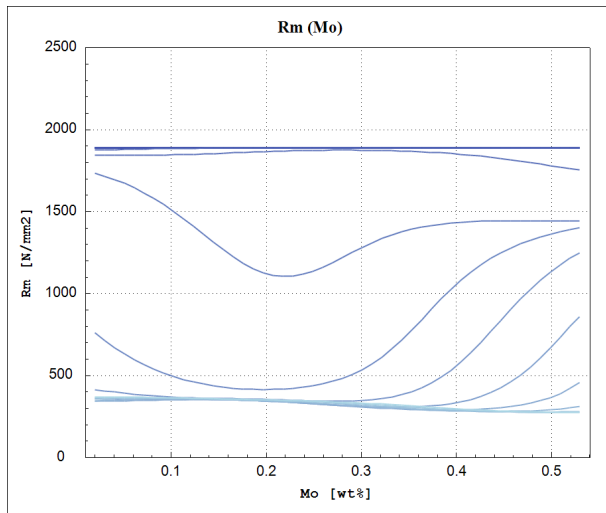


**Figure 232:** Tensile strength as a function of the Molybdenum concentration (Mo), calculated by the ANN model on centered verification point (red line) and centered training point (blue line).

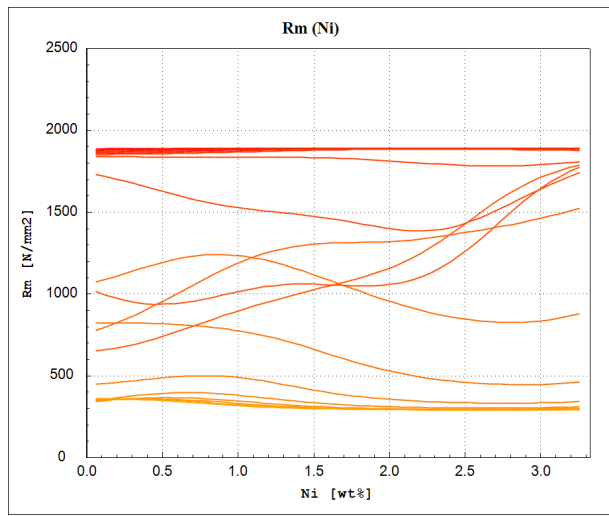
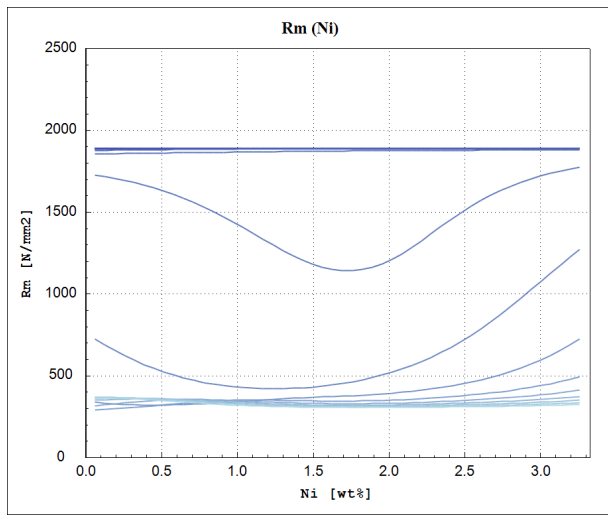


**Figure 233:** Tensile strength as a function of the Nickel concentration (Ni), calculated by the ANN model on centered verification point (red line) and centered training point (blue line).

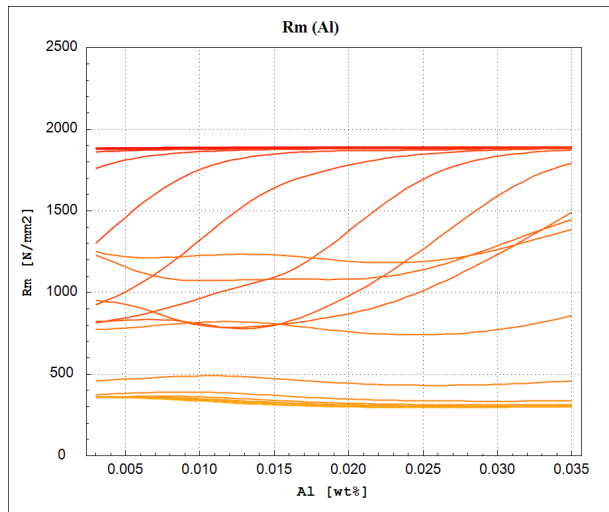
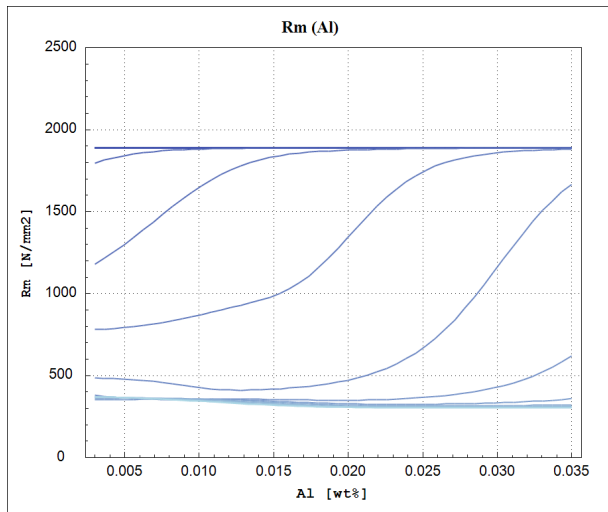


**Figure 234:** Tensile strength as a function of the Aluminium concentration (Al), calculated by the ANN model on centered verification point (red line) and centered training point (blue line).

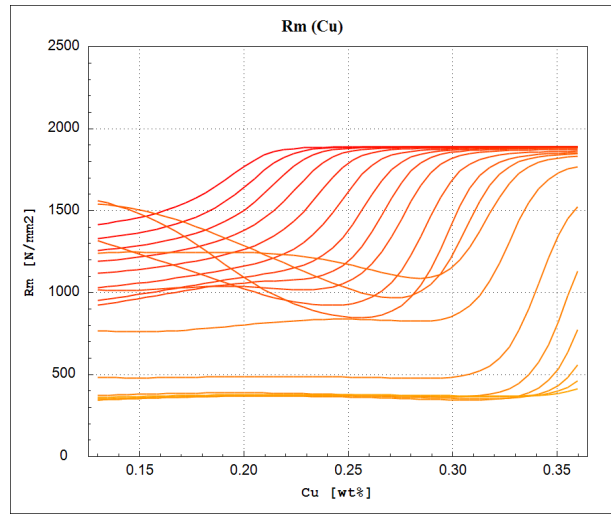
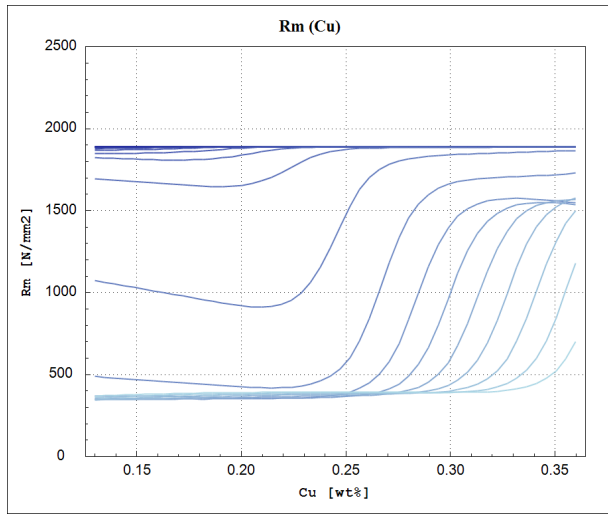


**Figure 235:** Tensile strength as a function of the Copper concentration (Cu), calculated by the ANN model on centered verification point (red line) and centered training point (blue line).

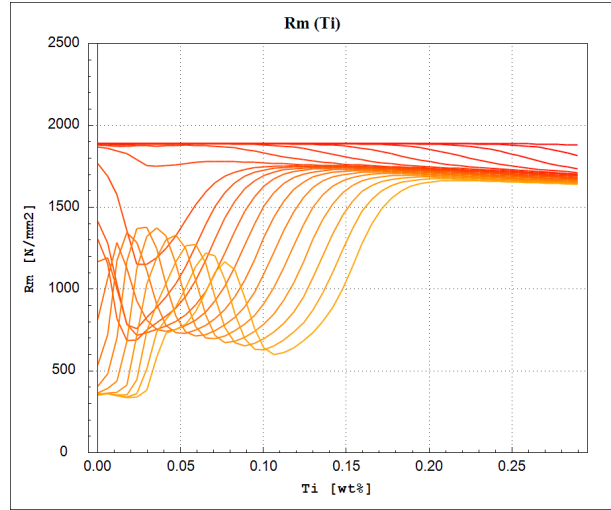
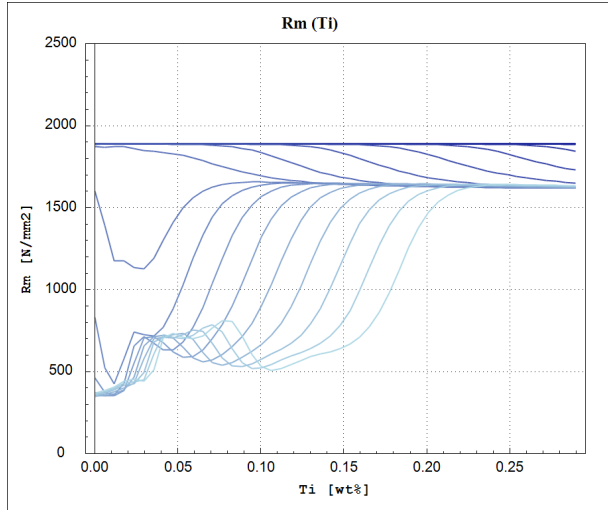


**Figure 236:** Tensile strength as a function of the Titanium concentration (Ti), calculated by the ANN model on centered verification point (red line) and centered training point (blue line).

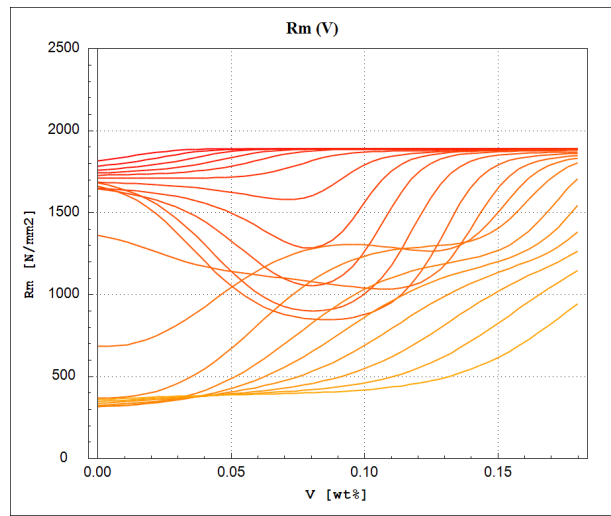
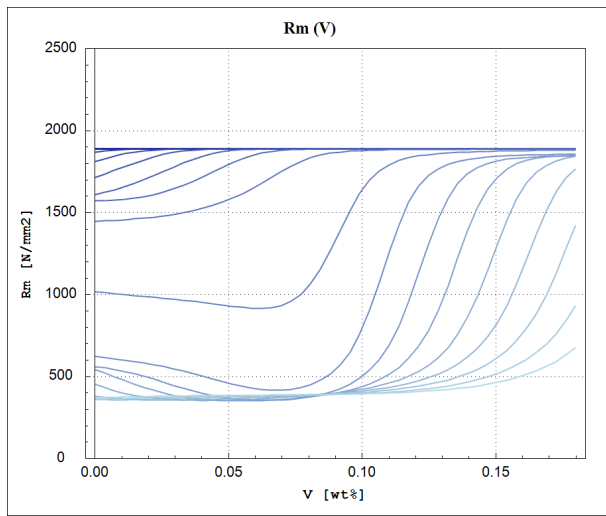


**Figure 237:** Tensile strength as a function of the Vanadium concentration (V), calculated by the ANN model on centered verification point (red line) and centered training point (blue line).

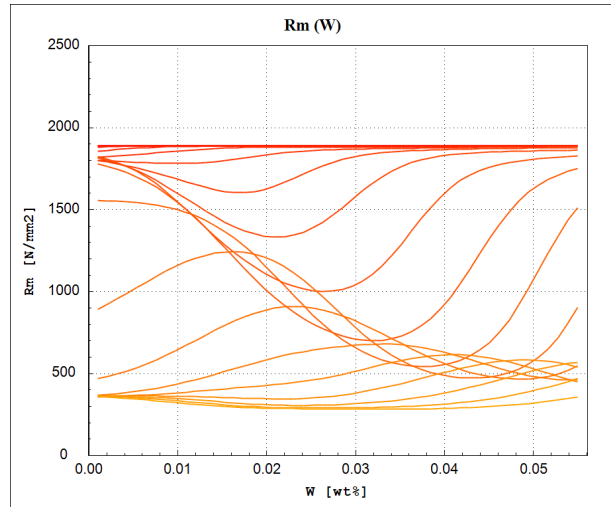
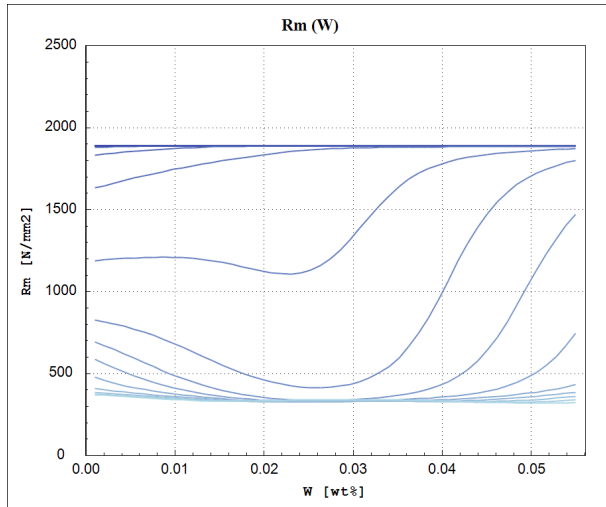


**Figure 238:** Tensile strength as a function of the Tungsten concentration (W), calculated by the ANN model on centered verification point (red line) and centered training point (blue line).

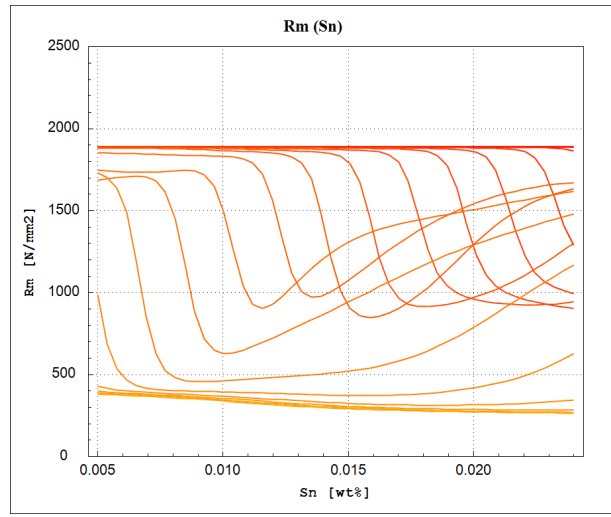
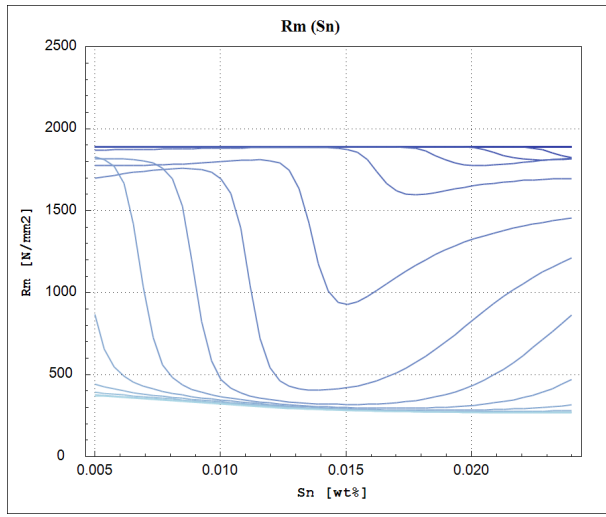


**Figure 239:** Tensile strength as a function of the Tin concentration (Sn), calculated by the ANN model on centered verification point (red line) and centered training point (blue line).

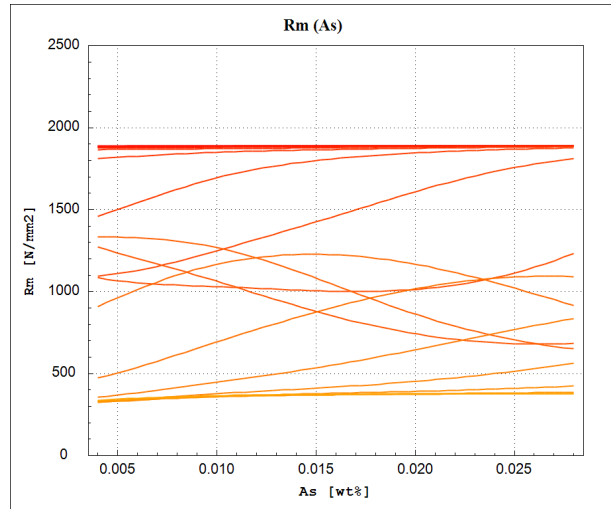
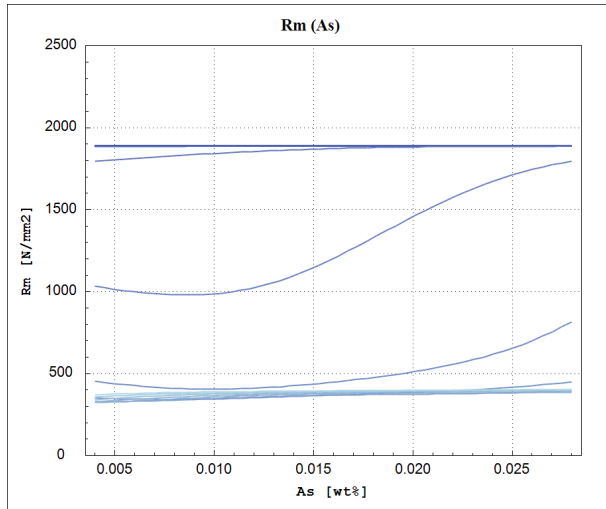


**Figure 240:** Tensile strength as a function of the Arsenic concentration (As), calculated by the ANN model on centered verification point (red line) and centered training point (blue line).

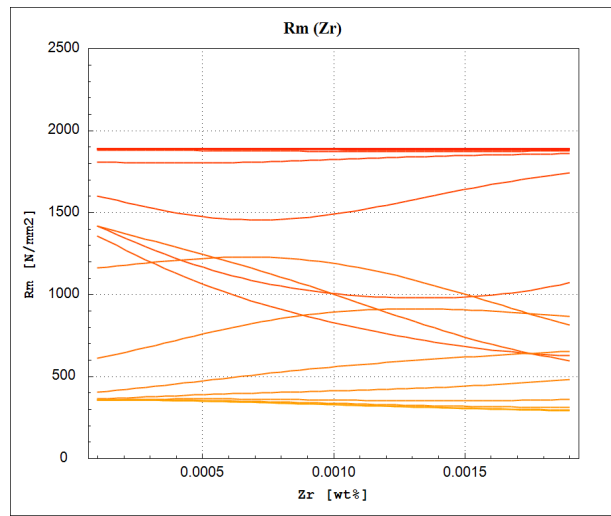
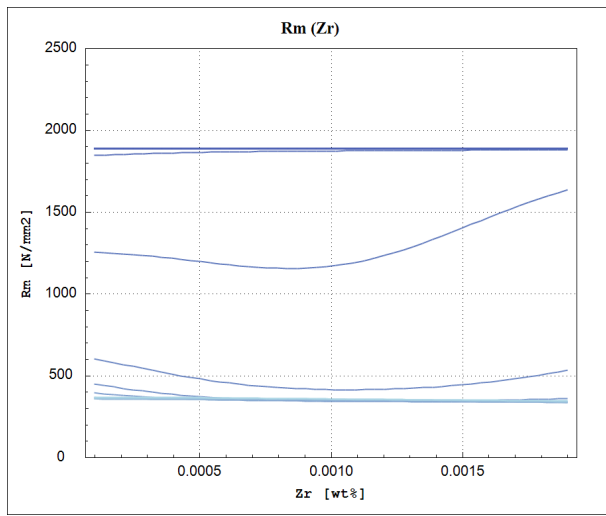


**Figure 241:** Tensile strength as a function of the Zirconium concentration (Zr), calculated by the ANN model on centered verification point (red line) and centered training point (blue line).

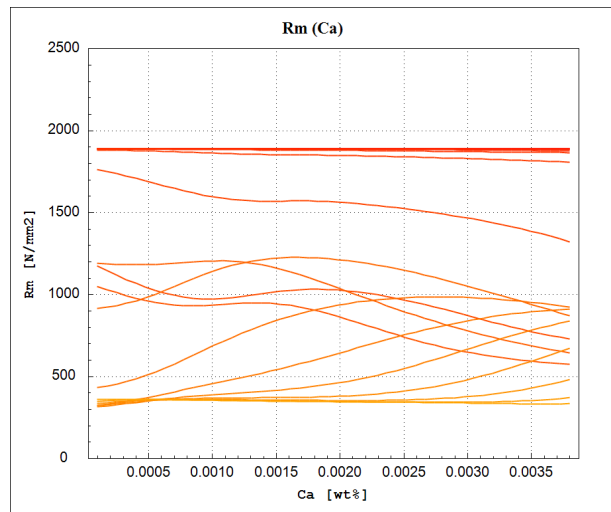
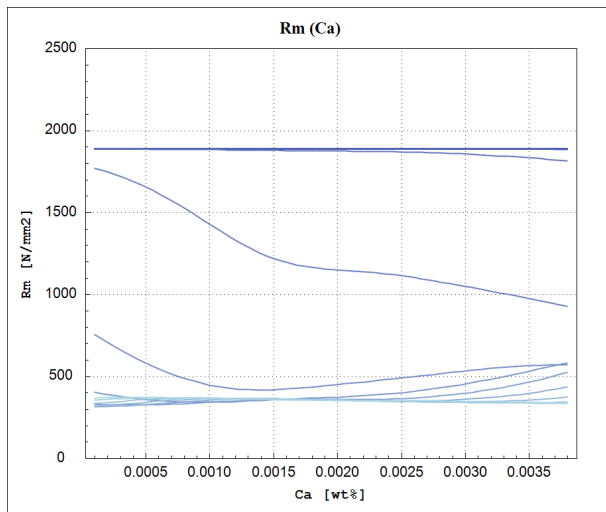


**Figure 242:** Tensile strength as a function of the Calcium concentration (Ca), calculated by the ANN model on centered verification point (red line) and centered training point (blue line).

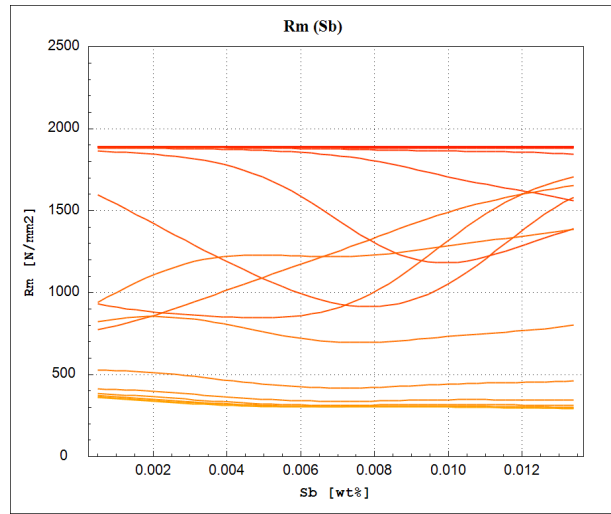
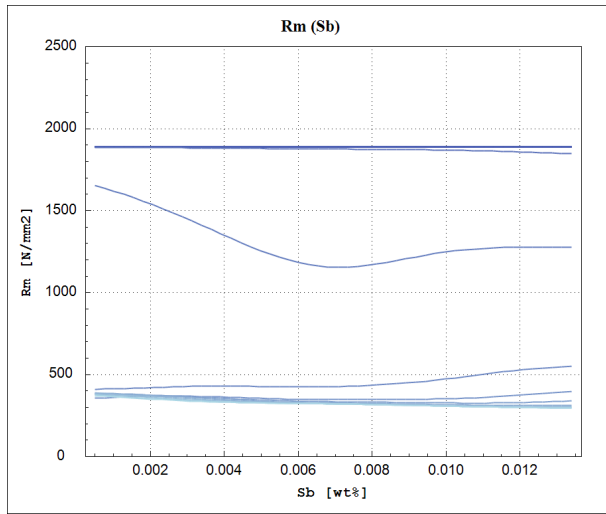


**Figure 243:** Tensile strength as a function of the Antimony concentration ( $Sb$ ), calculated by the ANN model on centered verification point (red line) and centered training point (blue line).

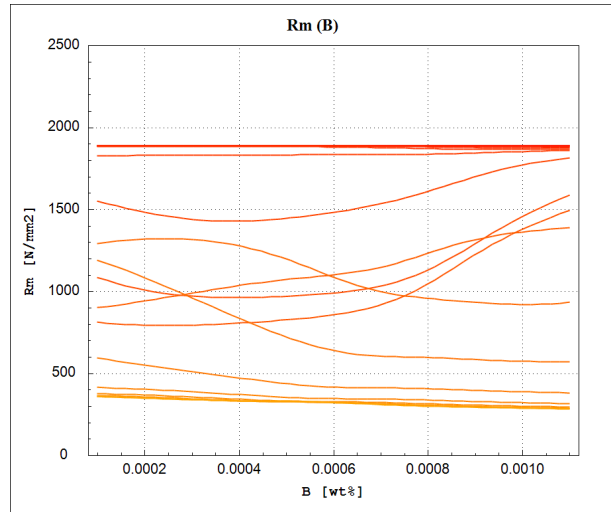
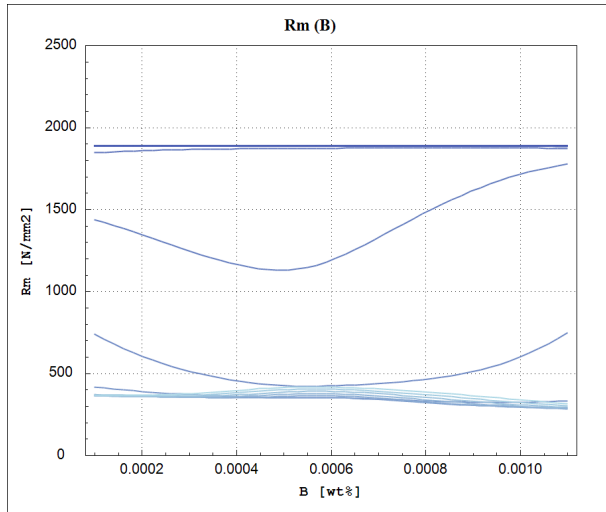


**Figure 244:** Tensile strength as a function of the Boron concentration ( $B$ ), calculated by the ANN model on centered verification point (red line) and centered training point (blue line).

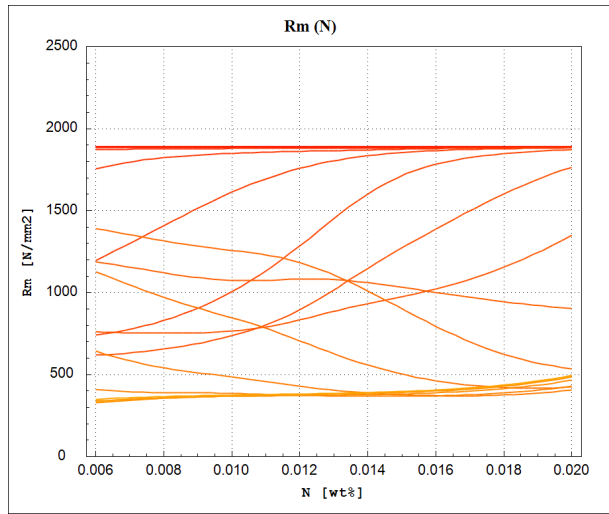
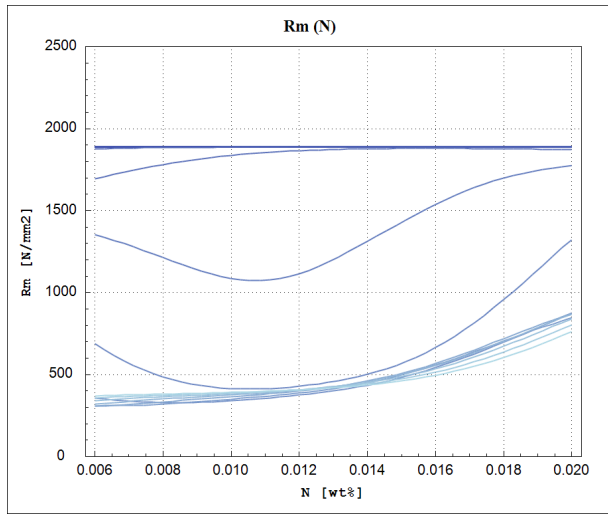


**Figure 245:** Tensile strength as a function of the Nitrogen concentration ( $N$ ), calculated by the ANN model on centered verification point (red line) and centered training point (blue line).

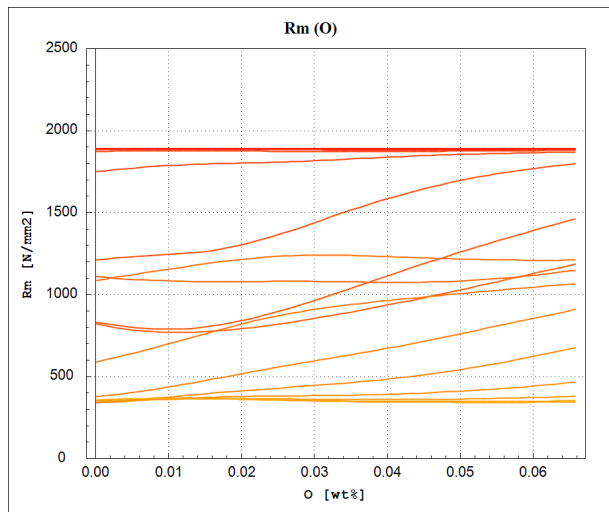
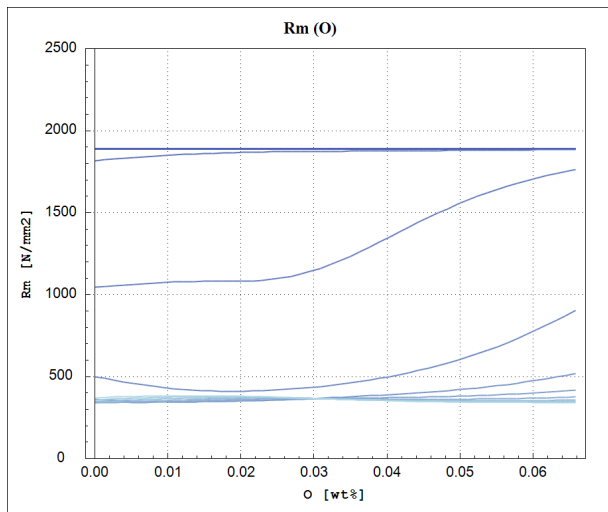


**Figure 246:** Tensile strength as a function of the Oxygen concentration ( $O$ ), calculated by the ANN model on centered verification point (red line) and centered training point (blue line).

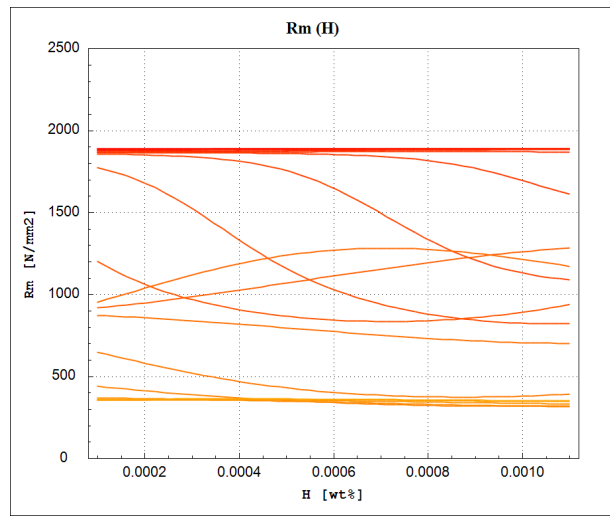
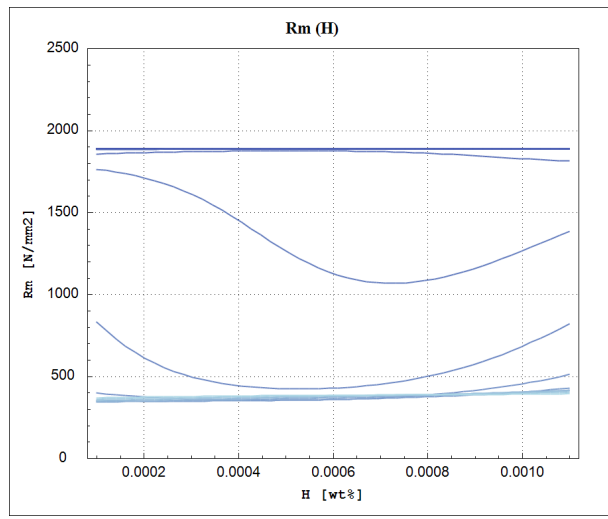


**Figure 247:** Tensile strength as a function of the Hydrogen concentration (H), calculated by the ANN model on centered verification point (red line) and centered training point (blue line).

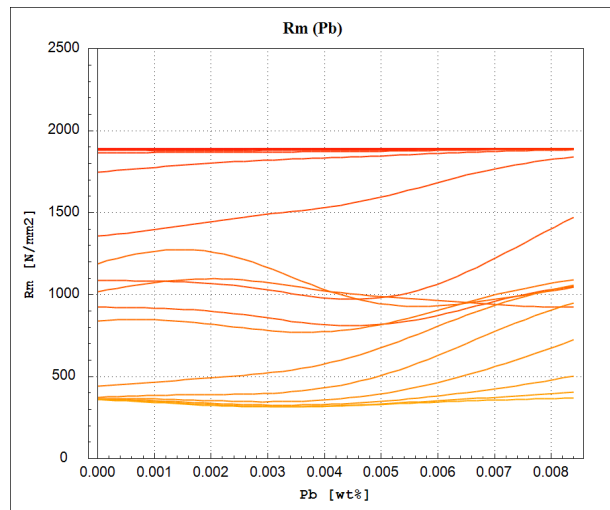
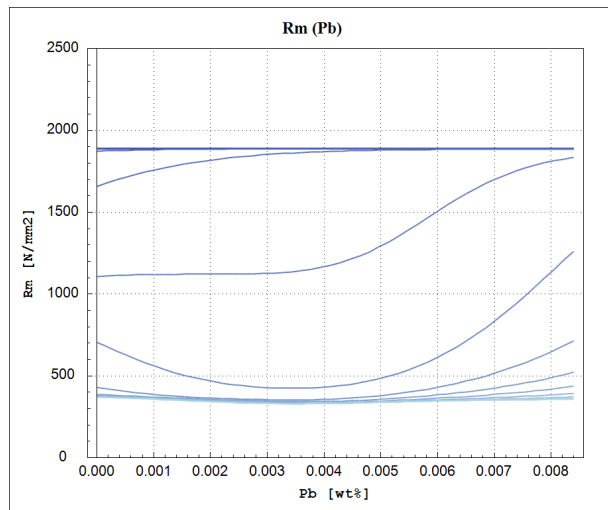


**Figure 248:** Tensile strength as a function of the Lead concentration (Pb), calculated by the ANN model on centered verification point (red line) and centered training point (blue line).

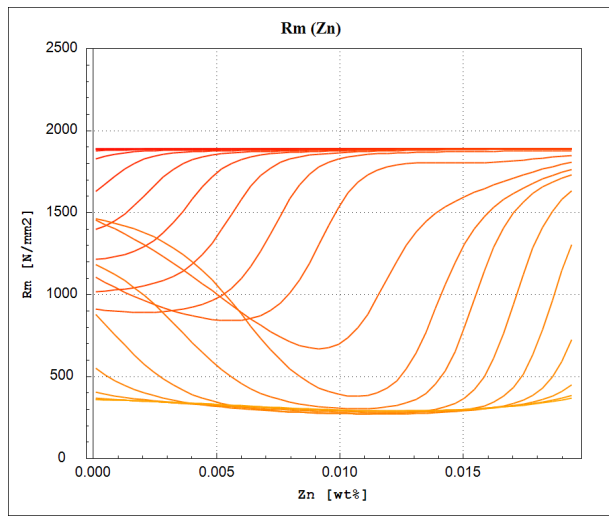
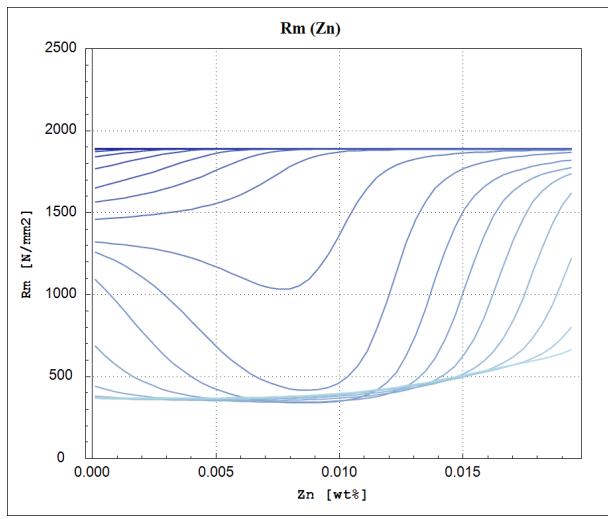


**Figure 249:** Tensile strength as a function of the Zinc concentration (Zn), calculated by the ANN model on centered verification point (red line) and centered training point (blue line).

### 5.2.3 Yield Stress ( $R_p$ )

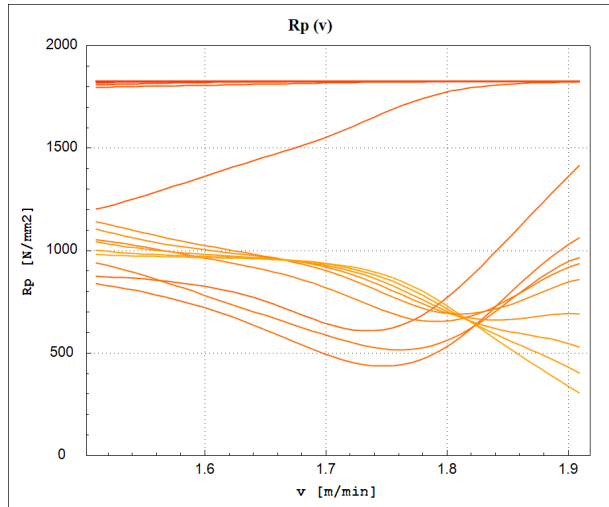
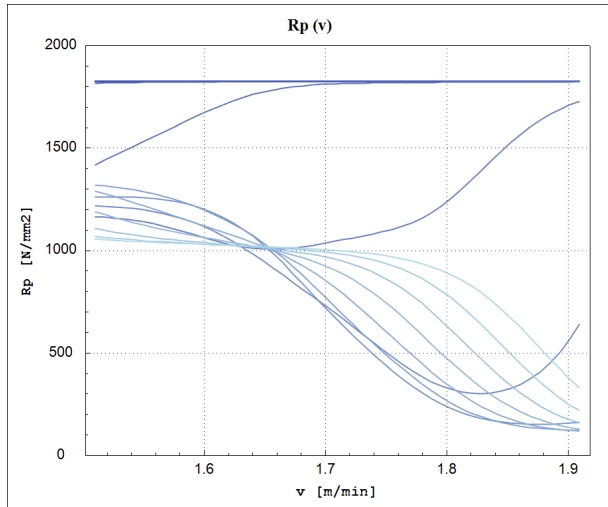


**Figure 250:** Yield stress as a function of the continuous casting speed, calculated by the ANN model on centered verification point (red line) and centered training point (blue line).

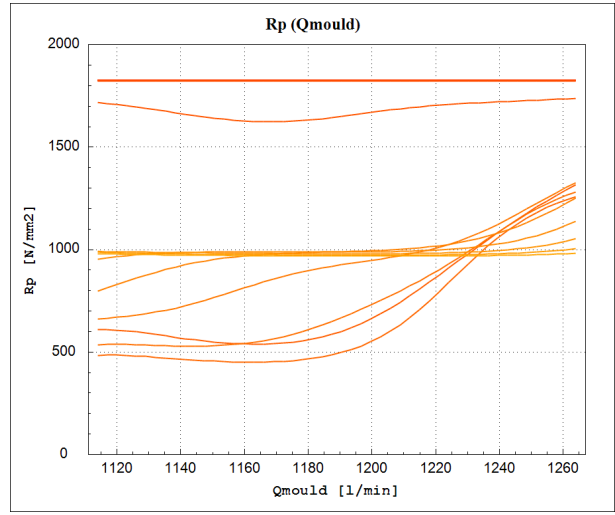
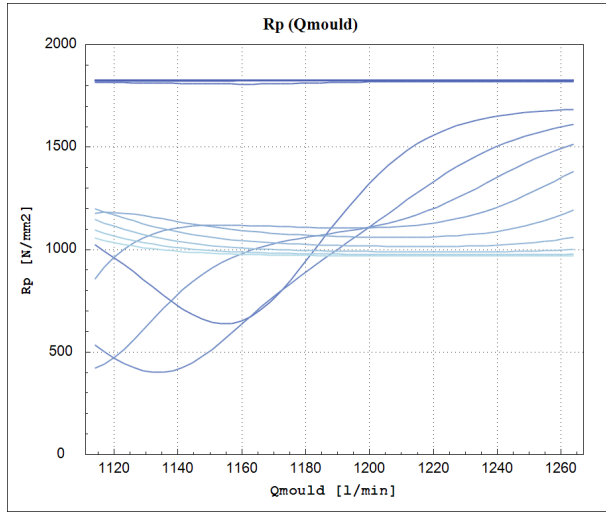


**Figure 251:** Yield stress as a function of the cooling flow rate in the mould, calculated by the ANN model on centered verification point (red line) and centered training point (blue line).

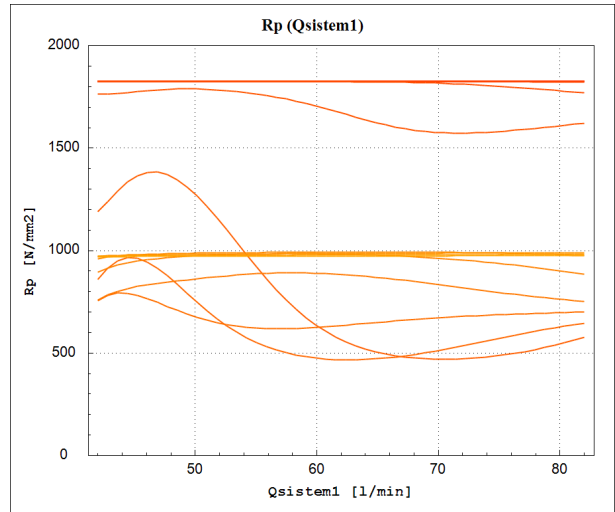
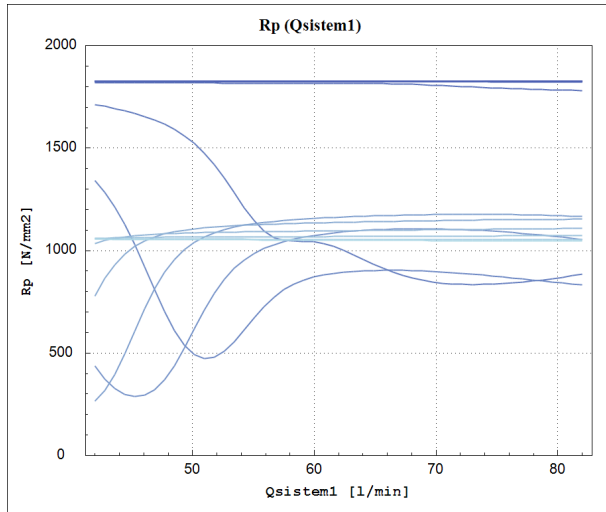


**Figure 252:** Yield stress as a function of the cooling flow rate in 1<sup>st</sup> spray system, calculated by the ANN model on centered verification point (red line) and centered training point (blue line).

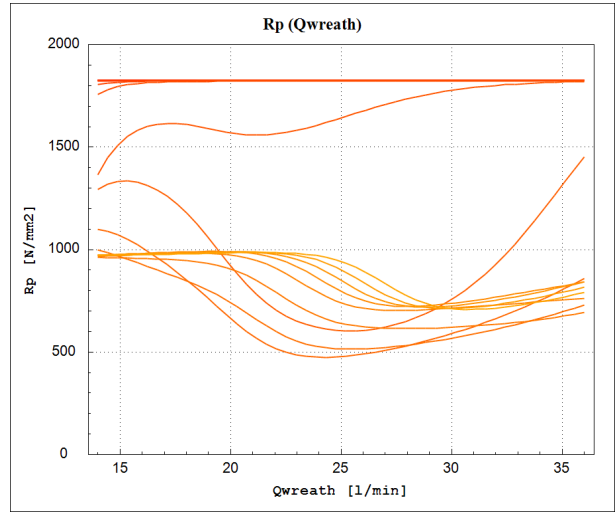
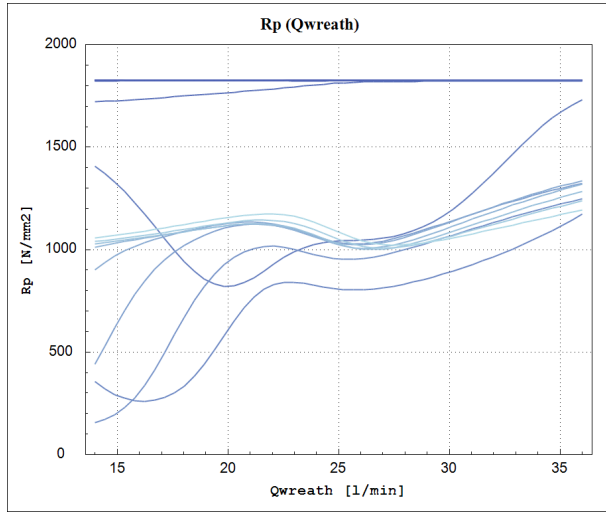


**Figure 253:** Yield stress as a function of the cooling flow rate in wreath spray system, calculated by the ANN model on centered verification point (red line) and centered training point (blue line).

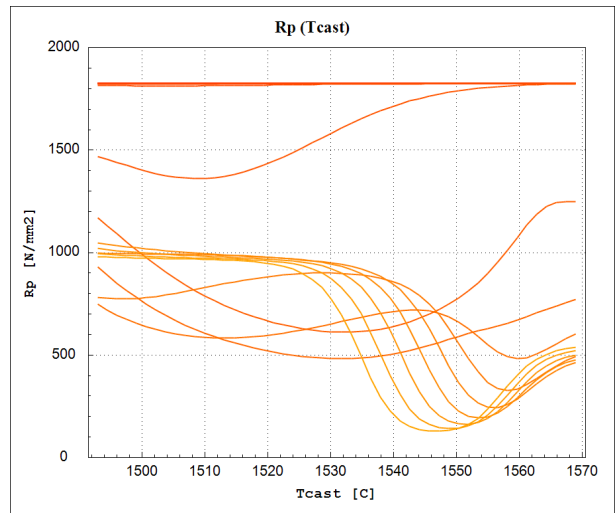
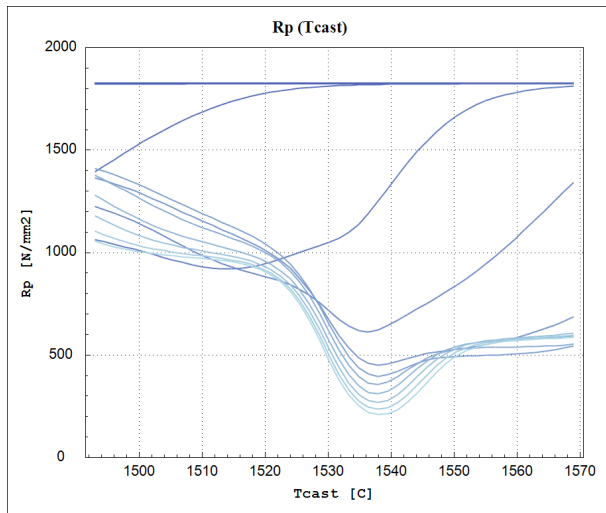


**Figure 254:** Yield stress as a function of the casting temperature, calculated by the ANN model on centered verification point (red line) and centered training point (blue line).

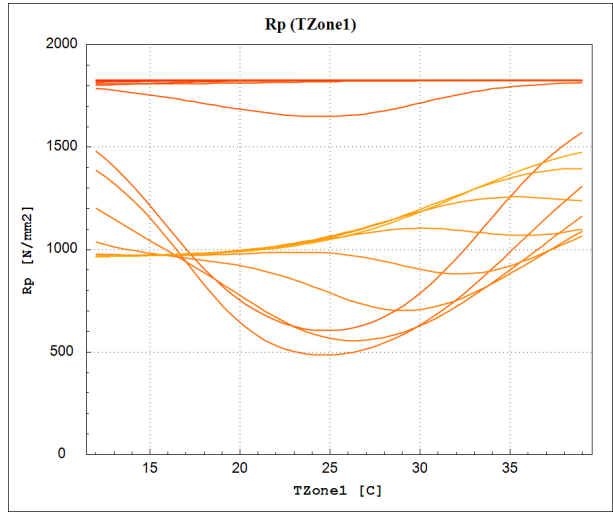
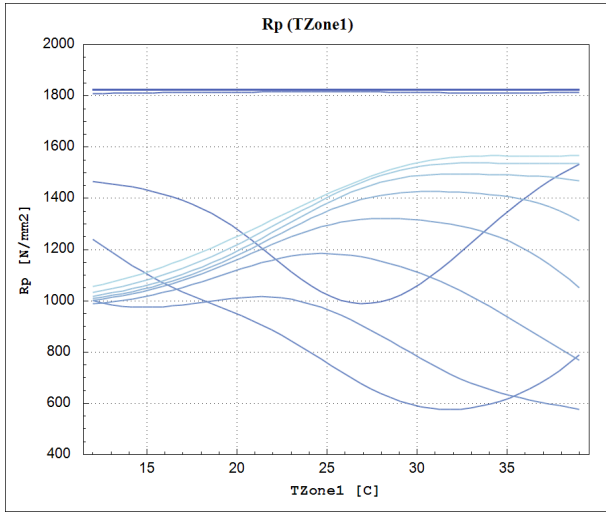


**Figure 255:** Yield stress as a function of the water temperature in Zone 1, calculated by the ANN model on centered verification point (red line) and centered training point (blue line).

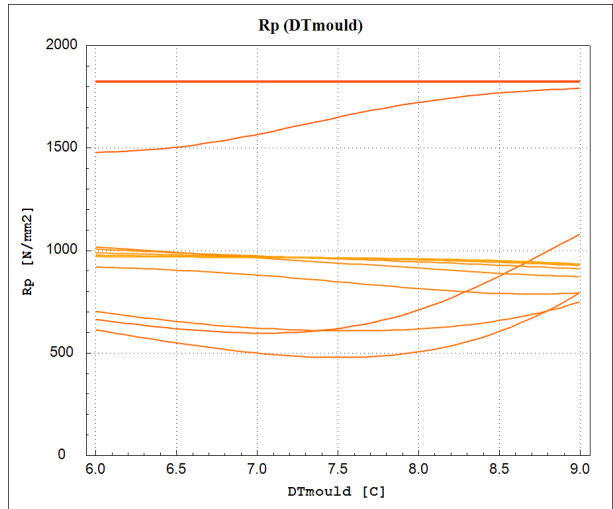
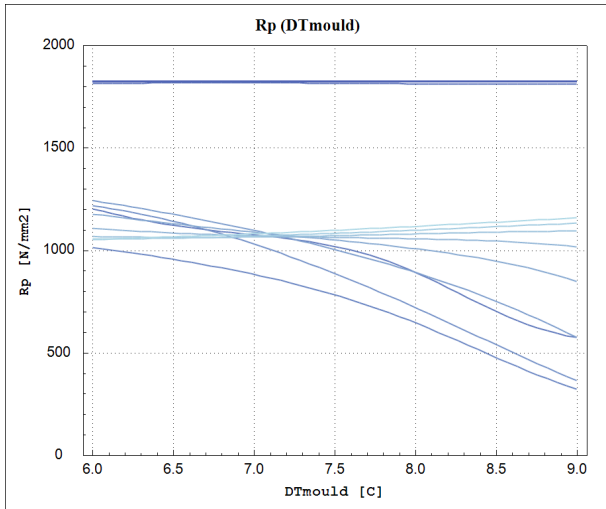


**Figure 256:** Yield stress as a function of the delta  $T$ , calculated by the ANN model on centered verification point (red line) and centered training point (blue line).

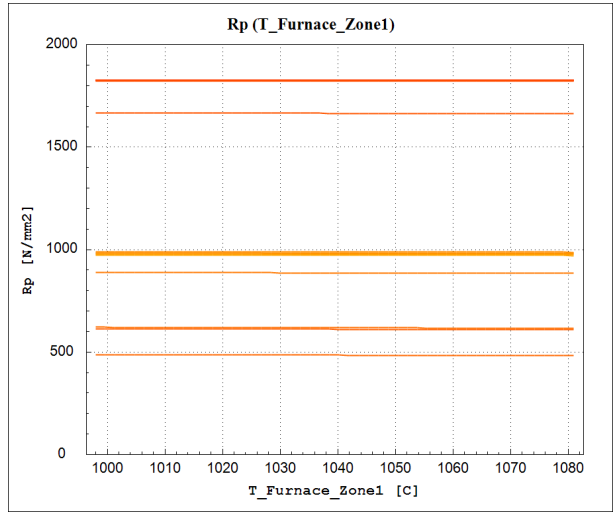
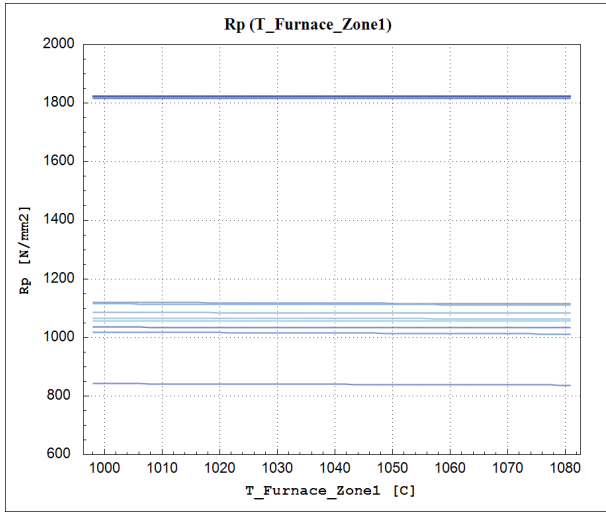


**Figure 257:** Yield stress as a function of the average on temperature in zone 1, calculated by the ANN model on centered verification point (red line) and centered training point (blue line).

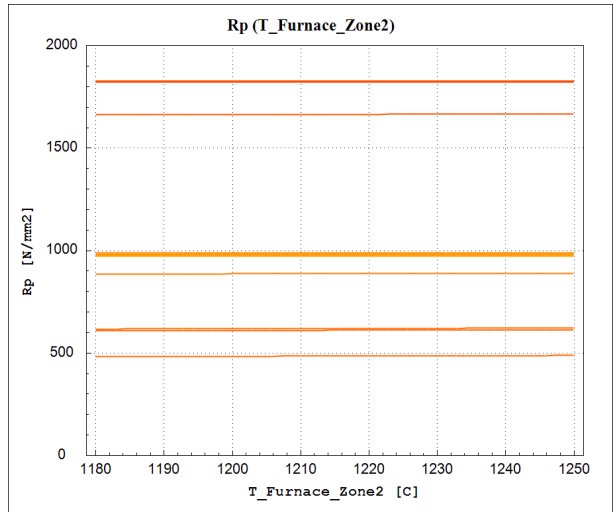
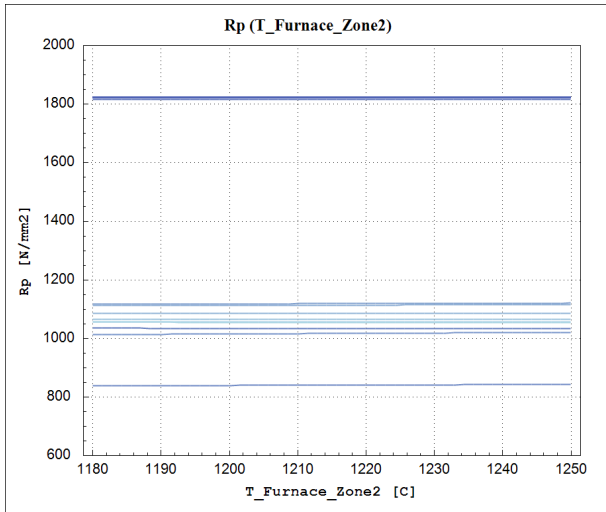


**Figure 258:** Yield stress as a function of the average on temperature in zone 2, calculated by the ANN model on centered verification point (red line) and centered training point (blue line).

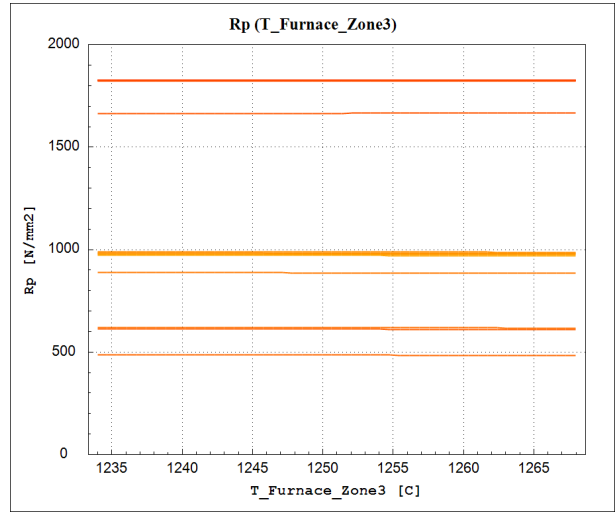
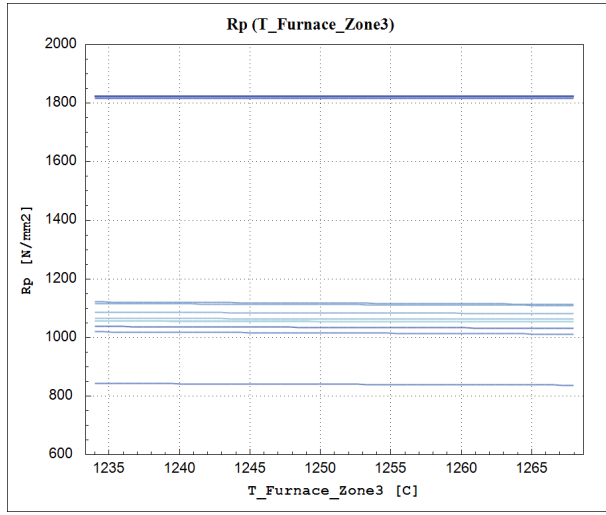


**Figure 259:** Yield stress as a function of the average on temperature in zone 3, calculated by the ANN model on centered verification point (red line) and centered training point (blue line).

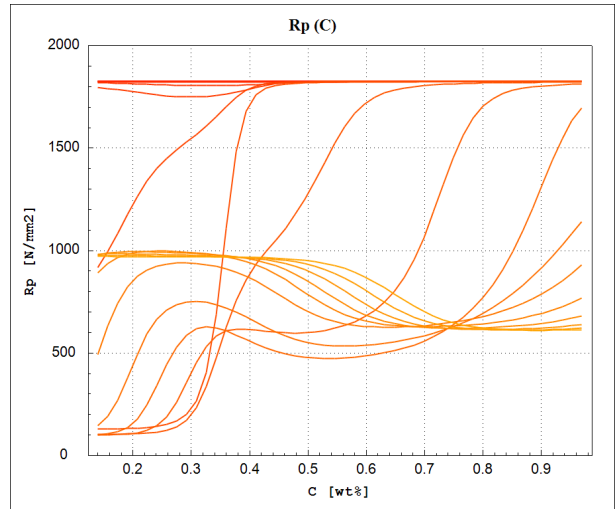
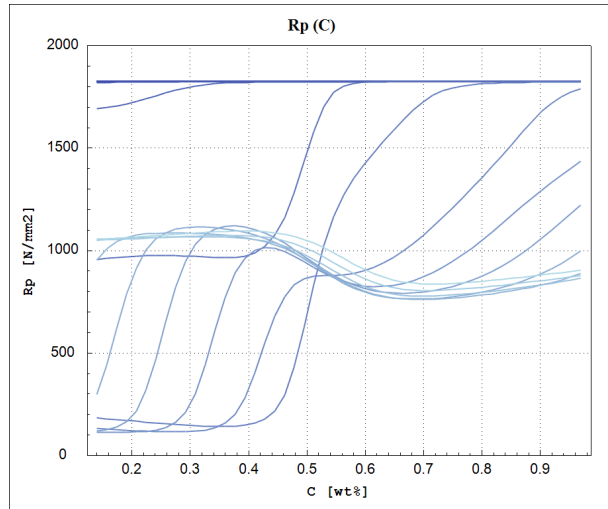


**Figure 260:** Yield stress as a function of the Carbon concentration (C), calculated by the ANN model on centered verification point (red line) and centered training point (blue line).

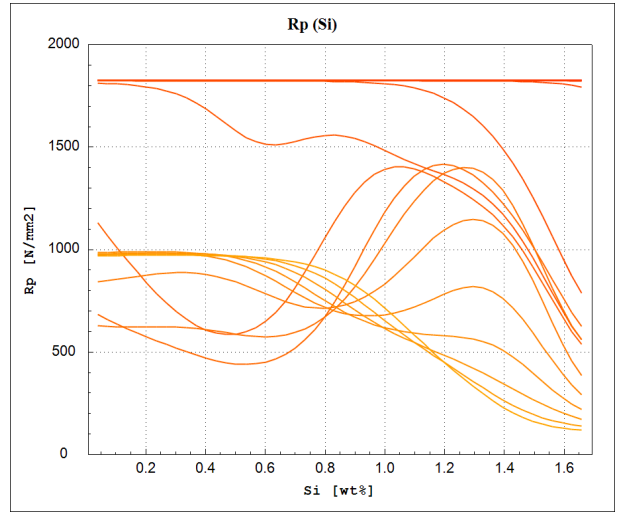
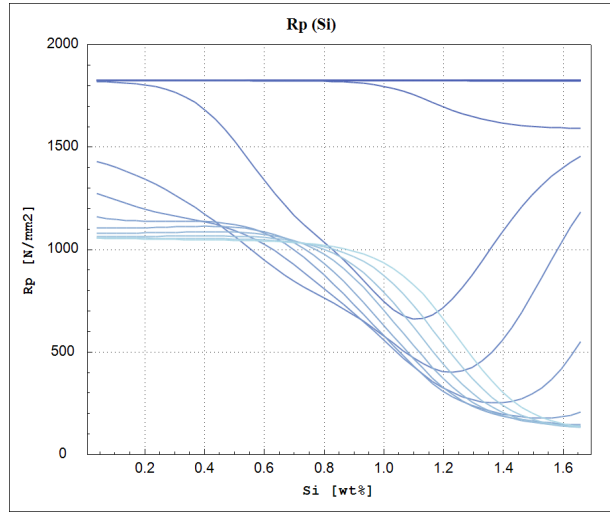


**Figure 261:** Yield stress as a function of the Silicon concentration (Si), calculated by the ANN model on centered verification point (red line) and centered training point (blue line).

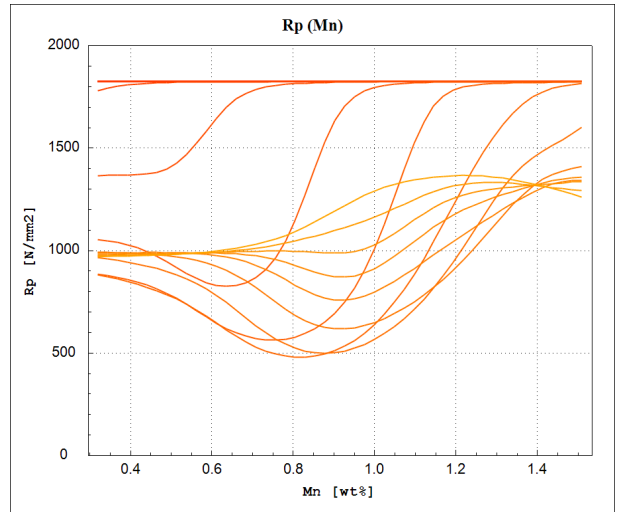
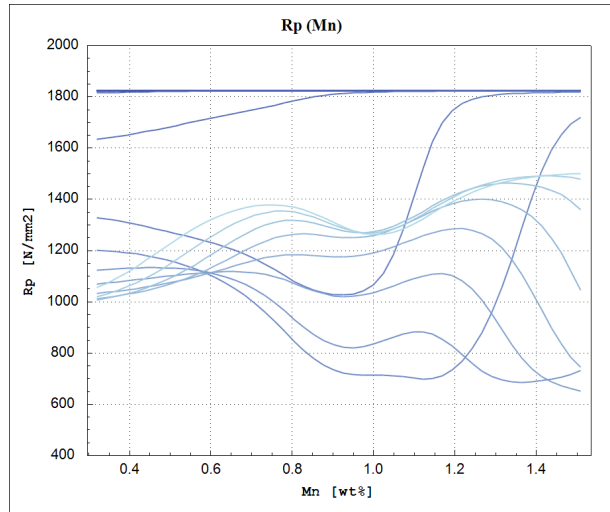


**Figure 262:** Yield stress as a function of the Manganese concentration (Mn), calculated by the ANN model on centered verification point (red line) and centered training point (blue line).

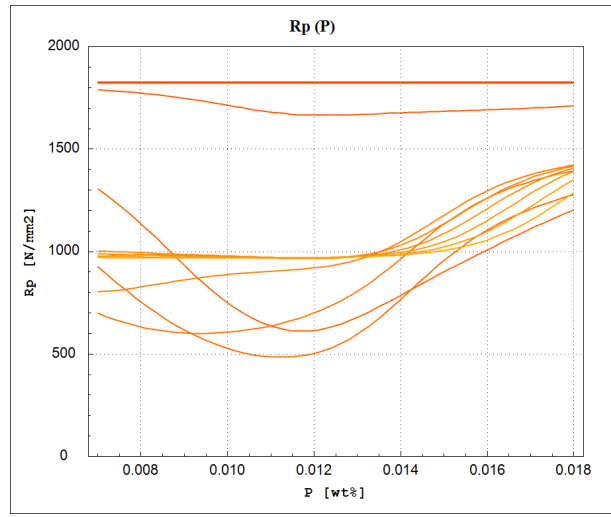
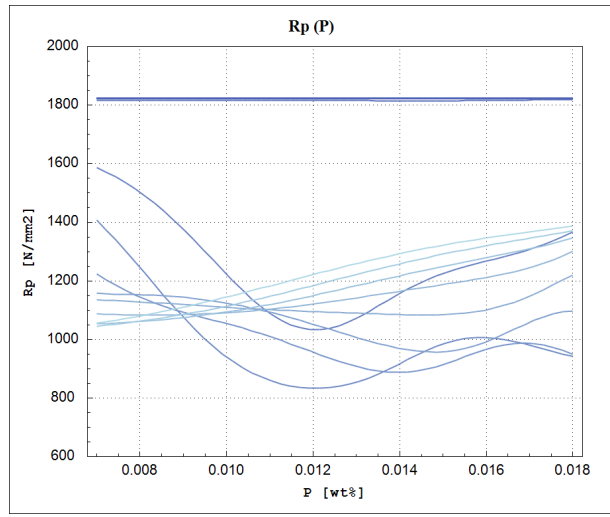


**Figure 263:** Yield stress as a function of the Phosphorus concentration (P), calculated by the ANN model on centered verification point (red line) and centered training point (blue line).

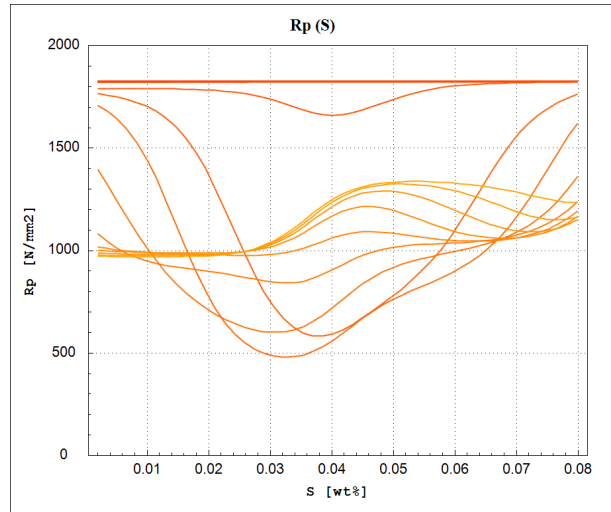
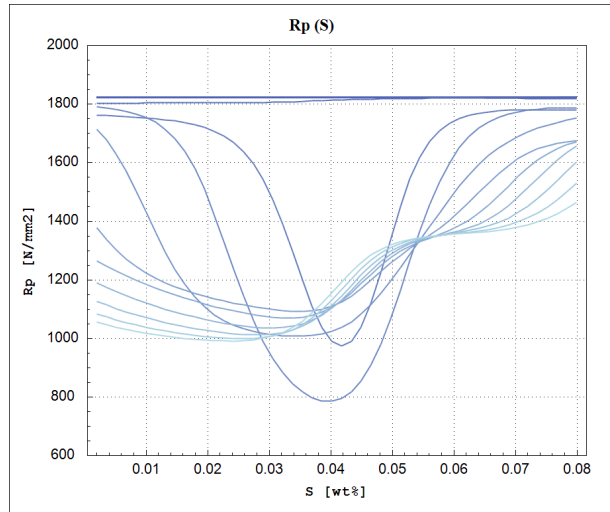


**Figure 264:** Yield stress as a function of the Sulphur concentration (S), calculated by the ANN model on centered verification point (red line) and centered training point (blue line).

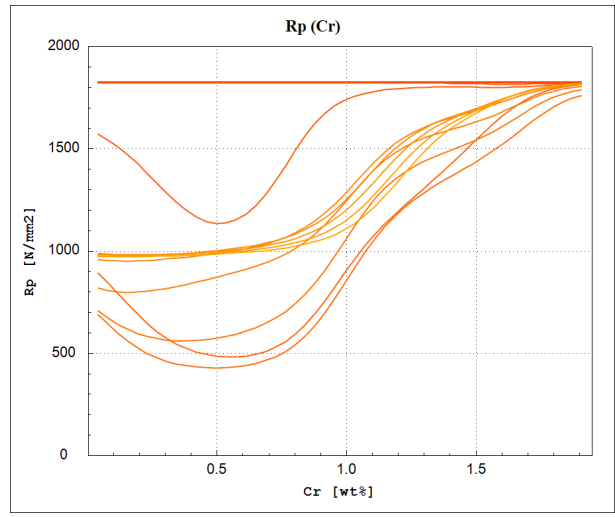
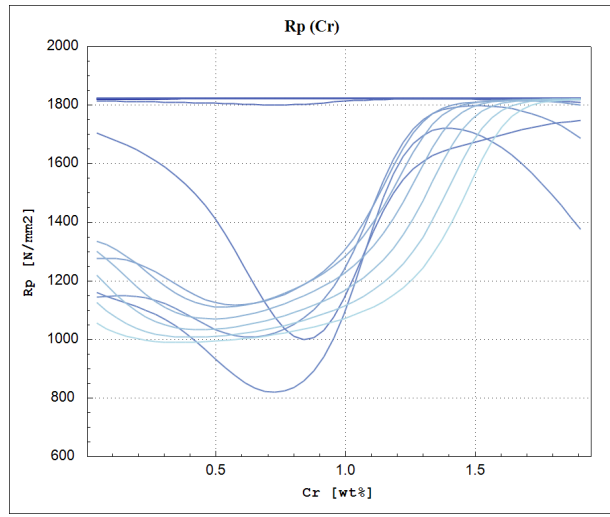


**Figure 265:** Yield stress as a function of the Chromium concentration (Cr), calculated by the ANN model on centered verification point (red line) and centered training point (blue line).

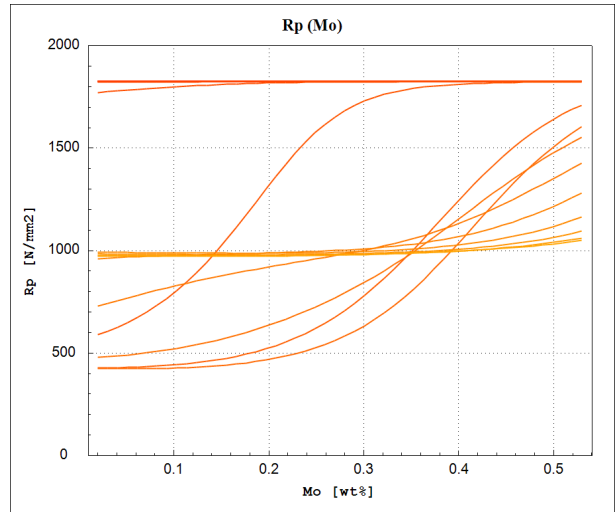
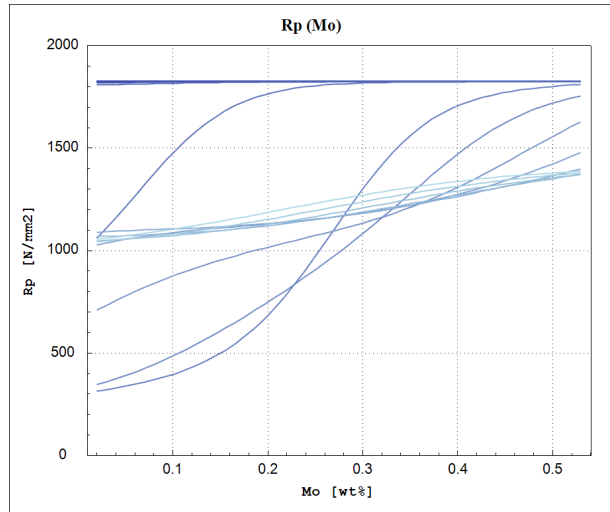


**Figure 266:** Yield stress as a function of the Molybdenum concentration (Mo), calculated by the ANN model on centered verification point (red line) and centered training point (blue line).

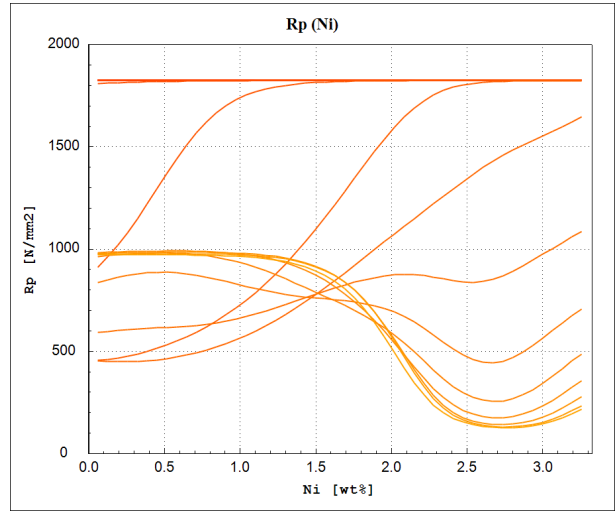
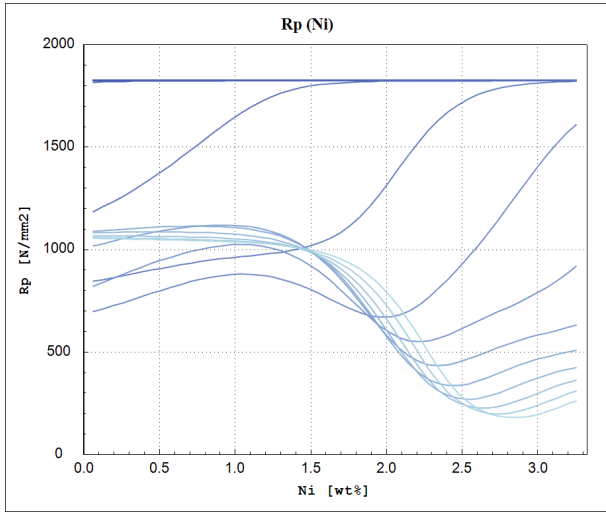


**Figure 267:** Yield stress as a function of the Nickel concentration (Ni), calculated by the ANN model on centered verification point (red line) and centered training point (blue line).

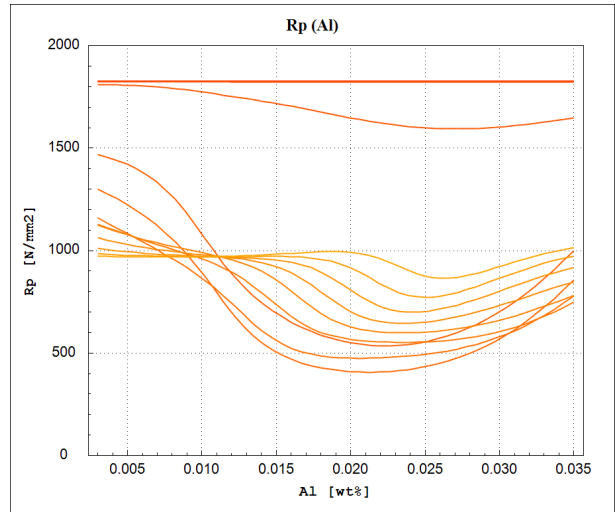
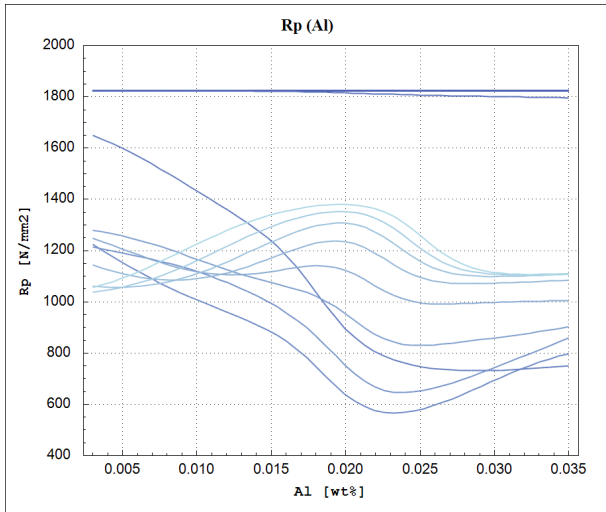


**Figure 268:** Yield stress as a function of the Aluminium concentration (Al), calculated by the ANN model on centered verification point (red line) and centered training point (blue line).

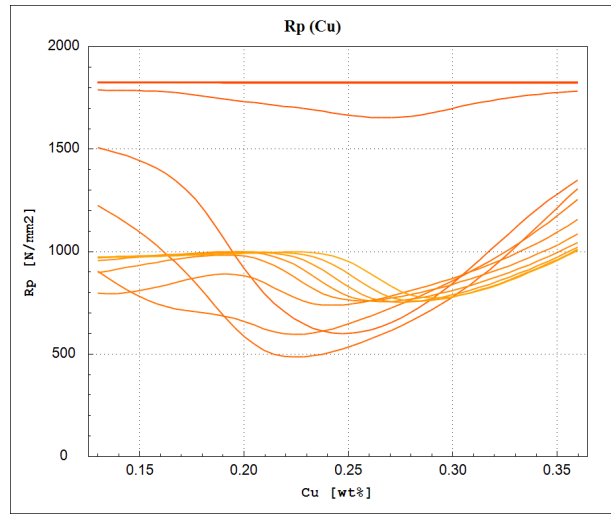
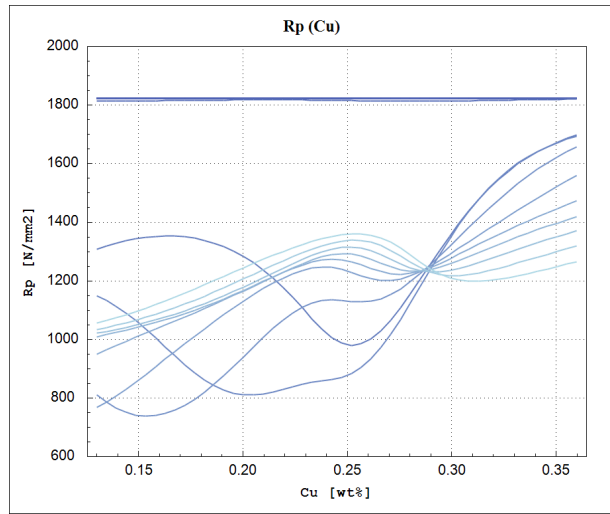


**Figure 269:** Yield stress as a function of the Copper concentration (Cu), calculated by the ANN model on centered verification point (red line) and centered training point (blue line).

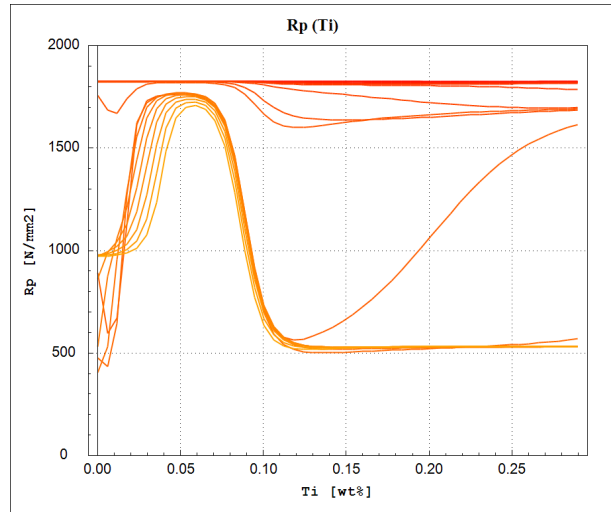
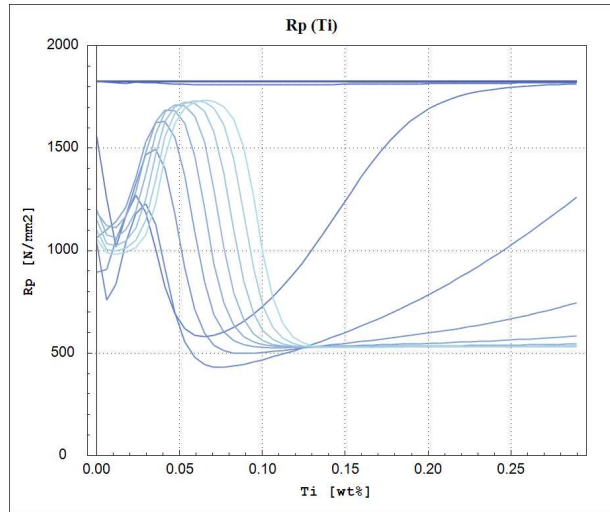


**Figure 270:** Yield stress as a function of the Titanium concentration (Ti), calculated by the ANN model on centered verification point (red line) and centered training point (blue line).

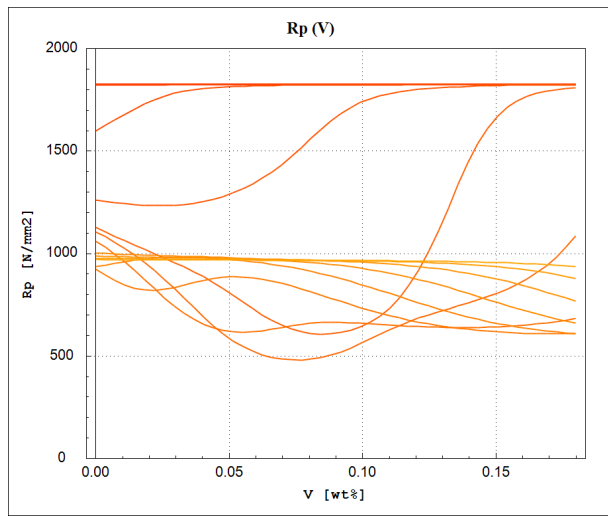
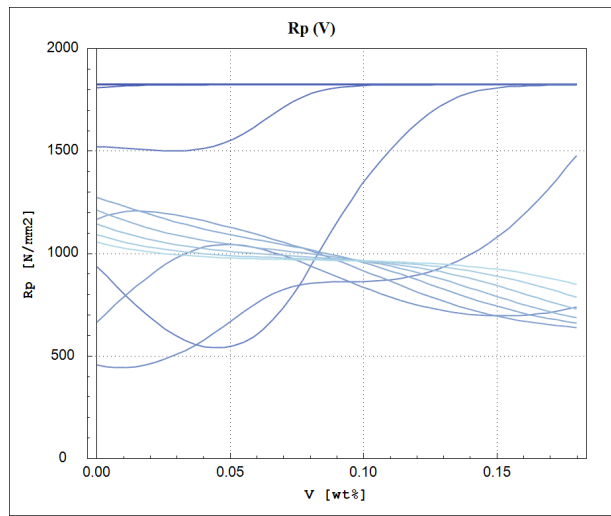


**Figure 271:** Yield stress as a function of the Vanadium concentration ( $V$ ), calculated by the ANN model on centered verification point (red line) and centered training point (blue line).

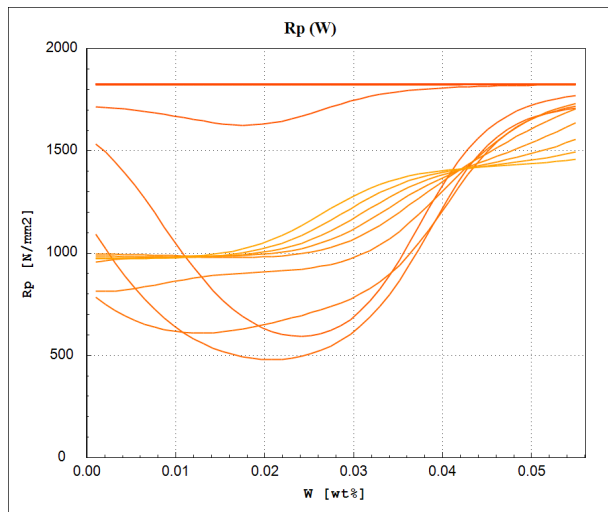
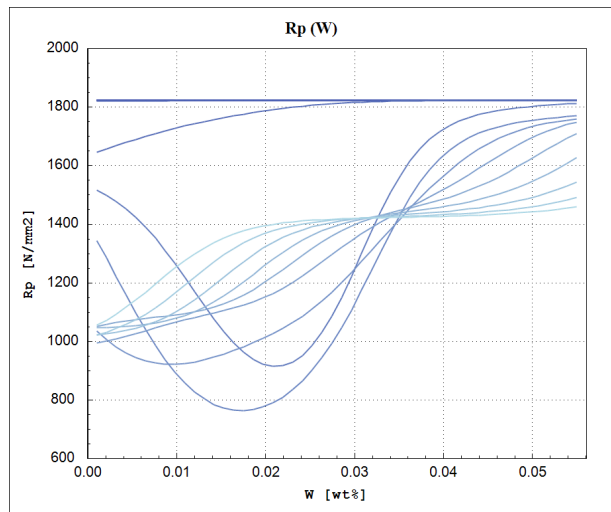


**Figure 272:** Yield stress as a function of the Tungsten concentration ( $W$ ), calculated by the ANN model on centered verification point (red line) and centered training point (blue line).

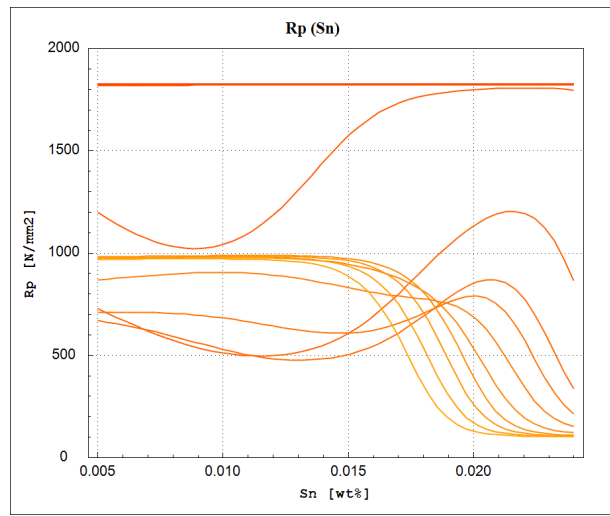
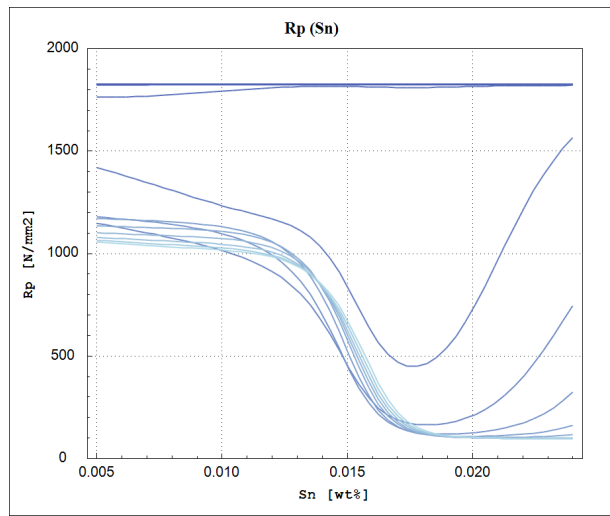


**Figure 273:** Yield stress as a function of the Tin concentration (Sn), calculated by the ANN model on centered verification point (red line) and centered training point (blue line).

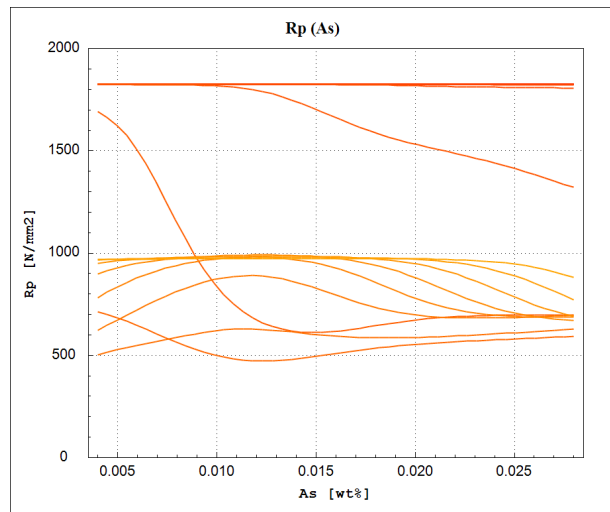
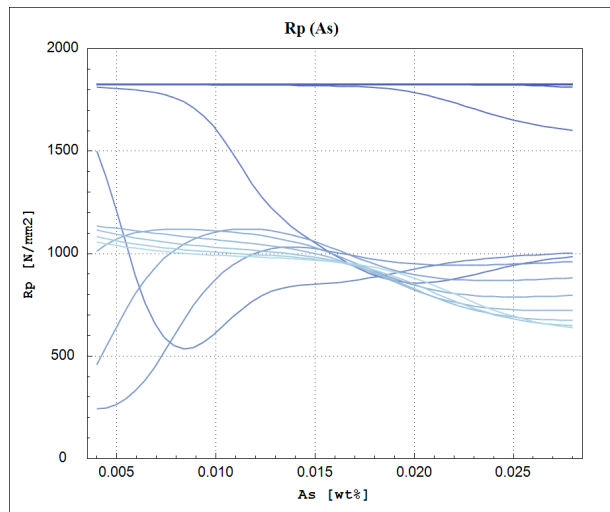


**Figure 274:** Yield stress as a function of the Arsenic concentration (As), calculated by the ANN model on centered verification point (red line) and centered training point (blue line).

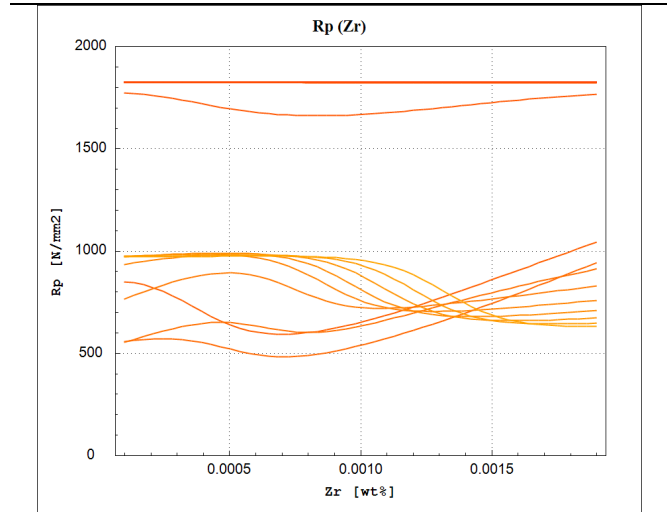
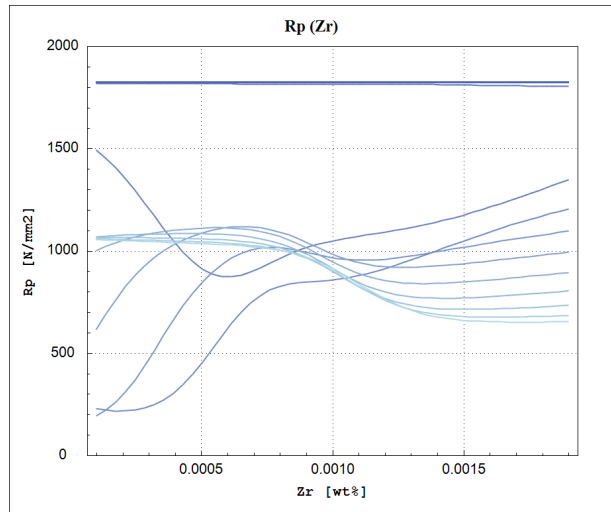


**Figure 275:** Yield stress as a function of the Zirconium concentration (Zr), calculated by the ANN model on centered verification point (red line) and centered training point (blue line).

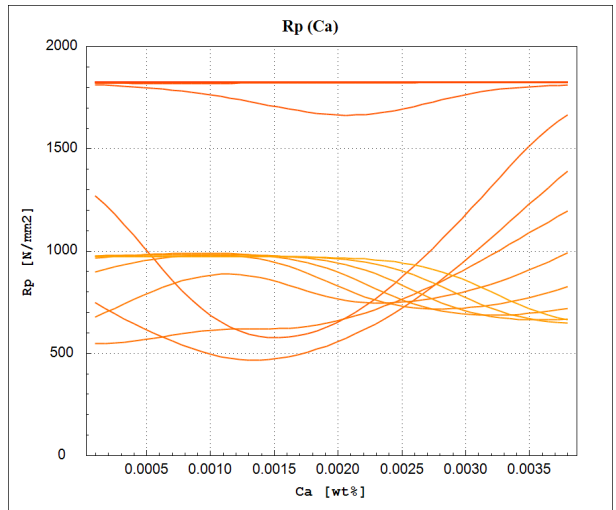
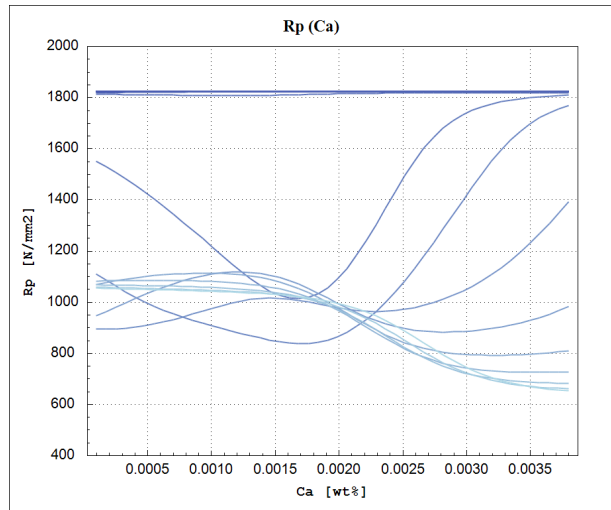


**Figure 276:** Yield stress as a function of the Calcium concentration (Ca), calculated by the ANN model on centered verification point (red line) and centered training point (blue line).

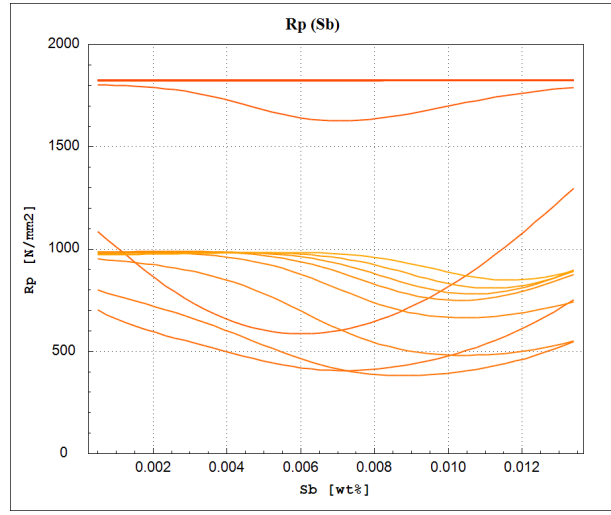
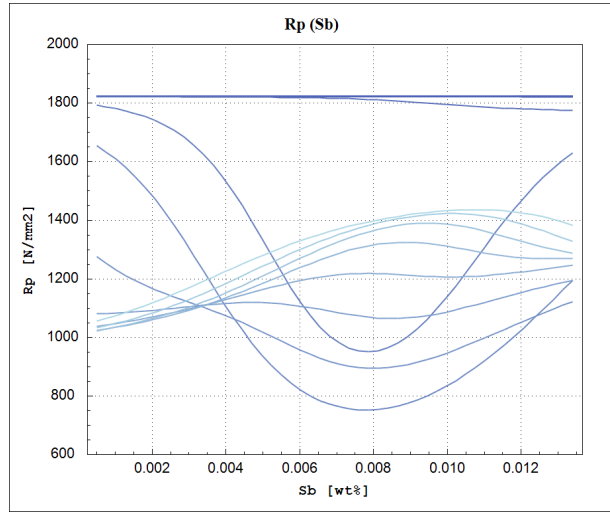


**Figure 277:** Yield stress as a function of the Antimony concentration (Sb), calculated by the ANN model on centered verification point (red line) and centered training point (blue line).

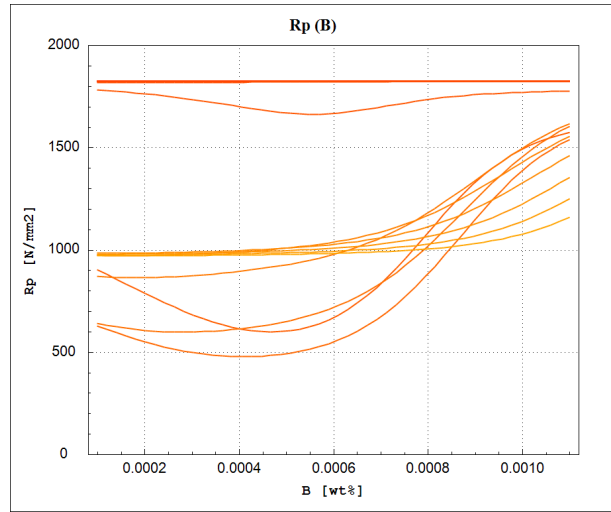
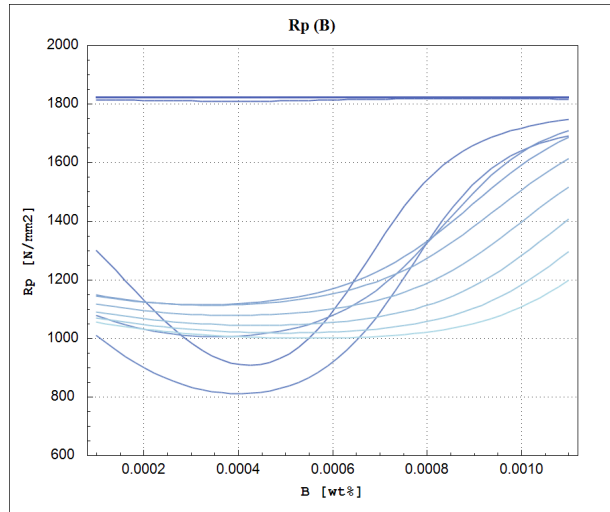


**Figure 278:** Yield stress as a function of the Boron concentration (B), calculated by the ANN model on centered verification point (red line) and centered training point (blue line).

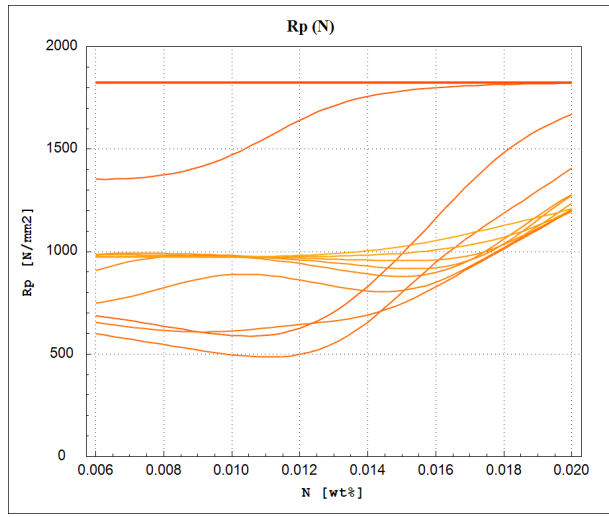
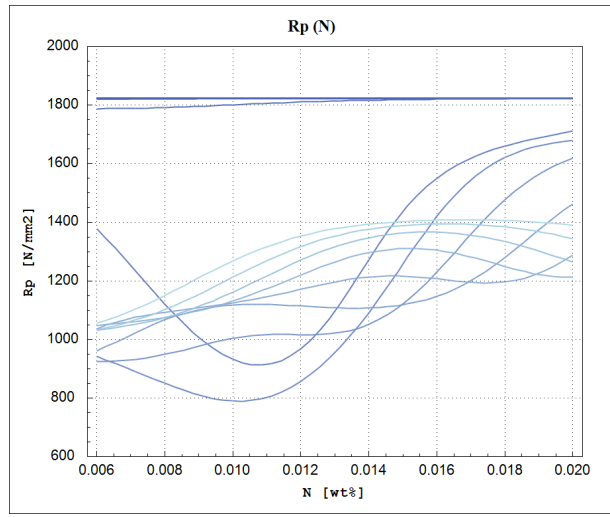


**Figure 279:** Yield stress as a function of the Nitrogen concentration (N), calculated by the ANN model on centered verification point (red line) and centered training point (blue line).

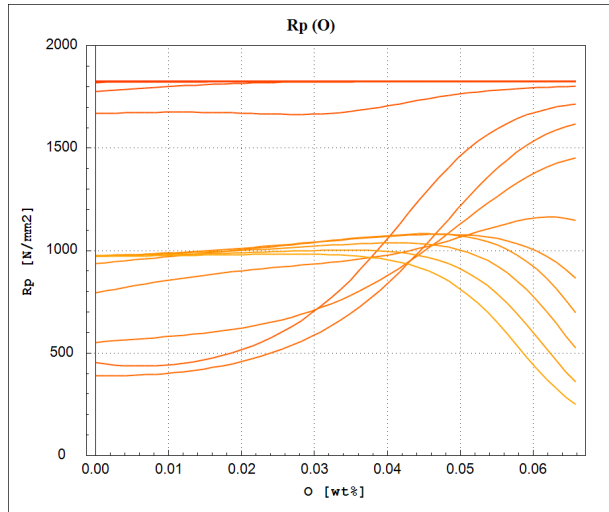
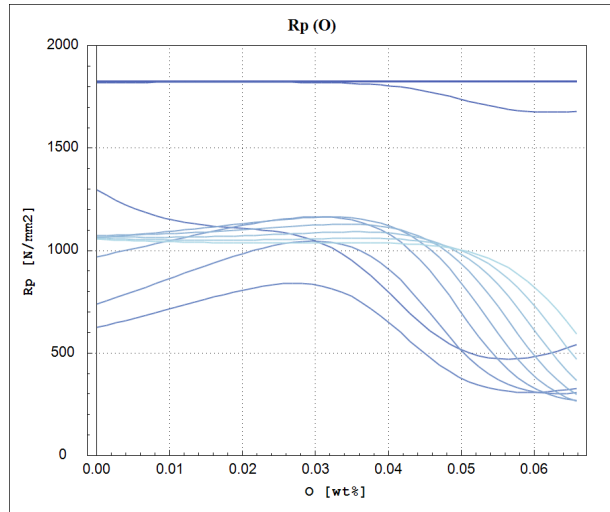


**Figure 280:** Yield stress as a function of the Oxygen concentration (O), calculated by the ANN model on centered verification point (red line) and centered training point (blue line).

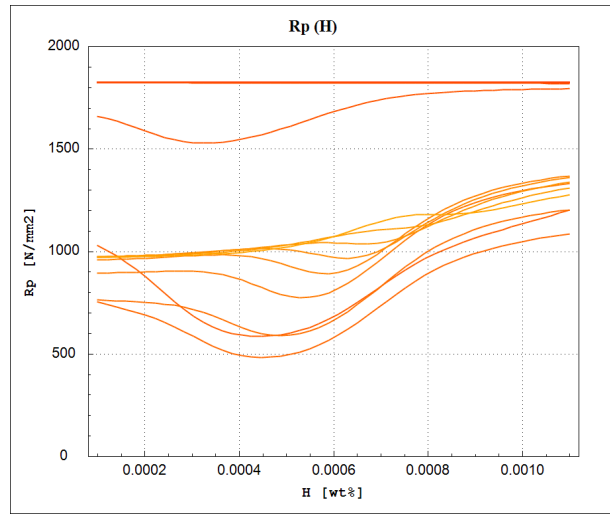
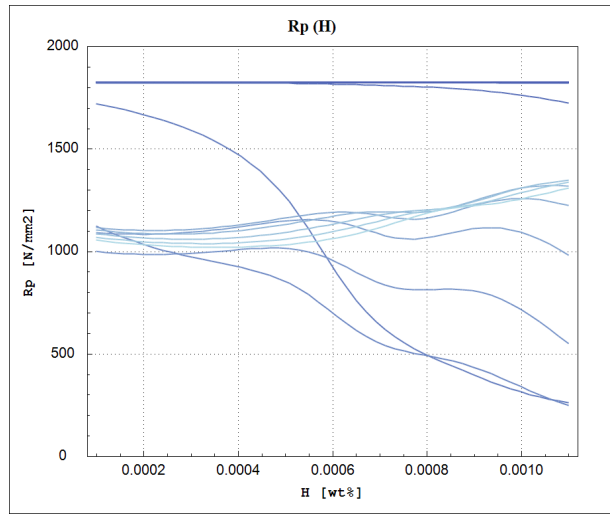


**Figure 281:** Yield stress as a function of the Hydrogen concentration (H), calculated by the ANN model on centered verification point (red line) and centered training point (blue line).

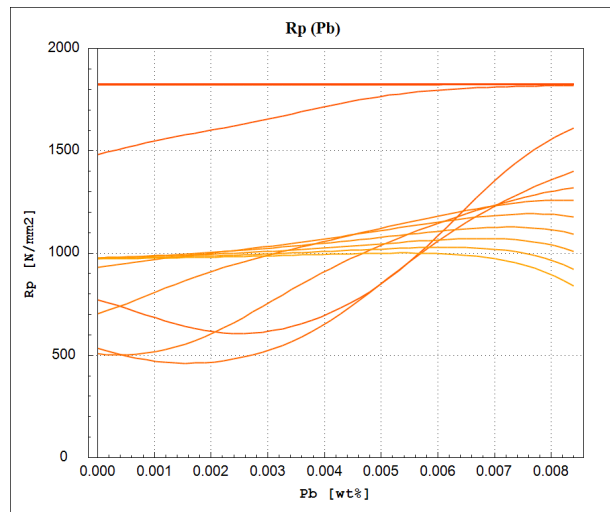
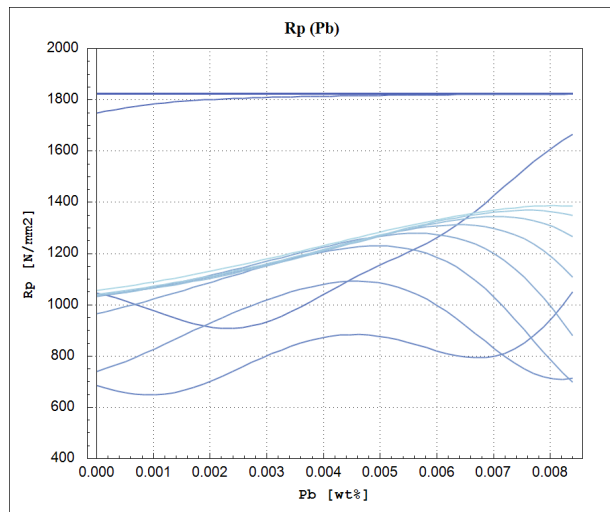


**Figure 282:** Yield stress as a function of the Lead concentration (Pb), calculated by the ANN model on centered verification point (red line) and centered training point (blue line).

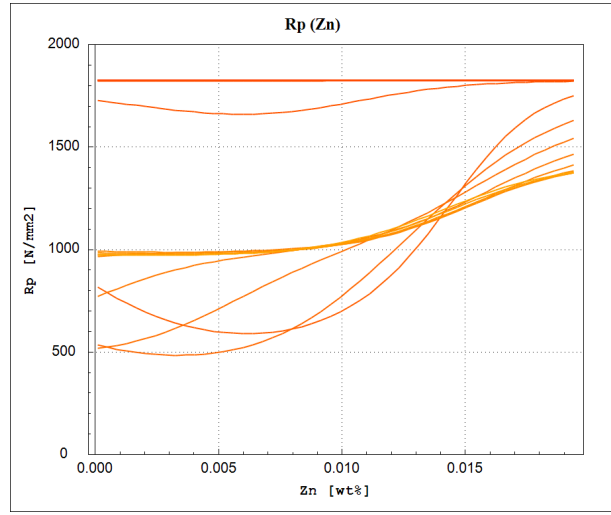
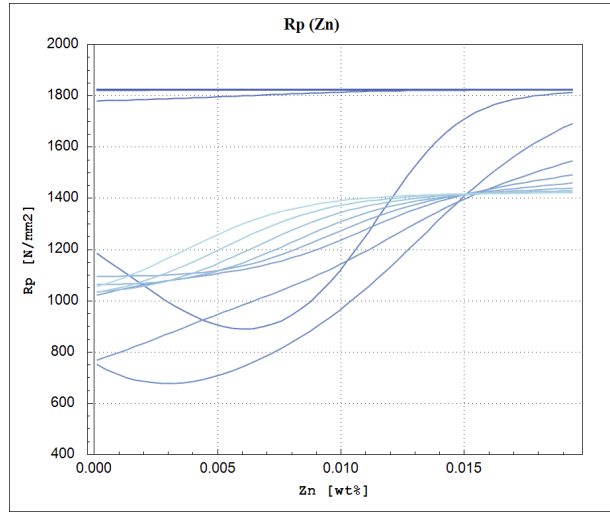


**Figure 283:** Yield stress as a function of the Zinc concentration (Zn), calculated by the ANN model on centered verification point (red line) and centered training point (blue line).

#### 5.2.4 Hardness After Rolling (HB)

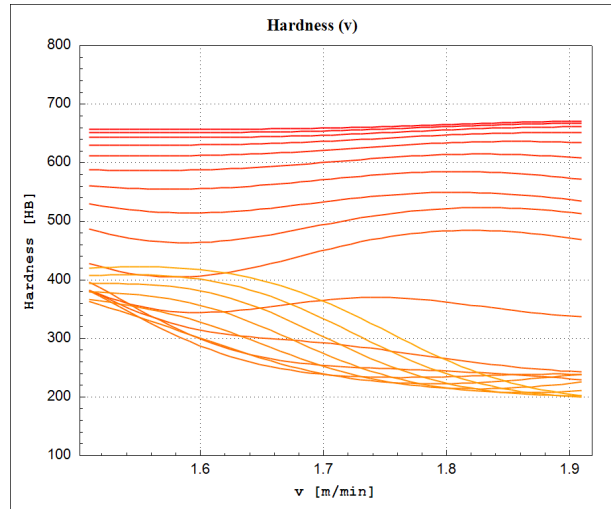
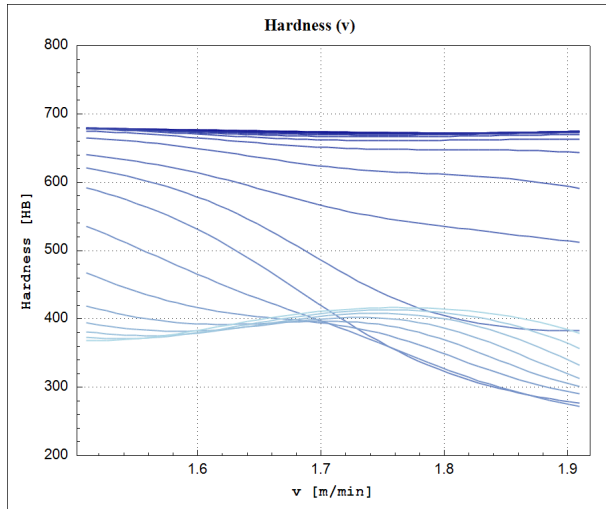


**Figure 284:** Hardness after rolling as a function of the continuous casting speed, calculated by the ANN model on centered verification point (red line) and centered training point (blue line).

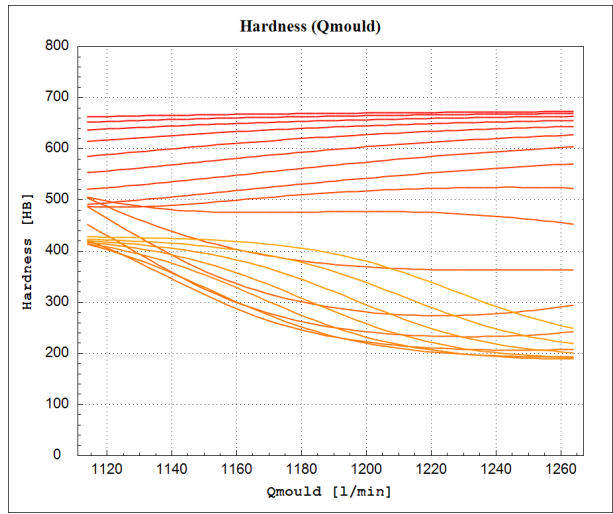
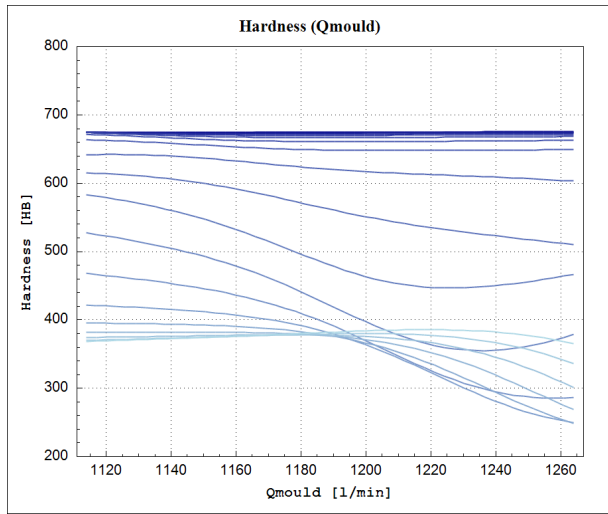


**Figure 285:** Hardness after rolling as a function of the cooling flow rate in the mould, calculated by the ANN model on centered verification point (red line) and centered training point (blue line).

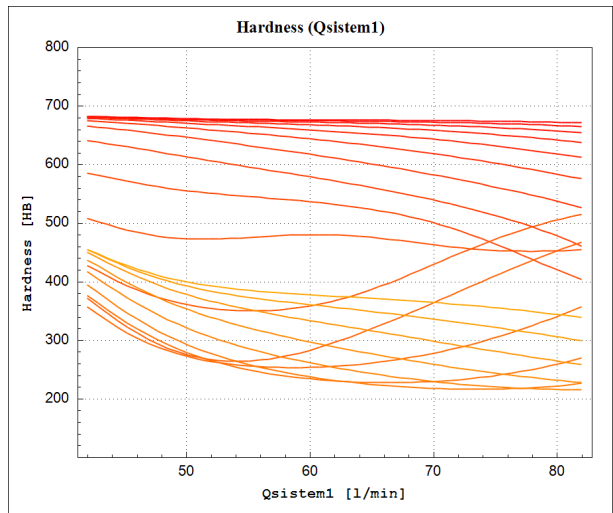
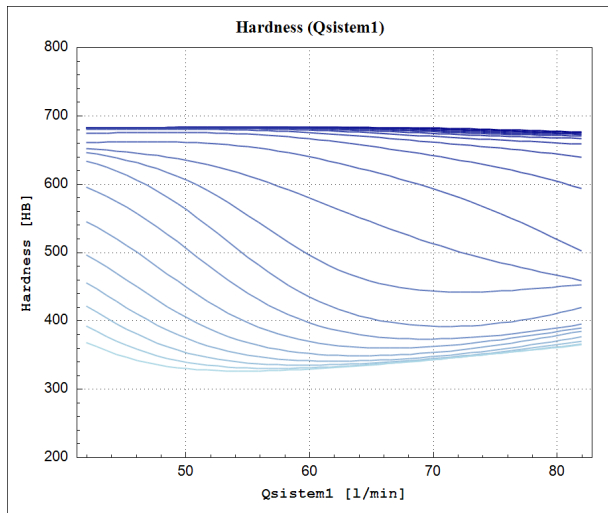


**Figure 286:** Hardness after rolling as a function of the cooling flow rate in 1<sup>st</sup> spray system, calculated by the ANN model on centered verification point (red line) and centered training point (blue line).

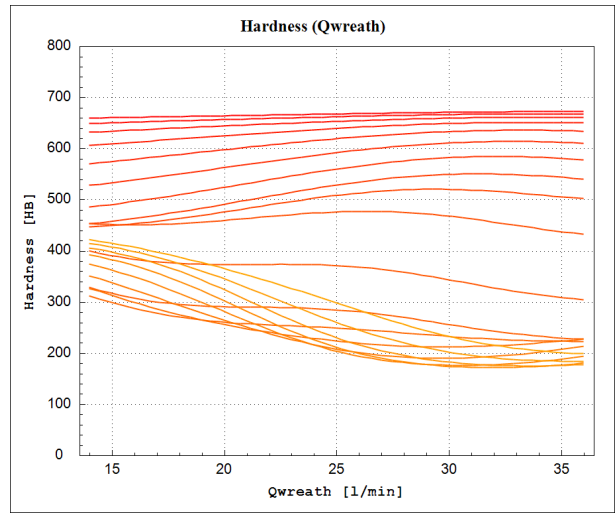
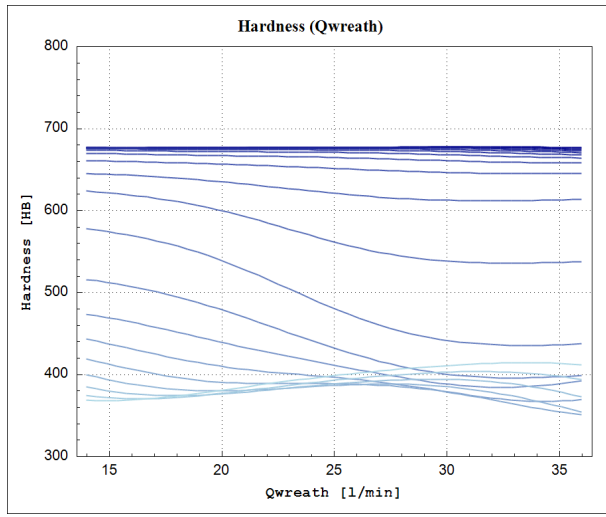


**Figure 287:** Hardness after rolling as a function of the cooling flow rate in wreath spray system, calculated by the ANN model on centered verification point (red line) and centered training point (blue line).

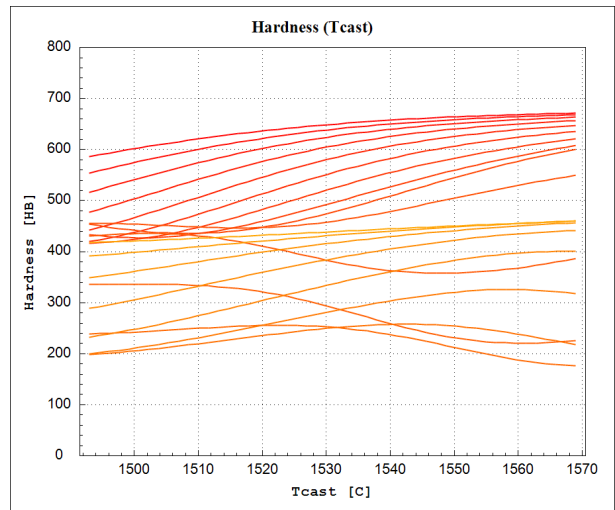
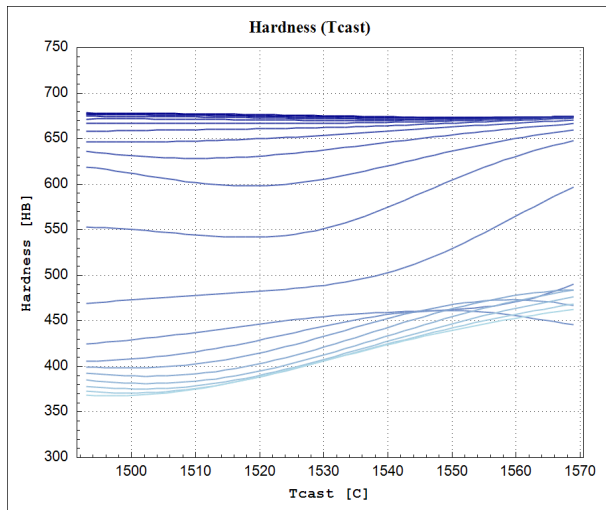


**Figure 288:** Hardness after rolling as a function of the casting temperature, calculated by the ANN model on centered verification point (red line) and centered training point (blue line).

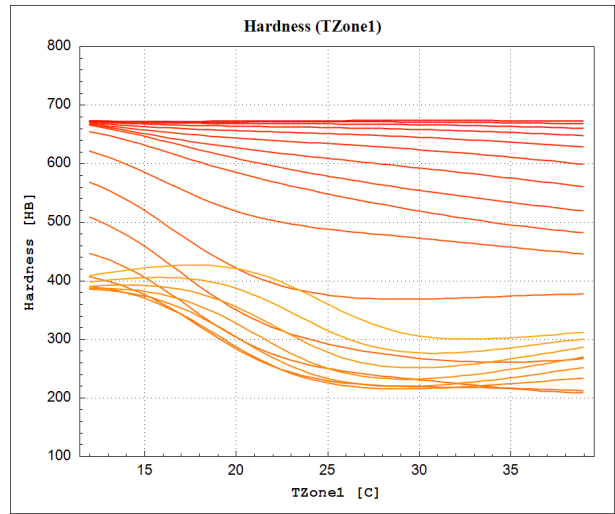
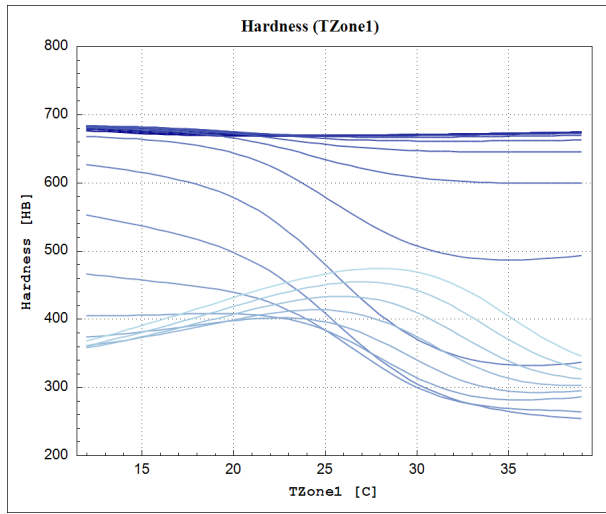


**Figure 289:** Hardness after rolling as a function of the water temperature in Zone 1, calculated by the ANN model on centered verification point (red line) and centered training point (blue line).

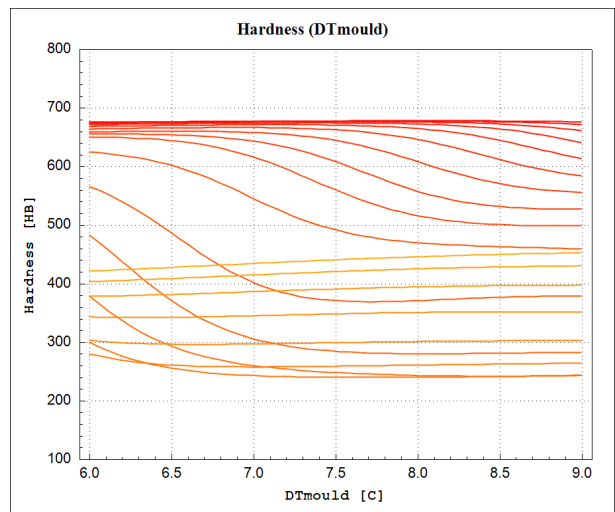
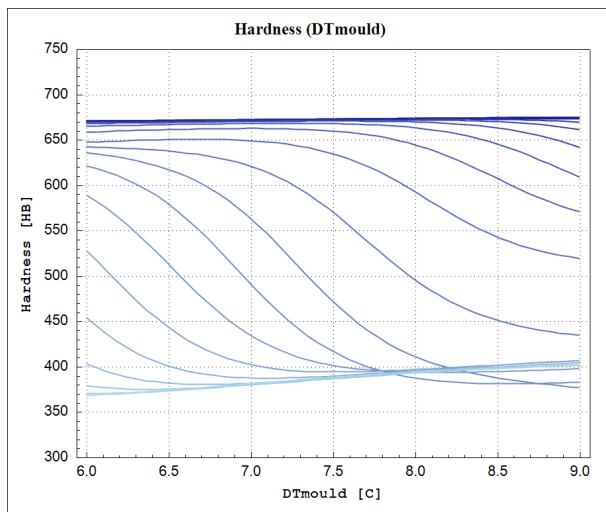


**Figure 290:** Hardness after rolling as a function of the delta T, calculated by the ANN model on centered verification point (red line) and centered training point (blue line).

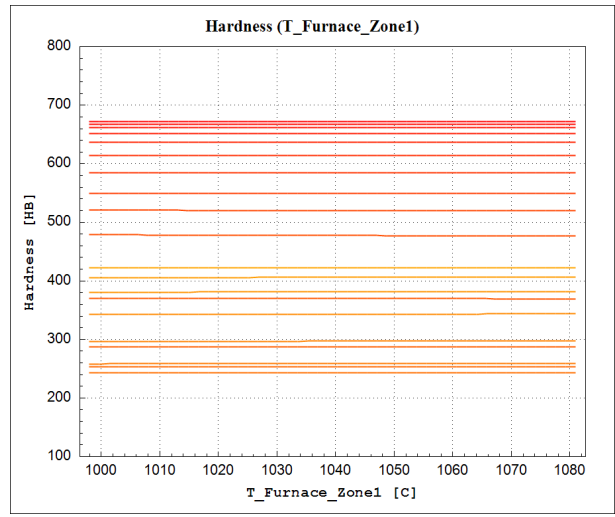
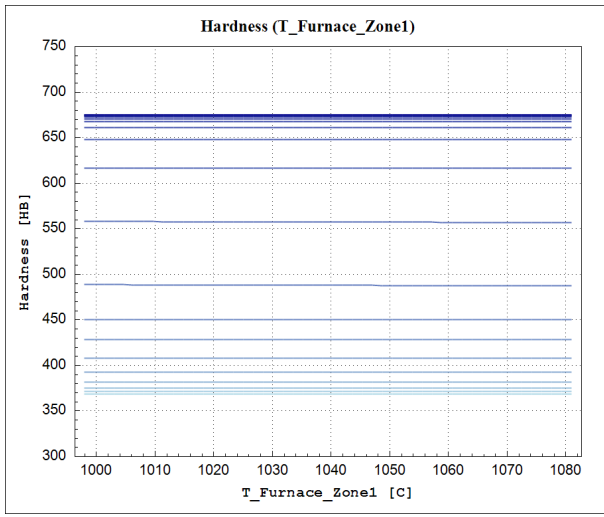


**Figure 291:** Hardness after rolling as a function of the average on temperature in zone 1, calculated by the ANN model on centered verification point (red line) and centered training point (blue line).

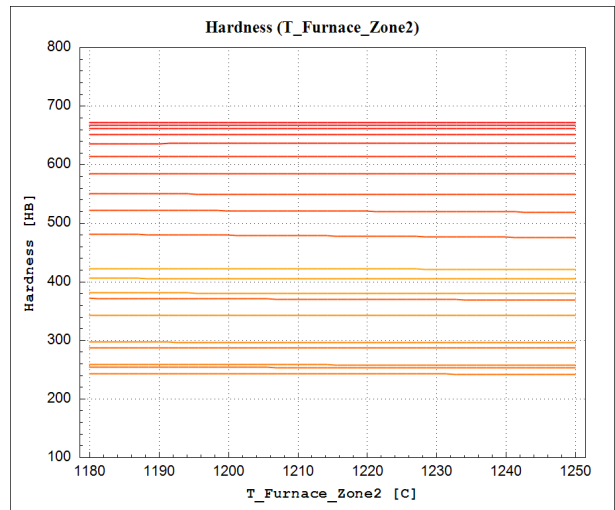
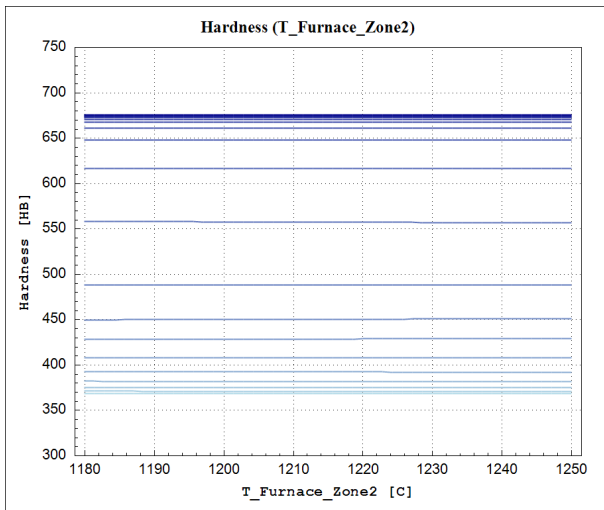


**Figure 292:** Hardness after rolling as a function of the average on temperature in zone 2, calculated by the ANN model on centered verification point (red line) and centered training point (blue line).

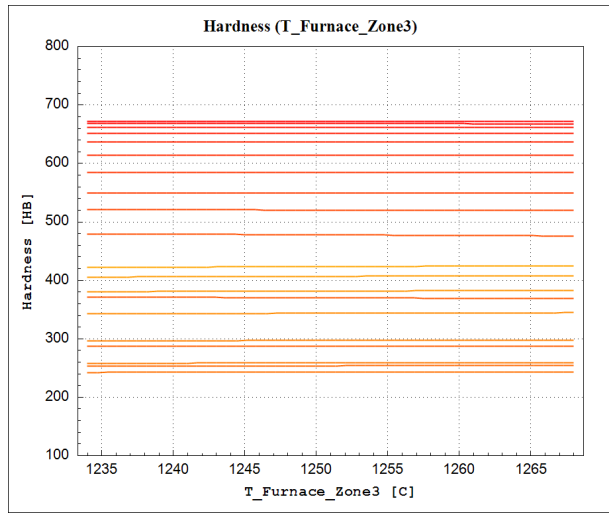
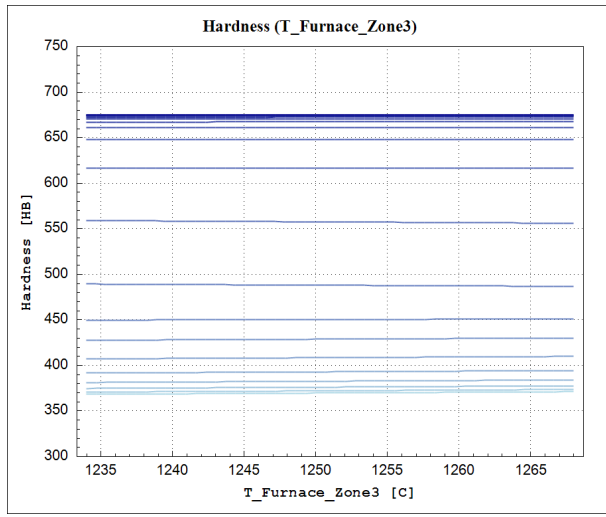


**Figure 293:** Hardness after rolling as a function of the average on temperature in zone 3, calculated by the ANN model on centered verification point (red line) and centered training point (blue line).

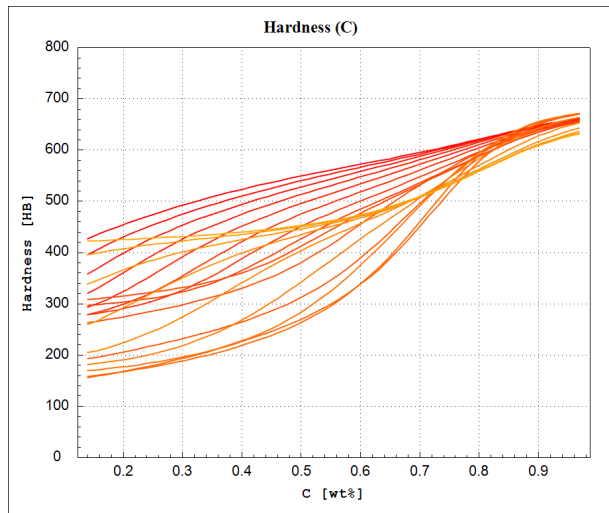
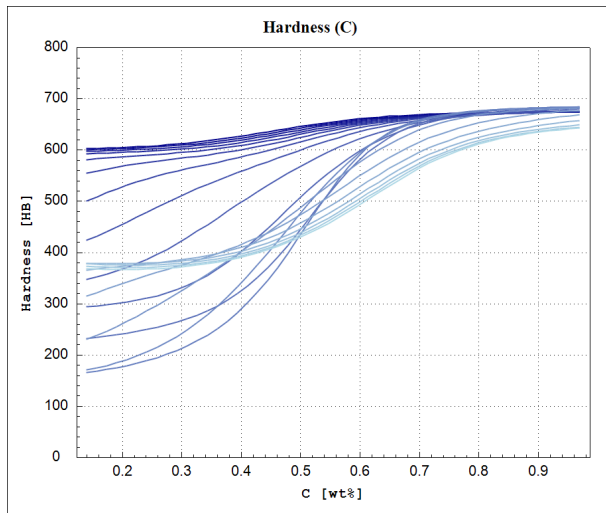


**Figure 294:** Hardness after rolling as a function of the Carbon concentration (C), calculated by the ANN model on centered verification point (red line) and centered training point (blue line).

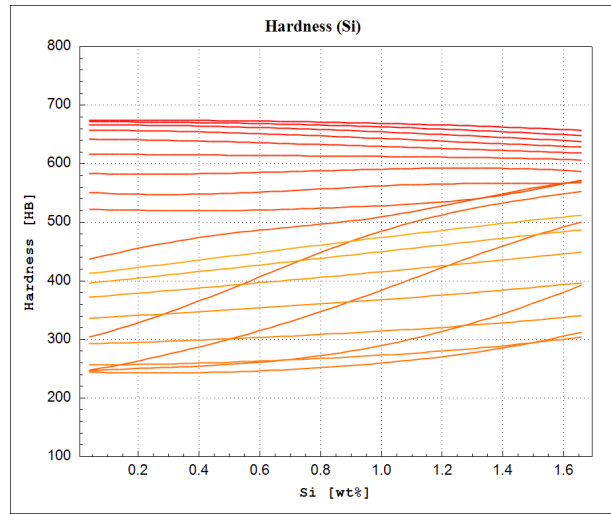
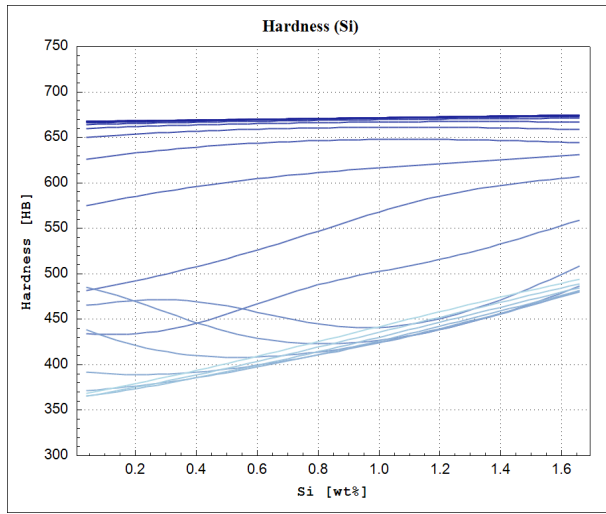


**Figure 295:** Hardness after rolling as a function of the Silicon concentration (Si), calculated by the ANN model on centered verification point (red line) and centered training point (blue line).

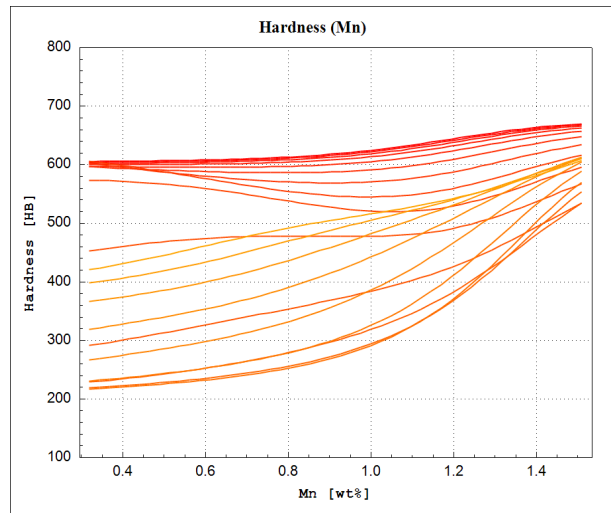
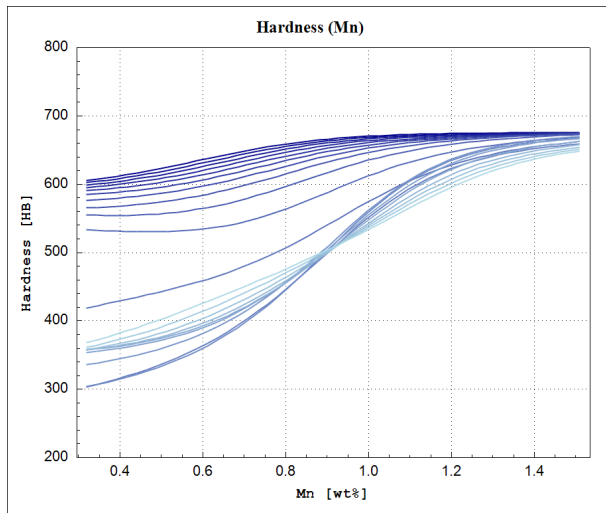


**Figure 296:** Hardness after rolling as a function of the Manganese concentration (Mn), calculated by the ANN model on centered verification point (red line) and centered training point (blue line).

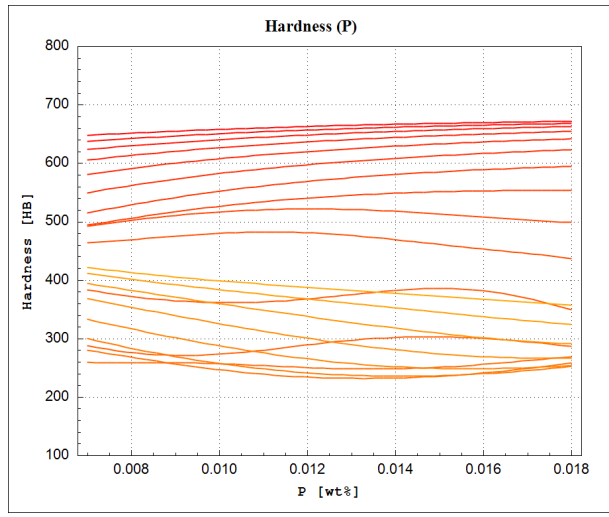
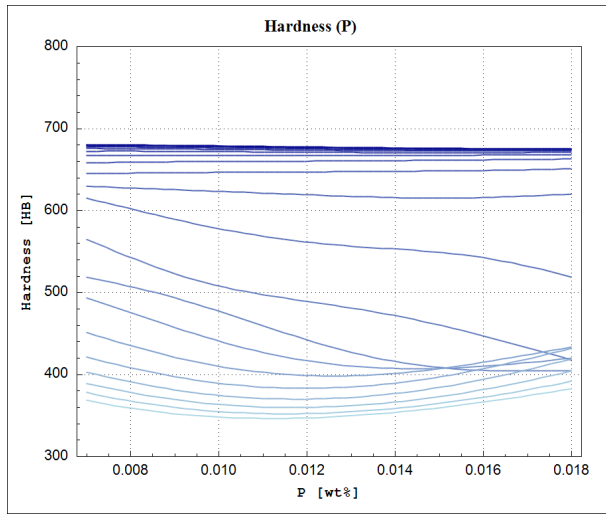


**Figure 297:** Hardness after rolling as a function of the Phosphorus concentration (P), calculated by the ANN model on centered verification point (red line) and centered training point (blue line).

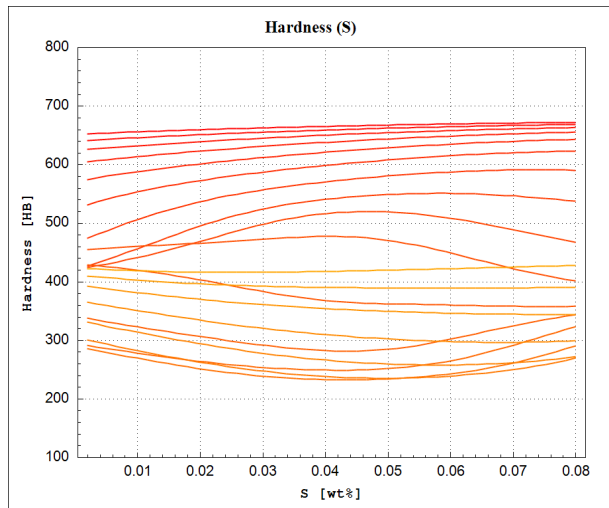
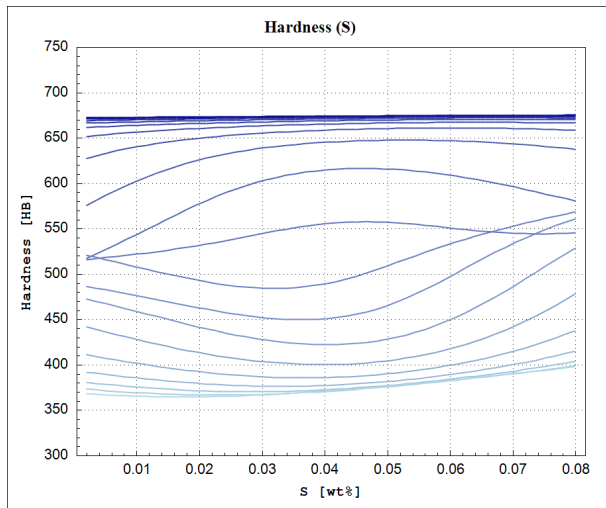


**Figure 298:** Hardness after rolling as a function of the Sulphur concentration (S), calculated by the ANN model on centered verification point (red line) and centered training point (blue line).

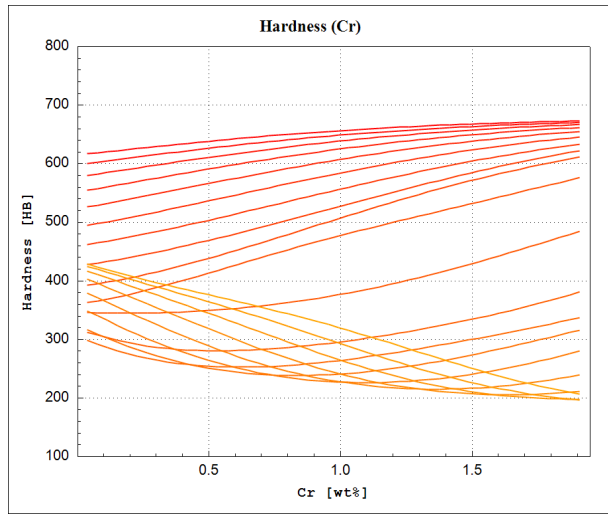
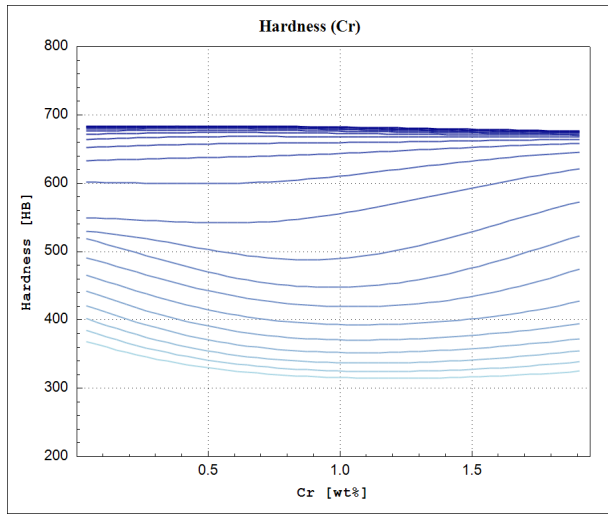


**Figure 299:** Hardness after rolling as a function of the Chromium concentration (Cr), calculated by the ANN model on centered verification point (red line) and centered training point (blue line).

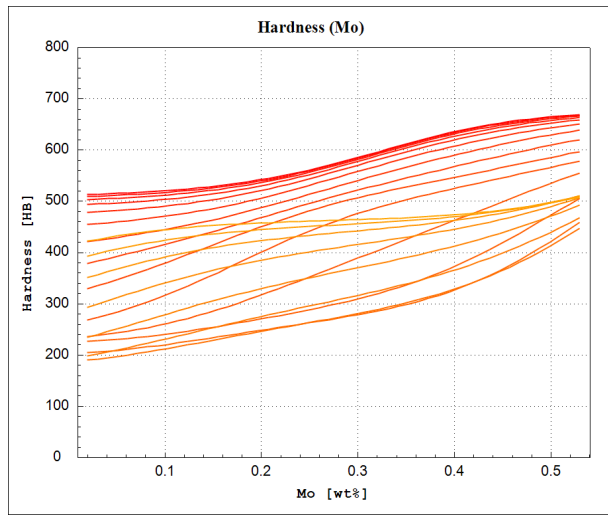
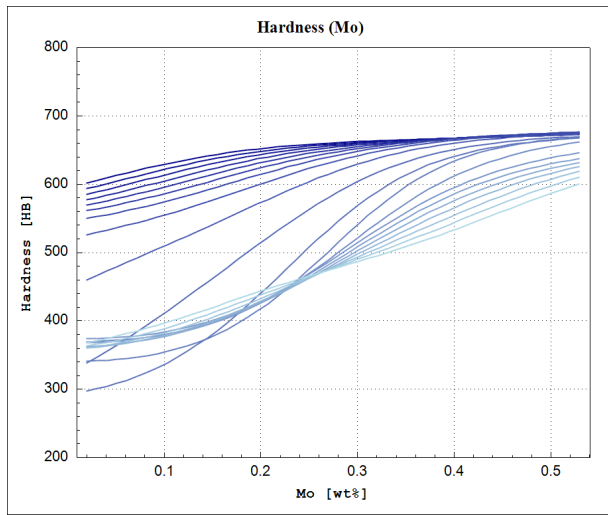


**Figure 300:** Hardness after rolling as a function of the Molybdenum concentration (Mo), calculated by the ANN model on centered verification point (red line) and centered training point (blue line).

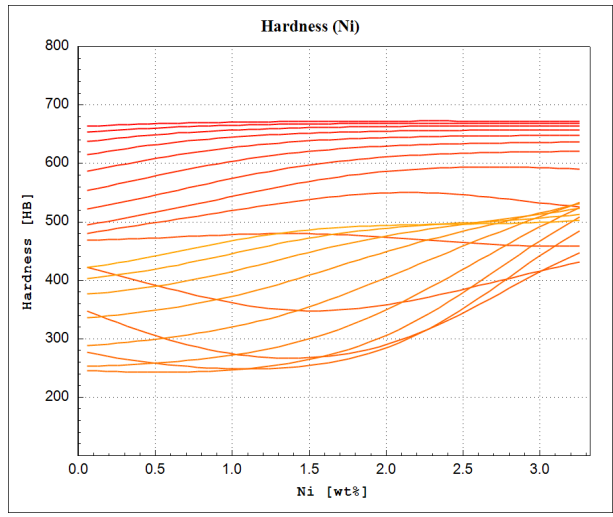
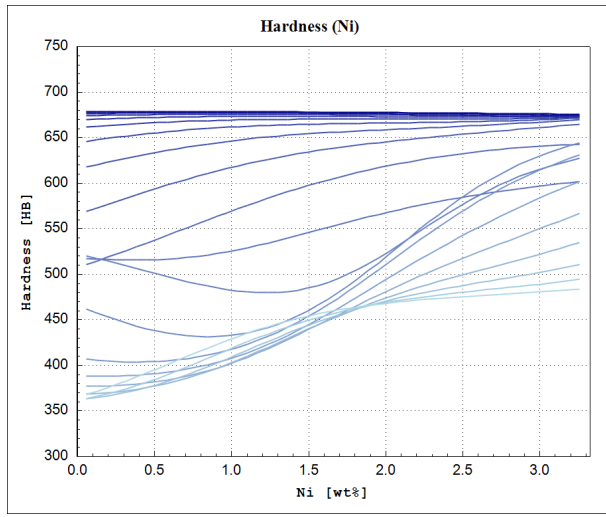


**Figure 301:** Hardness after rolling as a function of the Nickel concentration (Ni), calculated by the ANN model on centered verification point (red line) and centered training point (blue line).

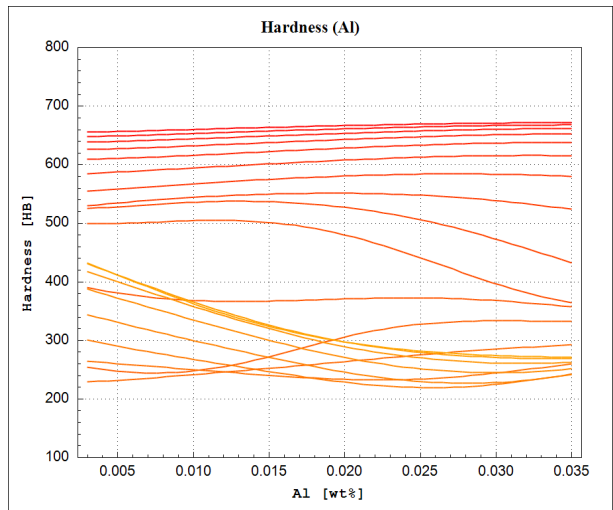
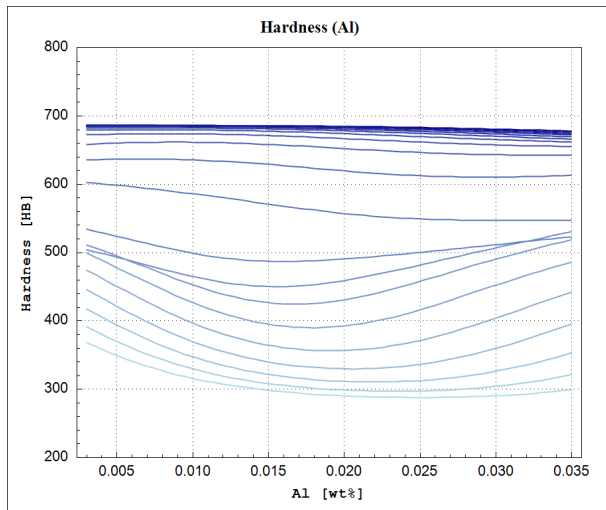


**Figure 302:** Hardness after rolling as a function of the Aluminium concentration (Al), calculated by the ANN model on centered verification point (red line) and centered training point (blue line).

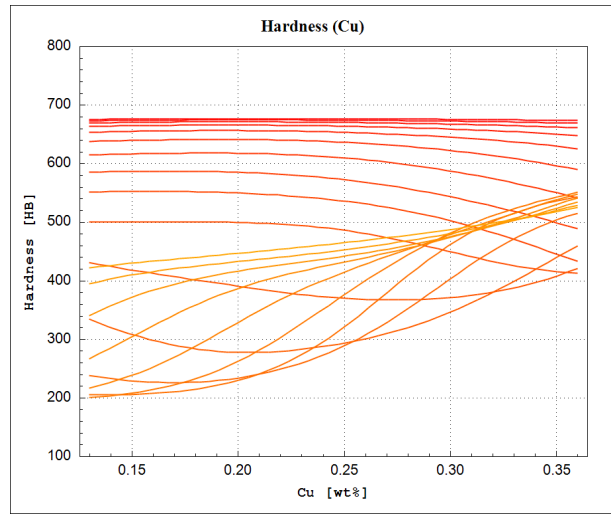
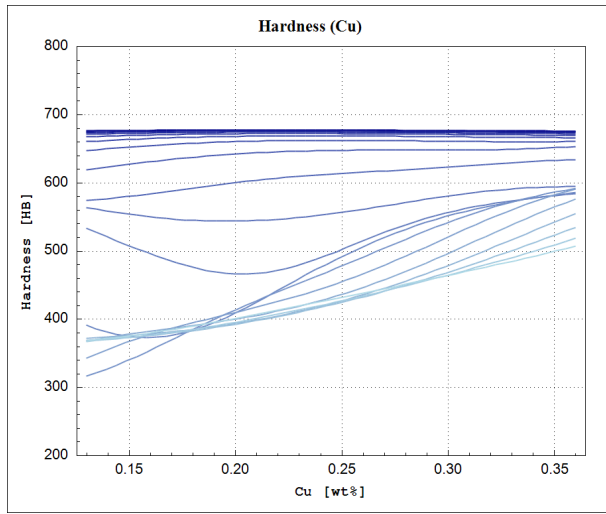


**Figure 303:** Hardness after rolling as a function of the Copper concentration (Cu), calculated by the ANN model on centered verification point (red line) and centered training point (blue line).

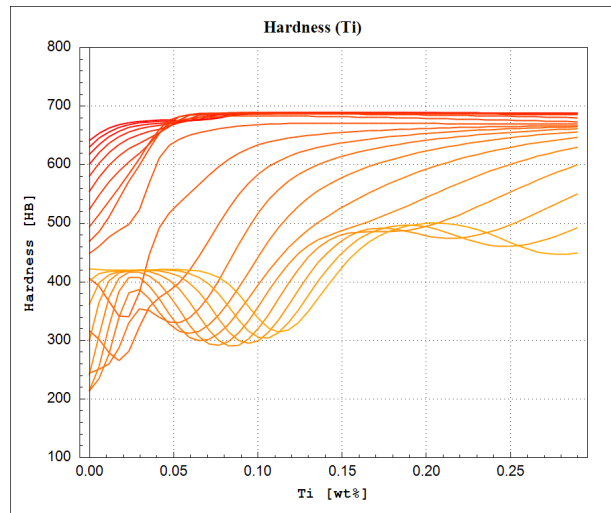
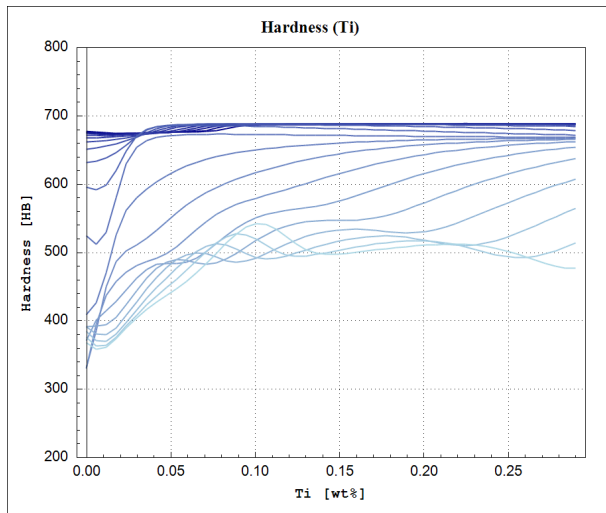


**Figure 304:** Hardness after rolling as a function of the Titanium concentration (Ti), calculated by the ANN model on centered verification point (red line) and centered training point (blue line).

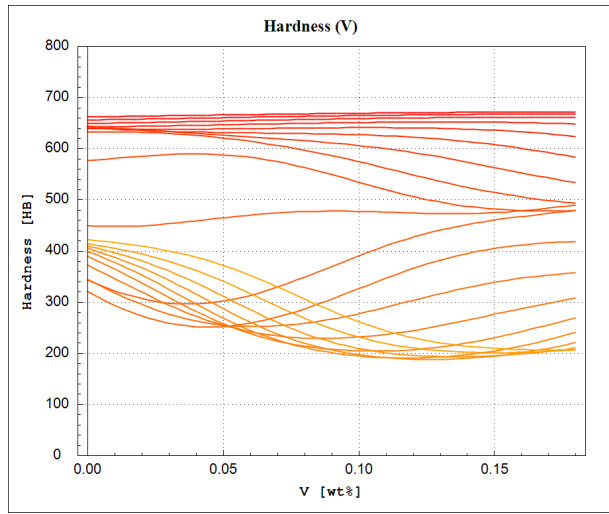
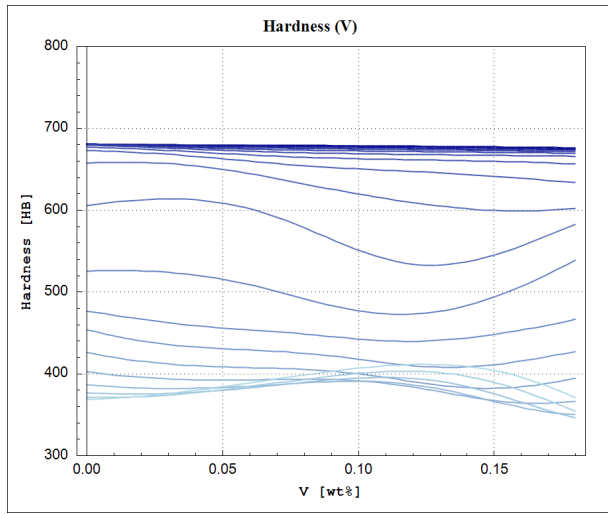


**Figure 305:** Hardness after rolling as a function of the Vanadium concentration (V), calculated by the ANN model on centered verification point (red line) and centered training point (blue line).

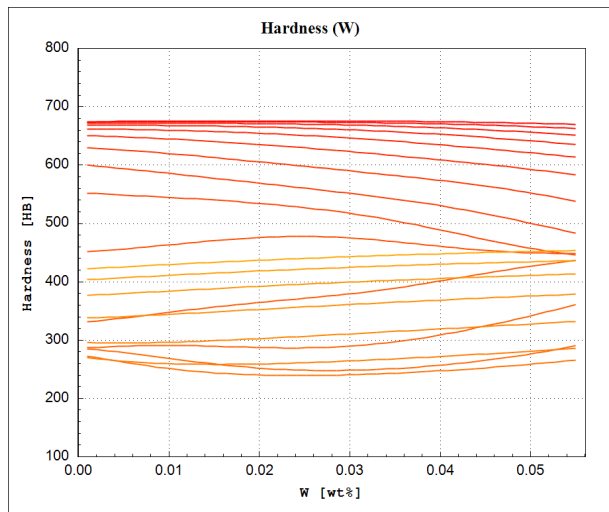
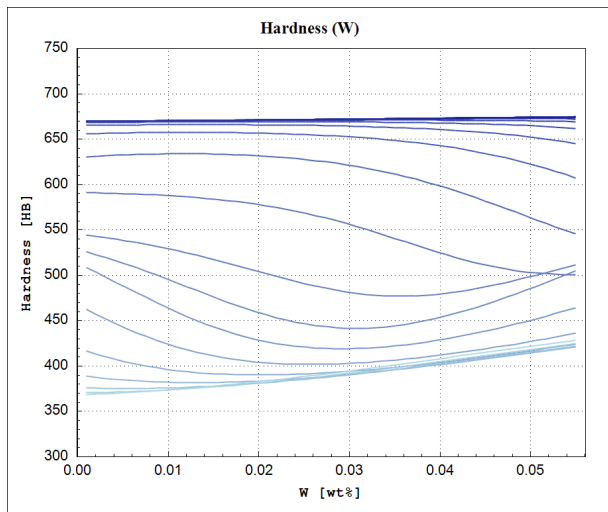


**Figure 306:** Hardness after rolling as a function of the Tungsten concentration (W), calculated by the ANN model on centered verification point (red line) and centered training point (blue line).

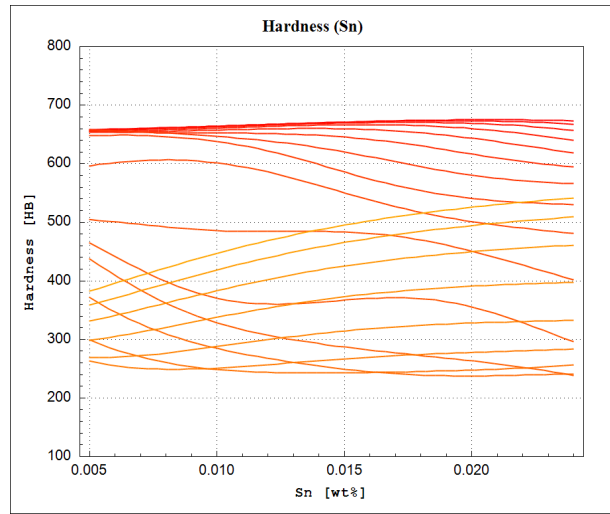
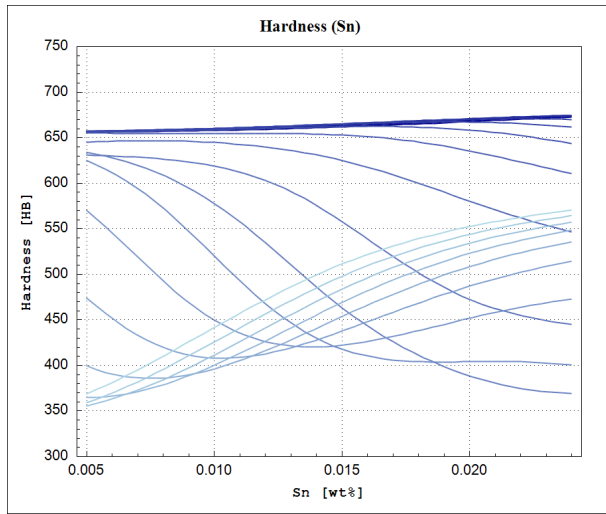


**Figure 307:** Hardness after rolling as a function of the Tin concentration (Sn), calculated by the ANN model on centered verification point (red line) and centered training point (blue line).

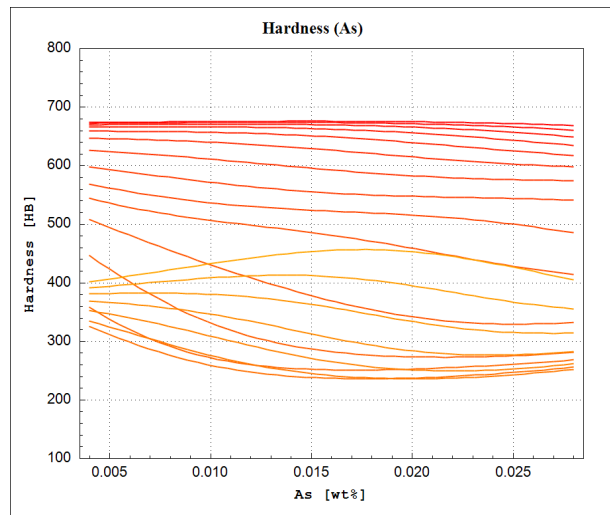
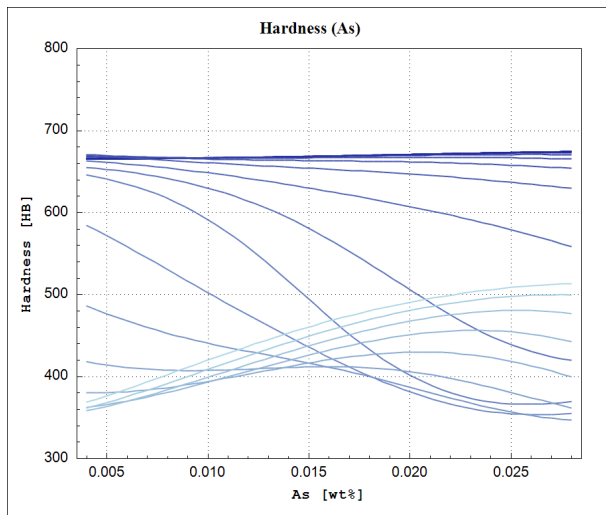


**Figure 308:** Hardness after rolling as a function of the Arsenic concentration (As), calculated by the ANN model on centered verification point (red line) and centered training point (blue line).

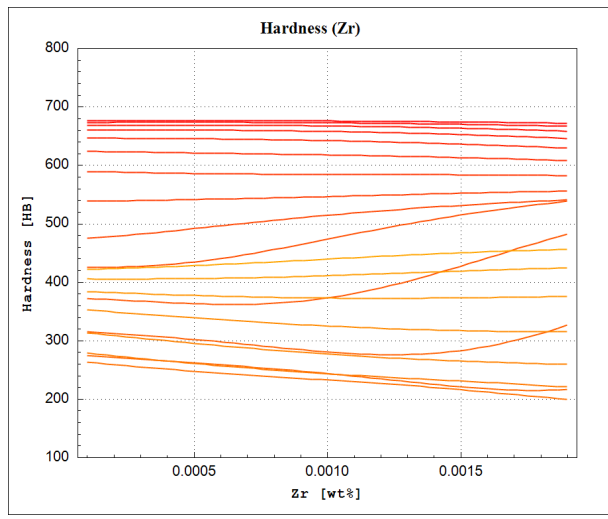
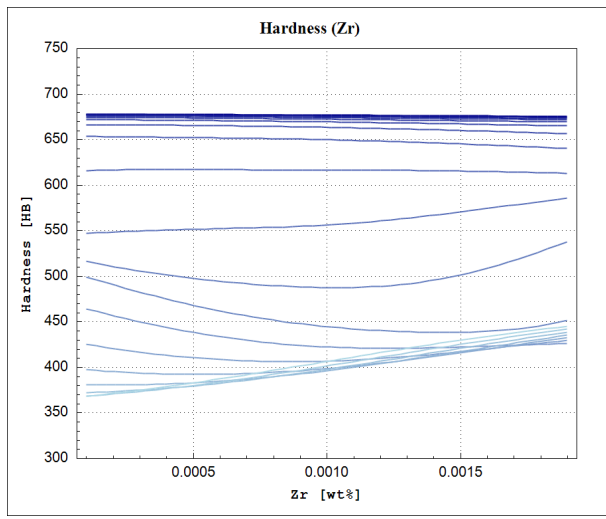


**Figure 309:** Hardness after rolling as a function of the Zirconium concentration (Zr), calculated by the ANN model on centered verification point (red line) and centered training point (blue line).

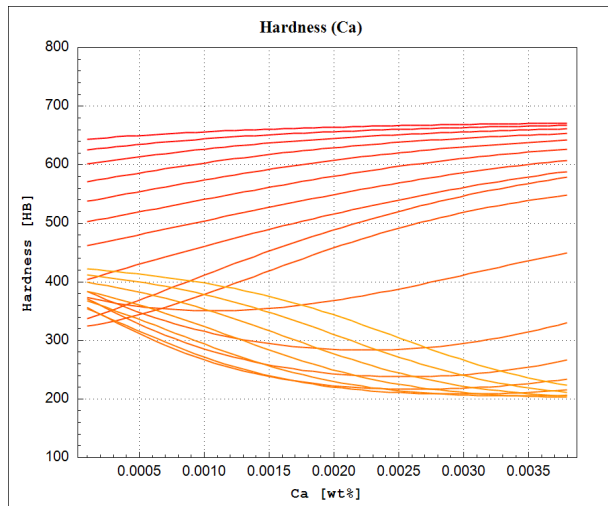
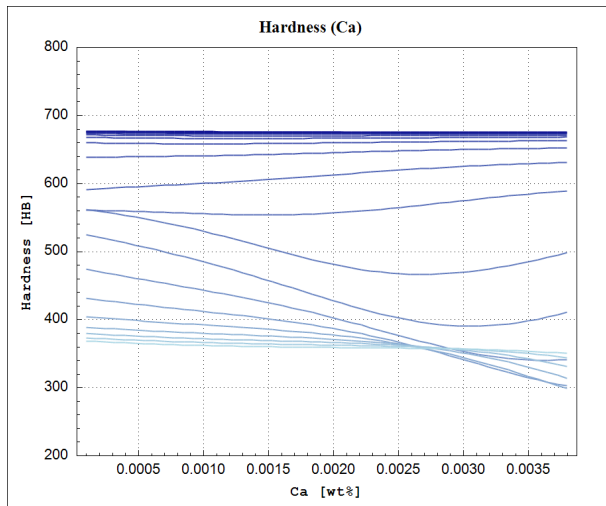


**Figure 310:** Hardness after rolling as a function of the Calcium concentration (Ca), calculated by the ANN model on centered verification point (red line) and centered training point (blue line).

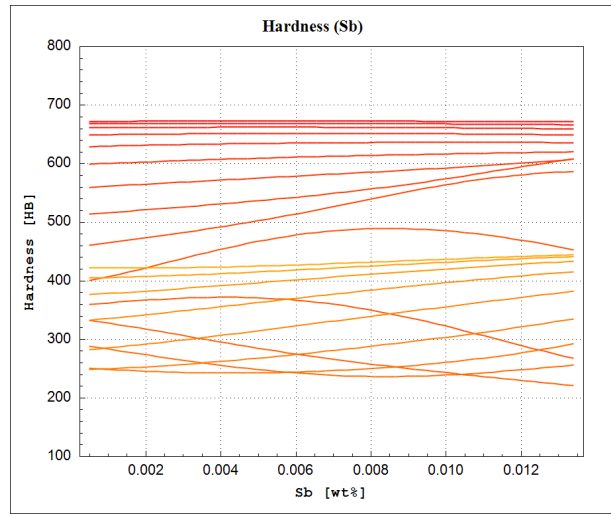
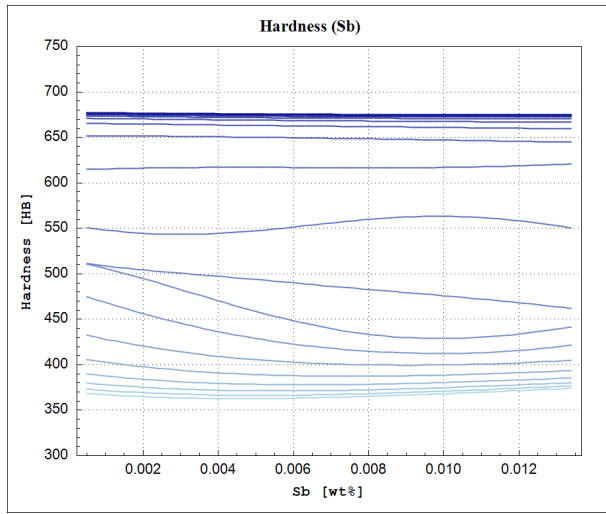


**Figure 311:** Hardness after rolling as a function of the Antimony concentration (Sb), calculated by the ANN model on centered verification point (red line) and centered training point (blue line).

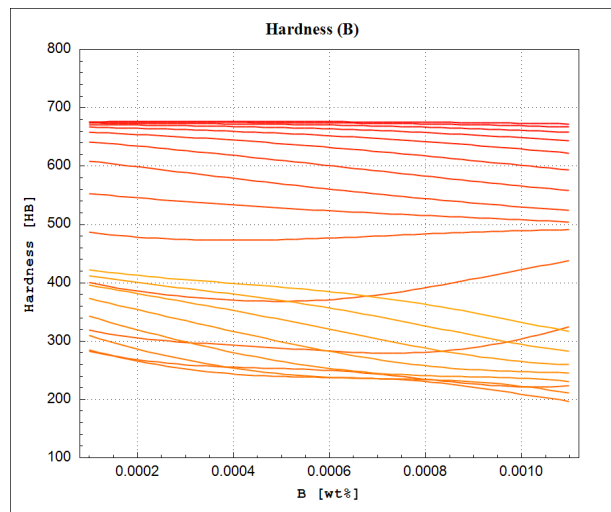
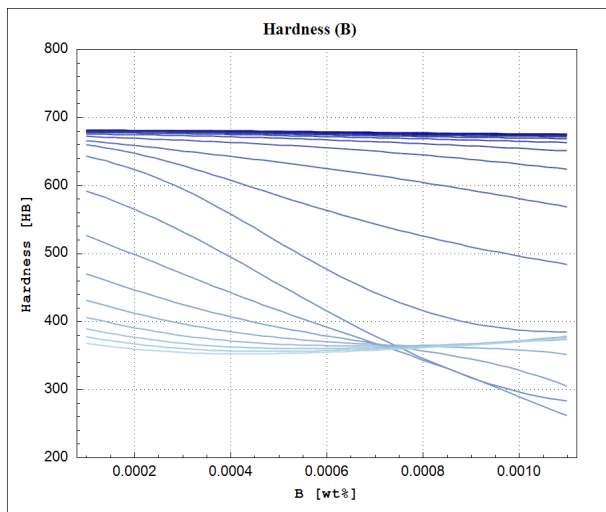


**Figure 312:** Hardness after rolling as a function of the Boron concentration (B), calculated by the ANN model on centered verification point (red line) and centered training point (blue line).

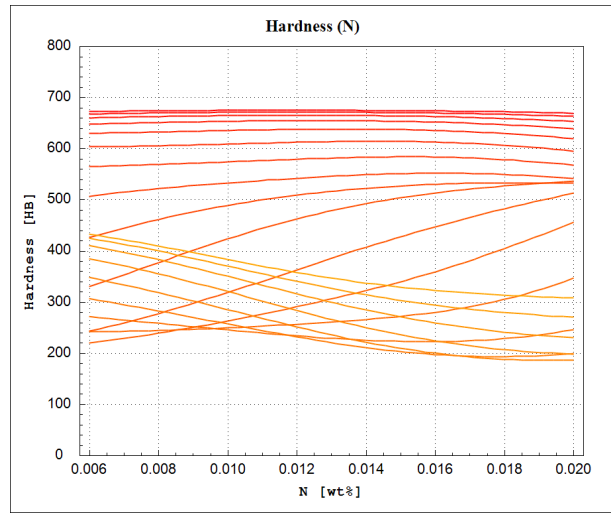
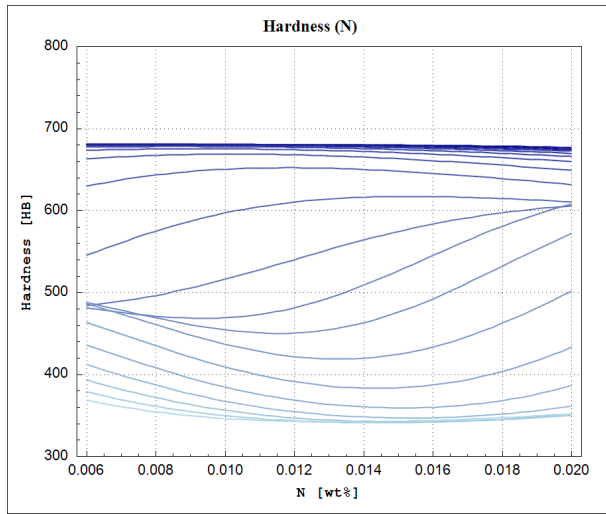


**Figure 313:** Hardness after rolling as a function of the Nitrogen concentration (N), calculated by the ANN model on centered verification point (red line) and centered training point (blue line).

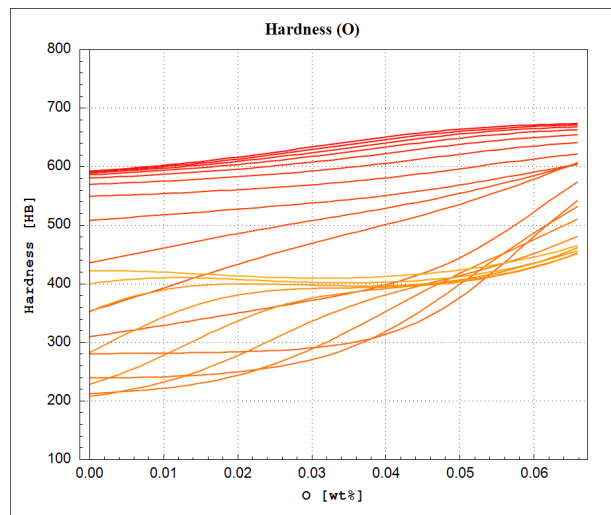
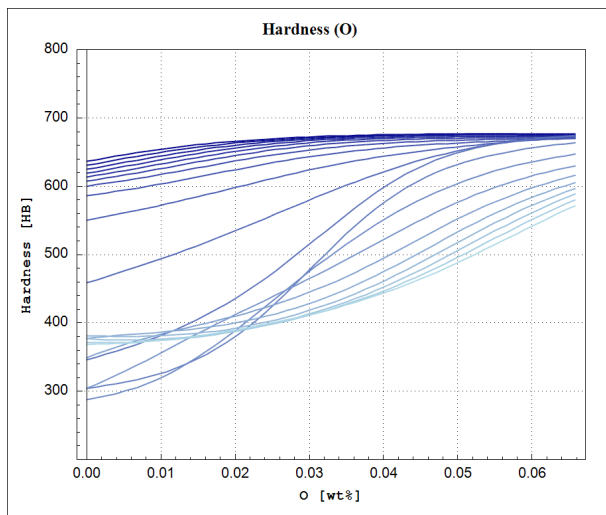


**Figure 314:** Hardness after rolling as a function of the Oxygen concentration (O), calculated by the ANN model on centered verification point (red line) and centered training point (blue line).

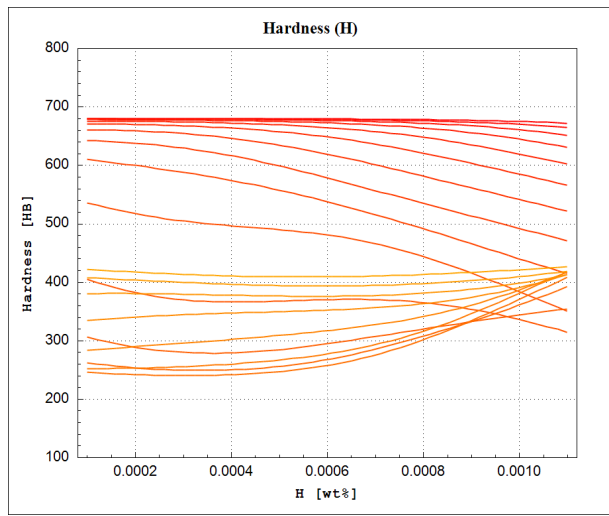
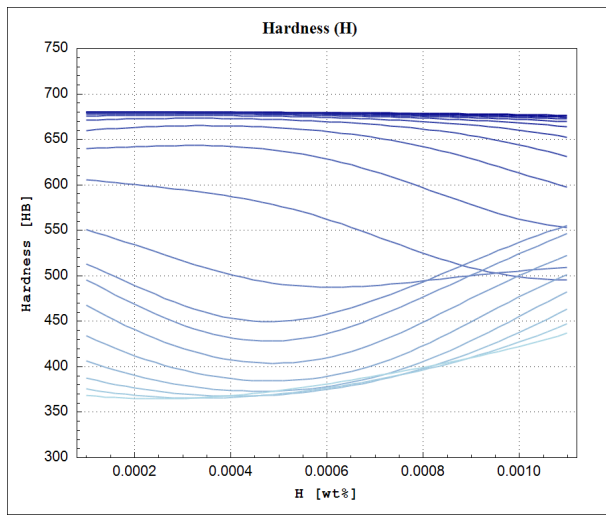


**Figure 315:** Hardness after rolling as a function of the Hydrogen concentration (H), calculated by the ANN model on centered verification point (red line) and centered training point (blue line).

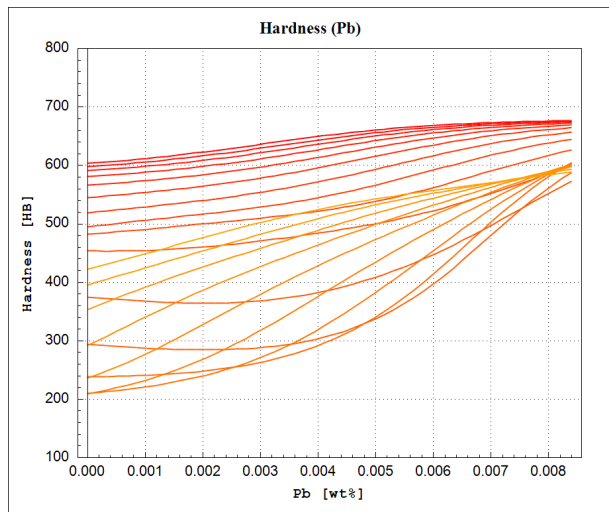
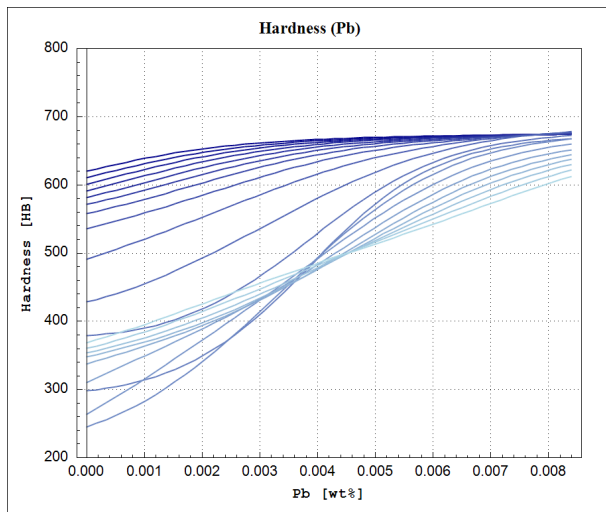


**Figure 316:** Hardness after rolling as a function of the Lead concentration (Pb), calculated by the ANN model on centered verification point (red line) and centered training point (blue line).

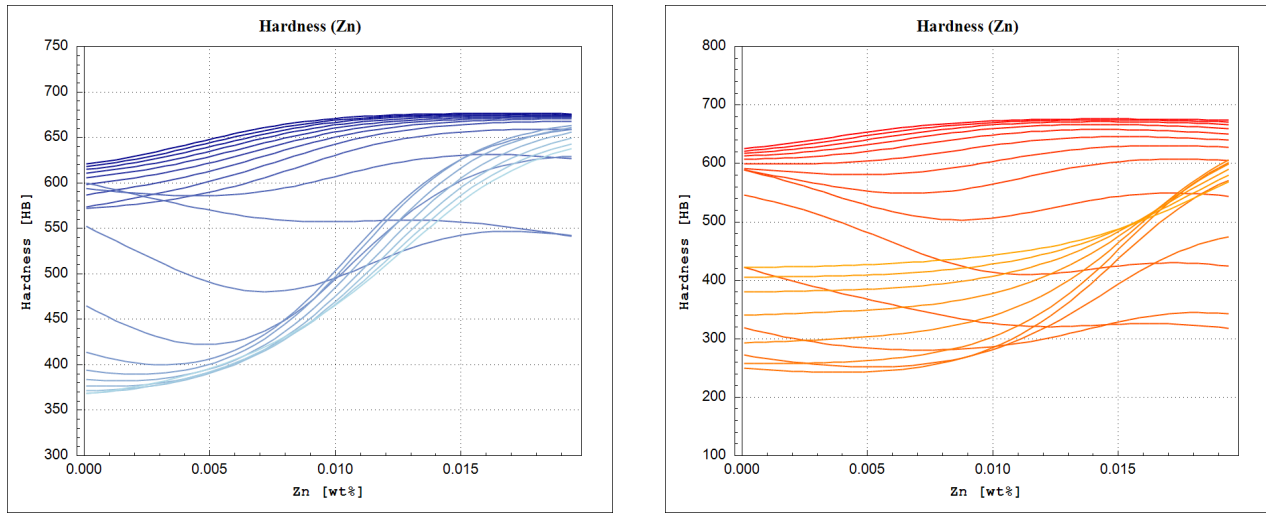


**Figure 317:** Hardness after rolling as a function of the Zinc concentration (Zn), calculated by the ANN model on centered verification point (red line) and centered training point (blue line).

### 5.2.5 Necking (Z)

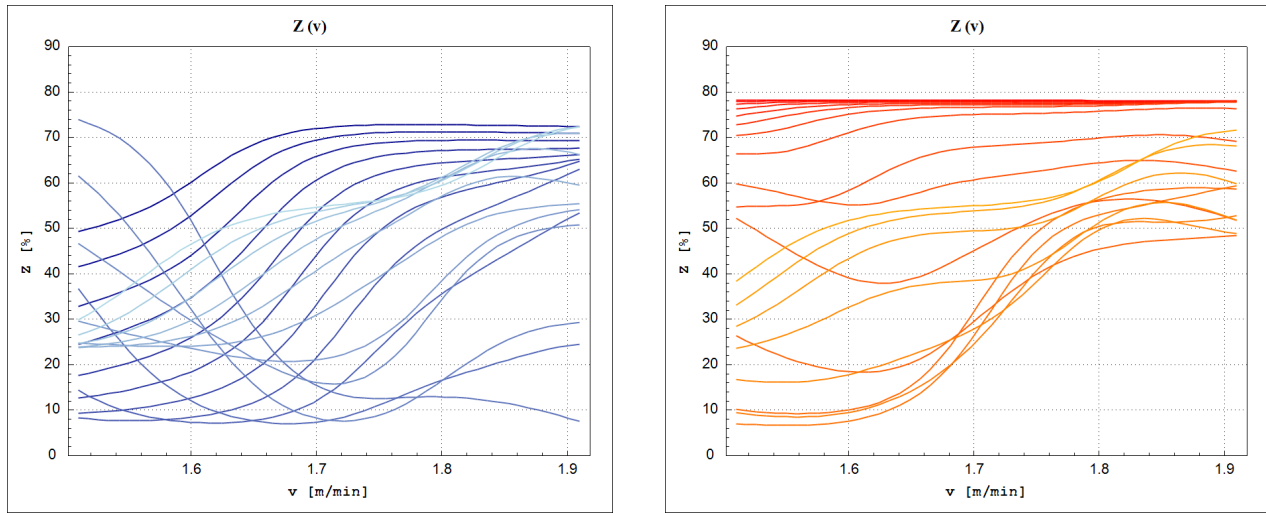


**Figure 318:** Necking as a function of the continuous casting speed, calculated by the ANN model on centered verification point (red line) and centered training point (blue line).

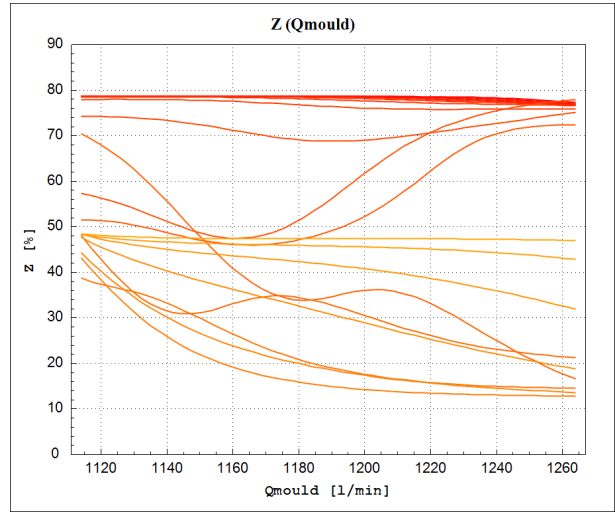
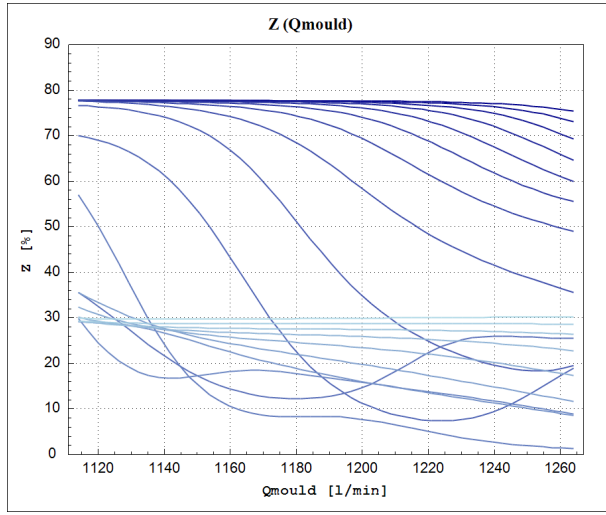


**Figure 319:** Necking as a function of the cooling flow rate in the mould, calculated by the ANN model on centered verification point (red line) and centered training point (blue line).

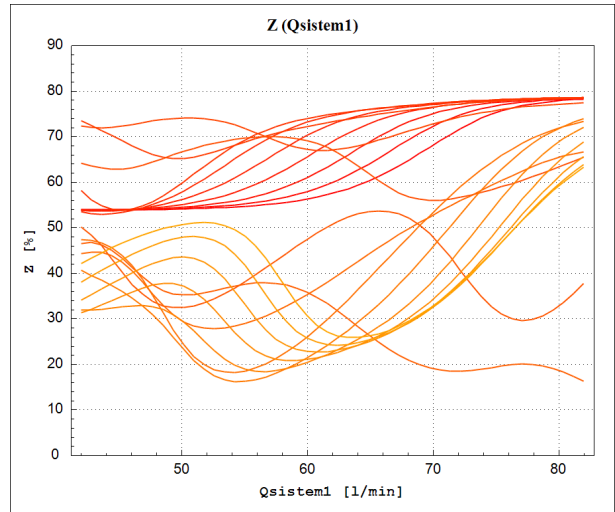
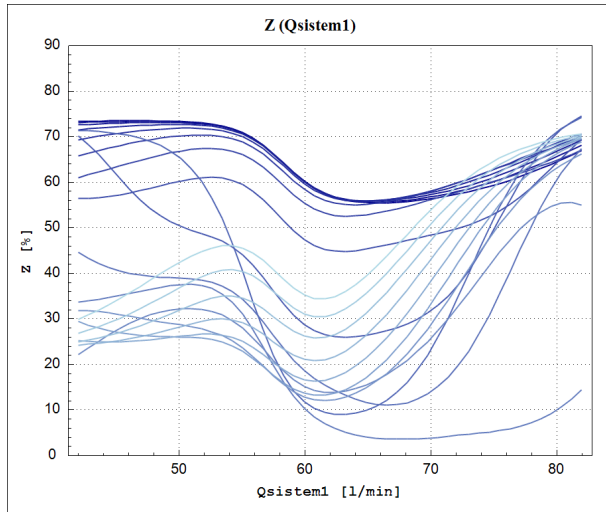


**Figure 320:** Necking as a function of the cooling flow rate in 1<sup>st</sup> spray system, calculated by the ANN model on centered verification point (red line) and centered training point (blue line).

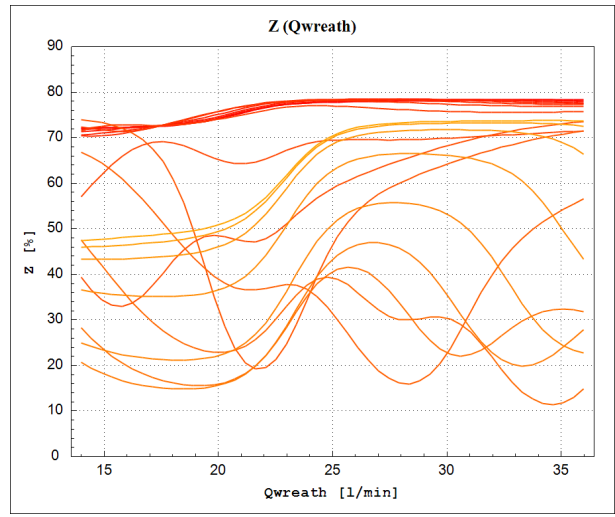
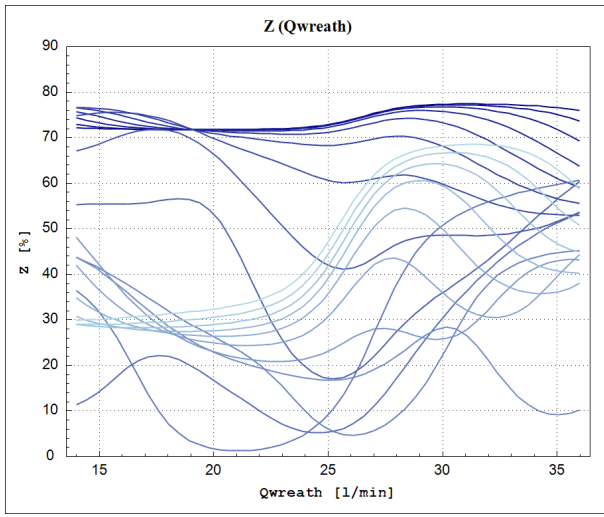


**Figure 321:** Necking as a function of the cooling flow rate in wreath spray system, calculated by the ANN model on centered verification point (red line) and centered training point (blue line).

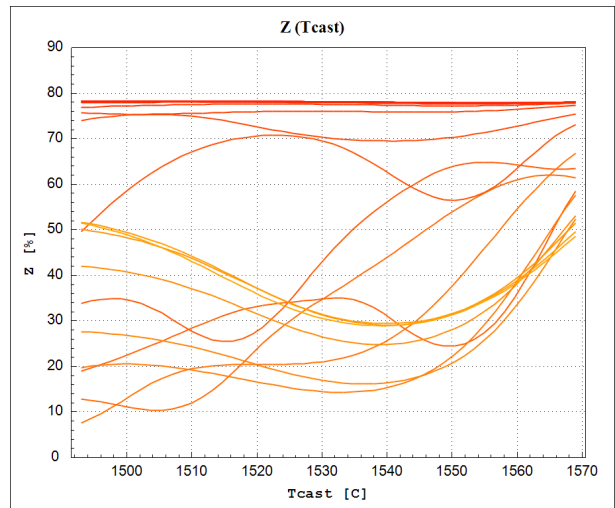
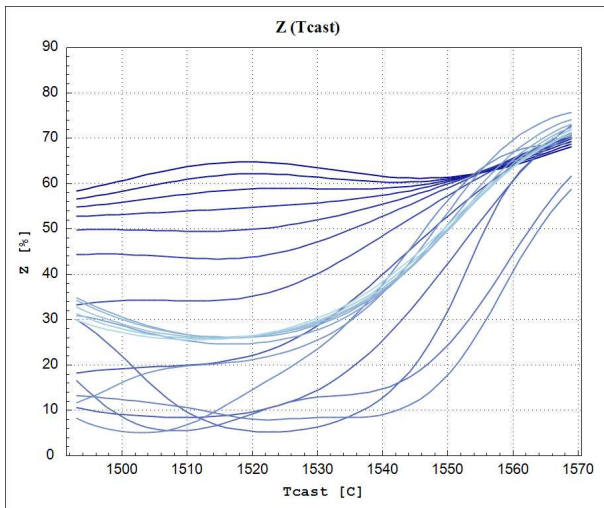


**Figure 322:** Necking as a function of the casting temperature, calculated by the ANN model on centered verification point (red line) and centered training point (blue line).

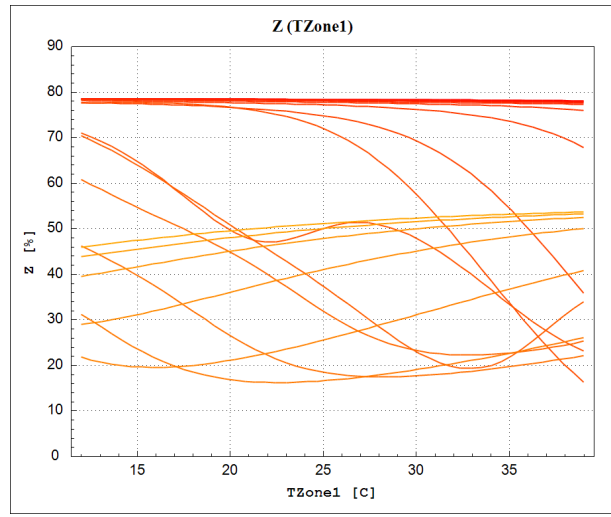
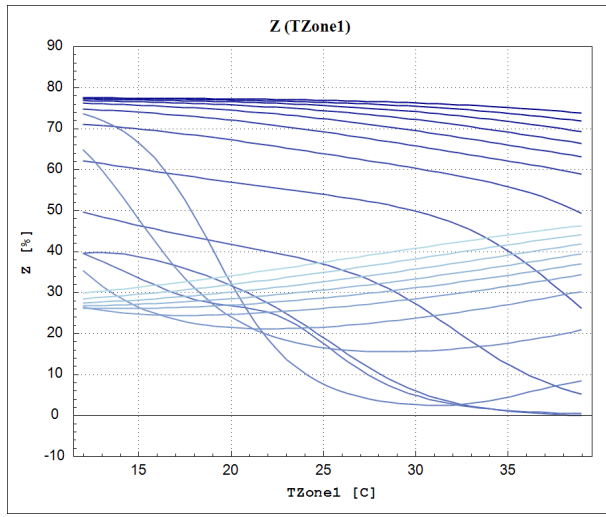


**Figure 323:** Necking as a function of the water temperature in Zone 1, calculated by the ANN model on centered verification point (red line) and centered training point (blue line).

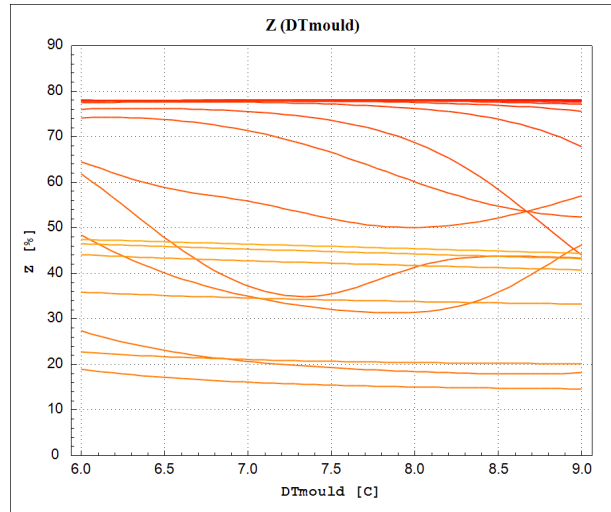
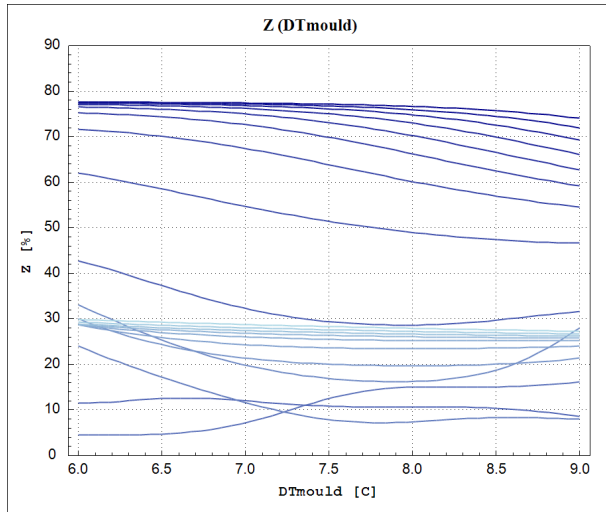


**Figure 324:** Necking as a function of the delta T, calculated by the ANN model on centered verification point (red line) and centered training point (blue line).

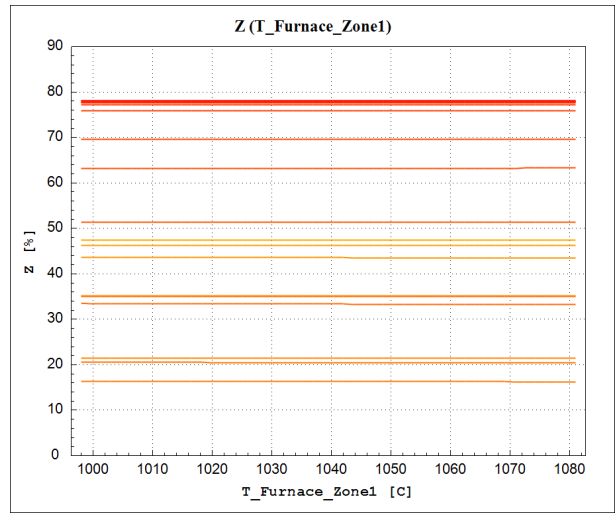
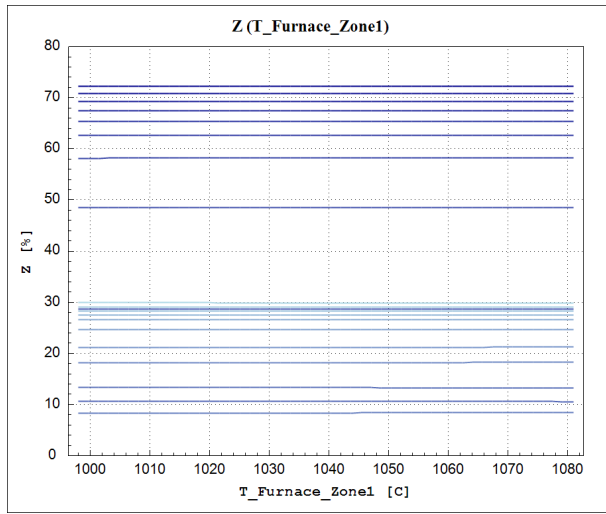


**Figure 325:** Necking as a function of the average on temperature in zone 1, calculated by the ANN model on centered verification point (red line) and centered training point (blue line).

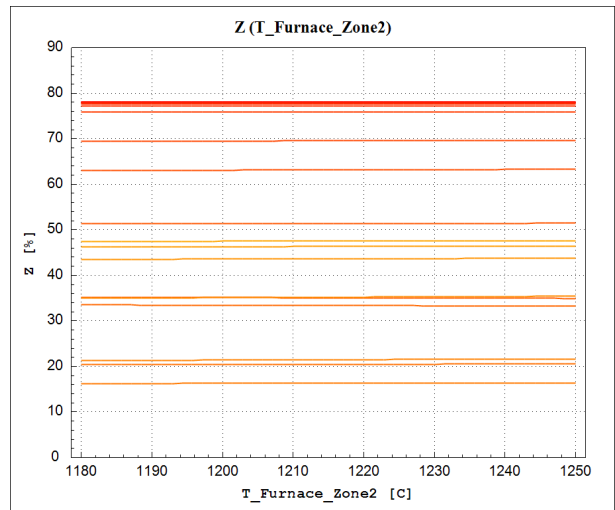
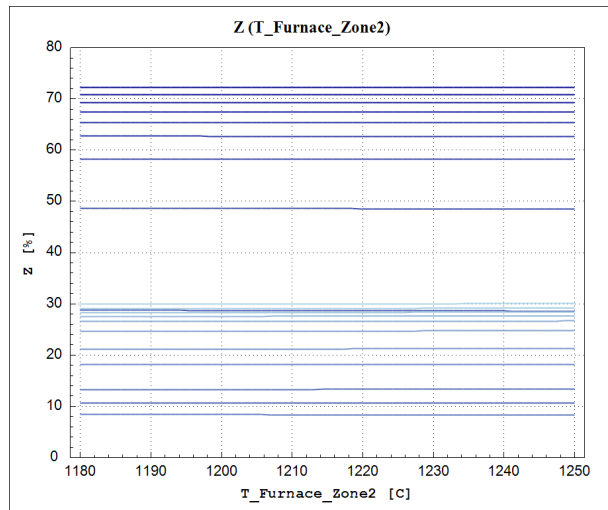


**Figure 326:** Necking as a function of the average on temperature in zone 2, calculated by the ANN model on centered verification point (red line) and centered training point (blue line).

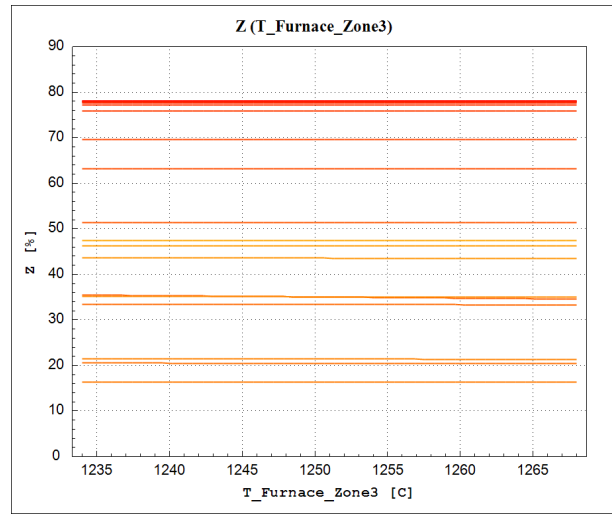
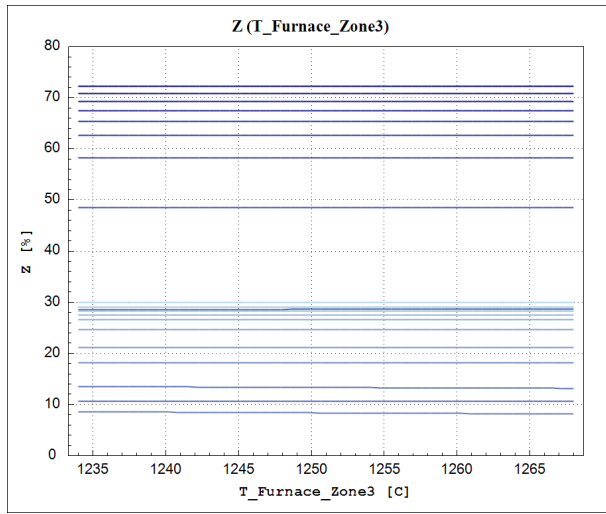


**Figure 327:** Necking as a function of the average on temperature in zone 3, calculated by the ANN model on centered verification point (red line) and centered training point (blue line).

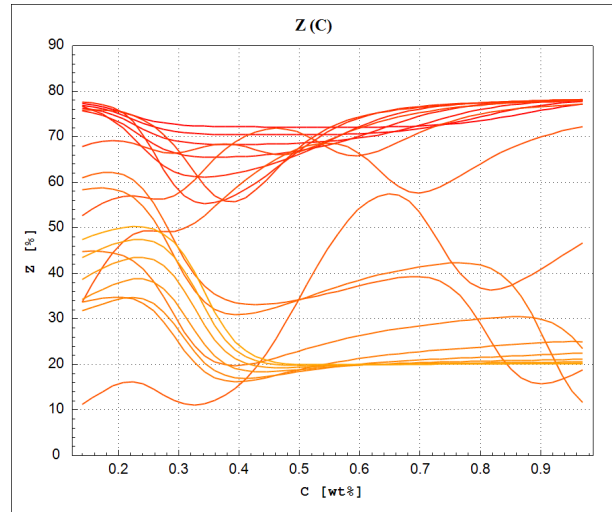
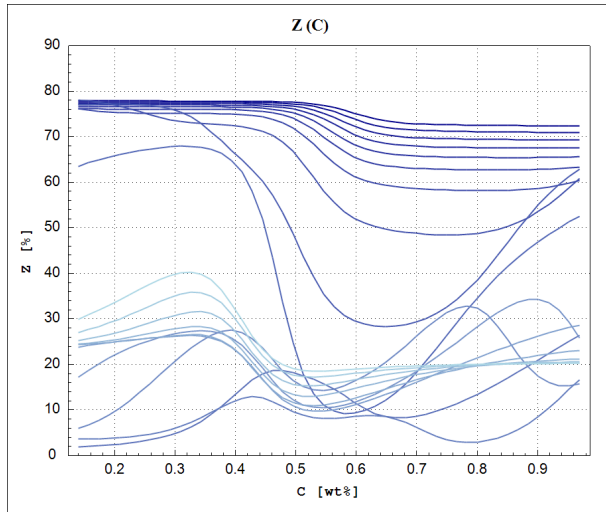


**Figure 328:** Necking as a function of the Carbon concentration (C), calculated by the ANN model on centered verification point (red line) and centered training point (blue line).

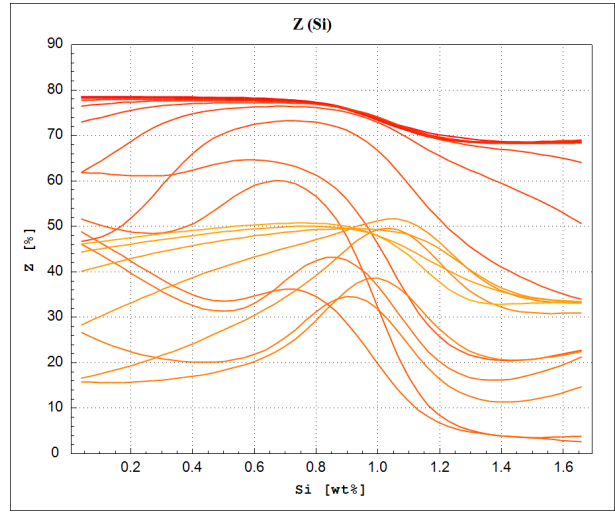
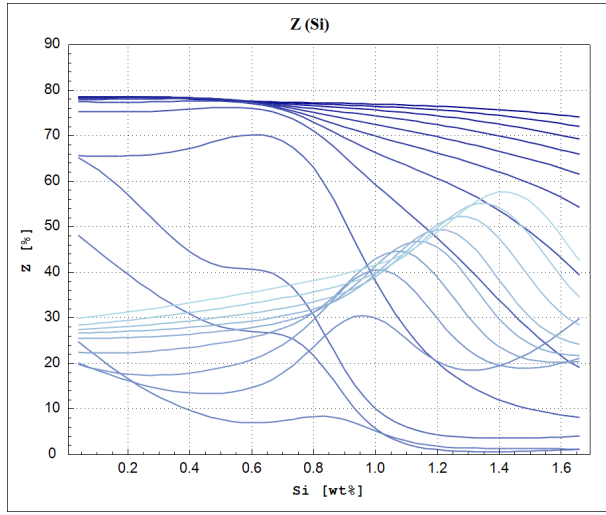


**Figure 329:** Necking as a function of the Silicon concentration (Si), calculated by the ANN model on centered verification point (red line) and centered training point (blue line).

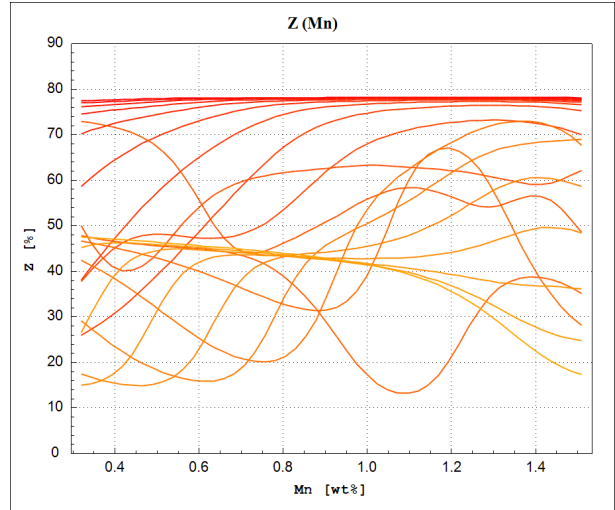
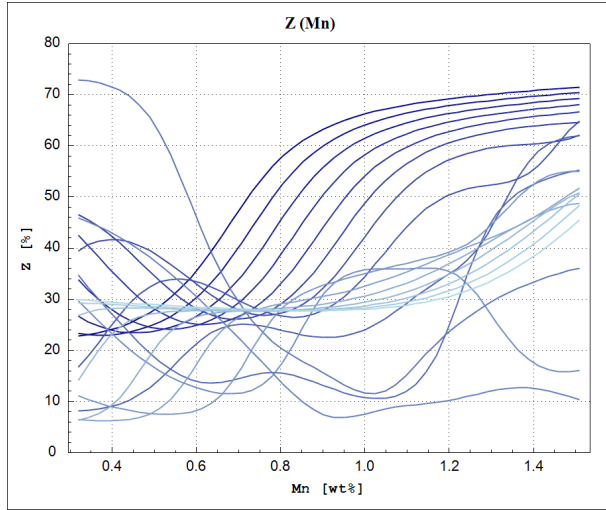


**Figure 330:** Necking as a function of the Manganese concentration (Mn), calculated by the ANN model on centered verification point (red line) and centered training point (blue line).

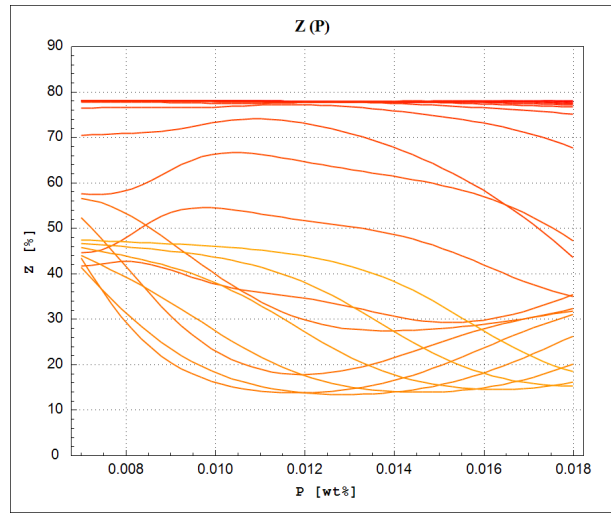
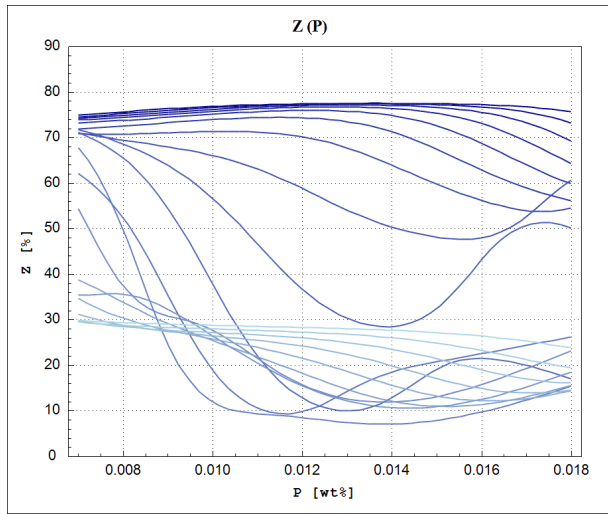


**Figure 331:** Necking as a function of the Phosphorus concentration (P), calculated by the ANN model on centered verification point (red line) and centered training point (blue line).

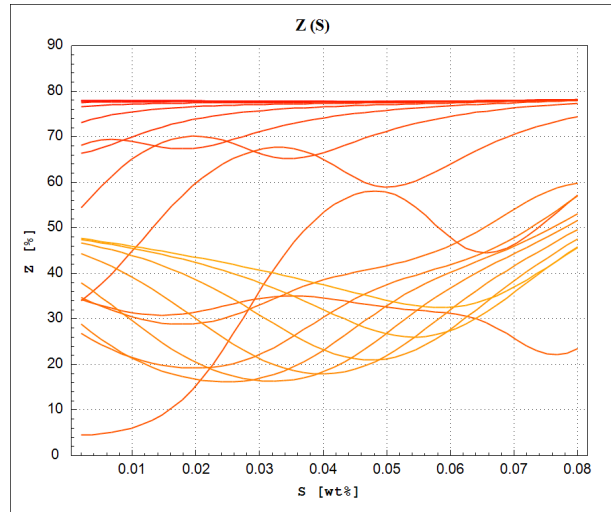
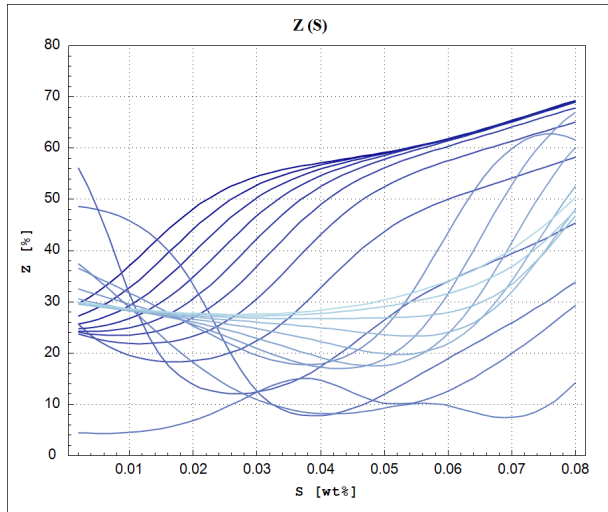


**Figure 332:** Necking as a function of the Sulphur concentration (S), calculated by the ANN model on centered verification point (red line) and centered training point (blue line).

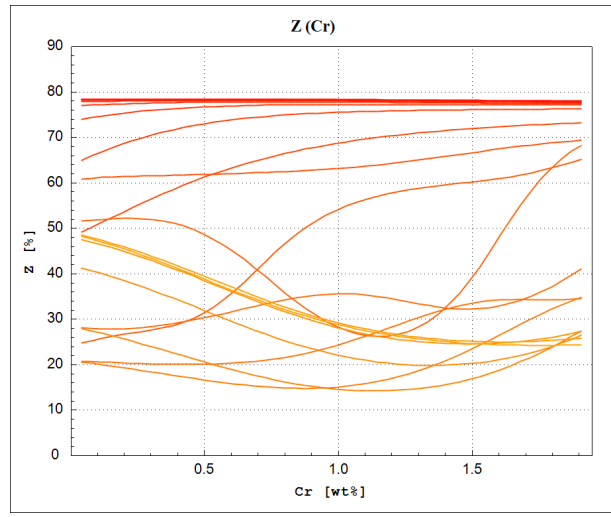
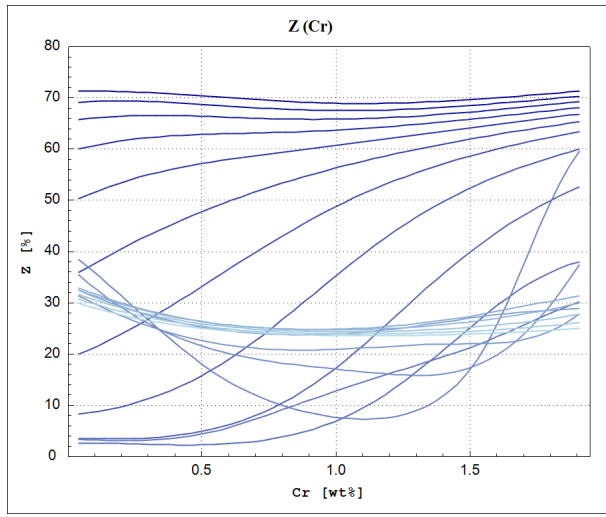


**Figure 333:** Necking as a function of the Chromium concentration (Cr), calculated by the ANN model on centered verification point (red line) and centered training point (blue line).

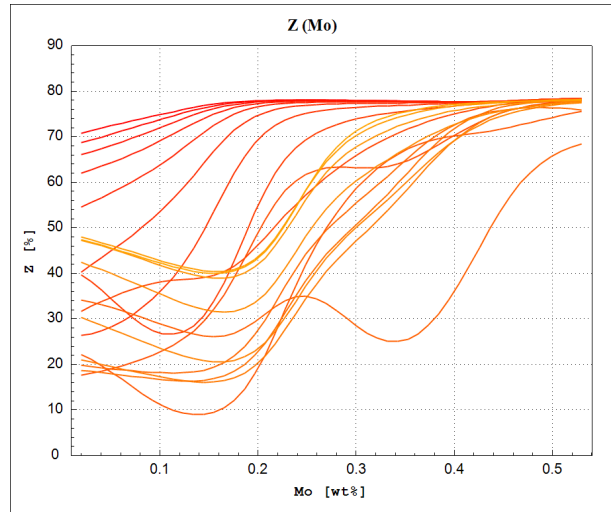
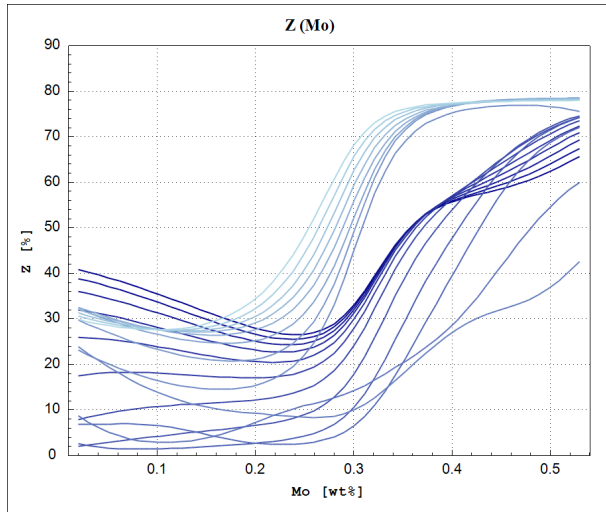


**Figure 334:** Necking as a function of the Molybdenum concentration (Mo), calculated by the ANN model on centered verification point (red line) and centered training point (blue line).

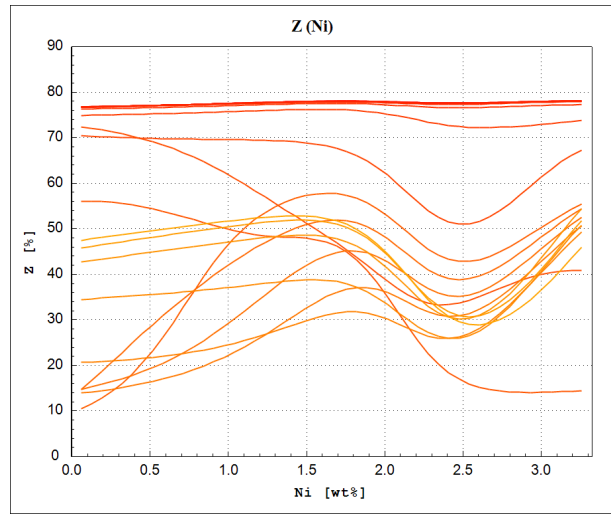
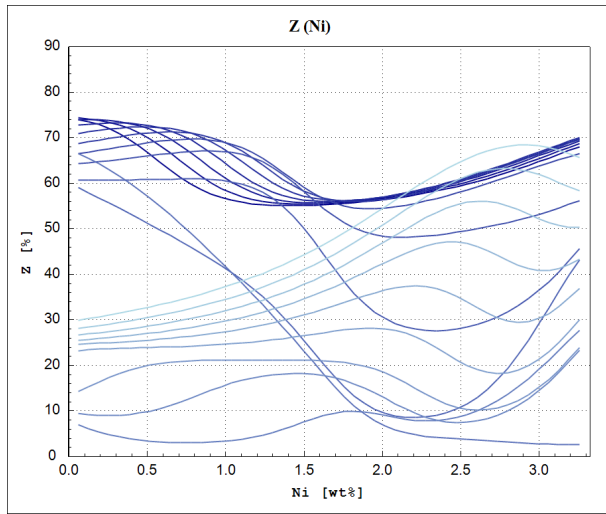


**Figure 335:** Necking as a function of the Nickel concentration (Ni), calculated by the ANN model on centered verification point (red line) and centered training point (blue line).

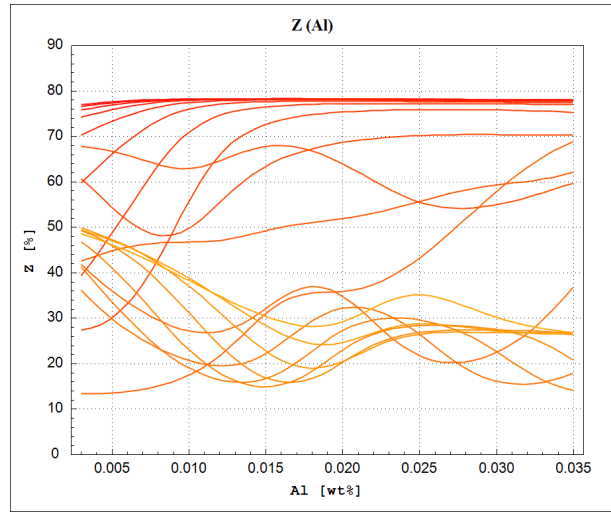
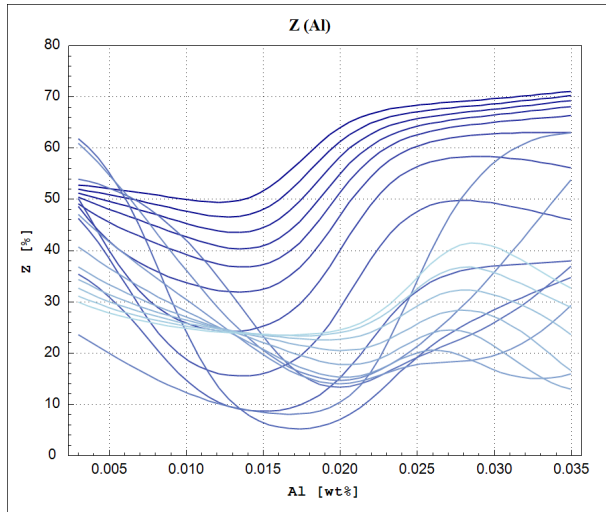


**Figure 336:** Necking as a function of the Aluminium concentration (Al), calculated by the ANN model on centered verification point (red line) and centered training point (blue line).

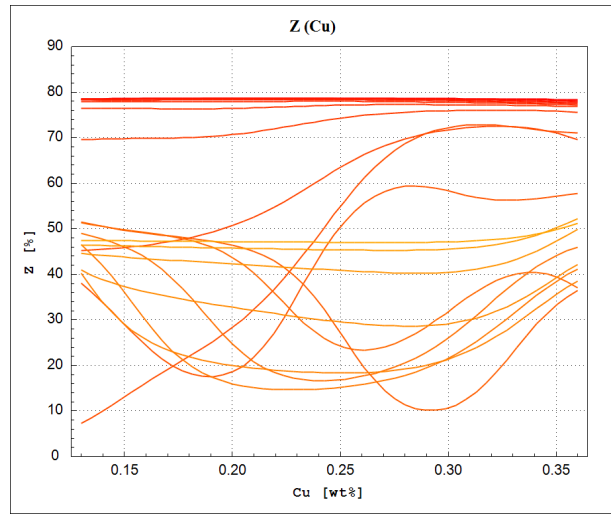
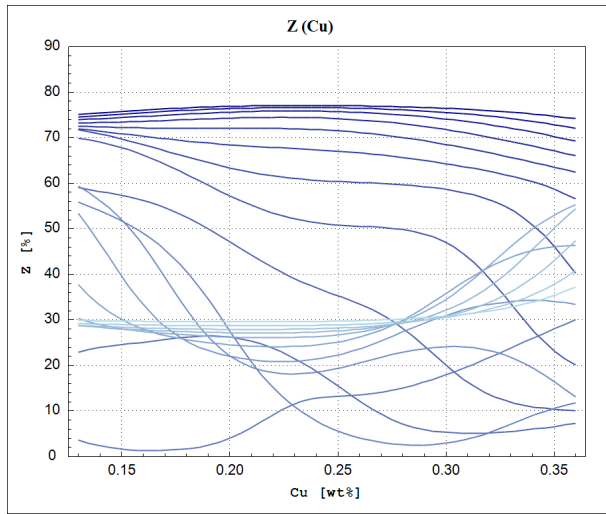


**Figure 337:** Necking as a function of the Copper concentration (Cu), calculated by the ANN model on centered verification point (red line) and centered training point (blue line).

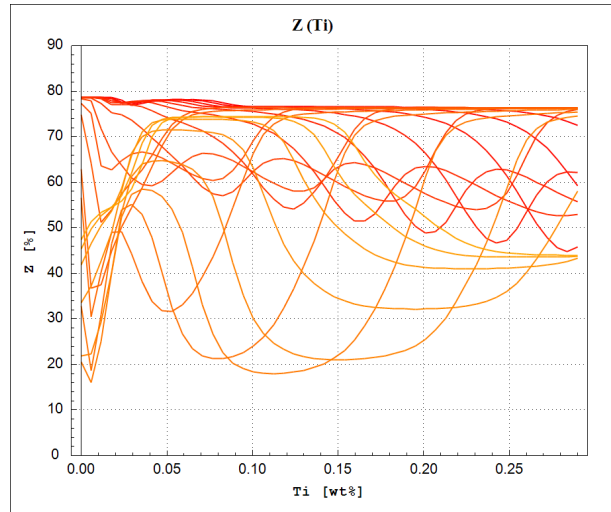
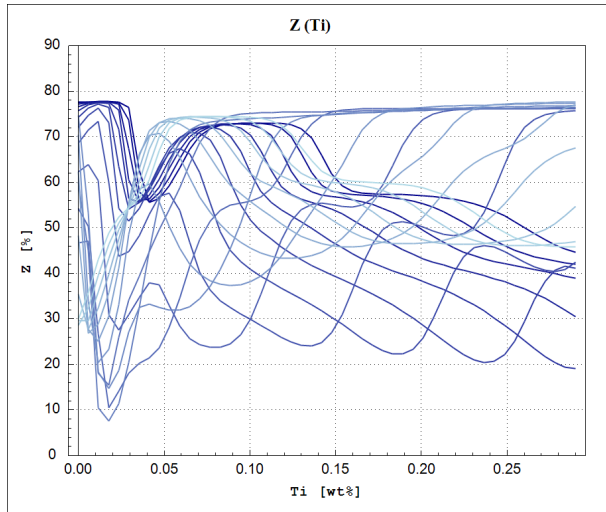


**Figure 338:** Necking as a function of the Titanium concentration (Ti), calculated by the ANN model on centered verification point (red line) and centered training point (blue line).

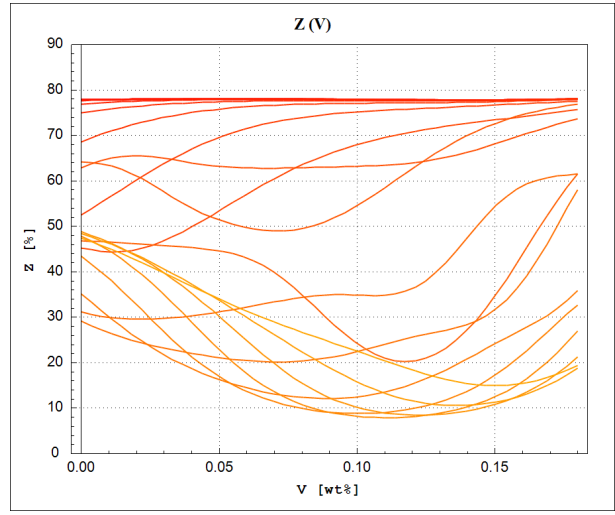
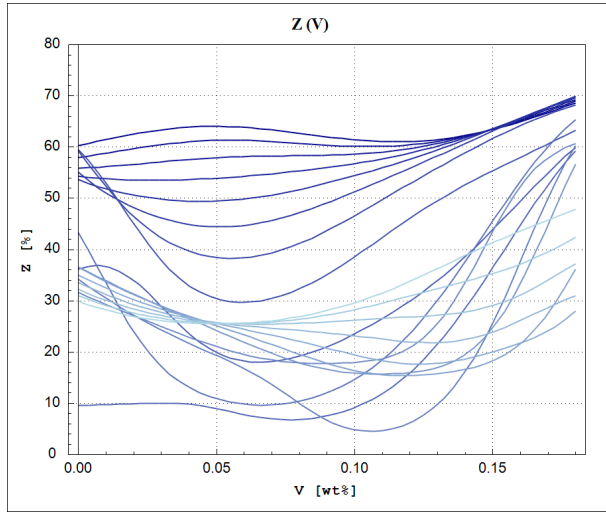


**Figure 339:** Necking as a function of the Vanadium concentration (V), calculated by the ANN model on centered verification point (red line) and centered training point (blue line).

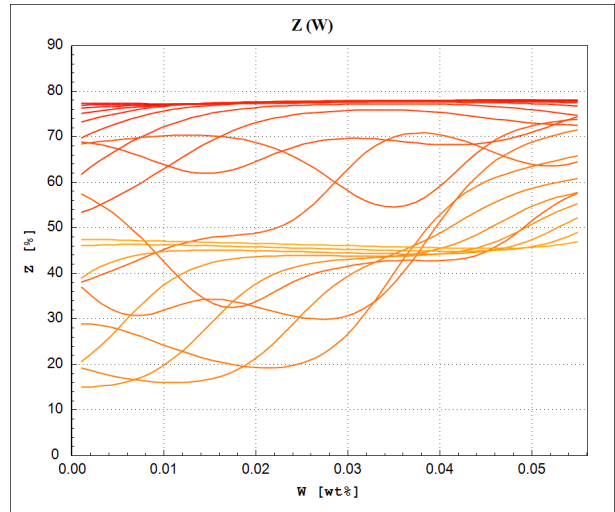
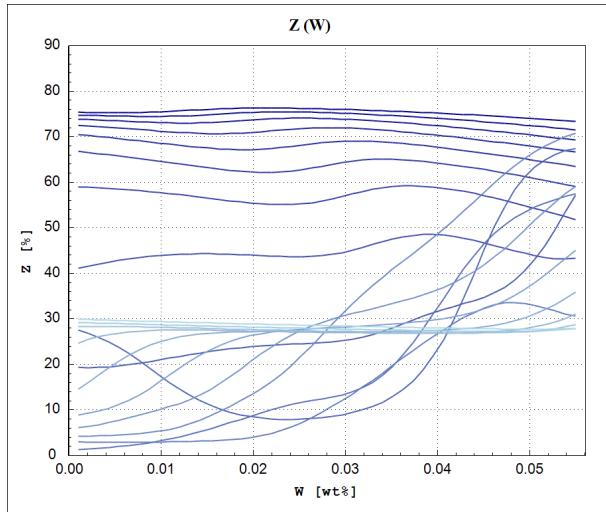


**Figure 340:** Necking as a function of the Tungsten concentration (W), calculated by the ANN model on centered verification point (red line) and centered training point (blue line).

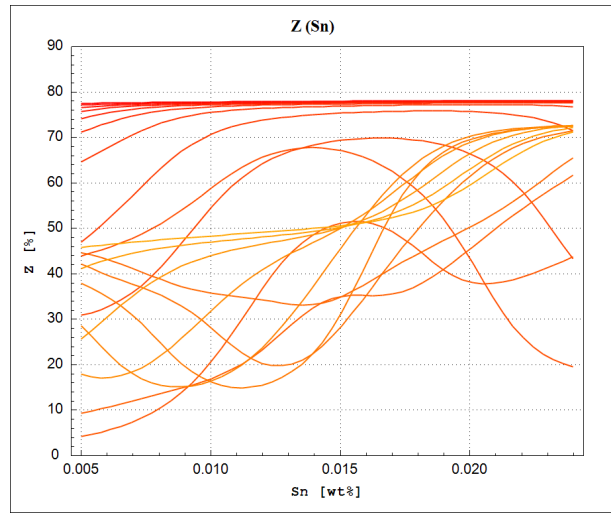
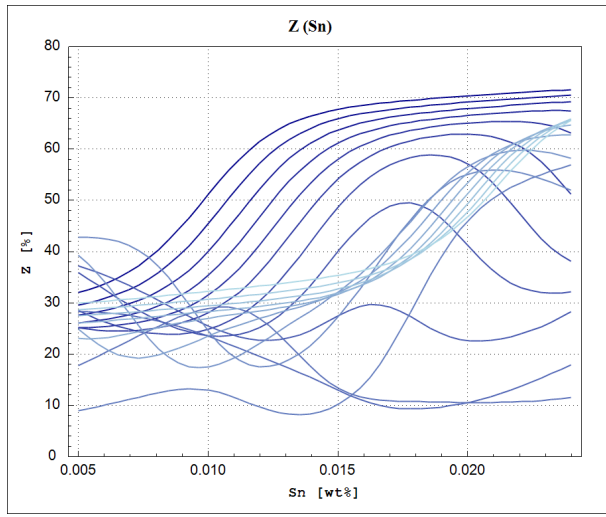


**Figure 341:** Necking as a function of the Tin concentration (Sn), calculated by the ANN model on centered verification point (red line) and centered training point (blue line).

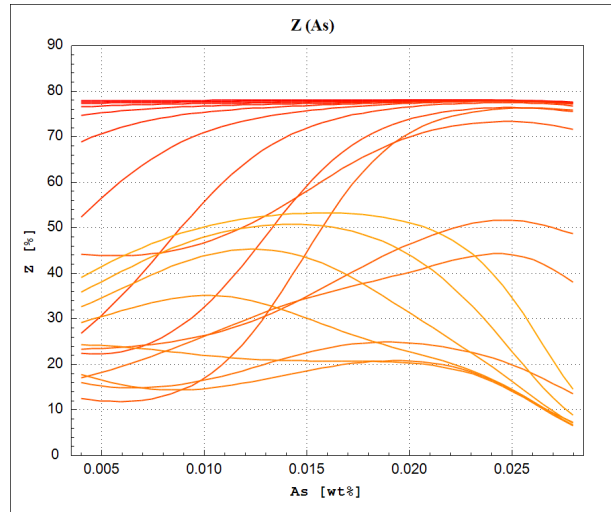
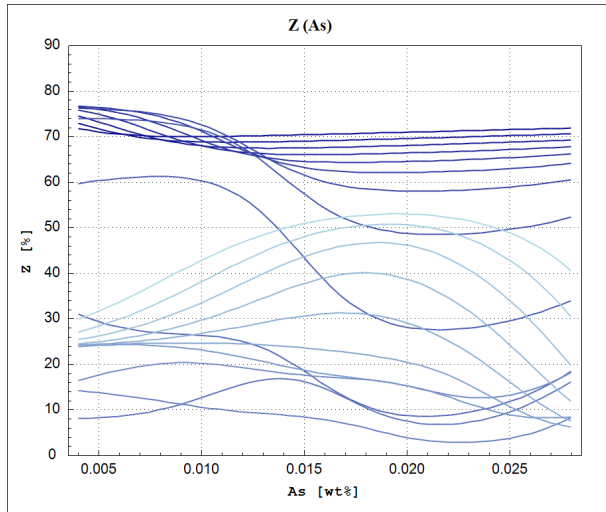


**Figure 342:** Necking as a function of the Arsenic concentration (As), calculated by the ANN model on centered verification point (red line) and centered training point (blue line).

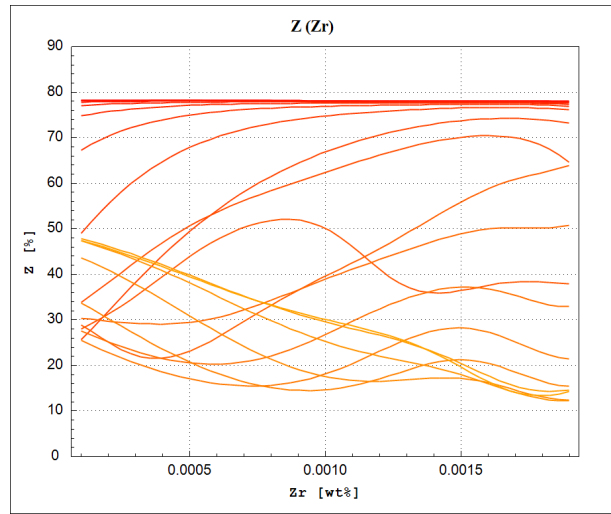
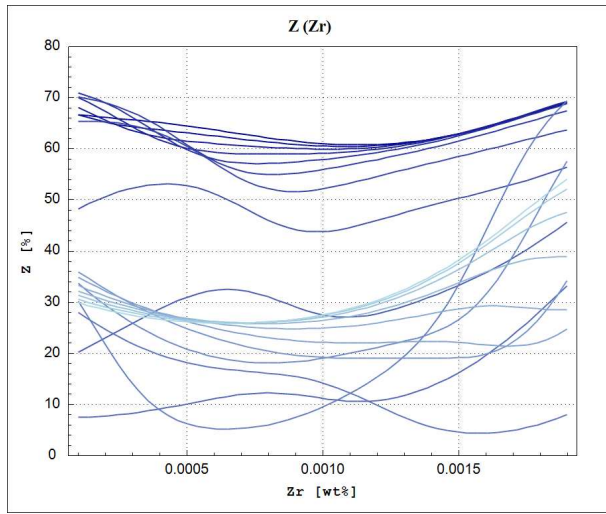


**Figure 343:** Necking as a function of the Zirconium concentration (Zr), calculated by the ANN model on centered verification point (red line) and centered training point (blue line).

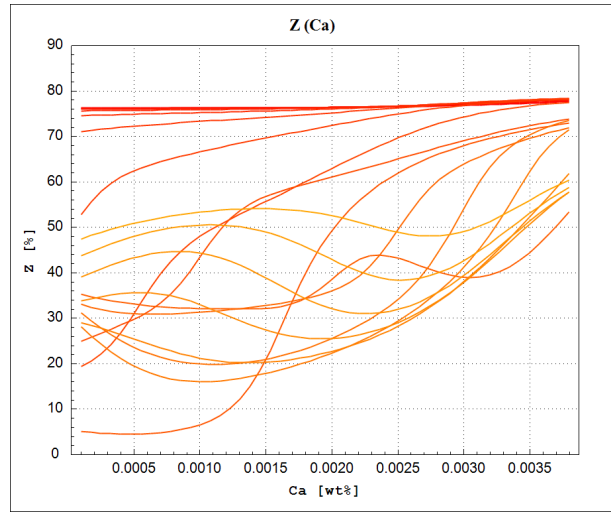
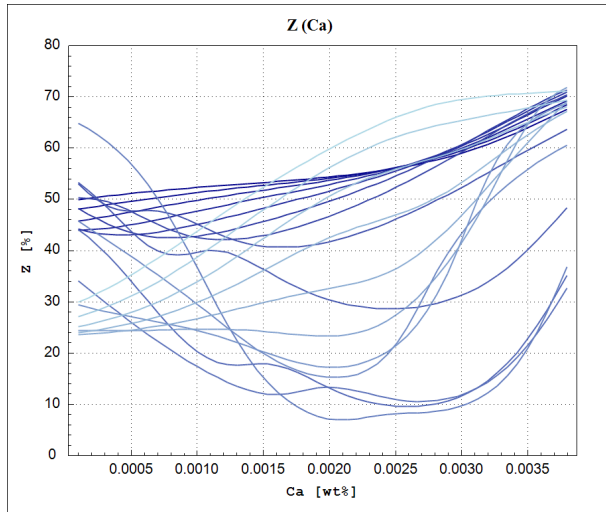


**Figure 344:** Necking as a function of the Calcium concentration (Ca), calculated by the ANN model on centered verification point (red line) and centered training point (blue line).

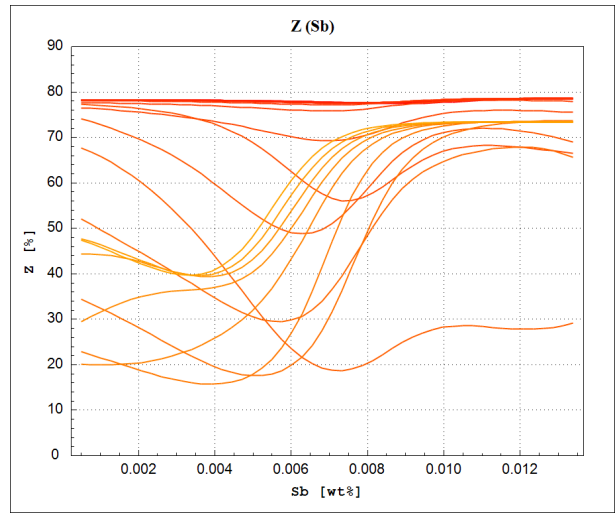
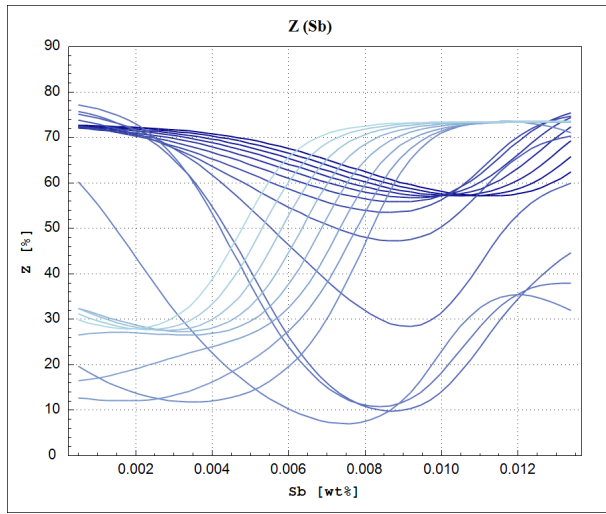


**Figure 345:** Necking as a function of the Antimony concentration (Sb), calculated by the ANN model on centered verification point (red line) and centered training point (blue line).

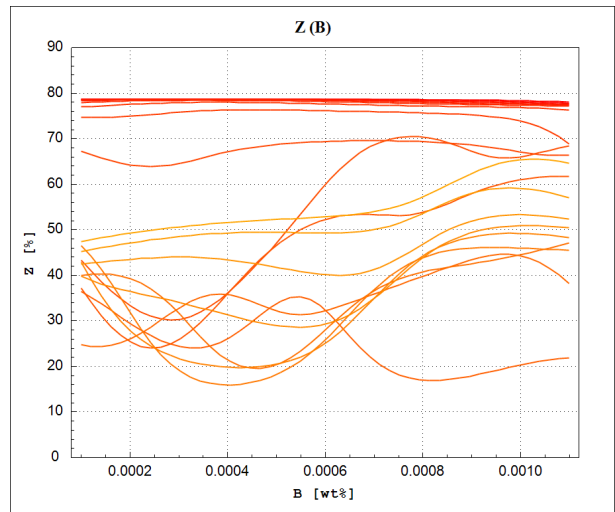
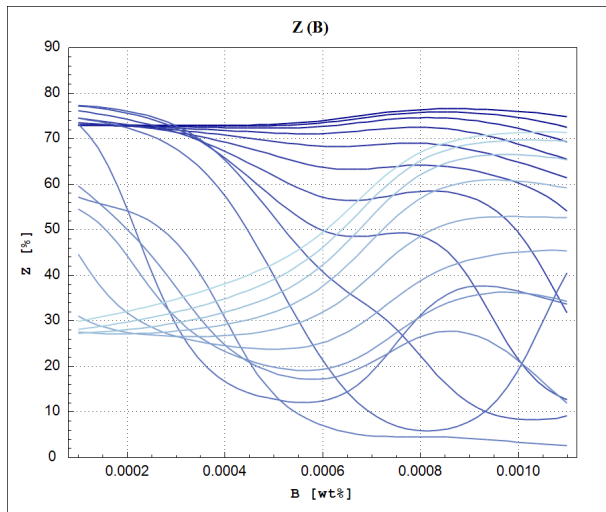


**Figure 346:** Necking as a function of the Boron concentration (B), calculated by the ANN model on centered verification point (red line) and centered training point (blue line).

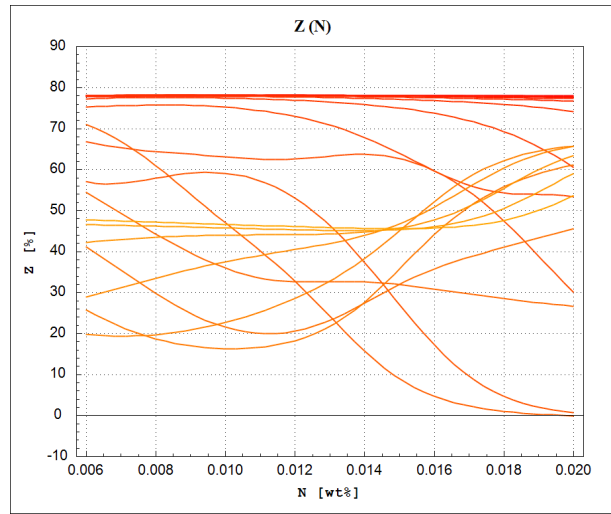
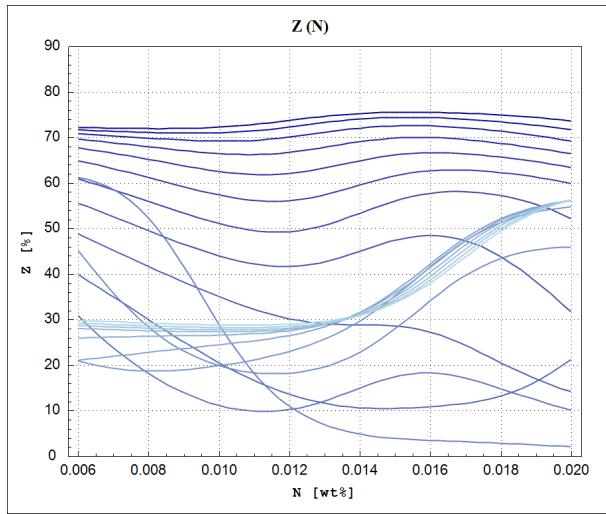


**Figure 347:** Necking as a function of the Nitrogen concentration (N), calculated by the ANN model on centered verification point (red line) and centered training point (blue line).

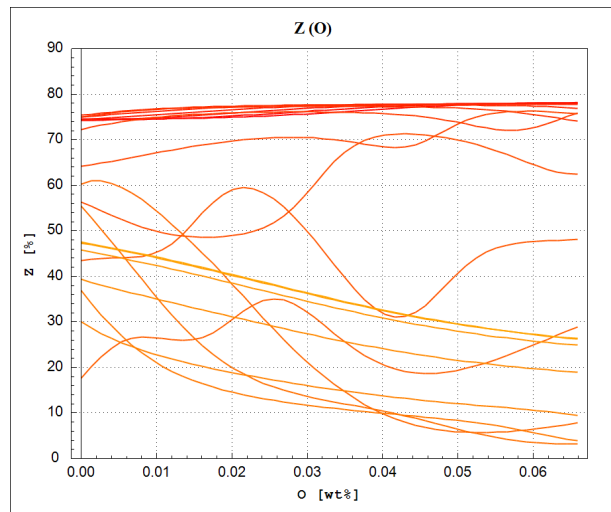
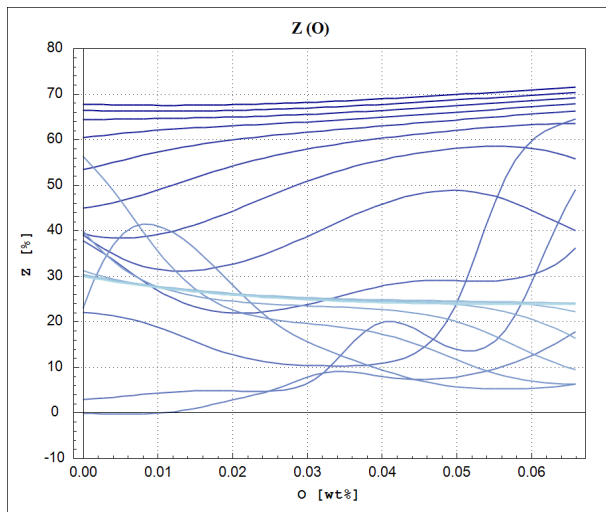


**Figure 348:** Necking as a function of the Oxygen concentration (O), calculated by the ANN model on centered verification point (red line) and centered training point (blue line).

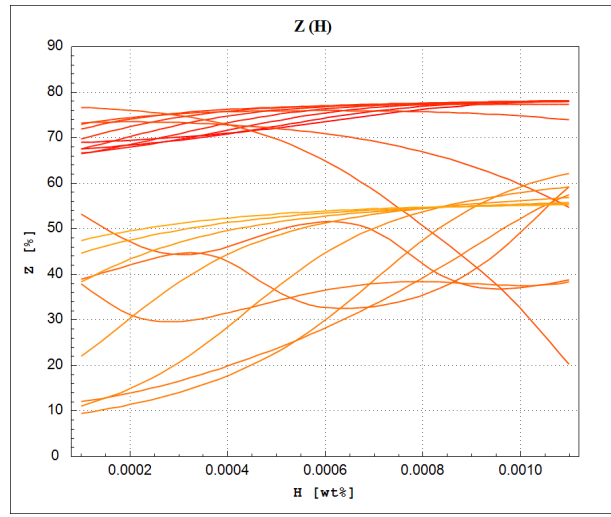
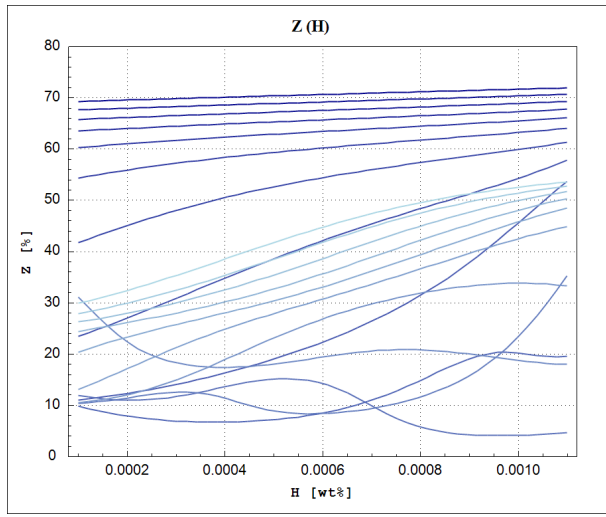


**Figure 349:** Necking as a function of the Hydrogen concentration (H), calculated by the ANN model on centered verification point (red line) and centered training point (blue line).

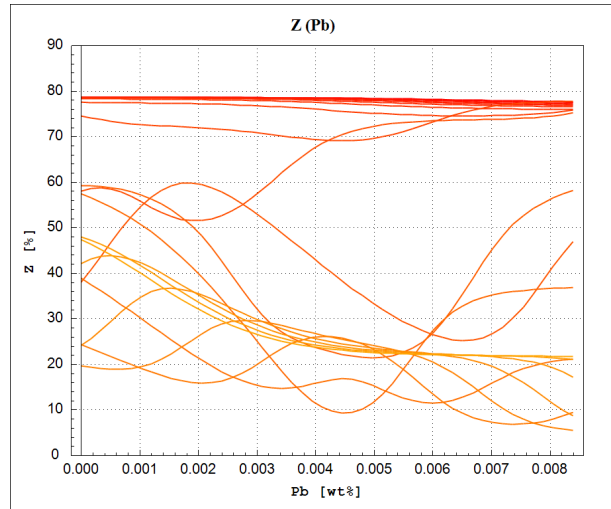
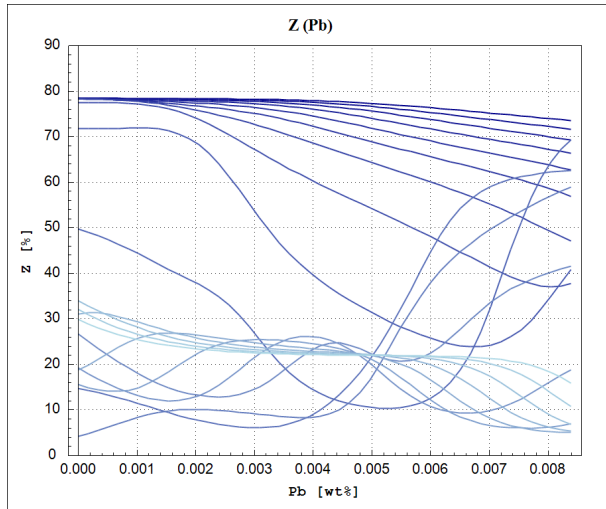


**Figure 350:** Necking as a function of the Lead concentration (Pb), calculated by the ANN model on centered verification point (red line) and centered training point (blue line).

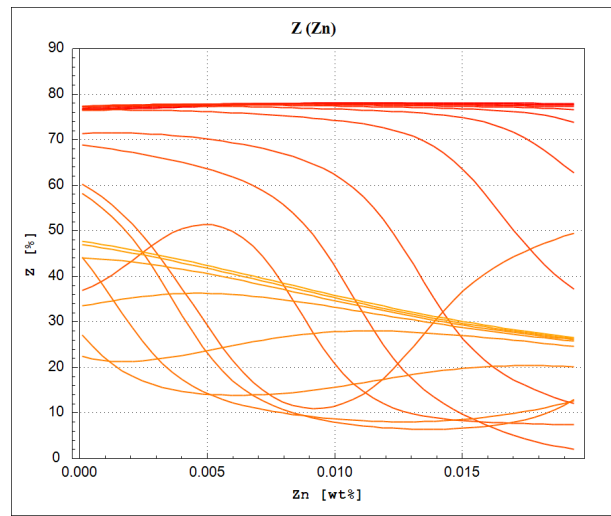
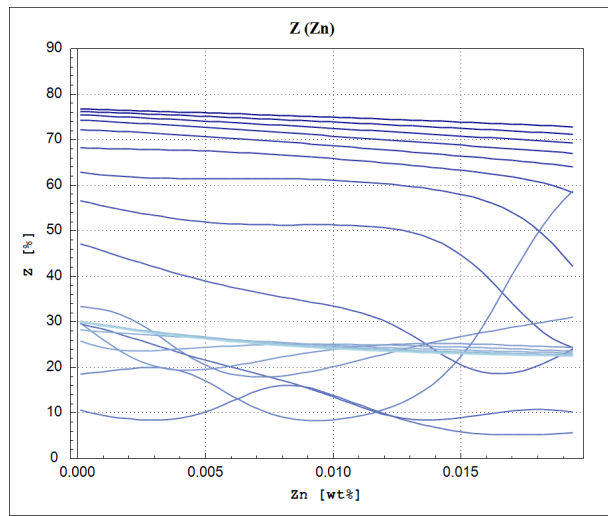


**Figure 351:** Necking as a function of the Zinc concentration (Zn), calculated by the ANN model on centered verification point (red line) and centered training point (blue line).

## 6 SENSITIVITY TESTS

The main purpose of these tests is to demonstrate the influence of different process parameters on 5 material properties. In each test we change one process parameter from minimum value to maximum value and verify the change in all material properties. The graph below shows how process parameters influence on outputs. The influence is represented in percentage of change of process parameter according to the range of that process parameter.

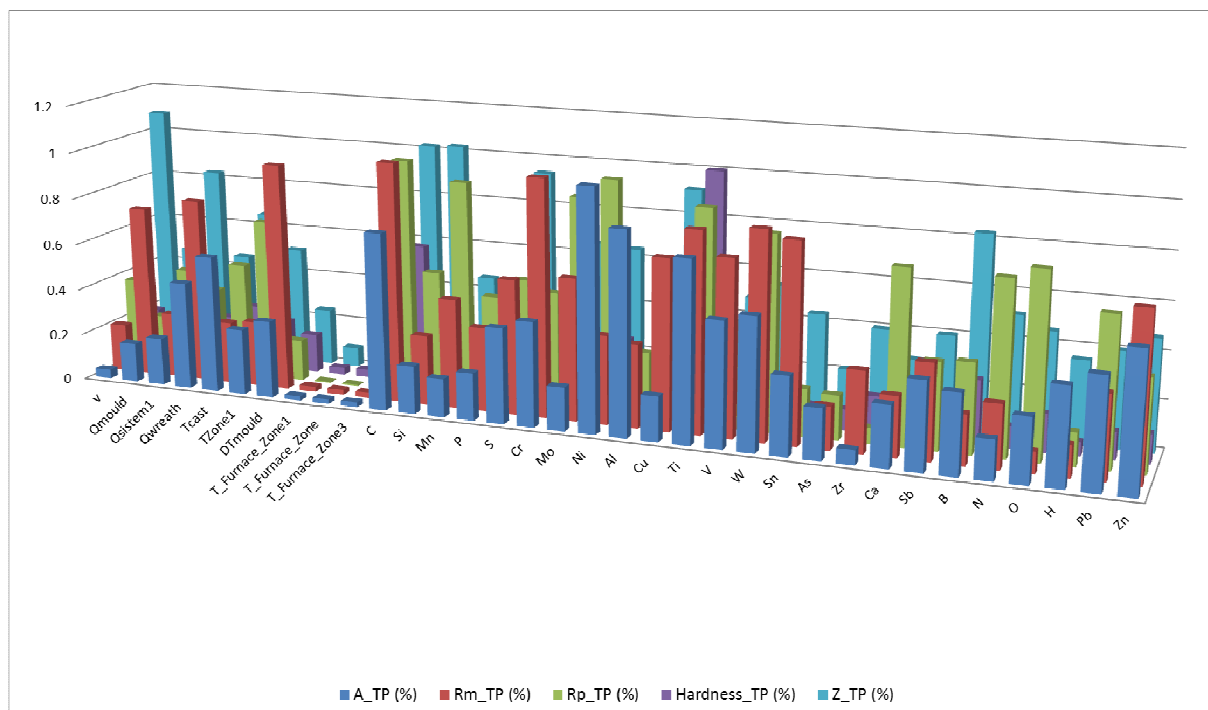


**Figure 352:** Influence on elongation (A), tensile strength ( $R_m$ ), yield stress ( $R_p$ ), hardness (HB) and necking (Z) by changing process parameters from minimum to maximum value.

### 6.1 Elongation (A)

Graph below shows the influence of different process parameters to elongation (A) for training point (blue columns) and verification point (red column). Process parameters are sorted from the most influential to the least influential. The influence is represented in percentage of change of process parameter according to the range of that process parameter.

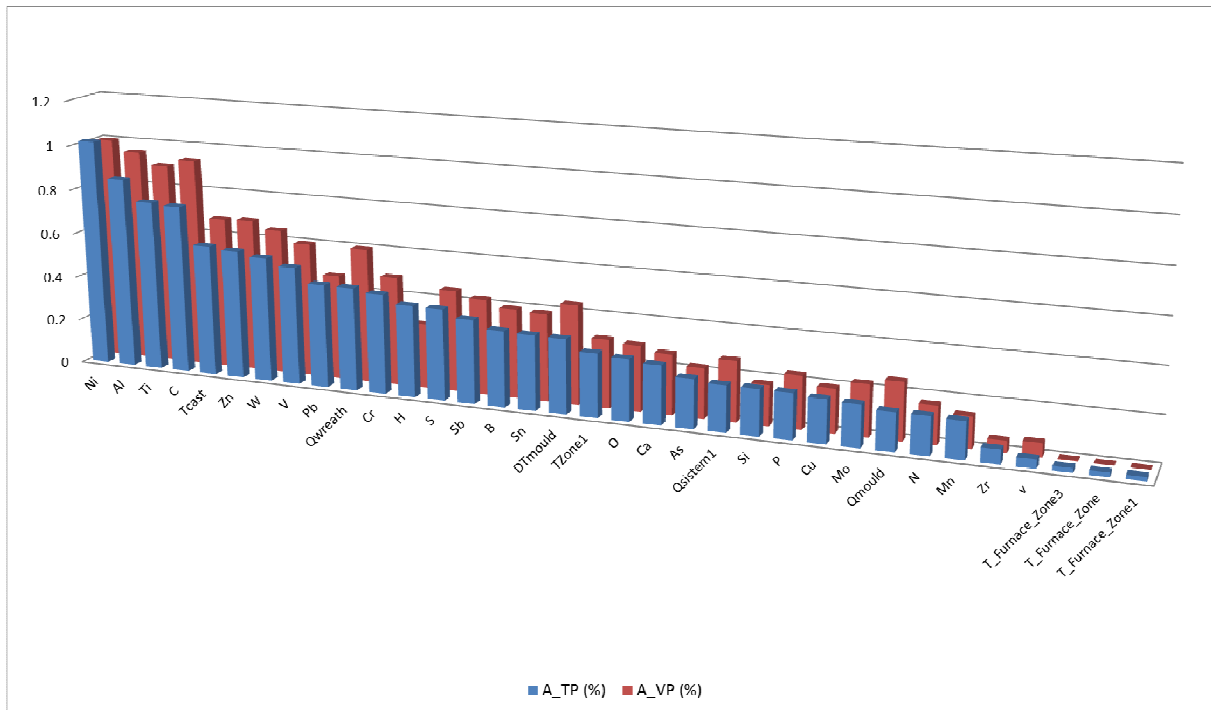


**Figure 353:** Influence on elongation (A) by changing process parameters from minimum to maximum value for training and verification point. Influence is shown in percentage of total range of elongation (A).

Influence of each process parameter on output is different. In the Figure 354 we can see the share of each process parameter in percentage among all process parameters when simulating elongation (A).

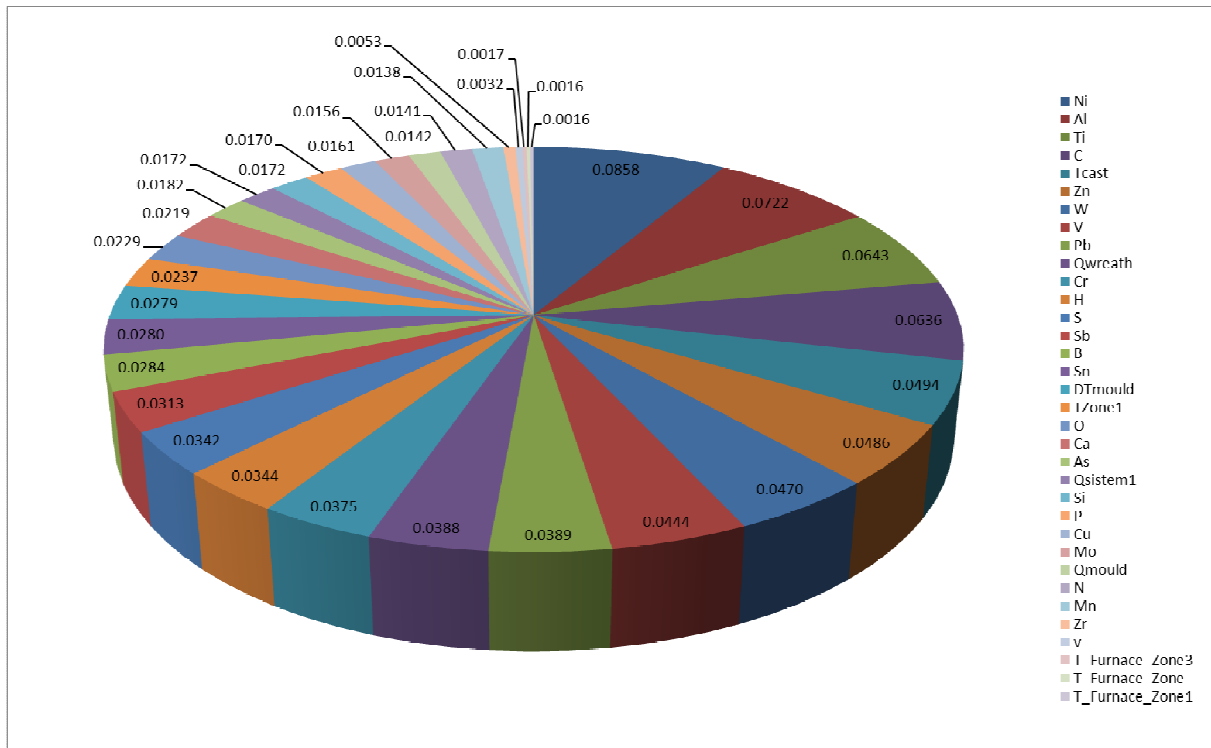


**Figure 354:** The share of each process parameter in percentage among all process parameters when simulating elongation (A).

## 6.2 Tensile Strength ( $R_m$ )

Graph below shows the influence of different process parameters to tensile strength ( $R_m$ ) for training point (blue columns) and verification point (red column). Process parameters are sorted from the most influential to the least influential. The influence is represented in percentage of change of process parameter according to the range of that process parameter.

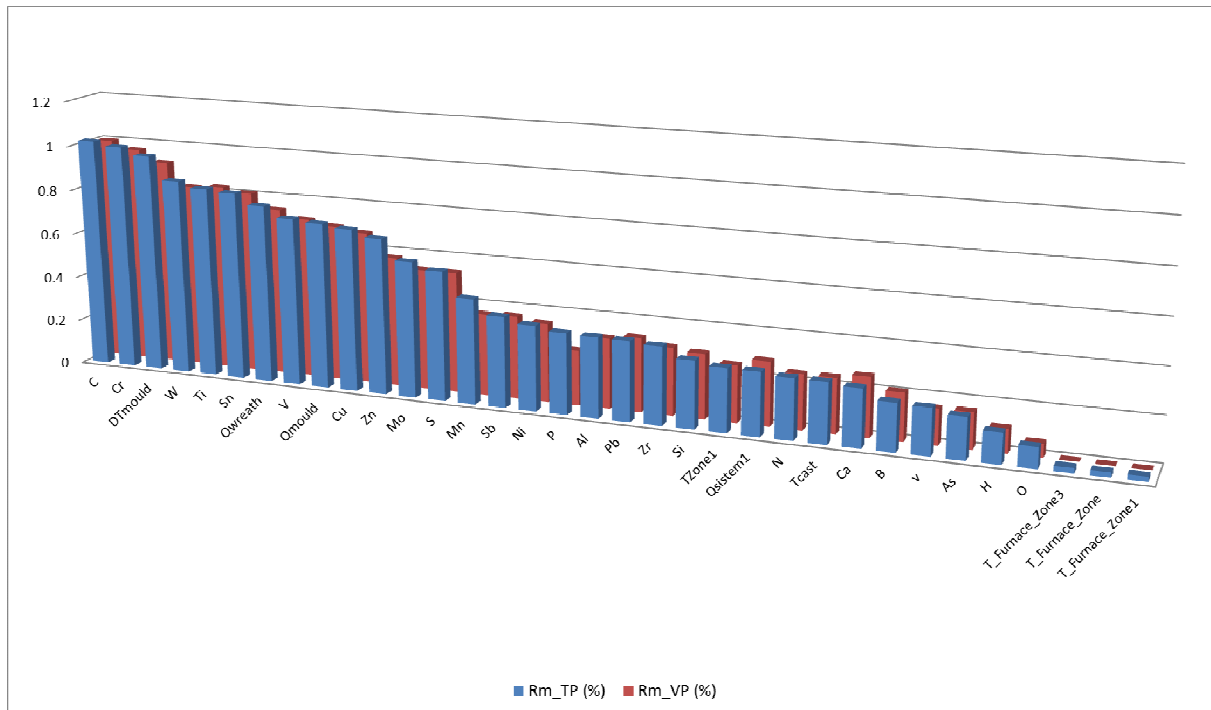


**Figure 355:** Influence on tensile strength ( $R_m$ ) by changing process parameters from minimum to maximum value for training and verification point. Influence is shown in percentage of total range of tensile strength ( $R_m$ ).

Influence of each process parameter on output is different. In the Figure 356 we can see the share of each process parameter in percentage among all process parameters when simulating tensile strength ( $R_m$ ).

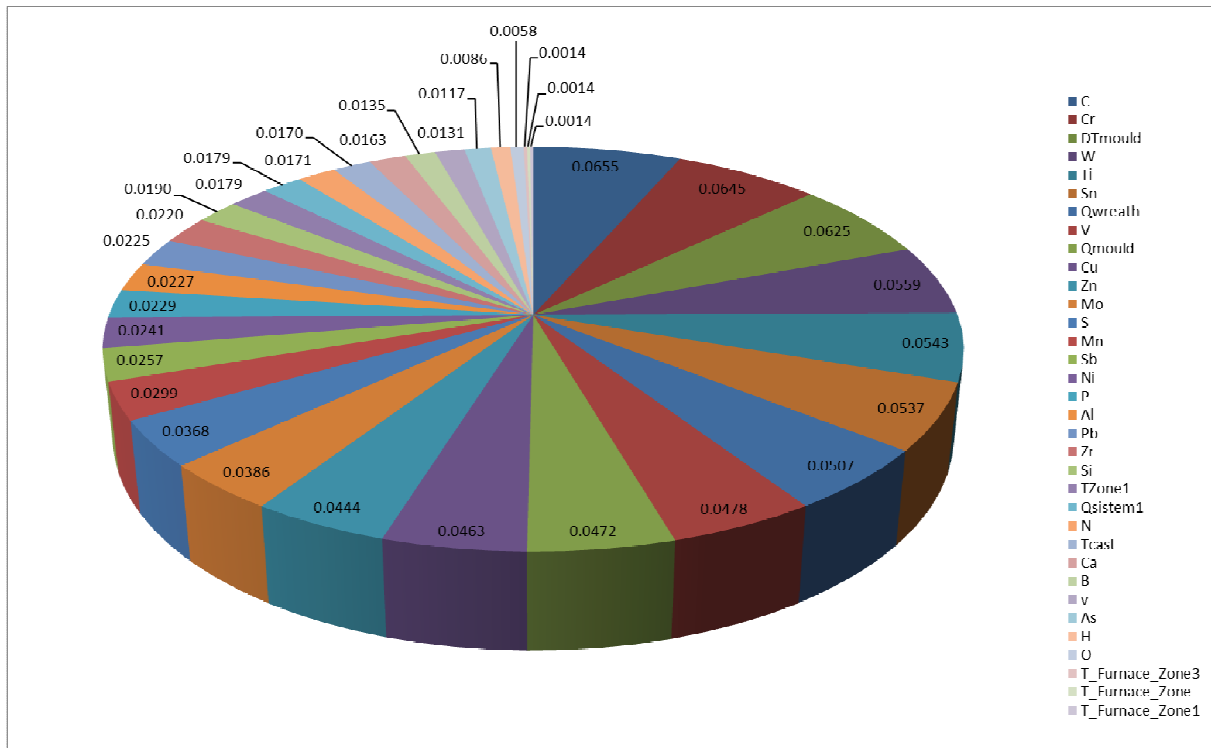


**Figure 356:** The share of each process parameter in percentage among all process parameters when simulating tensile strength ( $R_m$ ).

### 6.3 Yield Stress ( $R_p$ )

Graph below shows the influence of different process parameters to yield stress ( $R_p$ ) for training point (blue columns) and verification point (red column). Process parameters are sorted from the most influential to the least influential. The influence is represented in percentage of change of process parameter according to the range of that process parameter.

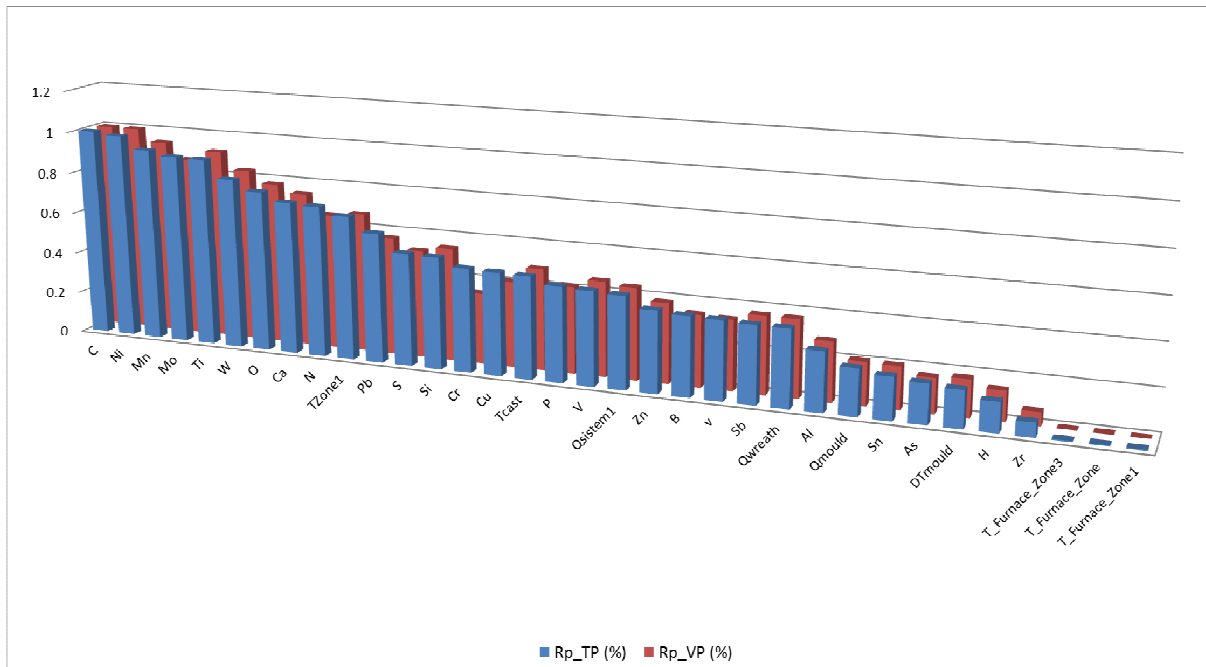


**Figure 357:** Influence on yield stress ( $R_p$ ) by changing process parameters from minimum to maximum value for training and verification point. Influence is shown in percentage of total range of yield stress ( $R_p$ ).

Influence of each process parameter on output is different. In the Figure 358 we can see the share of each process parameter in percentage among all process parameters when simulating yield stress ( $R_p$ ).

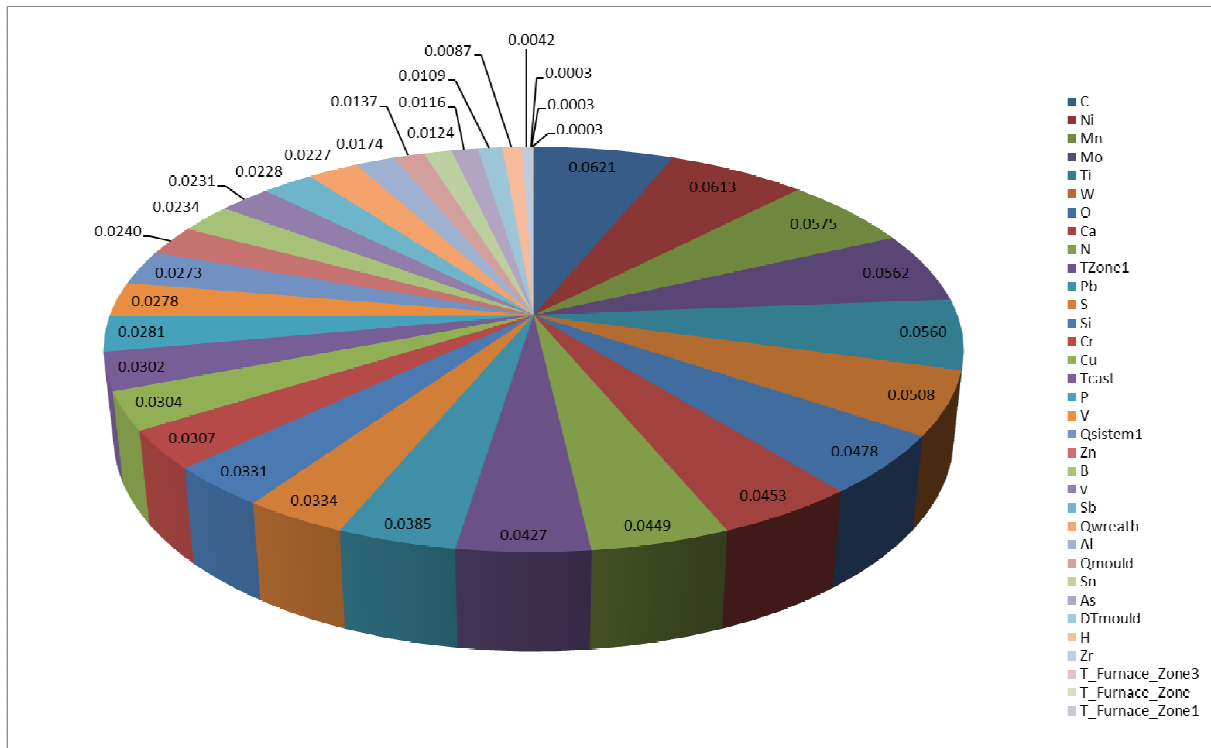


**Figure 358:** The share of each process parameter in percentage among all process parameters when simulating yield stress ( $R_p$ ).

#### 6.4 Hardness After Rolling (HB)

Graph below shows the influence of different process parameters to hardness after rolling (HB) for training point (blue columns) and verification point (red column). Process parameters are sorted from the most influential to the least influential. The influence is represented in percentage of change of process parameter according to the range of that process parameter.

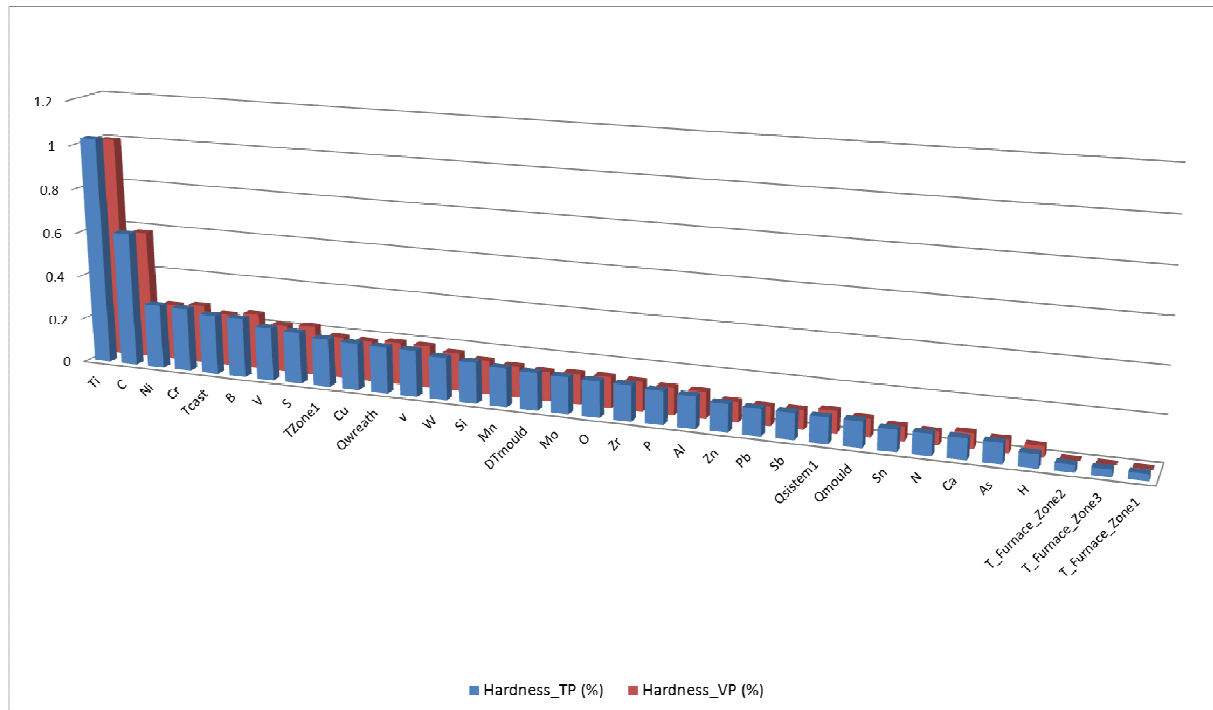


**Figure 359:** Influence on hardness after rolling (HB) by changing process parameters from minimum to maximum value for training and verification point. Influence is shown in percentage of total range of hardness after rolling (HB).

Influence of each process parameter on output is different. In the Figure 360 we can see the share of each process parameter in percentage among all process parameters when simulating hardness after rolling (HB).

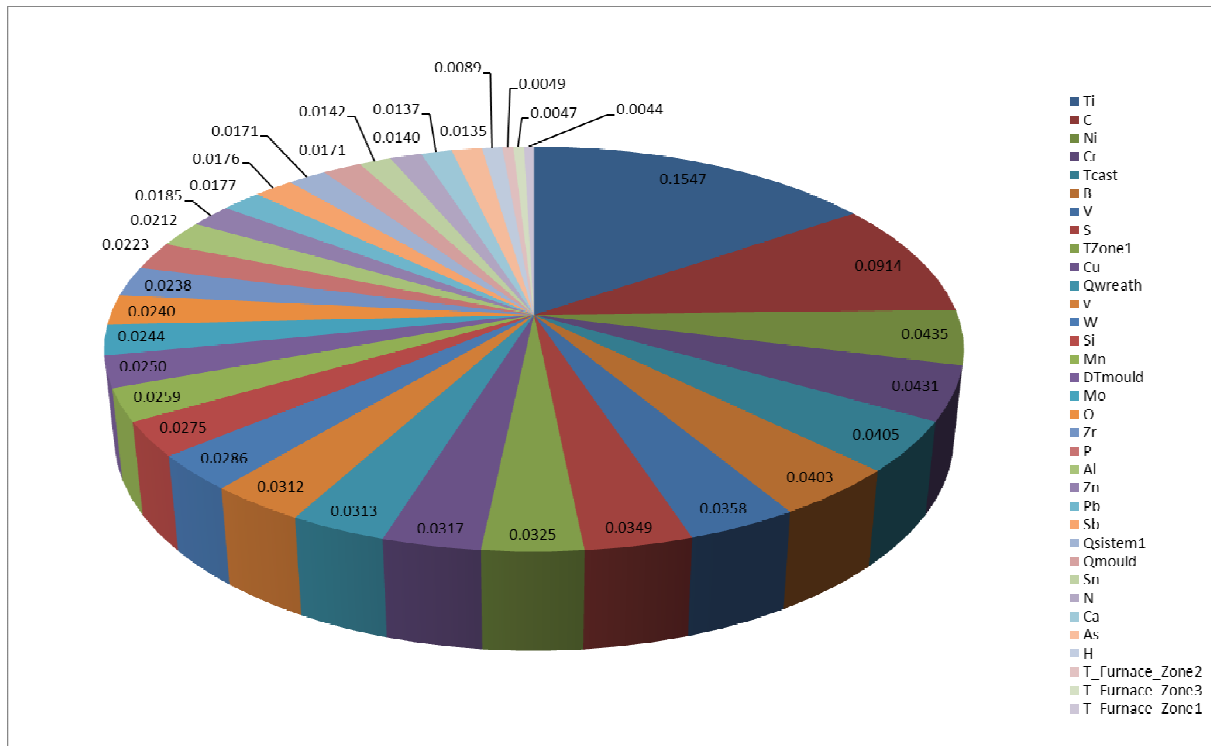


**Figure 360:** The share of each process parameter in percentage among all process parameters when simulating hardness after rolling (HB).

## 6.5 Necking (Z)

Graph below shows the influence of different process parameters to necking (Z) for training point (blue columns) and verification point (red column). Process parameters are sorted from the most influential to the least influential. The influence is represented in percentage of change of process parameter according to the range of that process parameter.

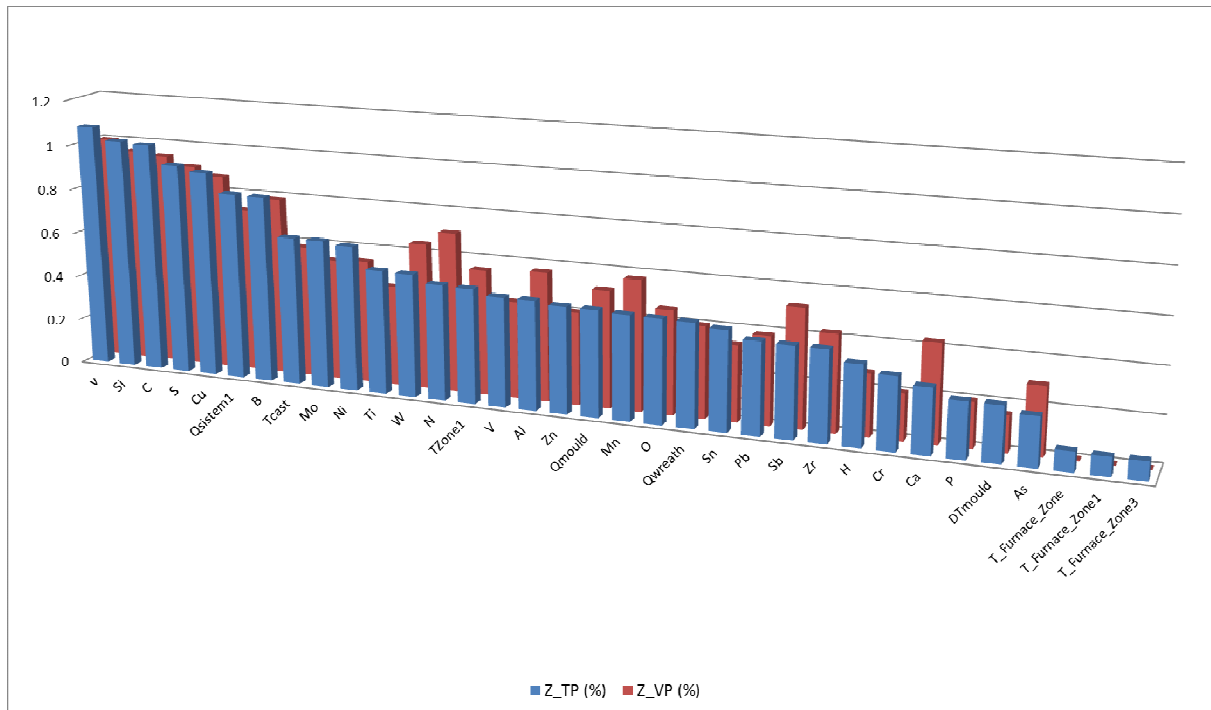


**Figure 361:** Influence on necking (Z) by changing process parameters from minimum to maximum value for training and verification point. Influence is shown in percentage of total range of necking (Z).

Influence of each process parameter on output is different. In the Figure 362 we can see the share of each process parameter in percentage among all process parameters when simulating necking (Z).

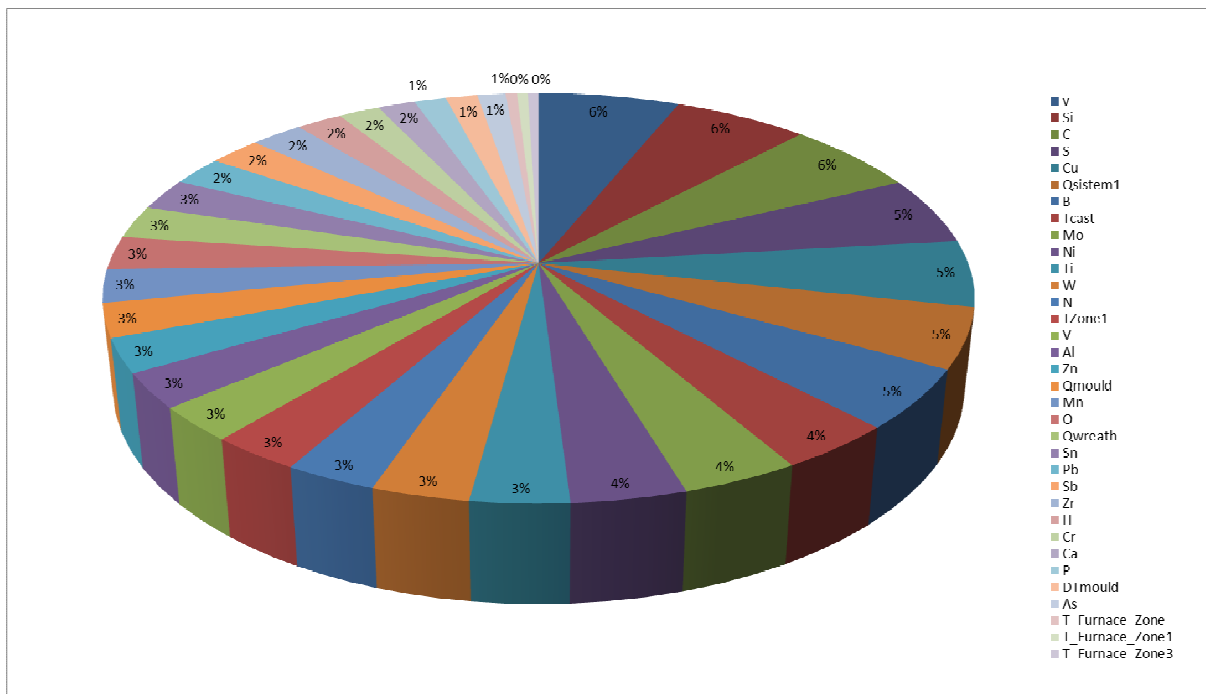


**Figure 362:** The share of each process parameter in percentage among all process parameters when simulating necking (Z).

## **References:**

- [1] Store Steel d.d. (2012). Available at: <http://www.store-steel.si/ProizvodniProgramE.asp>.
- [2] Aforge.Net, artificial intelligence library (2012). Available at: <http://www.aforgenet.com/>.
- [3] Grešovnik, I.; Kodelja, T.; Vertnik, R.; Šarler, B. (2012): Application of artificial neural networks to improve steel production process. Bruzzone, A. G.; Hamza, M. H. Proceedings of the 15th International Conference on Artificial Intelligence and Soft Computing, Napoli, Italy, pp. 249-255.
- [4] Grešovnik, I.; Kodelja, T.; Vertnik, R.; Senčič, B.; Kovacič, M.; Šarler, B. (2012): Application of artificial neural networks in design of steel production path. Computers, Materials and Continua, vol. 30, pp. 19-38.
- [5] Kodelja, T.; Grešovnik, I.; Vertnik, R.; Šarler, B. (2012): Topmost steel production design by using artificial neural networks through process modeling, 20<sup>th</sup> jubilee conference on materials and technology, Portorož, Slovenia.
- [6] Gresovnik, I. (2000): A General Purpose Computational Shell for Solving Inverse and Optimisation Problems - Applications to Metal Forming Processes, Ph. D. thesis, University of Wales Swansea, U.K..
- [7] Grešovnik, I. (2012): Optimization shell Inverse, <http://www2.arnes.si/~ljc3m2/inverse/index.html>.
- [8] Rodič, T., Grešovnik, I. (1998): A computer system for solving inverse and optimization problems. Engineering Computations, vol. 15.
- [9] Ibrahimbegovic, A., Grešovnik, I., Markovič, D., Melnyk, S., and Rodič, T. (2005): Shape optimization of two-phase inelastic material with microstructure. Engineering Computations, Vol. 22 Iss. 5/6, pp.605 - 645.
- [10] Grešovnik, I. (2007): The use of moving least squares for a smooth approximation of sampled data. Journal of Mechanical Engineering, vol. 9, pp. 582-598.
- [11] Grešovnik, I. (2009): Simplex Algorithms for Nonlinear Constrained Optimization Problems, technical report. Available at: <http://www2.arnes.si/~ljc3m2/igor/doc/rep/optalgsimplex.pdf>.
- [12] Grešovnik, I. (2012): IGLib.net - investigative generic library. Available at: <http://www2.arnes.si/~ljc3m2/igor/iglib/>.
- [13] Grešovnik, I. (2012): IOptLib – library for solving inverse and optimization problems. Available at: <http://www2.arnes.si/~ljc3m2/igor/iopplib/>.
- [14] Grešovnik, I.; Kodelja, T.; Vertnik, R.; Šarler, B. (2012): A software framework for optimization parameters in material production. Applied Mechanics and Materials, vol. 101, pp. 838-841.